Denitrification in Agricultural Surface Waters: Quantifying the Effect of Environmental Parameters and Hydrologic Connectivity on Nitrate Uptake and Microbial Communities

A Dissertation
SUBMITTED TO THE FACULTY OF
UNIVERSITY OF MINNESOTA
BY

Abigail Ann Tomasek

IN PARTIAL FULFILLMENT OF THE REQUIREMENTS
FOR THE DEGREE OF
DOCTOR OF PHILOSOPHY

Dr. Miki Hondzo

October 2017

Acknowledgements

This research would not have been possible without the support of numerous people. First, I would like to acknowledge my advisor Dr. Miki Hondzo, whose guidance and support were invaluable over these past four years. Thank you for pushing me when I needed it the most. I would also like to acknowledge Dr. Jessica Kozarek for her mentorship, instrumental project ideas, and continued support over the entirety of my PhD. Thank you to my committee member Dr. Michael Sadowsky for his instrumental contribution and research development for the microbiological work presented in this thesis, as well as his support and patience in sharing his knowledge. I would also like to thank my committee members Dr. Sebastian Behrens and Dr. Vaughan Voller for their helpful comments and advice.

In addition, I'd like to acknowledge the numerous people that have contributed equipment, ideas, and laboratory space that made this research possible. Thank you to Dr. Jacques Finlay, Andrea Little, and Shelly Rorer for use of the laboratory space to run denitrification assays and help with nutrient analysis. Thanks to Dr. Kurt Spokas and Martin du Saire for their instrumental and laboratory help with GC analysis, and to Dr. Rodney Venterea for providing guidance for nitrous oxide sampling. Dr. Ping Wang was invaluable to the progression and development of this research, and helped me, with incredible patience, in learning the fundamentals of qPCR. Thank you to Dr. Christopher Staley for his statistical and microbiological contributions. I'd like to acknowledge the help of numerous undergraduate students who contributed to this project, particularly Aileen Zebrowski, India Woodruff, and Rena Weiss. And thank you to Nicole Lurndahl for all of her contribution and analysis of microbial gene abundances, as well as her assistance with fieldwork. Long days in the ditches would not have been nearly as successful or enjoyable without you.

Funding for this project was provided by the Clean Water Research Program through the Minnesota Department of Agriculture with funding from the Minnesota Clean Water, Land, and Legacy Amendment, as well as by Agriculture and Food Research Initiative Competitive grant 2015-06019-23600 from the USDA National Institute of Food and Agriculture. Funding was also provided by the Freshwater Society

of Minnesota through the Moos Fellowship in Aquatic Biology. Thank you to the Anderson family, and Frank and Julie Tsai for their generous support of SAFL's graduate students, and whose donations allowed me to expand my knowledge and share my research. I would also like to acknowledge the SAFL Student Council Travel Award, the CEGE Travel Award, and the International Society for River Science (ISRS) Scholarship for providing financial support for conference travel.

Thank you to the St. Anthony Falls Laboratory in entirety. The exchange of ideas, the passion, and the vast knowledge of the faculty, staff, and students makes it a unique and special place, and I am grateful to have been able to be a part of the SAFL community. To the Flowers (Anne, Maria, and Zeinab), your friendship has carried me through. I cannot wait to see everything you women accomplish. Words cannot express my gratitude to the SAFL student body for their support and friendship during the entirety of this PhD. From the happy hours, to the weekend festivities, to hallway conversations, my PhD has actually been enjoyable due to all of you.

Thank you to all of my friends and family for the unconditional support over the past four years. This path has not been easy, academically or emotionally, and without your encouragement and love, I would not be here today.

Dedication

To my mother, for her unconditional love and support, for setting an example on how to be a strong woman in both STEM and in life, and for providing the foundation for my love of the natural world. To my father, for instilling in me the joy of science and research, for teaching me to wonder and to question, and for being an inspiration in kindness and generosity. To my brother. Your approach to life is something I aspire to. You are a hero in every sense of the word. To Michelle, Ari, and Hailey. I love you all.

Abstract

The development of synthetic fertilizer has led to increases in crop yields and allowed for global population growth over the past century. However, this increase in available nitrogen has greatly altered the global nitrogen cycle, including increased nitrate loading to surface water and groundwater in the Midwestern United States, with negative effects on human health and aquatic ecosystems. Therefore, there is a need for effective management strategies and an understanding of the mechanisms for nitrate transport and uptake. Denitrification, the microbiological reduction of nitrate to nitrogen gas, can be viewed as a net sink for reactive nitrogen in aquatic systems. Small areas, termed hot spots, and short time periods, termed hot moments, frequently account for a large portion of denitrification. This research focuses on identifying the environmental parameters and hydrologic regimes that promote denitrification, along with determining how parameters, denitrification rates, and microbiological communities are related at multiple temporal and spatial scales. At the finest scale, a recirculating laboratory flume was used to determine the effect of turbulence and organic carbon on denitrification rates and the microbial community. An outdoor experimental stream and flow-through basin in the Outdoor StreamLab at the St. Anthony Falls Laboratory (SAFL) were used to determine the effect of short-term inundation and periodic inundation on denitrification. At the largest scale, water and sediment samples were collected over two years from a field site in an agricultural watershed in Southern Minnesota. The objectives of this research were to: (1) determine how turbulence and organic carbon affect denitrification, (2) investigate how inundation and hydrologic connectivity leads to the formation of denitrification hot spots and hot moments, (3) quantify and correlate the driving environmental parameters

of microbial denitrification and the differences in these relationships for in-channel and riparian locations in an agricultural watershed, (4) develop and evaluate functional relationships between environmental parameters and denitrification rates, and (5) identify how denitrifying gene abundances, denitrification rates, and environmental parameters are related across a hydrologic gradient from channels to riparian areas.

Contents

List of Tables

List of Figures

1 Introduction

1.1 Dissertation Overview

The research conducted during my PhD, and discussed in this dissertation, focused on identifying the environmental parameters and hydrologic regimes that promote denitrification, along with determining how parameters, rates, and microbiological communities are related. This research was conducted at multiple temporal and spatial scales, ranging from laboratory to field-scale. The dissertation is organized into six chapters, described below.

- Chapter 1 provides an overview and introduction to the nitrogen cycle, microbial denitrification, and a more extensive explanation of the methodology used in this dissertation.
- Chapter 2 investigates the effect of small-scale turbulence and sediment carbon amendment on denitrification in a recirculating laboratory flume.
- Chapter 3 describes how short-term and longer duration inundation, as well as differing soil organic carbon, affect denitrification rates, microbial communities, and nitrous oxide emissions.
- Chapter 4 uses a scaling relationship to develop a predictive functional relationship to estimate denitrification rates using multiple independent environmental parameters, and discusses differing correlations between denitrification rates, environmental parameters, and gene abundances in a normal-flow year.
- Chapter 5 expands on Chapter 4 by investigating how correlations between denitrification rates, environmental parameters, and gene abundances differ between a normal and wet year and at locations with varying hydrologic connectivity, as well as providing a microbial community analysis to further validate spatial differences seen in denitrification rates.
- Chapter 6 provides a summary and conclusion of the dissertation results.

1.2 The Nitrogen Cycle

1.2.1 Introduction to the Nitrogen Cycle

All organisms require nitrogen (Elser et al., 2000). It is essential in living tissue where it serves as an integral part of enzymes, proteins, and DNA (Schlesinger and Burnhardt, 2013), and in plants, nitrogen content is related to the photosynthetic capacity, therefore affecting productivity and crop yields (Evans, 1989). The nitrogen cycle has a large number of transformations and pathways due to its number of oxidation states ranging from -3 to +5 (ammonia and nitrate, respectively) (Schlesinger and Burnhardt, 2013). While the denitrification and nitrification pathway were discovered over a century ago (Zumft, 1997), new pathways in the nitrogen cycle are still being discovered. For instance, dissimilatory nitrate reduction to ammonium (DNRA) has only been widely recognized for 35 years, anaerobic ammonium oxidation (anammox) was discovered in wastewater plants in the 1990s (Burgin and Hamilton, 2007), and complete ammonia oxidizers (comammox) were discovered in 2015 (Daims et al., 2015). Figure 1.1 shows the pathways in the nitrogen cycle (Daims et al., 2016).

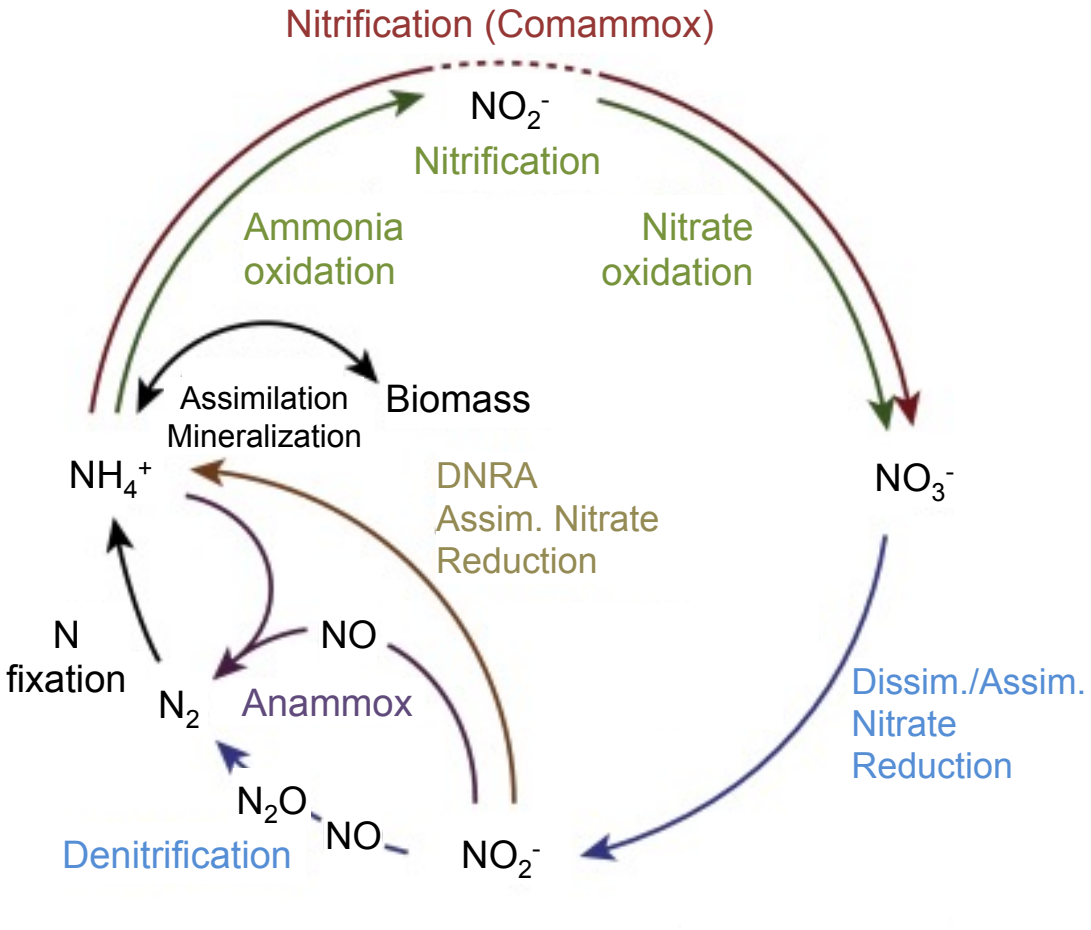

Figure 1.1. Biogeochemical nitrogen cycle with key processes in the cycle. The dashed line for comammox shows that nitrite is an intermediate but can be oxidized to nitrate by the same organism (Daims et al., 2016).

While nitrogen comprises approximately 78% of the atmosphere, it is in the form of nitrogen gas (N_2), which is unusable to most organisms. The triple bond holding the two nitrogen atoms together results in one of the most stable gasses and requires a large amount of energy to break the bond (946 kJ mol^{-1} compared to 498 kJ mol^{-1} for O_2) (Moore et al., 2010). Nitrogen availability limits plant growth in almost all natural environments (White and Brown, 2010), and in pre-industrial agriculture, nitrogen was

the most commonly yield-limiting nutrient (Smil, 2002). Some bacteria have overcome this barrier through nitrogen fixation in low-nitrogen environments. Due to the high energy cost, nitrogen fixation is influenced by the availability of carbon, with rates of symbiotic nitrogen fixation in plants often directly related to rates of photosynthesis (Bormann and Gordon, 1984), and nonsymbiotic, free-living, heterotrophic nitrogen fixers usually found in soils with high organic matter (Billings et al., 2003; Schlesinger and Burnhardt, 2013). In particular, leguminous plants are able to naturally supply nitrogen to agro-ecosystems through their symbiotic relationships with the nitrogen fixing *Rhizobia* in root nodules (Hayat et al., 2010; Jensen et al., 2012). Plants without the ability to fix their own nitrogen require nitrogen fertilizer additions to obtain acceptable crop yields. Historical evidence shows that adding manure to fields has been used since Neolithic times to increase nitrogen availability for crops (Bogaard et al., 2013). In the past century, synthetic fertilizers have largely replaced manure.

1.2.2 Anthropogenic Alteration of the Nitrogen Cycle

The Haber-Bosch process creates ammonia by reacting atmospheric nitrogen with hydrogen under high pressures and temperatures (Erisman et al., 2008). The process has been estimated to sustain approximately 40 percent of the global population (Smil, 2002), however it has increased the amount of global reactive nitrogen in the environment by 120 percent since 1970 (Galloway et al., 2008; Schlesinger, 2009), and it contributes nearly double the natural rate of terrestrial nitrogen fixation (Canfield et al., 2010). Meat consumption, which requires more fertilizer inputs to produce, has increased globally over the past century, and is therefore a major factor in agricultural nitrogen use (Howarth et al., 2002; Westhoek et al., 2014). Figure 1.2 from Erisman et al. (2008) shows global increases in population, an estimation of the global population without the use of Haber-Bosch fertilizer, the percentage of the population that is fed by the Haber-Bosch, average fertilizer inputs, and global meat production.

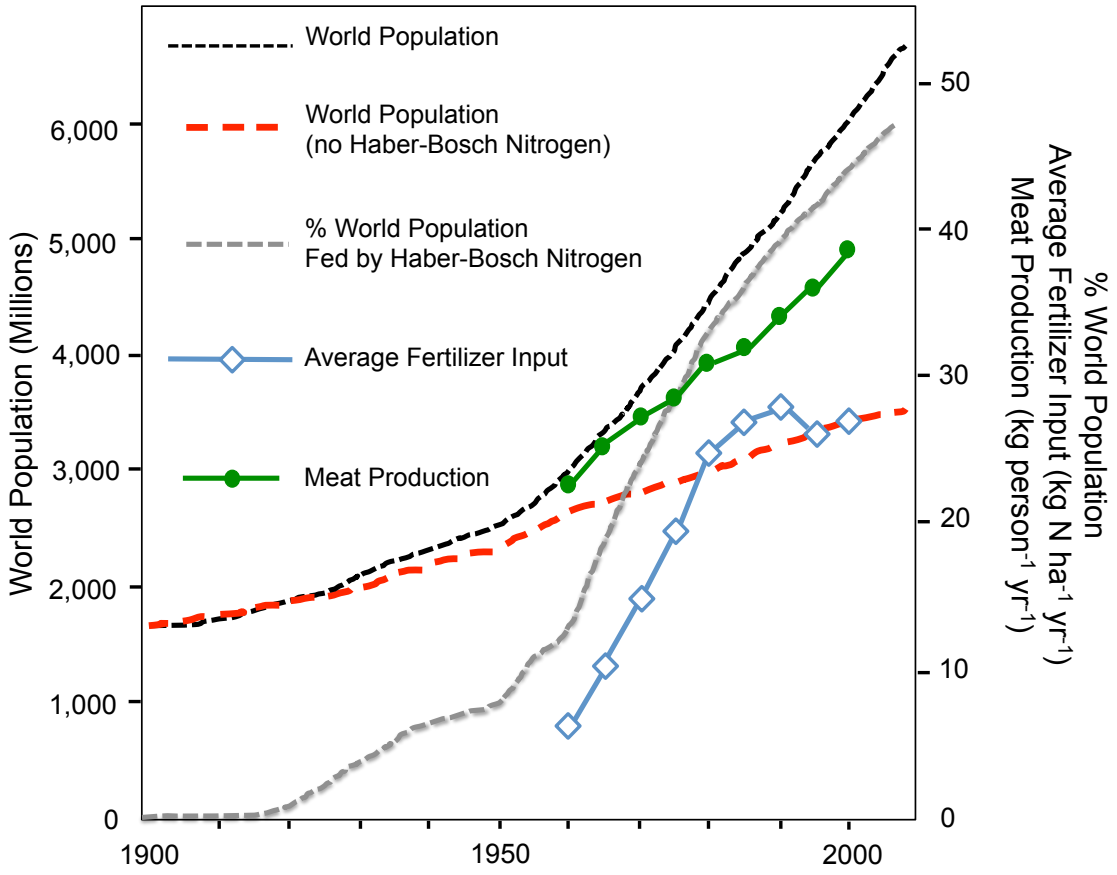

Figure 1.2. Change in the global population (black line), an estimate of the number of people that could be sustained without reactive nitrogen from the Haber-Bosch process (red dashed line), an estimate of the percentage of the world's population that is fed by Haber-Bosch derived nitrogen (black dashed line), average fertilizer use per hectare of land (blue symbols), and the increase in per capita meat production from 1990 to 2008 (Erisman et al., 2008).

Crops do not take-up all of the nitrogen applied to fields, resulting in nitrogen losses to the atmosphere (ammonia volatilization), through runoff, and leaching into ground and surface waters (Di and Cameron, 2002). Synthetic fertilizers are usually applied as ammonium or ammonia, which reacts with soil water to form ammonium. This readily converts to nitrate in soils through nitrification (Cameron et al., 2013; Robertson and Vitousek, 2009). Since most soils in the Midwestern United States are negatively charged, nitrate is not adsorbed by soil particles, allowing nitrate to leach through soil (Di

and Cameron, 2002). Studies have shown that up to 50-70 percent of the reactive nitrogen applied to soils is lost through hydrologic and gaseous pathways (Masclaux-Daubresse et al., 2010; Robertson and Vitousek, 2009). Similarly, Lasaletta et al. (2014) found that only 47 percent of reactive nitrogen applied to croplands is converted into harvestable product, but that globally, nitrogen use efficiency (the fertilizer recovery) has decreased since the 1960s while fertilizer inputs have increased. The Minnesota Pollution Control Agency (MPCA) and Minnesota Department of Agriculture (MDA) reported that in Minnesota, 63% of nitrogen applied to agricultural lands went into crops and food products, and that N fertilizer use efficiency has increased over the past decade (MPCA, 2013).

With increases in fertilizer applications, nitrogen loading to surface waters has correspondingly increased. Figure 1.3 shows increasing riverine nitrogen fluxes in several watersheds, including the Mississippi River watershed, in response to increasing net anthropogenic nitrogen inputs (Vitousek et al., 1997). Several studies have found that agriculture is a major source of increased nitrogen loading of watersheds over the past 50 years (NRC, 1993). In Minnesota, the MPCA estimated that approximately 70% of the nitrogen loading to surface waters was from agriculture statewide, but in the heavily agricultural Minnesota River Basin, this contribution was approximately 89 to 95% (MPCA, 2013). In the Mississippi River Basin, nitrate is the major contributor of the increased nitrogen loading in surface waters (Turner and Rabalais, 2003) (Figure 1.4).

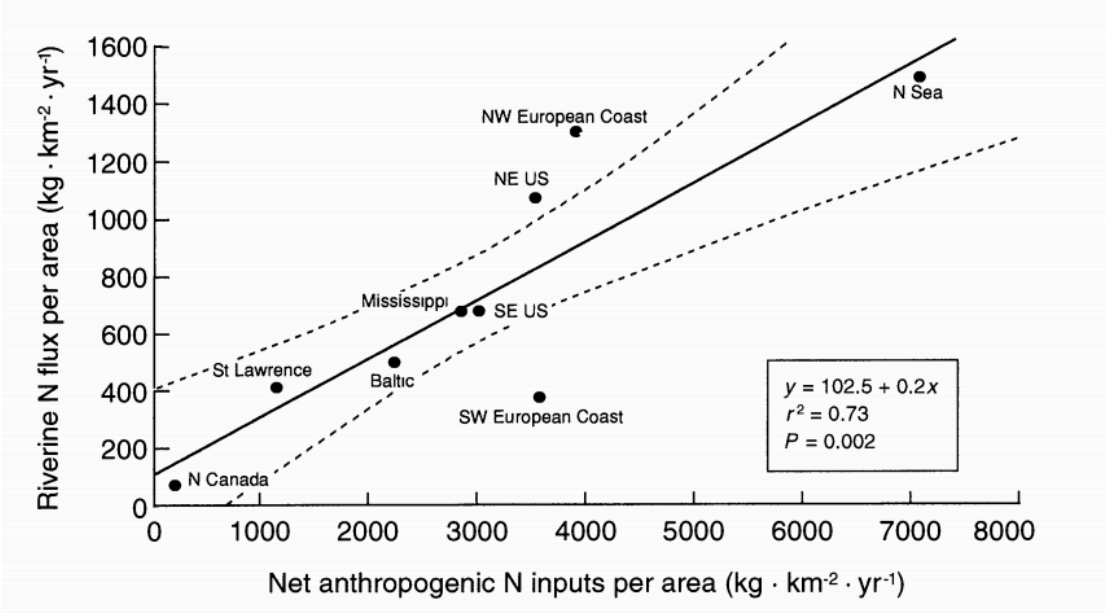

Figure 1.3. Export of total nitrogen from watersheds as a function of net anthropogenic inputs of nitrogen and their watersheds. Net anthropogenic inputs are: industrial N fertilizer + N fixation by legume crops + atmospheric inputs of oxidized N + net inputs of N in food and feedstock (Vitousek et al., 1997).

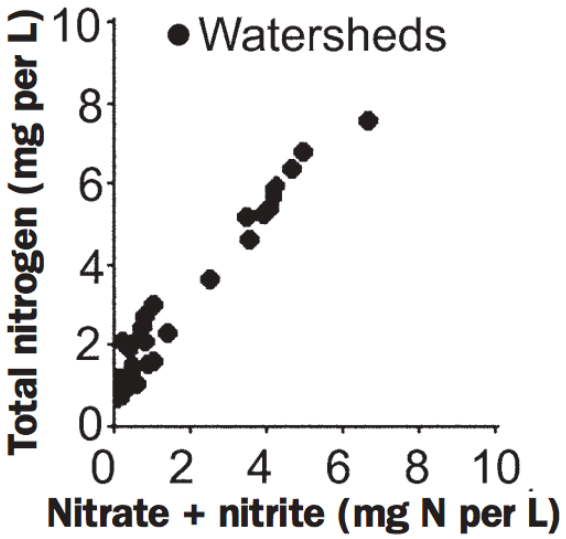

Figure 1.4. Relationship between total nitrogen and combined concentration of nitrate+nitrite for 42 subwatersheds in the Mississippi River Basin (Turner and Rabalais, 2003).

Nitrate delivery to surface waters in the agricultural Midwestern United States is exacerbated through the use of tile (field) drainage. Tile drains are implemented in areas with high water tables and work by directing soil-infiltrated water through a system of pipes installed below a field, thereby lowering the water table below the soil-saturated zone for optimal crop growth. However, these tiles serve as direct conduits of high nitrate water to surface waters, reducing residence time, and short-circuiting the system and reducing soil microbial processes such as denitrification. In watersheds that are drained, tiles (and field pipe drain systems) are the primary conduit of nitrate export from watersheds, and almost all nitrate export occurs during high-discharge events (Royer et al., 2006). In Minnesota during a normal precipitation year, cropland tile drainage contributes 37% of the nitrogen load to Minnesota's waters statewide and 67% in the heavily-tiled Minnesota River Basin; these contributions increase to 43% and 72%, respectively, during a wet year (MPCA, 2013). Comparing tile and non-tile drained systems, nitrate leaching into groundwater in the karstic landscape of the Lower Mississippi River Basin contributes 58% of nitrogen delivered to surface waters, whereas in the Minnesota River Basin, cropland groundwater only contributes 16% of nitrogen to surface waters (MPCA, 2013).

1.2.3 Health and Ecological Impacts of Increased Nitrate Loading

Ingestion of high-nitrate containing water has potential consequences on human health. One concern is methemoglobinemia, which decreases the oxygen carrying capacity of hemoglobin, particularly in infants, leading to blue baby syndrome. Cases have been reported in infants using water above the drinking water standard of 10 mg $N\text{-}NO_3^- L^{-1}$ (Fan and Steinberg, 1996). Other potential health risks that have been reported include gastroenterological conditions, cardiac disease, hypertension, diseases of the central nervous system, mutagenicity, contribution to the risks of non-Hodgkin's lymphoma and bladder and ovarian cancers, spontaneous abortions, and respiratory tract infections; however the literature is conflicted as to what conditions nitrate-laden water can cause and at what concentration (Camargo and Alonso, 2006; Ellis et al., 1998; Ward et al., 2005). Only public water systems treat drinking water for nitrate, whereas in agricultural

areas, where there is a higher chance for nitrate contamination, drinking water from private wells is not treated (Manassaram et al., 2006). Recommended water quality limits have been proposed as 2.9 to 3.6 mg $N\text{-}NO_3^-$ L^{-1} based on toxicity data (CCME, 2003), and as low as 1.0 mg L^{-1} for total nitrogen (TN) to prevent aquatic ecosystems from undergoing acidification and eutrophication (Camargo and Alonso, 2006). Nitrate concentrations in the Midwestern United States are routinely greater than even the 10 mg $N\text{-}NO_3^-$ L^{-1} drinking water standard (MPCA, 2013), indicating that measures are needed to reduce nitrogen loading in these areas.

Water containing high nitrate concentrations also has a wide range of potential ecological effects. A few of these include a delay in hatching of fish and amphibian eggs, reduced growth rates in fish and amphibians, declined species diversity, disruption of molting and emergence in insects and crustaceans, alteration of the food web, and a reduction in net photosynthesis and net productivity (Camargo and Alonso, 2006). The Gulf of Mexico hypoxic zone is one of the largest in the world and is predominately caused by nitrate export from the Mississippi River watershed to the Gulf (Turner et al., 2006). Nitrogen availability often limits the rate of net primary production in the ocean (Schlesinger and Burnhardt, 2013), and is the primary limiting nutrient for oceanic phytoplankton biomass accumulation (Howarth, 2008; Rabalais, 2002). When a pulse of nitrate enters the ocean, it stimulates phytoplankton growth. As the remains of the phytoplankton settle, they are decomposed by bacteria. This decomposition consumes oxygen, reducing the dissolved oxygen of the water, and hypoxic areas develop.

In February of 2015, the Hypoxia Task Force set the goal of reducing the extent of the hypoxic zone in the Gulf of Mexico to 5,000 km^2 by 2025 (EPA, 2015). The hypoxic zone in the summer of 2017 was the largest since mapping began in 1985 (NOAA, 2017), and was nearly three times greater than this targeted size (Figure 1.5). One possibility is that high May discharge in the Mississippi River basin increased the flux of nitrate to the Gulf of Mexico, but the fact that the size of the hypoxic zone is not decreasing suggests that current nitrogen management strategies are not enough.

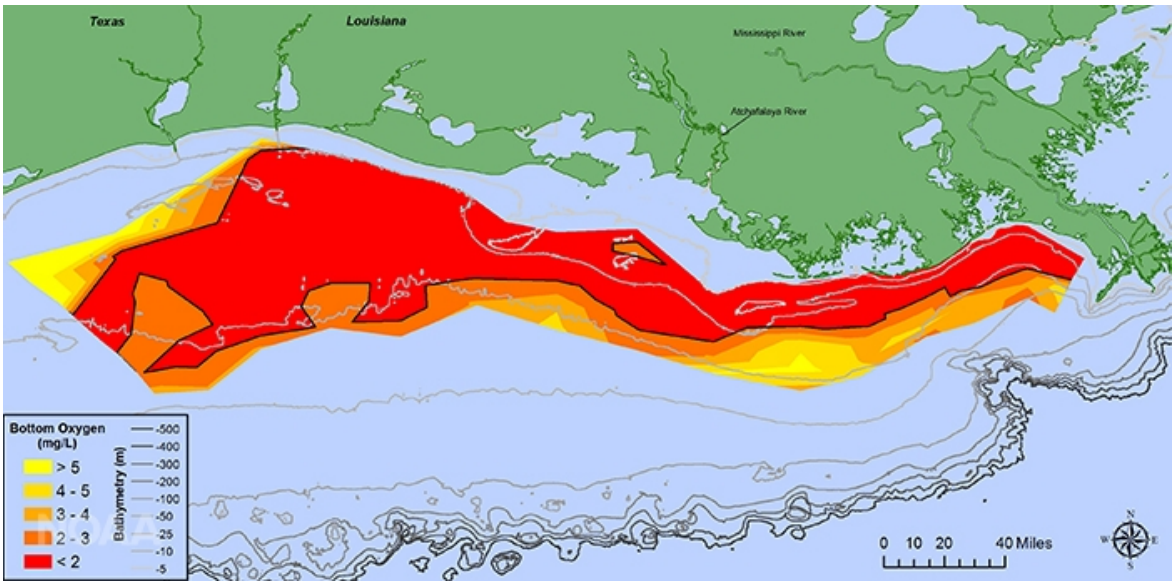

Figure 1.5. Hypoxic zone in the Gulf of Mexico in July 2017 (N. Rabalais, LSU/LUMCON)

1.2.4 Current Legislation

Currently, the only Minnesota legislation for improving water quality in agricultural ditches is a mandatory 16.5 ft (5 m) buffer strip between the top edge of the channel and the field (Minnesota Statutes, 2017). Buffer strips may be effective for certain water quality goals, such as bank stabilization and reducing suspended sediment (Strock et al., 2010), and for water quality in un-tiled agricultural areas (Smith et al., 2008a). However, research has shown they are not effective in reducing nitrogen loads in agricultural areas that are tile drained (Janssen et al., 2013; Osborne and Kovacic, 1993), even when buffer strips were up to 20 m wide (Kahle et al., 2013). In order for buffer strips to work in tile drained systems, water would need to be as overland flow, which only occurs in extreme weather events. Other practices, such as controlled draining, constructed wetlands, and bioreactors, are purely voluntary for farmers to implement. As the global population continues to increase, and with continued reliance on synthetic fertilizer use, a better understanding of nitrate uptake processes, and how to effectively implement this knowledge, is essential for the future health of our waters.

1.3 Denitrification

1.3.1 Overview of Denitrification

Denitrification is the stepwise microbial reduction pathway of aqueous nitrate to nitrogen gas (Figure 1.6). There are two types of pathways for nitrate reduction, assimilatory and dissimilatory (Table 1.1). Assimilatory nitrate reduction occurs when a more reduced nitrogen species (e.g. NH_3) is not available. This process cannot be viewed as a net loss of inorganic nitrogen since inorganic nitrogen is converted to organic nitrogen and released back into the environment (Van Rijn et al., 2006). In contrast, complete denitrification reduces nitrate to nitrogen gasses, which is then released to the atmosphere, thereby acting as a net sink for reactive nitrogen. For wetlands, streams, and riparian sediment, particularly in high nitrate environments, studies have shown that denitrification has the highest activity compared to other nitrogen-cycling pathways (Kim et al., 2016; Morrissey et al., 2013; Nogaro and Burgin, 2014; Scott et al., 2008; Washbourne et al., 2011; Welti et al., 2012).

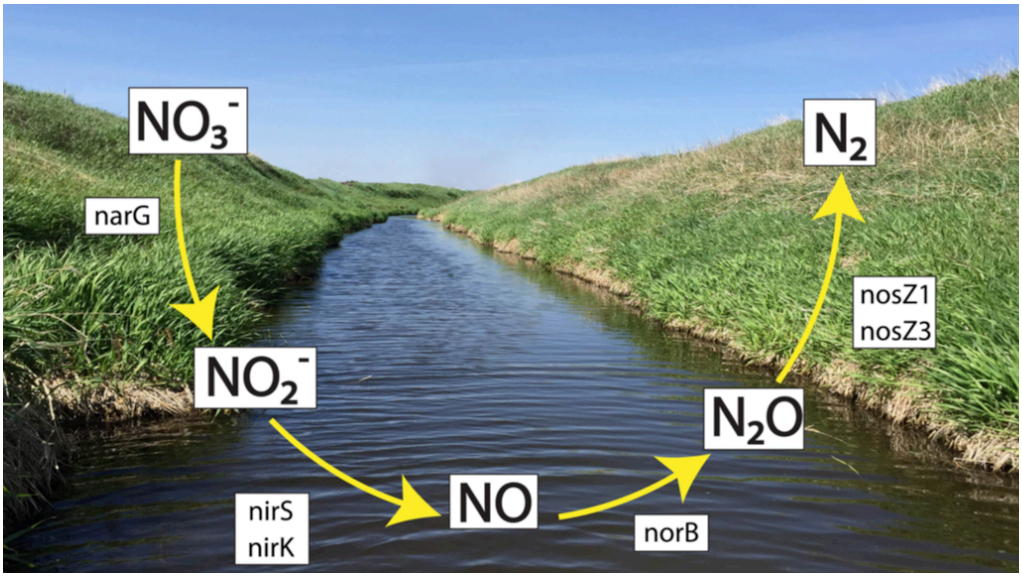

Figure 1.6. The complete denitrification pathway from nitrate (NO_3^-) to nitrogen gas, along with the genes encoding for the enzymes for each step in the process.

Table 1.1. Biological nitrate reduction for both assimilatory and dissimilatory pathways, along with the organisms that perform each pathway (Van Rijn et al., 2006).

Process	Regulators	Organisms
Assimilatory Nitrate Reduction ($NO_3^- \rightarrow NO_2^- \rightarrow NH_4^+$)	NH_4^+	Plants, fungi, algae, bacteria
Dissimilatory Nitrate Reduction		
Dissimilatory Nitrate Reduction to Ammonia ($NO_3^- \rightarrow NO_2^- \rightarrow NH_4^+$)	O_2, C/N	Anaerobic and facultative anaerobic bacteria
Denitrification ($NO_3^- \rightarrow NO_2^- \rightarrow NO \rightarrow N_2O \rightarrow N_2$)	O_2, C/N	Facultative anaerobic bacteria

Denitrification is largely a heterotrophic process performed by facultative aerobes. Denitrifiers are mainly *Proteobacteria* (Madigan et al., 2018), but are metabolically and phylogenetically diverse (Cheneby et al., 2000; Rich et al., 2003) due to the high oxidative potential of nitrate (Chen and Strous, 2013) and the high energy yield of the pathway (Table 1.2). Some nitrate reducers only perform certain steps in denitrification, for instance *E. coli* only reduces nitrate to nitrite (Madigan et al., 2018), while others, like *P. aeruginosa* (Arat et al., 2015) can complete the entire pathway.

While complete denitrification reduces NO_3^- completely to N_2, incomplete denitrification instead stops at N_2O. This is of global concern since N_2O is a greenhouse gas with 300-times the warming potential of CO_2 (Ravishankara et al., 2009). N_2O emissions account for approximately 6 percent of the anthropogenic greenhouse effect (Stehfest and Bouwman, 2006), but are increasing globally. Approximately 84 percent of global anthropogenic nitrous oxide emission is attributed to agriculture (Smith et al., 2008b), emphasizing the need to consider how environmental conditions affect the N_2O yield, or the proportion of nitrate that is reduced incompletely to N_2O instead of fully to N_2.

Table 1.2. Common reduction and oxidation half reactions (Schlesinger and Burnhardt, 2013).

Reduction		E° (V)	Oxidation		E° (V)
(A)	$1/4O_2(g) + H^+ + e^- = 1/2H_2O$	+0.813	(L)	$1/4CH_2O + 1/4H_2O = 1/4CO_2 + H^+ + e^-$	-0.485
(B)	$1/5NO_3^- + 6/5H^+ + e^- = 1/10N_2{}^+3/5H_2O$	+0.749	(M	$1/2CH_4 + 1/2H_2O = 1/2CH_3OH + H^+ + e^-$	+0.170
(C)	$1/2MnO^2(s) + 1/2HCO_3 + 3/2H^+ + e^- = 1/2MnCO_3 + H_2O$	+0.526	(N)	$1/8HS^- + 1/2H_2O = 1/8SO_4^{2-} + 9/8H^+ + e^-$	-0.222
(D)	$1/8NO_3^- + 5/4H^+ + e^- = 1/8NH_4{}^+3/8H_2O$	+0.363	(O)	$FeCO_3(s) + 2H_2O = FeOOH(s) + HCO_3(10^{-3}) + 2H^+ + e^-$	-0.047
(E)	$FeOOH(s) + HCO_3(10^{-3}) + 2H^+ + e^- = FeCO_3(s) + 2H_2O$	-0.047	(P)	$1/8NH_4{}^+3/8H_2O = 1/8NO_3^- + 5/4H^+ + e^-$	+0.364
(F)	$2/3CH_2O + H^+ + e^- = 1/2CH_3OH$	-0.178	(Q)	$1/2MnCO^3(s)+H_2O=1/2MnO_2(s)+1/2\ HCO_3(10^{-3})+3/2H^++e^-$	+0.527
(G)	$1/8SO_4^{2-} + 9/8H^+ + e^- = 1/8HS^- + 1/2H_2O$	-0.222			
(H)	$1/8CO_2 + H^+ + e^- = 1/8CH_4{}^+1/4H_2O$	-0.244			
(I)	$1/6N_2 + 4/3H^+ + e^- = 1/3NH_4$	-0.277			

Examples	Combinations	ΔG° (W) pH = 7 (kJ eq-1)
Aerobic Respiration	(A) + (L)	-125
Denitrification	(B) + (L)	-119
Nitrate reduction to ammonium	(D) + (L)	-82
Fermentation	(F) + (L)	-27
Sulfate reduction	(G) + (L)	-25
Methane fermentation	(H) + (L)	-23
Methane Oxidation	(A) + (M)	-62
Sulfide oxidation	(A) + (N)	-100
Nitrification	(A) + (P)	-43
Ferrous oxidation	(A) + (O)	-88
Mn(II) oxidation	(A) + (Q)	-30

1.3.2 Denitrification Hot Spots and Hot Moments

Small areas, termed hot spots, and short time periods, termed hot moments, frequently account for a large proportion of active denitrification. While the exact mechanisms for the formation of hot spots and hot moments are unknown, it is hypothesized that they form at the convergence of ideal organic carbon (Perryman et al., 2011; Pinay et al., 2000), nitrate concentrations (Inwood et al., 2007), soil water content (Pinay et al., 2007), oxygen conditions, water velocity (Arnon et al., 2007b; O'Connor and Hondzo, 2008a), and floodplain location (Roley et al., 2012a; Roley et al., 2012b), and in areas with established bacterial communities. Determining the correlation between these environmental parameters and denitrification rates is important for designing management strategies that promote the formation of hot spots and hot moments, and also for modeling efforts in order to effectively estimate nitrate uptake.

Fluctuations of water levels can cause the creation of denitrification hot spots and hot moments. For instance, a study found that small-scale variations in topography within the riparian zone had large effects on denitrification, where areas of small depressions (riparian zone hollows) accounted for 1% of the catchment area, but >99% of the total denitrification (Duncan et al., 2013). Similarly, enhanced denitrification has been identified with periodic inundation of riparian areas (Burt et al., 2002; Gu et al., 2012, Scott et al., 2014; Shrestha et al., 2014), and in restored floodplains that created near-channel riparian areas (Kaushal et al., 2008; Roley et al., 2012a). Therefore, reconnecting agricultural ditches with their floodplains, or creating inset floodplains in the ditches themselves, could enhance inundation frequency and water level fluctuations, thereby increasing denitrification rates. This concept has been placed into practice by modifying conventional agricultural ditches into two-stage ditches (Figure 1.7).

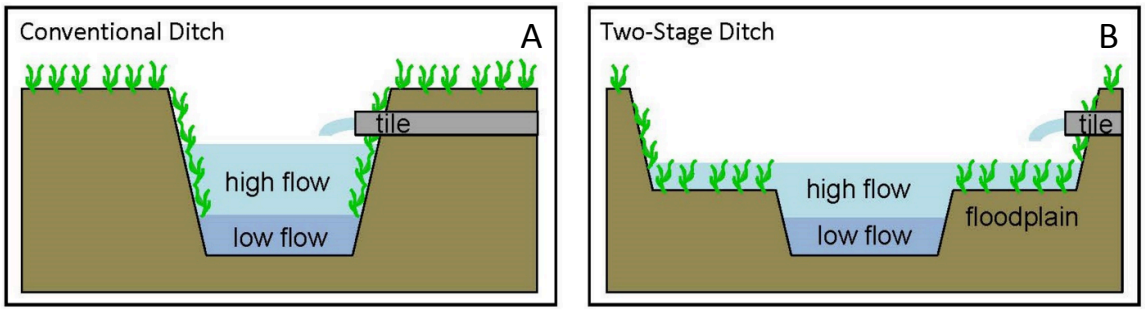

Figure 1.7. Schematic of a (A) conventional agricultural ditch and (B) a modified two-stage ditch (Powell et al., 2007).

Wetting and drying can increase denitrification rates through changes in nutrient availability and redox conditions. Initial wetting of previously dry soil can lead to a pulse release of nutrients (Baldwin and Mitchell, 2000; Corstanje and Reddy, 2004; Shenker et al., 2005). Fluctuations in water levels cause variations in redox potentials, stimulating different biogeochemical processes (Fiedler et al., 2007; Jones et al., 2014). Also, fluctuating water levels and the switch between aerobic and anaerobic conditions can lead to paired nitrification-denitrification reactions. Under dry conditions, soils are typically under aerobic conditions in the upper portion of the soil profile, where ammonia can be converted to nitrate through nitrification. When soil becomes inundated, soil pores fill with water and anaerobic conditions develop, and the newly synthesized nitrate can then be denitrified (Baldwin and Mitchell, 2000; Dong et al., 2012), leading to greater denitrification rates than if nitrification had not occurred.

1.3.3 Denitrification Genes

Functional genes encoding for enzymes used in each step in the denitrification pathway have been identified. The genes and the enzyme they encode for in order of the denitrification pathway are: *narG* or *napA* for nitrate reductase enzymes, *nirK* or *nirS* for nitrite reductase, *norB* or *cnorB* for nitric oxide reductase, and *nosZ-I* and *nosZ-II* for nitrous oxide reductase. Figure 1.8 shows each step of denitrification, the functional gene used in this dissertation, and the corresponding enzyme. Synthesis and activity of the first

enzyme in the denitrification process, nitrate reductase, is repressed by oxygen, and since all subsequent enzymes are coordinately regulated, the synthesis of all enzymes in the denitrification pathway is repressed by oxygen (Madigan et al., 2018). In literature, the *nir* and *nos* genes are the most frequently investigated in denitrification studies due to the *nir* genes being unique to denitrifiers (Zumft, 1997), and because the *nosZ* genes encodes for the final step in denitrification and therefore has implications for nitrous oxide emission. Historically, the *nosZ* gene was thought to be only associated with denitrifiers, but recent studies have found *nosZ* genes in Bacteria and Archaea that possess no other denitrification genes (Harter et al., 2017; Sanford et al., 2012). This demonstrates that denitrification is a community process, where some bacteria may only be able to complete a portion of the pathway, while others may contain all genes necessary to perform the full pathway.

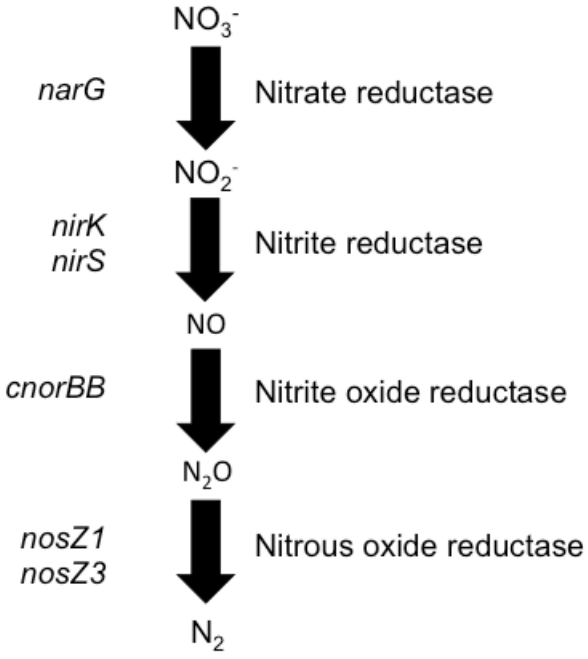

Figure 1.8. Denitrification pathway along with the corresponding functional genes quantified in this dissertation and the enzymes responsible for each step in the pathway.

The reduction of nitrite to nitric oxide is performed by either a copper-containing nitrite reductase (encoded for by *nirK*), or a cytochrome cd_1 nitrite reductase (encoded for by *nirS*). The two enzymes are evolutionarily unrelated (Zumft, 1997), and it is assumed that while the *nirS* gene is more abundant in the environment, *nirK* appears to be spread across a wider number of taxa (Decleyre et al., 2016). Previous research has shown that there is a greater co-occurrence of *nirS*, *nor*, and *nos* genes compared to *nirK*, *nor*, and *nos* (Graf et al., 2014), suggesting that denitrifiers containing *nirK* instead of *nirS* may contribute more to nitrous oxide emissions (Decleyre et al., 2016)

The gene encoding for the final step of denitrification occurs in two clades, *nosZ-1* and *nosZ-II*, and the abundances from the two clades varies among environmental conditions (Jones et al., 2013; Sanford et al., 2012). There are many pathways that can lead to the production of N_2O, but the only known biological pathway for its removal is through its reduction to N_2 catalyzed by the nitrous oxide reductase enzyme (Yoon et al., 2016). The *nosZ* gene for clade II occurs more frequently than clade I when other denitrification genes are not present, and both clades exhibit differential patterns with nitrous oxide (Yoon et al., 2016). It has also been suggested that the *nosZ-II* gene may be correlated with negative N_2O fluxes (Graf et al., 2014). In this study, *nosZ1* is used to identify *nosZ1*, and *nosZ3* represents an overlap between the two clades; *nosZ2* for the *nosZ-II* clade was not used for analysis due to unreliable results.

1.4 Methodology

While an overview of the methodology is provided in each chapter, this section provides a more detailed explanation of the methods used for potential denitrification assays and the quantification of gene abundances.

1.4.1 Denitrification Assays

Denitrification assays were performed using a modified acetylene block method (Groffman et al., 2009; Loken et al., 2016). Acetylene stops the denitrification pathway at nitrous oxide by blocking the conversion of nitrous oxide to nitrogen gas. Denitrification

rates are then quantified from the accumulation of nitrous oxide over time, which is easier to quantify than nitrogen gas due to the high atmospheric concentration of N_2.

After collecting soil cores, cores were stored at 4°C until analysis, and were analyzed within 3 days of collection (Findlay et al., 2011). For the potential denitrification assays, soil cores were homogenized and roots and rocks were removed, and 40 ± 3 g of soil was added to pre-weighed 125 mL glass Wheaton bottles. Two assays for potential denitrification were run, denitrification under site conditions (DeN) and under non-nutrient limiting conditions (DEA). For both assays, 10 mg L^{-1} chloramphenicol was added to site water to prevent de novo synthesis of microbial enzymes, to extend the liner portion of N_2O accumulation, and to reduce bottle effects (Bernot et al., 2003, Smith and Tiedje, 1979). For nutrient amended assays, nitrate as KNO_3 (100 mg N L^{-1}), carbon as glucose (40 mg C L^{-1}), and phosphorus as dihydrogen phosphate (13.84 mg P L^{-1}) was added to site water. For both assays, 40 mL of site-specific water with chloramphenicol and with or without nutrients was added to the corresponding bottles, and bottles were weighed to obtain the exact volume of liquid in the bottle (V_L). Bottles were capped and flushed with helium (He) for 5 minutes to create anoxic conditions. Acetylene (C_2H_2) was bubbled through Nanopure water to remove impurities, collected in a gas-sampling bag, 10 mL were injected into the Wheaton bottles, and bottles were allowed to rest for 20 minutes prior to the initial gas sample to allow for the C_2H_2 to diffuse into the sediment.

Gas samples were collected in 10 mL glass Agilent vials. Vials were capped using 20 mm silicone treated septa, sealed with 20 mm hold punched vial seals, and flushed for 1 minute with He. Blank sample vials were ran with every batch of samples. When measuring N_2O accumulation, 10 mL of gas was removed from each bottle using a 10 mL syringe and needed, 5 mL were ejected into the air, and 5 mL were injected into a flushed vial. Times for sample collection were recorded. After initial sample collection, bottles were placed on a rolling table to maintain slurried conditions and incubated for 2-4 hours. For a subset of bottles, periodic gas samples were collected during the incubations to ensure a linear production rate of N_2O. For these bottles, after a sample was collected, 10 mL of a 90% He 10% C_2H_2 mixture was added back to the bottles. After the final sample

was collected, bottles were uncapped, filled with water, and weighed to obtain the headspace volume (V_G) (subtracting the liquid weight, soil weight, and bottle weight from the weight of the bottle filled with water).

Gas samples were run on a Hewlett-Packard 5890 gas chromatograph (GC) equipped with an electron capture detector (ECD) and a headspace autosampler. Samples were run simultaneously to two different analytical GC columns, a capillary column (RTX-624; 30 m x 0.25 μm; 1.5 mL min^{-1} He flow rate) contained in a GC oven (40 to 275°C at 10°C min^{-1}) and that was connected to a mass spectrometer (MS; Perkin Elmer Clarus T600), and a packed column (Porapak Q, 6.4 mm x 1.8 m; Restek Corp; Bellefonte, PA) connected to a thermal conductivity sensor (TCD, 75°C) and a flame ionization detector (FID, 180°C) (Borchard et al., 2014). The flow rates for the ECD, TCD, and FID were helium at 30 ml min^{-1} and CH_4-Ar at 45 mL min^{-1}, helium at 30 ml min^{-1}, and helium at 12 mL min^{-1}, respectively.

Calculation of denitrification rates is determined from the linear accumulation of N_2O over time. N_2O concentrations measured by the GC are as ppb. Concentrations are converted to μg N_2O-N L^{-1} using the ideal gas law (Equation 1.1), where $C_{M,G}$ is the mass per volume concentration in μg N_2O-N L^{-1} headspace, C_V is the volume per volume concentration in ppb, M is the molecular weight of N in N_2O (28 μg N_2O-N per μmol of N_2O), P is the barometric pressure in atmospheres, R is the rate constant (0.08206 L atm mol^{-1} K^{-1}), and T is the air temperature in K.

$$C_{M,G} = \frac{C_V M P}{R T} \qquad \text{(Equation 1.1)}$$

The Bunsen coefficient is required to calculate total gas by accounting for gas in both the liquid and gas phase. Since the assays are done in slurried conditions, it can be assumed that N_2O in the liquid and gas phase are in equilibrium. The equation for Bunsen correction is shown in Equation 1.2, where M is the amount of N_2O in the liquid and gas phase, $C_{M,G}$ is the N_2O concentration in the gas phase (Equation 1.1), V_G is the volume

of the gas (headspace volume), V_L is the liquid volume (the amount of site-specific water added to each bottle), and B is the Bunsen coefficient (0.632 at 20°C and 0.544 at 25°C).

$$M = C_{M,G}\left(V_G + \left(V_L + B\right)\right) \qquad \text{(Equation 1.2)}$$

The amount of N_2O in the liquid and gas phase is converted to the potential denitrification rate using Equation 1.3, where DN is the denitrification rate, M_f is the final amount of N_2O, M_i is the initial amount of N_2O, D_w is the dry soil weight (amount of soil added to each bottle corrected to dry weight using the measured moisture content), and t is the incubation time.

$$DN = \frac{M_f - M_i}{D_W\ t} \qquad \text{(Equation 1.3)}$$

For this dissertation, denitrification rates were converted into an areal weight using Equation 1.4, where DN_A is the areal denitrification rate, DN is the calculated denitrification rate, ρ_b is the soil bulk density, and 5 is assuming that denitrification predominately occurs in the top 5 cm of the sediment

$$DN_A = DN(\rho_b)(5) \qquad \text{(Equation 1.4)}$$

There are several reported limitations to the acetylene block method, including the inhibition of nitrification and nitrification-denitrification, suppression of microbial respiration in the presence of C_2H_2, incomplete diffusion of C_2H_2 into sediment resulting in incomplete blockage of N_2O to N_2, and decomposition of C_2H_2 by C_2H_2-consuming microbes (Felber et al., 2012; Groffman et al., 2006; Seitzinger et al., 1993). However, over short incubation times and with the addition of chloramphenicol, denitrification rates measured using the acetylene block method are similar to other methods (Bernot et al., 2003; Roley et al., 2012a). Also, this method is appropriate when addressing denitrification hot spots and measuring potential denitrification for the comparison of

sites (Groffman et al., 2006), and for using denitrification as an indirect measure of microbial functional diversity (Cavigelli and Robertson, 2000). The research in this dissertation did not consider potential denitrification rates as exact rates of denitrification, but rather the acetylene block rates were used to compare differences in the potential rate of the soil to denitrify between sites under different environmental conditions. Using the same methodology to determine denitrification rates for all experiments and for collected soil from the field allowed for the rates of all sites to be compared. For the purposes of this dissertation, the acetylene block was an appropriate method for estimating denitrification rates.

1.4.2 Quantitative Polymerase Chain Reaction (qPCR)

Quantitative polymerase chain reaction (qPCR) was used to determine the abundances of 16S rRNA, along with six genes in the denitrification pathway (*narG*, *nirS*, *nirK*, *norB*, *nosZ1*, and *nosZ3*). Specifications for the primers, qPCR reactions, and protocols are provided in Table 1.3. Reactions were performed in 96 well plates, with each reaction volume totaling 20 µl. All reactions contained 10 µl iTaq™ Universal SYBR®Green Supermix, the amount of primer specified in Table 1.3, and enough DI water to total 15 µl. To this, 5 µl of DNA template was added to each well.

For each plate, negative controls (DNA-free water in place of DNA template), along with six known standard concentrations were run. Standards were made using gBlock gene fragments (Integrated DNA Technologies, Inc, Coralville, IA) from the primers in Table 1.3, with the exception of *nirS* for which plasmid standards were used due to the poor efficiency obtained when using the gBlock. Using the stock concentration, the size of the plasmid, and the size of the plasmid insert, standards were made for 30, 300, 3000, 30000, 300000, and 3000000 copy numbers. For qPCR, a threshold level is set, and the location where the reaction curve crosses this threshold is the C_t value, meaning the number of cycles it takes to detect a meaningful signal. Plotting the C_t values versus the logarithm of the known concentration standards provides the standard curve (Figure 1.9), which is then used to quantify the abundances of genes in the environmental samples from the samples' C_t values.

Table 1.3. qPCR specifications for each gene. Acknowledgement: Nicole Lurndahl and Dr. Ping Wang

Gene Name	Primer Set	Primer Sequence	qPCR Specifications	PCR/qPCR protocol	Ref.
BAC515F (16S rRNA)	U515F U806R	GTGCCAGCMGCCGCGGTAA GGACTACHVGGGTWTCTAAT	0.8 µl each primer	(95°C:30s, 50°C:30s, 72°C:30s) x40	(P.Wang and M.Sadowsky, not published)
cnorBB	cnorB-BF cnorB-BR	AIGTGGTCGAGAAGTGGCTCTA TCTGIACGGTGAAGATCACC	0.8 µl each primer 50 ng BSA	(95°C:30s, 60°C:30s, 72°C:30s) x46	(C. E. Dandie et al. 2007)
narG	narG_1960m2fE narG_2050m2R	TAYGTSGGGCAGGARAAACTG CGTAGAAGAAGCTGGTGCTGTT	0.5 µl each primer	(95°C:15s, 58°C:30s, 72°C:30s) x46	(López-Gutiérrez et al. 2004), (Kandeler et al. 2006)
nirK	nirK876F nirK1040R	ATYGGCGGVCAYGGCGA GCCTCGATCAGRTTRTGGTT	0.5 µl each primer	(95°C:30s, 63°C →58°C [-1°C/cycle] :30s, 72°C:30s) x51	(Bru et al. 2011; Petersen et al. 2012)
nirS	m-cd3AF m-R3cd	AACGYSAAGGARACSGG GASTTCGGRTGSGTCTTSAYGAA	2 µl each primer Plasmid standard	(95°C:30s, 63°C:58°C [-1°C/cycle] :30s, 72°C:30s, 81°C:30s) x55	(Hallin and Lingren 1999; Kandeler et al. 2009)
nosZ1	nosZ_F nosZ_1622R	CGYTGTTCMTCGACAGCCAG CGSACCTTSTTGCCSTYGCG	1.2 µl each primer	(95°C:30s, 65°C:30s, 72°C:30s) x51	(Rosch, Mergel, and Bothe 2002)
nosZ3	nosZ2F nosZ2R	CGCRACGGCAASAAGGTSMSSGT CAKRTGCAKSGCRTGGCAGAA	1.2 µl each primer	(95°C:30s, 65°C→60°C [-1°C/cycle] :30s, 72°C:30s) x51	(Bru et al. 2011; Petersen et al. 2012)

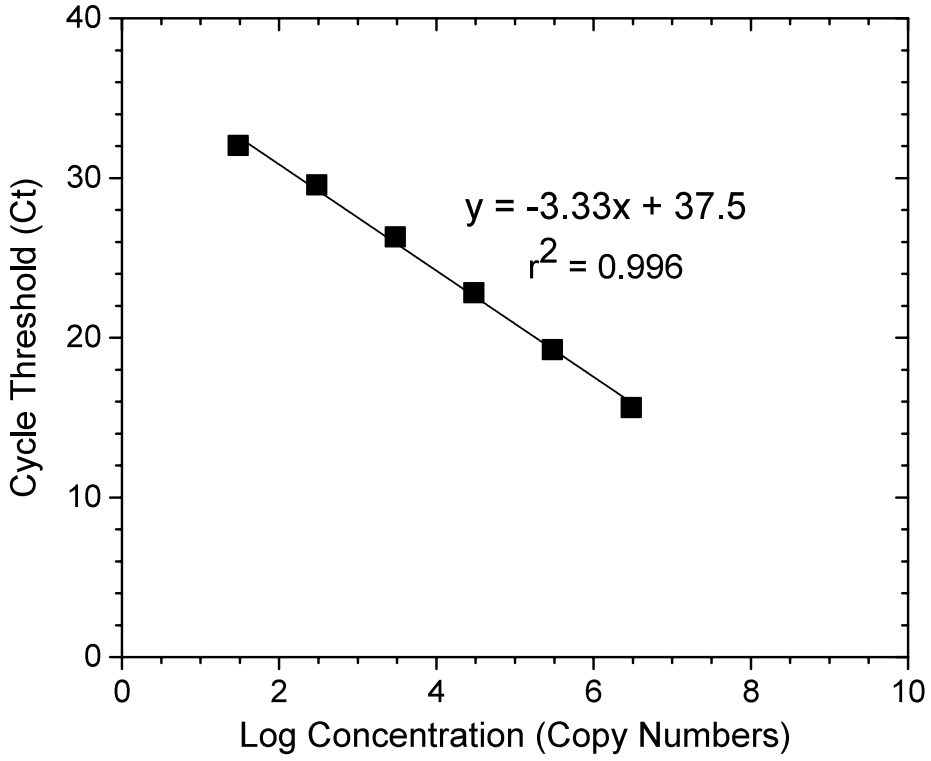

Figure 1.9. Standard curve for 16S rRNA for flume experiments (Chapter 2).

2 The Effects of Turbulence and Carbon Amendments on Nitrate Uptake and Microbial Gene Abundances in Stream Sediment

2.1 Overview

Understanding the mechanisms governing nitrate uptake in aquatic ecosystems is paramount in mitigating the negative impact of increased anthropogenic nitrogen loading on water quality. An experimental laboratory flume with agricultural sediment and carbon-amended sediment was used to evaluate the effect of turbulent fluid-flow above rough sediment on oxygen uptake, nitrate uptake, and sediment bacterial gene abundances. The transport of dissolved oxygen to the sediment scaled with the friction velocity and sediment roughness height. Results demonstrated that nitrate uptake was mediated by turbulence levels, quantified by friction velocity, above the sediment-water interface. Maximum nitrate uptake for amended and unamended sediment occurred under mid-range of friction velocities from 0.75 to 1.25 cm s^{-1}, which corresponds to Reynolds numbers from 2010 to 4320. High turbulence levels in the water column above the sediment with friction velocities larger than 1.5 cm s^{-1}, or Reynolds numbers larger than 6000, as well as low turbulence with friction velocities less than 0.50 cm s^{-1} or Reynolds numbers less than 1000, were determined to minimize nitrate uptake by the sediment. Carbon-amended sediment had approximately 100 times greater nitrate uptake fluxes compared to field-collected unamended sediment. The laboratory assays revealed that the terminal electron acceptor for denitrification in carbon-amended sediment was largely nitrous oxide rather than dinitrogen. For unamended sediment experiments, gene abundances significantly increased over the course of the experiments for mid-range friction velocities; increases were not seen in the low ($u_* = 0.51$ cm s^{-1}) and high ($u_* = 1.31$ cm s^{-1}) friction velocities. Gene abundances did not significantly increase in any experiments for carbon-amended sediment. The results of this study could provide guidance in promoting fluid-flow conditions in streams and channels to maximize nitrate uptake in agricultural watersheds by the sediment. Maintaining optimal friction velocities

could facilitate sustained nitrate uptake and reduce nitrogen loading to higher-order streams.

2.2 Introduction

Anthropogenic activity has greatly altered the global nitrogen (N) cycle over the past century. Increases in reactive nitrogen has several consequences, including alteration of biogeochemical cycling (Fowler et al., 2013; Howarth et al., 2011; Liu et al., 2013), human health effects (Powlson et al., 2008; Townsend et al., 2003; Ward et al., 2010; Wolfe and Patz, 2002), and ecological consequences (Camargo and Alonso, 2006; Compton et al., 2011; Doney, 2010; Vitousek et al., 1997). In 2017, eutrophication of the Gulf of Mexico, due predominately from N loading from the Mississippi River (Rabalais et al., 2007; Vitousek et al., 1997), was the largest size since measurements began in 1985 (NOAA, 2017), indicating that excess nitrogen loading is still a problem despite current management practices. Therefore, effective management and restoration practices are essential in mitigating the effects of anthropogenic N delivery to water bodies.

Denitrification, the microbial reduction of nitrate (NO_3^-) to nitrogen gas (N_2), and dissimilatory nitrate reduction to ammonia (DNRA) are the only known pathways in the N cycle that permanently remove reactive N from aquatic systems. Assimilation removes NO_3^- from ecosystems, but this serves as only a short-term N removal mechanism, where the assimilated N can later be remineralized and released as ammonia (NH_4^+) to the water column (O'Brien et al., 2012). For wetlands, streams, and riparian sediment, particularly in high nitrate environments, studies have shown that denitrification activity is greatest compared to the activity of other N-cycling pathways (Kim et al., 2016; Morrissey et al., 2013; Nogaro and Burgin, 2014; Scott et al., 2008; Washbourne et al., 2011; Welti et al., 2012). Denitrification rates are controlled by the interplay of several parameters, including soil organic carbon and quality and concentration (Dodla et al., 2008; Pinay et al., 2000; Perryman et al., 2011), water velocity (Arnon et al., 2007b), sediment oxygen conditions (O'Connor and Hondzo, 2008a), and nitrate concentrations (Inwood et al., 2007). Increasing sediment organic matter increases denitrification rates when nitrate concentrations are not limiting (Tomasek et al., 2017), however increases in carbon

quality (decreasing carbon to nitrogen ratio), can lead to increases in incomplete denitrification and therefore release of nitrous oxide (Huang et al., 2004).

Fluid flow velocity in a channel interacts with the streambed and channel geometry and generates turbulence in the water column. Turbulence promotes momentum fluxes towards the sediment-water interface and mediates nutrient supply to the sediment. Higher turbulence implies larger energy dissipation rates (ε) and friction velocities (u_*), and smaller Kolmogorov and Bachelor turbulence length scales (η_K, η_B,) (Jimenez, 2012, Ecke, 2005). Turbulent mixing in the water column maintains uniform dissolved oxygen (DO) and nitrate (NO_3^-) concentrations away from the sediment-water interface. In the proximity of the sediment-water interface, turbulence promotes faster transport of DO and NO_3^- to the streambed (Lorke et al., 2003; O'Connor and Hondzo, 2008a; O'Connor and Hondzo, 2008b). The previous studies have largely focused on the effect of turbulence on DO transport over a smooth sediment bed. However, this study focuses on turbulent transport over a rough sediment surface. This study expands on previous work by determining how sediment from a stream in an agriculturally-dominated watershed responds to changing turbulence conditions above the sediment-water interface, how gene abundances vary due to fluid-flow conditions, and how the availability of a high-quality carbon affects nitrate uptake rates.

This research used a recirculating flume to investigate how small-scale turbulence and oxygen diffusion affected denitrification rates under varying water velocities and with carbon amendments. The objectives of this study were (1) quantify how varying turbulence conditions effect the delivery of oxygen into sediments, (2) determine the interaction between oxygen delivery and nitrate uptake in sediments with and without a carbon amendment, and (3) evaluate how bacteria responding to differing turbulence by quantifying microbial gene abundances.

2.3 Methods

2.3.1 Experimental Setup

Experiments were conducted using a recirculating flume at the St. Anthony Falls Laboratory (SAFL), University of Minnesota. The flume is rectangular and 7.6 m long by 0.2 m wide with water depth maintained on average at 0.06 m. The inflow to the flume is located at the upstream end, and the outflow is positioned at the downstream end. The inflow and outflow locations are connected through PVC piping with a speed-controllable centrifugal pump, which was used to control the discharge of the water through the flume. Three flow straighteners (honeycombs with an approximate diameter of 5 mm) were used at the upstream end of the flume to facilitate uniform flow distribution at the flume entrance. The test section was positioned approximately 3 m downstream of the flume entrance

Sediment used for the experiment was collected from the Seven Mile Creek, Minnesota, which is located in an agriculturally dominated watershed (SMC-1, see Tomasek et al., 2017). Collected sediment was homogenized in a concrete mixer to minimize potential differences among experiments due to sediment heterogeneity in the field. After homogenization, sediment was stored in 19 L sealed buckets at 4°C. Sediment depth in the flume was 5 cm since the majority of denitrification has been shown to occur in the top 5 cm (Inwood et al., 2007). Silicone ice cube trays (5 cm x 5 cm x 5 cm) placed on the bottom of the flume were used to hold the sediment during the experiments to ensure consistent sediment depth along the length of the flume, and to minimize sediment disruption during sampling.

Each experiment was conducted for two weeks. Sediment was placed in the ice cube trays, water dechlorinated through a granular activated carbon filter was added to the flume, and the water was recirculated at a low velocity for two days before starting the experiment to equilibrate the sediments. After two days, approximately 50 L of water was drained from the flume, 13 g KNO_3^- was thoroughly mixed into the drained water, after which the water was added back to the flume. The water velocity was raised to the targeted experimental velocity, and samples were taken incrementally over the two-week

experimental duration. A Velmex BiSlide actuator and VXM stepping motor (Velmex, Inc) mounted on a sliding traverse was used to collect velocity and dissolved oxygen (DO) profiles along the flume and over the flume depth.

Carbon additions were used on a subset of the experiments to determine how carbon quality and quantity effects nitrate uptake and microbial gene abundances. Ground soybean meal (10 kg) was added to collected agricultural sediment (105 kg), the sediment was homogenized, and stored at 4°C until used. Experimental protocol for the soy-amended sediment followed the same procedure as for unamended sediment as described in the above paragraph.

2.3.2 Turbulence and Dissolved Oxygen Measurements

Water velocity was measured using an acoustic-Doppler Velocimeter (ADV) (Nortek Vectrino, Sandvika, Norway). For each experiment, velocity point measurements at known depths were collected several times over the experimental duration. Velocity measurements were collected for 2 minutes at a sampling rate of 200 Hz (0.005 s), thus generating 24,000 velocity measurements at each measuring location. The 24,000 measurements were time-averaged to determine a single velocity at each location. Sampling depths for the velocity measurements were controlled using the Velmex controller. The depth-averaged velocity (U) was determined by integrating the velocity profiles and normalizing by water depth. The Reynolds number for each flow was calculated using $Re = (UR_H)/\nu$, where R_H is the hydraulic radius, and ν is the temperature-adjusted kinematic viscosity of a fluid. Shear velocities (u_*), or the vertical flux of momentum from the water column to the sediment-water interface, were quantified using the scaling relationship between time-averaged water velocity and the natural logarithm of the corresponding depth (Biron et al., 2004; Schlicting, 1987).

Turbulence parameters were also calculated from collected velocity measurements. Energy dissipation (ε) was obtained using the log-law estimation by Equation 2.1, which has been shown to be similar to other methods for estimation (O'Connor and Hondzo, 2008b), where u_* is shear velocity, k is the von Karman constant, and y is the difference between the upper and lower limit of the log-law depth used to

find u_*. The Kolmogorov (η_K) and Batchelor scales (η_B) were quantified using Equation 2.2 and 2.3, respectively.

$$\varepsilon = \frac{u_*^{\,3}}{\kappa y} \qquad \text{(Equation 2.1)}$$

$$\eta_K = \left(\frac{\nu^3}{\varepsilon}\right)^{1/4} \qquad \text{(Equation 2.2)}$$

$$\eta_B = \left(\frac{D^2\nu}{\varepsilon}\right)^{1/4} \qquad \text{(Equation 2.3)}$$

DO microprofiles were collected several times during each experimental run. DO was measured at known depths in the water column and in the sediment using an optical DO sensor (PreSens, Precision Sensing). The sensor has a spatial resolution of 0.05 mm and a response time of less than 3 s. For point measurements, the depth of the sensor was adjusted, and DO concentrations were recorded for at least 2 minutes after DO concentrations had stabilized. Each measuring point is the average of DO concentrations for at least 360 data points.

DO delivery to sediments can be estimated by using Fick's First Law and the thin-film theory (O'Connor and Hondzo, 2008b) (Equations 2.4 and 2.5), where J is the DO flux to the sediment, D is molecular diffusion coefficient, δ_c is the diffusive sublayer thickness (DSL), C_B is the DO concentration of the bulk water above the sediment, and C_S is the DO concentration at the sediment-water interface. The DSL thickness can be quantified by combining Equations 2.4 and 2.5 and solving for δ_c (Equation 2.6).

$$J = \frac{-D}{\delta_C}\left(C_B - C_S\right) \qquad \text{(Equation 2.4)}$$

$$J = -D\left(\frac{dC}{dy}\right)\Bigg|_{y=0} \qquad \text{(Equation 2.5)}$$

$$\delta_C = \frac{\left(C_B - C_S\right)}{\left.\frac{dC}{dy}\right|_{y=0}} \qquad \text{(Equation 2.6)}$$

2.3.3 Soil Parameters and Nitrate Flux

Soil water content, bulk density, and organic matter were quantified for the experiments. A 60 mL syringe with the end cut off was used to collect a sediment core, the volume of the sediment was measured, the sediment was weighed, and dried for 24 h or until the weight did not change. The dry weight was then recorded and normalized by the sediment volume to obtain the soil bulk density. Dried soil was ground with a mortal and pestle, passed through a 2 mm sieve, and 5 g was weighed into a crucible and combusted at 550°C for 4 h. The muffled weight was recorded and normalized by the dry weight to obtain the soil organic matter (Heiri et al., 2001).

Water samples were collected over the experimental duration to quantify nitrate concentrations. Samples were filtered using pre-combusted Whatman 0.7 μm GF/F filters and analyzed on a Lachat QC800 Autoanalyzer (Hach Company) using the cadmium reduction method (Kazemzadeh and Ensafi, 2001). Nitrate uptake was linear over time, and uptake fluxes were calculated according to Equation 2.7, where J_{NO3} is nitrate flux, C_{NO3} is nitrate concentration, t is time, V_W is volume of water, and A_S is surface area of the sediment.

$$J_{NO3} = \frac{V_W}{A_S}\left(\frac{dC_{NO3}}{dt}\right) \qquad \text{(Equation 2.7)}$$

Potential denitrification rates under flume conditions (DeN) with nitrate addition and non-nutrient limiting conditions (DEA) were calculated on a subset of the experiments. For determining DeN and DEA rates at initial conditions (pre), sediment was placed in the flume, left for the two-day equilibration period, and removed immediately prior to starting the experiment. For post experimental conditions (post), sediment was collected at the end of the two-week experimental duration. DeN and DEA rates were calculated using a modified acetylene block method (Groffman et al., 2009;

Loken et al., 2016), where acetylene is used to block denitrification at N_2O. For both DeN and DEA, chloramphenicol (10 mg L^{-1}) was added to stop de novo protein synthesis and to extend the linear period of N_2O accumulation (Tiedje et al., 1989). Nitrate additions (100 mg N L^{-1} as potassium nitrate) were added to DeN assays to account for the variable nitrate concentrations between experiments. For DEA assays, nitrate (100 mg N L^{-1} as potassium nitrate), carbon (40 mg C L^{-1} as glucose), and phosphate (13.84 mg P L^{-1} as potassium dihydrogen phosphate) were added to flume water. A gas chromatograph (5890 series II, Hewlett-Packard) equipped with an electron capture headspace autosampler (Hewlett-Packard 7694) was used to measure N_2O accumulation over time, and rates were corrected using the Bunsen solubility coefficient (Tiedje, 1982). Areal rates for denitrification were calculated by normalizing DeN and DEA rates by the bulk density and assuming that most denitrification occurs in the top 5 cm of sediment (Arango et al., 2007, Inwood et al., 2007). DeN and DEA rates measure the combination of incomplete and complete denitrification. Incomplete denitrification rates were calculated concurrently with DeN and DEA rates using the same method as described above except without the addition of acetylene.

2.3.4 Microbial Gene Abundances

Abundances of three genes, 16S rRNA, *nirS*, and *nosZ3* were quantified over the duration of the 2-week experiments for a subset of experimental runs. Samples were collected in an autoclaved 10 mL syringe with the end cut off, and immediately transferred to a -20°C freezer. DNA was extracted from 0.5 g collected sediment using DNeasy PowerSoil Kits (QIAGEN, Germany) following the manufacturers protocol. Abundances were quantified using qPCR on an ABI Prism 7500 Fast Real-Time PCR System (Applied Biosystems). The specific primers used were U515F and U806R (BAC515F) for 16S rRNA (Wang and Qian, 2009), m-cd3AF and m-R3cd for *nirS* (Rosch et al., 2002), and nosZ2F and nosZ2R for *nosZ3* (Bru et al., 2011). Gene copy numbers were normalized by the moisture content to obtain the number of copy numbers per gram of dry soil. The qPCR efficiencies for all genes ranged from 80% to 110% with R^2 values over 0.99 for all calibration curves.

2.3.5 Continuous Flume Experiment with Different Carbon Amendments

The same flume as described above was used to determine denitrification rates for three sediment types and four velocities, along with a stagnant control condition. Sediment and water were collected from the agricultural ditch at SMC-1 in the Seven Mile Creek watershed. Sediment was homogenized and split into three types, one that was left as collected (the control sediment), one that was amended with ground corn stover collected from a field in Minnesota, and one amended with ground soybean meal. Field collected sediment was augmented to 10% organic carbon for the amended experiments.

Experimental setup was similar to the experiment described above. Ice cube trays were used to divide the three sediment treatments. Each tray contains six 5x5x5 cm compartments, and 12 trays were used for each sediment type. Trays were placed in a randomly generated orientation. Once sediment was in place, the flume was filled with the field-collected water using a peristaltic pump at a rate of 1 L min^{-1}. Initial water depth was 5 cm, which represented approximately 45 gallons of field-collected water. Water depth was adjusted by adding spiked deionized water at the beginning of every new flow rate to maintain this depth. Water was spiked to a concentration of 10 mg $N\text{-}NO_3^-$ L^{-1}.

Each velocity was run for 2 weeks. The water was then drained, sediment was collected to determine denitrification potential, the flume was refilled with the drained water, and a new velocity was started. Horizontal and vertical velocity profiles were collected over each sediment type using an ADV. Similarly, DO profiles were collected for each sediment type.

2.3.6 Statistics

Statistical analysis was performed using Jmp Version 13.0 (SAS Institute Inc.). Regressions were used to determine significant (α = 0.05) relationships between flow conditions, turbulence scales, and nitrate uptake. The significance level was set as α = 0.05 for all analysis. ANOVA analyses were used to determine the correlation between flow conditions and gene abundances. Tukey's post-hoc tests were used for ANOVA analyses that were significant.

2.4 Results

2.4.1 Velocity and Dissolved Oxygen Measurements

Fourteen independent experiments were conducted at specified fluid-flow conditions in the experimental flume. Depth-averaged velocities for the unamended experiments ranged from 2.8 to 16.8 cm s^{-1}, and from 5.3 to 15.5 cm s^{-1} for the soy-amended experiments (Table 2.1). The flow in the flume was in the turbulent regime with a range of Reynolds numbers form 1070 to 6090. In the proximity of the sediment-water interface, the longitudinal time-averaged velocities followed the turbulent log-law velocity profile typical for a rough sediment surface (Figure 2.1) by Equation 2.8, where κ is the von Karman constant, k_s is the average sediment roughness height, u_* is the friction velocity, and B is the additive constant.

$$\frac{u}{u_*} = \frac{1}{\kappa}\ln\left(\frac{y}{k_s}\right) + B \qquad \text{(Equation 2.8)}$$

The slope of the time-averaged velocities versus the natural logarithm of depth with coefficients of determinations of at least 89% was used to estimate u_* (Table 2.1). The viscous sublayer thickness (δ_v) at the sediment-water interface was determined using Equation 2.9, where ν is the temperature-adjusted kinematic viscosity. The δ_v ranged from 0.7 to 2.2 mm, while the k_s ranged from 3 to 7 mm. Since $k_s/\ \delta_v > 1$, the roughness elements interacted directly with the turbulent velocities in the proximity of the sediment. The roughness Reynolds numbers, Re_* (Equation 2.10) ranged from 30 to 130, indicating turbulent flow over completely rough surface ($Re_* > 60$) and transitionally rough conditions ($Re_* < 60$) in the flume (Schlicting, 1987).

$$\delta_\nu \approx 11\frac{\nu}{u_*} \qquad \text{(Equation 2.9)}$$

$$Re_* = \frac{u_* k_s}{\nu} \qquad \text{(Equation 2.10)}$$

The Kolmogorov length scale, η_K, is the smallest length scale where inertial forces still dominate over viscous forces, and the Batchelor length scale, η_B, is where scalar (dissolved oxygen) fluctuations are dampened out by molecular diffusion in a turbulent flow (Table 2.1). The Batchelor length scale ranged from 0.009 to 0.02 mm, and was much smaller than the average sediment roughness height of 5 mm. Since $k_s / \eta_B >> 1$, the roughness of the sediment dominated the gradients of DO in the proximity of the sediment.

Eleven DO microprofiles were collected for different fluid flow conditions above and into the sediment using two different carbon concentrations (unamended and soy-amended). For each DO profile, the sediment-water interface was detected from the change in the DO gradient due to the different diffusion coefficients in the water and sediment. Figure 2.2 displays three representative DO profiles for unamended sediment and three profiles for soy-amended sediment under similar fluid-flow conditions in the flume. DO concentrations decreased towards the sediment due to the DO uptake by the sediment. In this region, DO distribution approaches a straight line and intersects the bulk time-averaged concentration (C_B) at the vertical distance (δ_C) above the sediment-water interface. The δ_C is the DSL thickness and is estimated using Equation 2.6 for each DO profile (Table 2.1). In general, δ_C decreases with increasing Reynolds number or friction velocity. A scaling relationship between the δ_C and Re_* is depicted in Figure 2.3. The plot indicates a power law scaling where δ_C decreases with increasing Re_* ($\delta_C \sim Re_*^{-7/5}$). As outlined in Equation 2.4, smaller δ_C implies higher DO flux into the sediment for a given concentration difference ($C_B - C_S$) above the sediment.

Table 2.1. Fluid-flow conditions for unamended and amended sediment experiments. U is the depth-averaged velocity, u_* is the friction velocity, Re is the dimensionless Reynolds number based on U and the hydraulic radius, ε is the energy dissipation rate, η_K is the Kolmogorov length scale, η_B is the Batchelor length scale, δ_C is diffusive sublayer thickness, and T is the temperature of the water during each experimental.

Type	U (cm s^{-1})	u_* (cm s^{-1})	Re	ε (m^2 s^{-3})	η_K (mm)	η_B (mm)	δ_C	T (°C)
Unam.	2.77	0.51	1070	3.06E-05	0.423	0.0196	0.98	20.5
Unam.	3.12	0.69	1200	3.61E-05	0.413	0.0187	1.15	19.7
Unam.	4.52	0.60	1690	2.10E-05	0.485	0.0213	2.12	18.7
Unam.	5.16	0.75	2010	1.04E-04	0.318	0.0144	1.17	19.6
Unam.	9.74	1.04	2690	2.30E-04	0.256	0.0118	0.78	20.5
Unam.	11.4	1.02	4700	1.76E-04	0.263	0.0129	0.61	22.9
Unam.	11.7	1.24	4320	2.40E-04	0.252	0.0117	0.24	20.8
Unam.	12.6	1.38	5410	4.20E-04	0.219	0.0102		20.7
Unam.	16.8	1.31	6090	2.38E-04	0.248	0.0119	0.23	21.8
Soy	5.31	0.67	1560	7.33E-05	0.381	0.0153	0.90	15.9
Soy	6.25	0.74	2210	1.02E-04	0.332	0.0143	0.55	18.1
Soy	13.2	1.12	5180	2.99E-04	0.234	0.0112		21.9
Soy	15.5	1.53	5380	5.76E-04	0.185	0.009	0.18	22.7

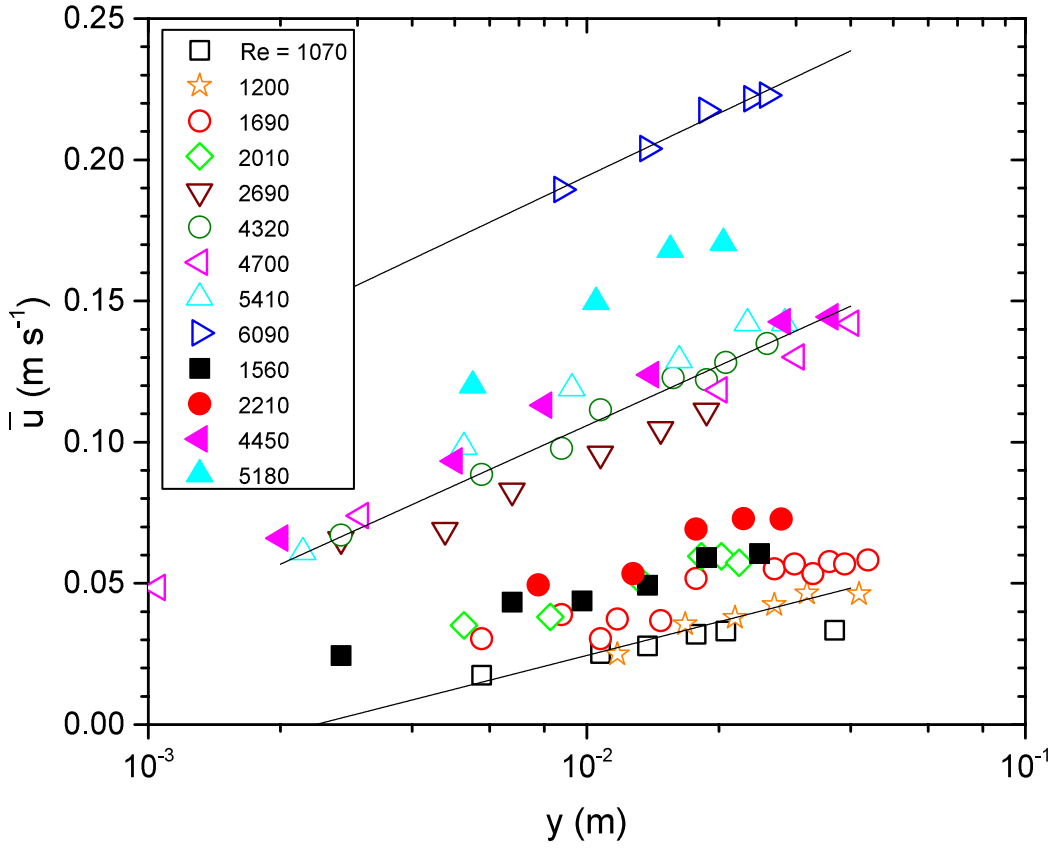

Figure 2.1. Time-averaged velocities (ū) at multiple corresponding depths from the sediment-water interface upward (y) for experiments. Points shown represent the velocity data that depicted the log-law velocity distribution above the sediment-water interface. The three linear lines are examples of lines of best fit for the velocity data profiles at Re = 1200, 4320, and 6090. The slope of each line was used to determine the corresponding friction velocity (u_*).

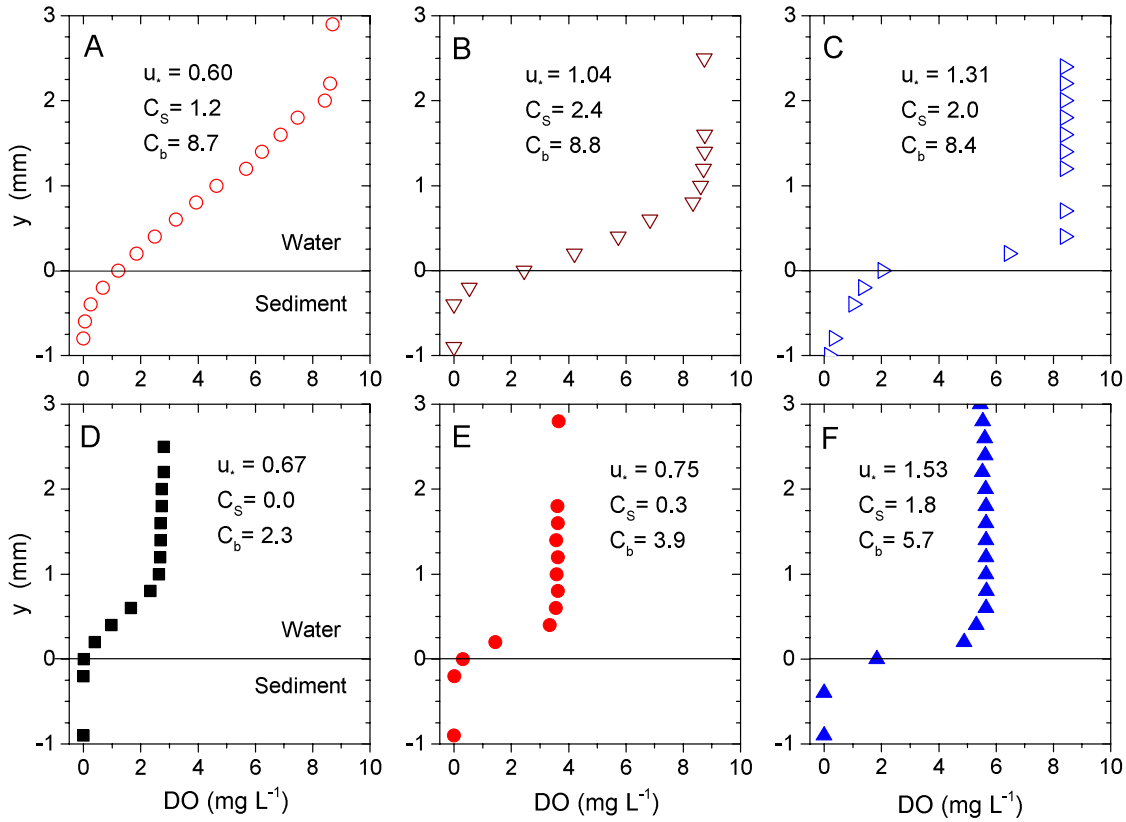

Figure 2.2. Time-averaged dissolved oxygen (DO) profiles for unamended sediment under (A) low friction velocity, (B) mid-range friction velocity, and (C) high friction velocity, and for soy-amended sediment under (D) low friction velocity, (E) mid-range friction velocity, and (F) high friction velocity, where y is the vertical distance from the sediment-water interface, C_S is the DO concentration at the sediment-water interface, and C_B is the bulk DO concentration.

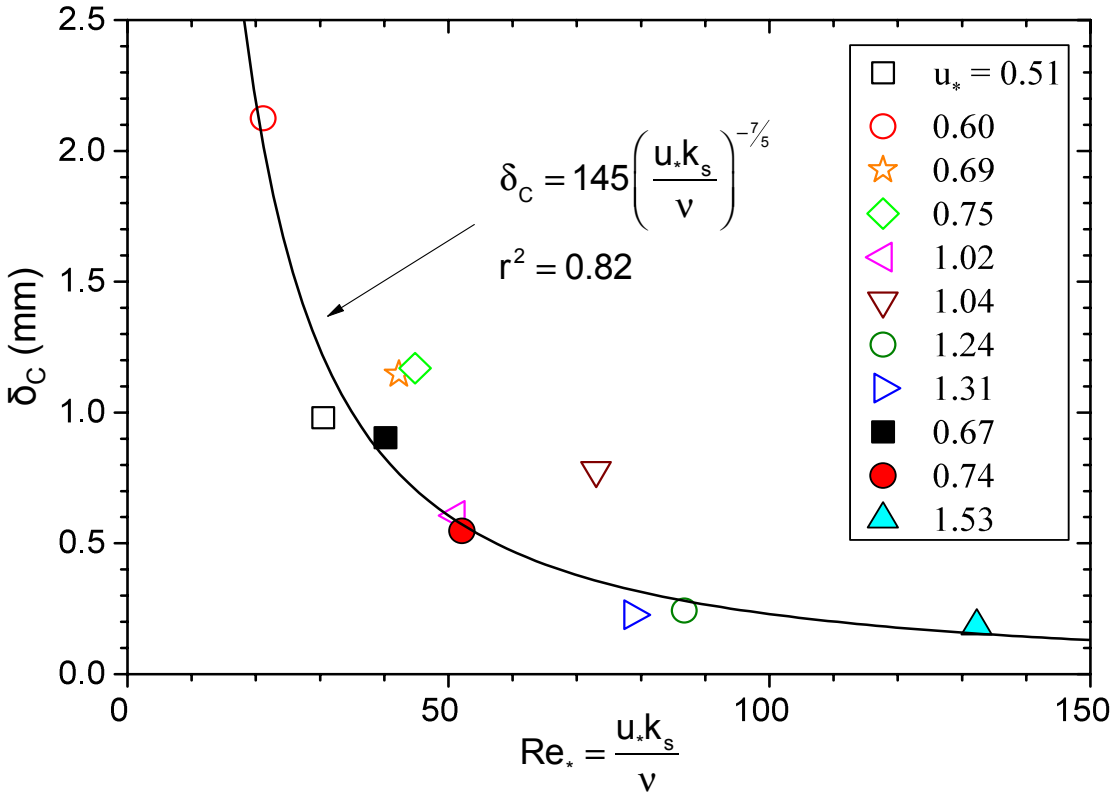

Figure 2.3. Diffusive sublayer thickness (δ_C) versus the roughness Reynolds number (Re_*). The equation shown displays the power law decay of δ_C with increasing roughness Reynolds number.

2.4.2 Effect of Turbulence and Carbon Amendment on Nitrate Uptake

Soy-amended sediment had greater sediment organic matter than unamended sediment (average of 8.2% and 2.1%, respectively). In addition, the soy-amended sediment had lower bulk density than unamended sediment (0.90 and 1.38 g cm^{-3}). Water nitrate concentrations at the beginning of the independent experiments ranged from 9.21 to 11.5 mg $N\text{-}NO_3^-$ L^{-1} for unamended experiments and 8.81 to 12.2 mg $N\text{-}NO_3^-$ L^{-1} for soy-amended experiments. Nitrate uptake was zero-order over time, and linear regressions were used to determine the uptake rate (Figure 4). Fitted regressions were significant (α = 0.05) for all experiments except for unamended sediment with friction velocities (u_*) of 1.24 and 1.38. These experiments also had the lowest uptake rates. Nitrate flux rates were

determined using the uptake rate as determined by the regressions $\left(\frac{dC_{NO3}}{dt}\right)$ in Equation 2.7.

Final concentrations at the end of the experiments differed based on the friction velocity. For soy-amended experiments, nitrate concentrations in the water column were below the minimum detection limit (0.01 mg $N\text{-}NO_3^-$ L^{-1}) by the end of all experiments. Figure 2.4 shows the change in nitrate concentrations over time for a subset of unamended and soy-amended experiments, where C/C_0 is the nitrate concentration at the time since the start of the experiment normalized with the nitrate concentration at the beginning of the experiment (C_0). Nitrate uptake was very low, almost zero, for the experiment with the most intensive turbulence (u_* = 1.24 cm s^{-1}), followed by the experiment with smallest turbulence level (u_* = 0.5) for the unamended runs. Nitrate uptake in the soy-amended experimental runs was much faster than for unamended, with slowest uptake in the experiment with the lowest turbulence level (u_* = 0.74), followed by the greatest turbulence level (u_* = 1.53 cm s^{-1}). Nitrate for the mid-range friction velocity (u_* = 1.18 cm s^{-1}) soy-amended experiment was almost immediately uptaken, with only two time periods having nitrate concentrations above the minimum detection limit.

Maximum nitrate uptake occurred when friction velocities ranged from 0.75 to 1.1 cm s^{-1} (corresponding to Reynolds numbers from 2010 to 4700) for unamended sediment, and from 1.0 to 1.25 cm s^{-1} (corresponding to a Reynolds number of 5180 to 5380) for soy-amended sediment (Figure 2.5). Nitrate fluxes for soy-amended sediment experiments were nearly 100 times greater than for unamended sediment. Overall, maximum nitrate uptake occurred at mid-range friction velocities from 0.75 to 1.25 cm s^{-1} (corresponding to a Reynolds number from 2010 to 4320). High-friction velocities, larger than 1.5 cm s^{-1} (Reynolds number greater than 5000), and low-friction velocities, smaller than 0.50 cm s^{-1} (Reynolds number smaller than 1000), minimized nitrate uptake by the sediment. There was no nitrate uptake quantified in the experiment with the highest friction velocity (u_* = 1.38 cm s^{-1}).

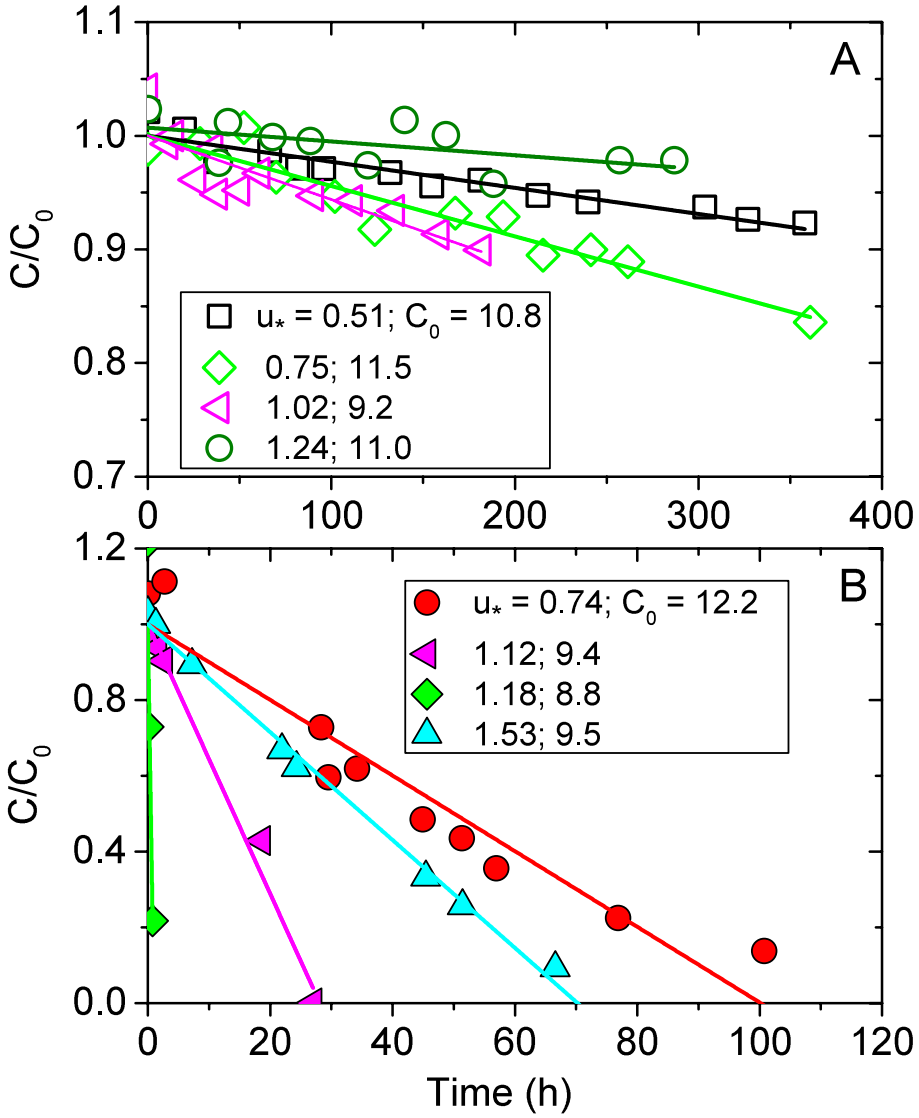

Figure 2.4. Time series of nitrate concentration in the flume (C) normalized by the nitrate concentration at the beginning (t = 0) of the experiment (C_0) for a subset of (A) a unamended sediment, and (B) soy-amended sediment experiments. The slopes of the straight lines indicate the corresponding rate of change of nitrate in the water column $\left(\frac{dC_{NO3}}{dt}\right)$.

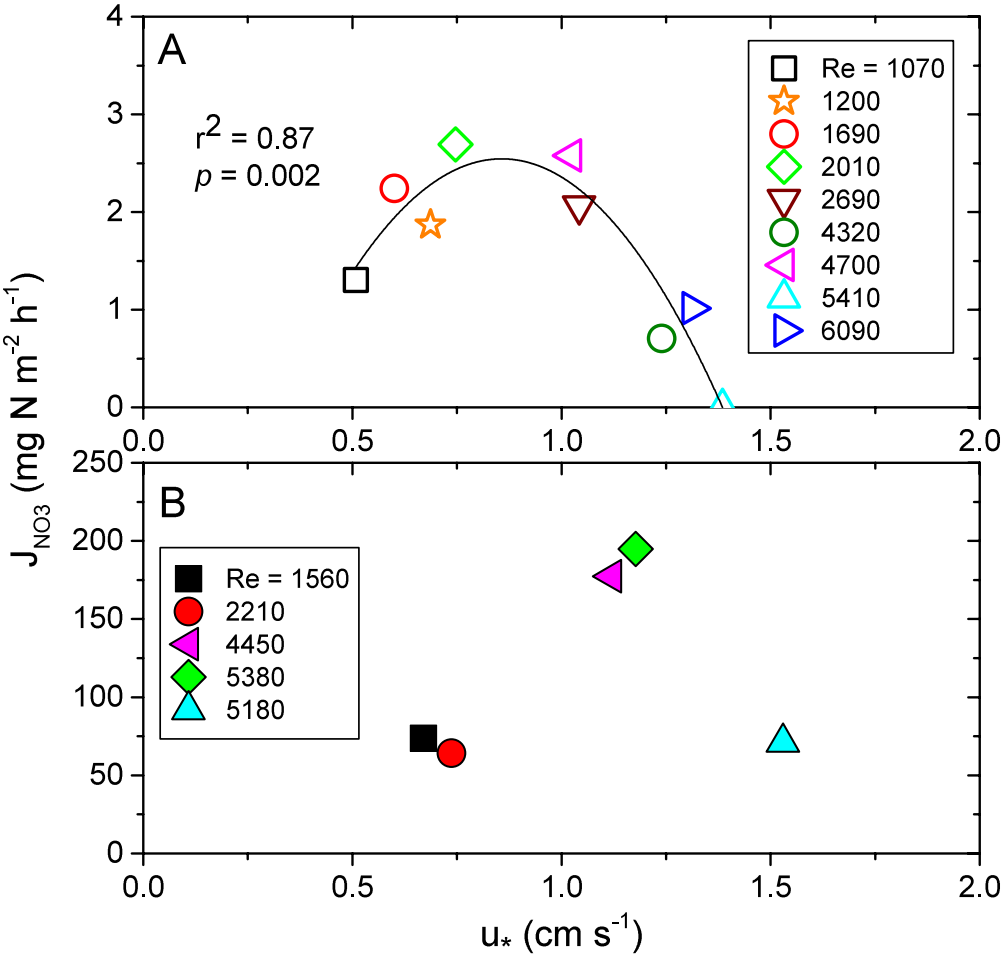

Figure 2.5. Nitrate flux (J_{NO3}) verses friction velocity (u_*) for (A) unamended sediment, and (B) soy-amended sediment at the corresponding Reynolds numbers and friction velocities in the flume.

2.4.3 Comparison Between Denitrification Potential and Nitrate Flux

Potential denitrification rates quantified using the acetylene block method were compared to nitrate fluxes as measured directly from nitrate consumption over time in the experimental flume. Table 2.2 shows direct nitrate fluxes (J_{NO3}), with complete and incomplete potential denitrification rates for assays with acetylene (C_2H_2) and nitrate added (DeN C_2H_2 in table), complete and incomplete denitrification for assays with nitrate, phosphate, and glucose added (DEA C_2H_2 in table), incomplete potential

denitrification rates as measured by assays without C_2H_2 (DeN and DEA no C_2H_2 in table), and the ratio of incomplete to incomplete plus complete denitrification (N_2O yield). While soy-amended sediment had much greater J_{NO3} rates, DeN and DEA rates were similar for unamended and soy-amended sediment. However, N_2O yield of the soy-amended sediment was much greater than the unamended sediment.

Table 2.2. Uptake variables for a subset of unamended and soy-amended sediment experimental runs. Re is the Reynolds number, time is whether soil cores were taken before or after the 2-week experiment, and u_* is the friction velocity. J_{NO3} is the nitrate flux as measured from flume nitrate concentrations over time. DeN C_2H_2 is denitrification potential with acetylene (C_2H_2) as an indicator for complete and incomplete denitrification for assays with flume water spiked with nitrate. DEA C_2H_2 is potential complete and incomplete denitrification for assays with flume water spiked with nitrate, phosphate, and glucose. DeN No C_2H_2 is potential incomplete denitrification for assays with flume water spiked with nitrate. DEA No C_2H_2 is potential incomplete denitrification for assays with flume water spiked with nitrate, phosphate, and glucose. N_2O yield is the ratio of incomplete to incomplete and complete denitrification for DeN and DEA assays.

Type	Re	Time	u_* (m s^{-1})	J_{NO3} (mg N m^{-2} h^{-1})	DeN C_2H_2 (mg N m^{-2} h^{-1})	DEA C_2H_2 (mg N m^{-2} h^{-1})	DeN No C_2H_2 (mg N m^{-2} h^{-1})	DEA No C_2H_2 (mg N m^{-2} h^{-1})	N_2O Yield DeN	N_2O Yield DEA
Unam.	1070	Post	0.51	1.30	28.3	37.4	3.0	4.1	11%	11%
Unam.	1690	Pre	0.60	2.24	42.9	53.1	1.0	12.7	2%	24%
Unam.	1690	Post	0.60	2.24	26.0	36.3	0.9	4.6	4%	13%
Unam.	2010	Pre	0.75	2.69	36.4	44.9	2.6	0.2	7%	0.4%
Unam.	2690	Pre	1.04	2.06	48.8	63.6	2.1	13.0	4%	21%
Unam.	2690	Post	1.04	2.06	35.1	43.4	1.1	5.4	3%	12%
Unam.	4700	Pre	1.02	2.58	44.7	51.4	3.2	4.3	7%	8%
Unam.	6090	Pre	1.31	1.04	30.0	37.8	1.0	7.3	4%	20%
Unam.	6090	Post	1.31	1.04	35.5	45.3	1.0	6.5	3%	14%
Soy	1560	Post	0.67	73.8	23.7	22.4	21.1	22.5	89%	101%
Soy	2210	Pre	0.74	64.2	34.1	33.1	28.5	33.5	84%	101%
Soy	2210	Post	0.74	64.2	17.4	19.8	15.0	15.3	86%	77%
Soy	4450	Post	1.18	195	NA	34.8	NA	26.4	NA	76%

Nitrate uptake, as measured by the acetylene block method (denitrification potential), and from direct measurements of nitrate concentration of flume water over time (J_{NO3}) is shown in Figure 2.6. The closed symbols represent potential denitrification assays run with flume water amended with nitrate (DeN), and open symbols represent assays with nitrate, carbon, and phosphate added (DEA). Both DeN and DEA rates were over an order of magnitude greater than J_{NO3} rates. The trend between J_{NO3} and DeN was not significant ($r^2 = 0.29$, $p = 0.14$). Similarly, the trend between DEA and J_{NO3} was also not significant ($r^2 = 0.34$, $p = 0.10$. Since there is not a significant trend between J_{NO3} and either DeN or DEA, differences in nitrate uptake for the individual experiments cannot solely be attributed to differences in sediment characteristics (differences in the potential of the soil to denitrify) between experiments.

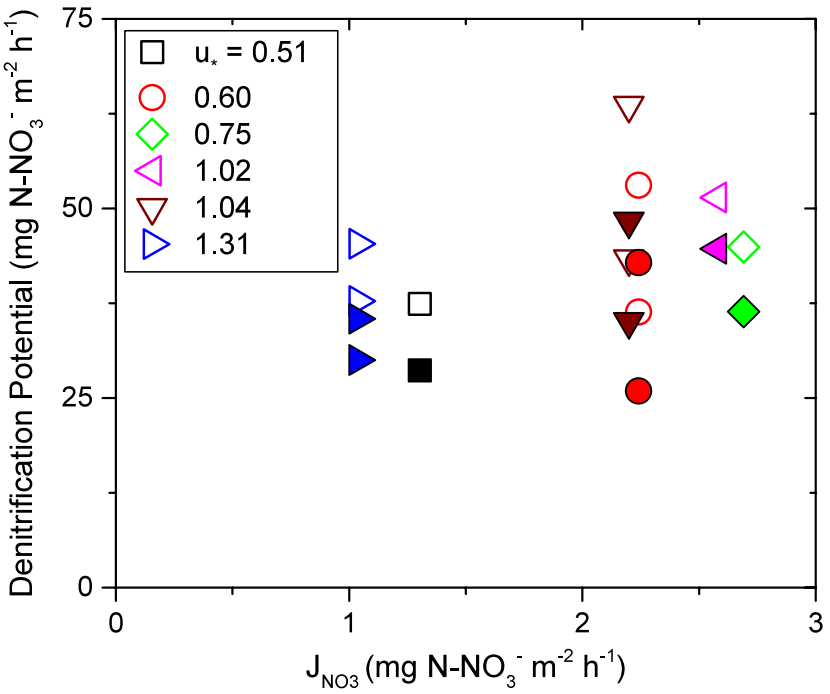

Figure 2.6. Comparison of nitrate uptake rates as measured by the acetylene block method (denitrification potential) and from direct nitrate measurements over time (J_{NO3}). Closed symbols represent rates for flume water with nitrate added, and open symbols represent rates for flume water with nitrate, phosphate, and glucose added. All symbols represent the average potential denitrification of the triplicate assays.

2.4.4 Microbial Gene Abundances Under Varying Turbulence

Gene abundances over the experimental duration for 8 experiments, and with 4 different Reynolds numbers for unamended and soy-amended sediment, are shown in Figure 2.7. For the unamended runs, the significantly lowest gene abundances were on the first day of the start of the experiment for the mid-range friction velocities of 0.75 and 1.04 cm s^{-1} for 16S rRNA (p = 0.001 and p = 0.035, respectively), *nirS* (p = 0.005 and p = 0.05, respectively) and *nosZ3* (p = 0.001 and p = 0.032, respectively). For the experiment with the lowest friction velocity for unamended runs (0.5 cm s^{-1}), abundances of *nosZ3* were significantly lowest on the first day of the experiment and on day 12 (p = 0.002). Gene abundances for *nirS* decreased over time in soy-amended sediment for the experiment with a friction velocity of 0.67 cm s^{-1} (p = 0.01). Similarly, gene abundances of *nosZ3* in soy-amended sediment decreased over time in the experiment with a friction velocity of 0.74 cm s^{-1}. There were no other significant relationships for gene abundances in unamended sediment for the experiment with a low friction velocity (u_* = 0.51 cm s^{-1}) or high friction velocity (u_* = 1.31 cm s^{-1}), or for soy-amended sediment experiments. Gene abundances were significantly greater in soy-amended sediment compared to unamended sediment for 16S rRNA ($p < 0.001$) and *nosZ3* (p = 0.008), but not for *nirS*.

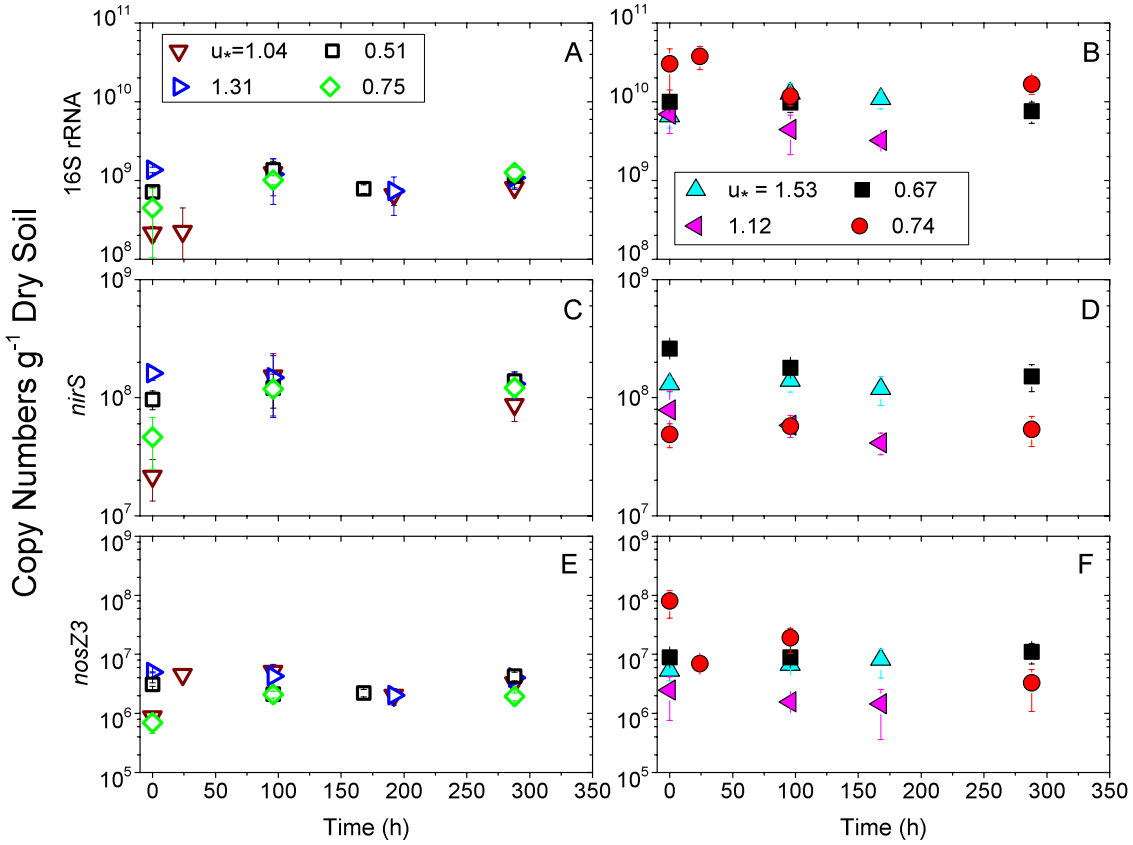

Figure 2.7. Gene abundances as copy numbers per gram of dry soil in unamended sediment for (A) 16S rRNA, (C) *nirS*, and (E) *nosZ3*, and in soy-amended for (B) 16S rRNA, (D) *nirS,* and (F) *nosZ3* under varying fluid-flow conditions. Symbols represent the average of the triplicate samples and error bars represent ± the standard deviation.

2.4.5 Continuous Flume Experiment

The three sediment types exhibited different patterns in denitrification rates. DEA rates were greatest in the soy-amended sediment, but all three sediments had similar DeN rates. Soy-amended sediment had the greatest DEA rates after the 5 cm s^{-1} experimental run, whereas corn-amended sediment increased with increasing velocity (Figure 2.8). Denitrification rates as measured by the decrease in nitrate concentrations over time were second order and were greatest for the two lower velocities. Since the experiments were run in order of increasing order and with the same sediment throughout the entire

duration of the experiment, time also could have been a factor in the differential denitrification rates.

Biofilm growth occurred on the surface of the soy and corn-amended sediment, but was absent from the control sediment (Figure 2.10). The biofilm growth affected both velocity flows and dissolved oxygen profiles for the amended sediment. Flow patterns became increasingly different with faster velocities, which was also longer into the experimental duration where biofilm had more time to develop (Figure 2.11, Figure 2.12, and Figure 2.13). The biofilm for the corn-amended sediment was thicker than the soy-amended, causing a smaller water depth above the corn treatments, and resulting in faster flows over the corn treatments. DO profiles for the amended sediment turned anoxic in the biofilm before reaching the sediment (Figure 2.14). The biofilm of the corn-amended sediment was thicker than for the soy-amended, and DO decreased rapidly from the water column into the biofilm.

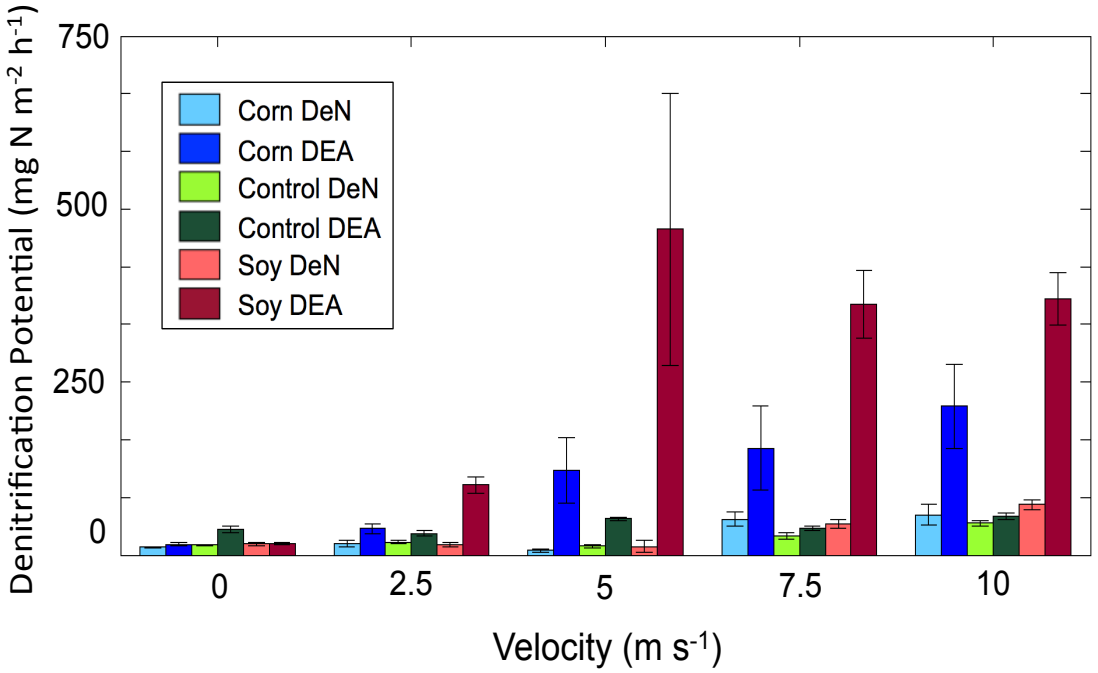

Figure 2.8. Denitrification potential under flume conditions (DeN) and with non-nutrient limiting conditions (DEA) using the acetylene block method for the three sediment types, the stagnant control velocity, and four velocity experiments.

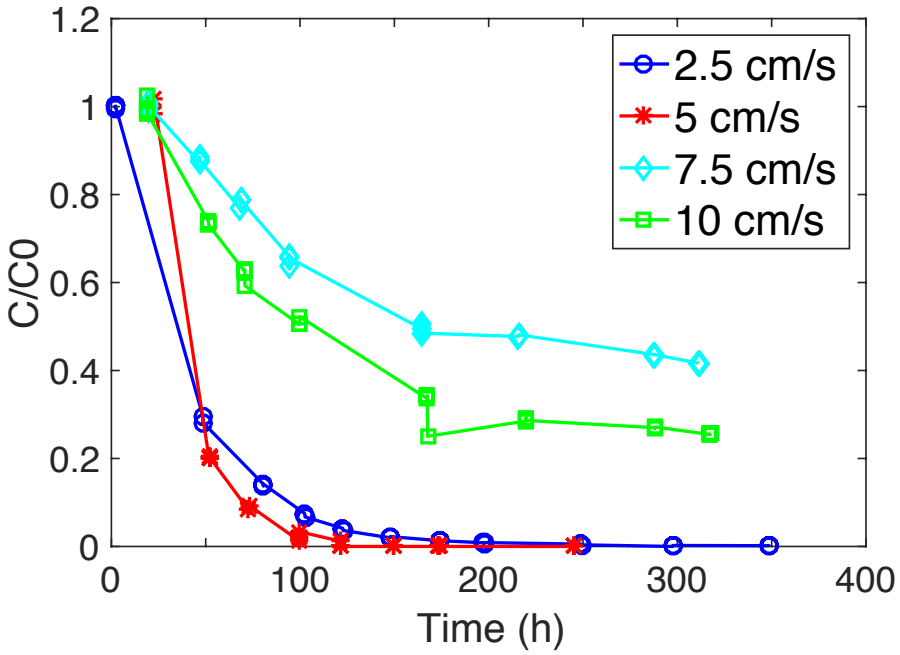

Figure 2.9. Nitrate concentration over time for the four experimental flume velocities.

Figure 2.10. Biofilm formation over each sediment type. Soy and corn amended sediment each had a visibly distinct biofilm growing on the sediment surface, whereas there was no biofilm formation on the control sediment.

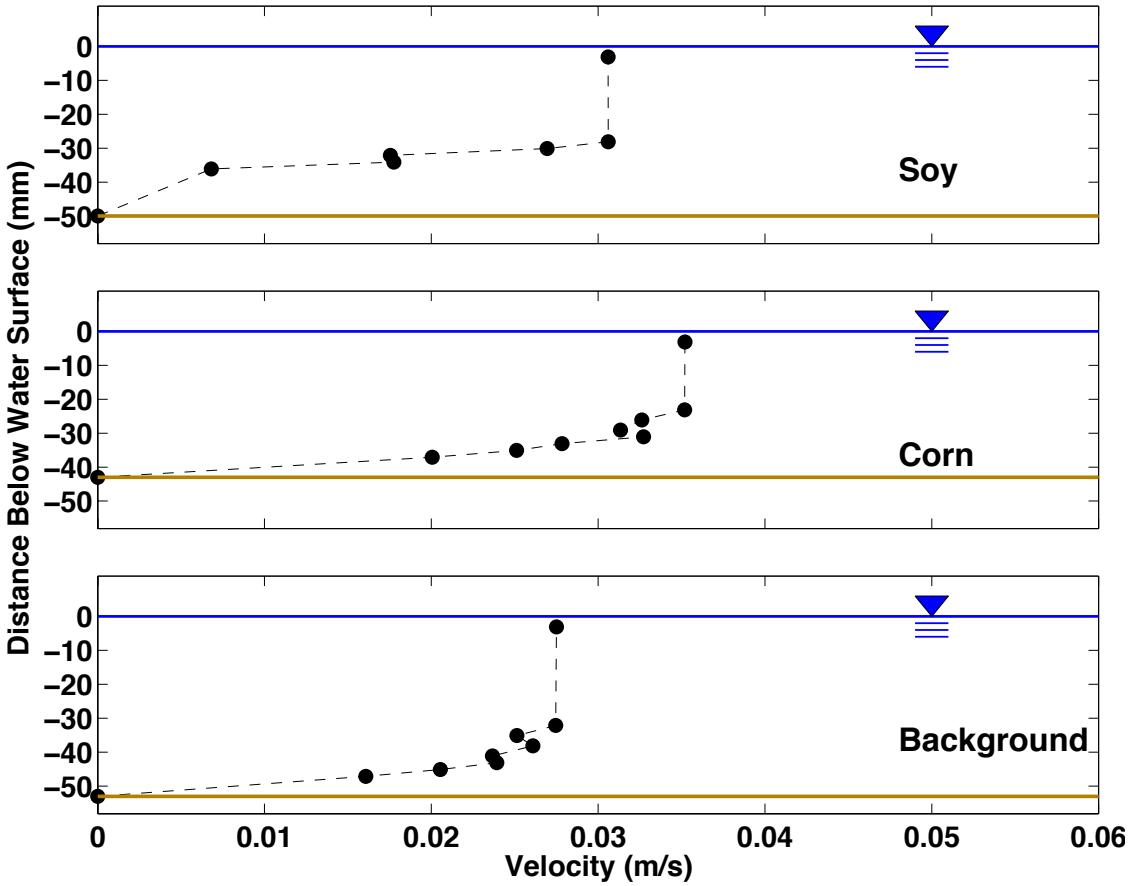

Figure 2.11. Velocity profiles over each treatment for 2.5 cm/s.

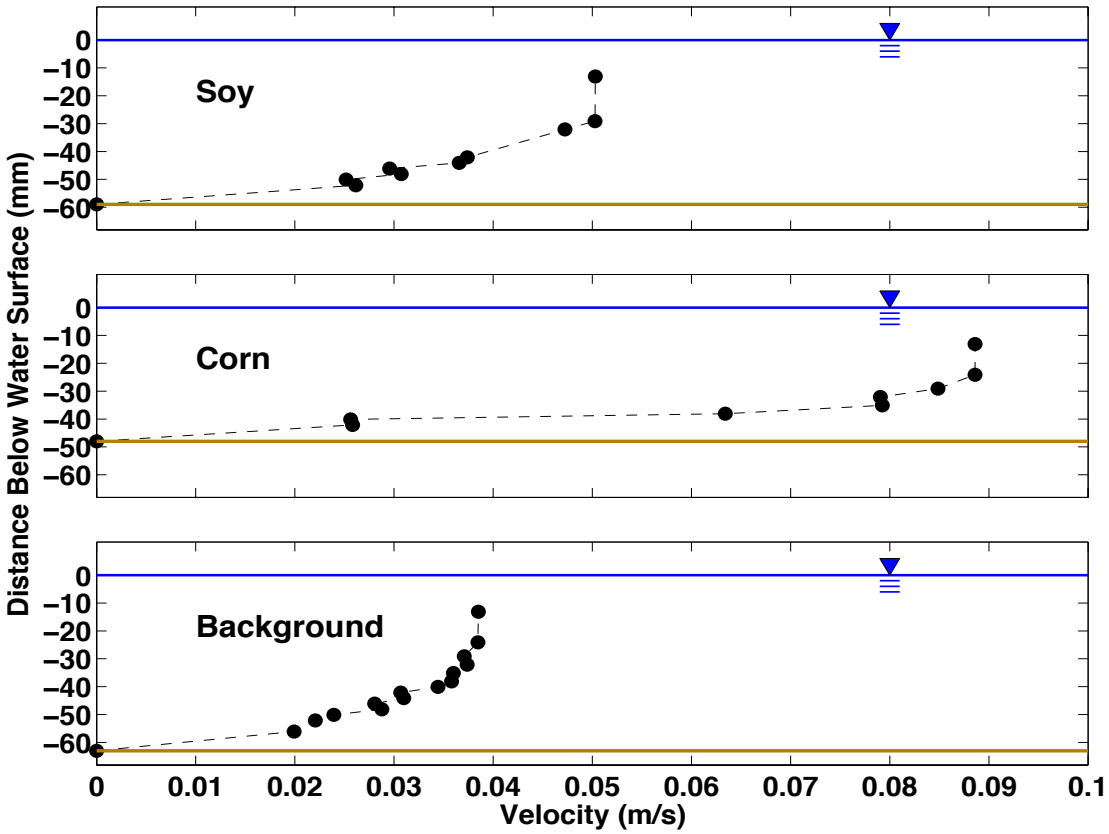

Figure 2.12. Velocity profiles over each treatment for 5 cm/s.

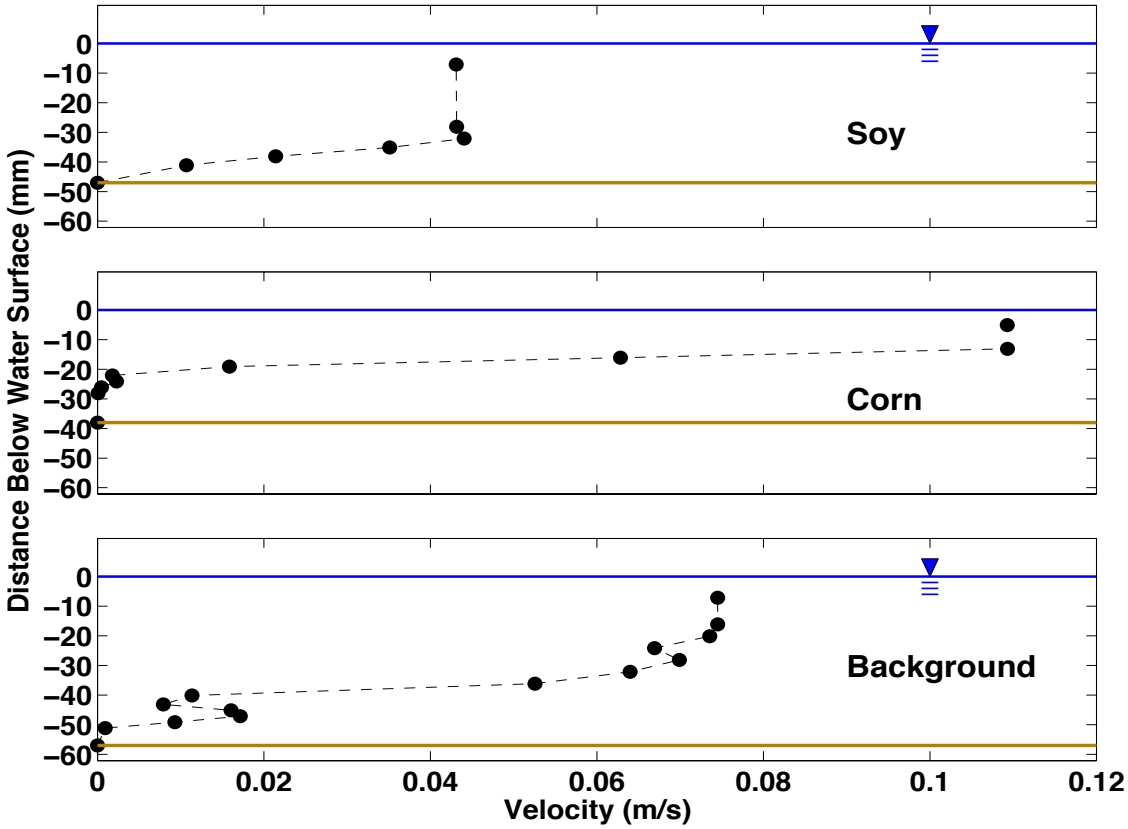

Figure 2.13.Velocity profiles over each treatment for 7.5 cm/s.

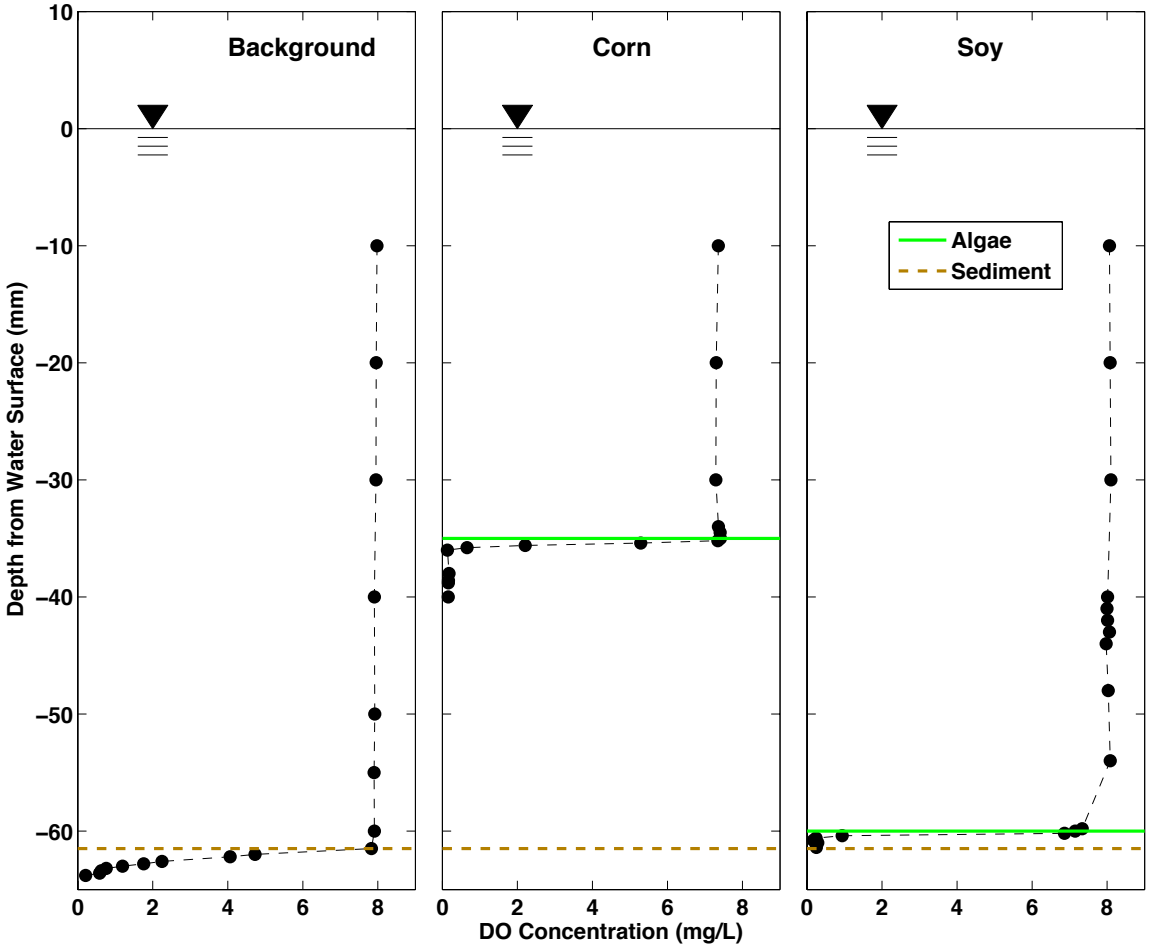

Figure 2.14. DO profiles in each treatment during 5 cm/s.

2.5 Discussion

2.5.1 The Evaluation of Turbulence and Carbon on Denitrification

Denitrification is a difficult process to measure (Groffman et al., 2006), and studies have largely focused on large-scale field investigations or small-scale laboratory experiments utilizing sediment-core techniques. The use of a recirculating flume enables direct measurement of nitrate uptake over time, and allows for easy manipulation of variables such as water velocity, which would be very difficult in field-scale investigations. Also, flume experiments enable two separate ways to estimate denitrification, quantifying

nitrate flux rates based on direct measurements of nitrate uptake over time, and using collected soil cores for the acetylene block method.

Two types of sediment were used in the flume experiments, as-collected field sediment and soy-amended sediment. While fluid-flow conditions had similar effects on nitrate uptake for both types of sediment, nitrate uptake was much faster in soy-amended sediment. Soy-amended sediment had greater sediment organic matter contents and lower bulk densities than unamended sediment, which has been shown to relate to higher denitrification rates (Tomasek et al., 2017). Soybean meal has a low carbon to nitrogen (C:N) ratio, approximately 5.4 (Van Kessel et al., 2000), indicating a high carbon quality that can readily be used by bacteria. Previous studies showed that readily biodegradable organic carbon increased rates of denitrification (Henderson et al., 2010; Sirivedhin and Gray, 2006), but that low C:N ratios produce large N_2O emissions (Huang et al., 2004). Similarly, denitrification assays showed that the majority of denitrification that was occurring in soy-amended sediment was as incomplete denitrification, with DeN N_2O yields of 86.3% compared to 4.9% for unamended sediment, and DEA N_2O yields of 93% compared to 13.7% for unamended sediment (Table 2.2). Gene abundances for 16S rRNA and *nosZ3* were significantly greater for soy-amended sediment compared to unamended sediment, but the abundance of *nirS*, a gene unique to denitrifiers (Zumft, 1997), was not significantly different between sediment types.

Nitrate uptake varied based on fluid-flow conditions, with maximum uptake rates occurring at overall friction velocities between 0.75 to 1.25 cm s^{-1} for unamended and soy-amended sediment. Increasing fluid flow led to increasing Reynolds numbers, friction velocity, and energy dissipation, and decreasing Kolmogorov and Batchelor length scale and diffusive sublayer. Similarly, increasing fluid flow increased the DO concentration gradient near the sediment-water interface. Since DO flux is directly related to the DO concentration gradient, and inversely related δ_C (Equations 2.4 and 2.5), increasing fluid-flow would increase the flux of oxygen into the sediments. This can be seen in Figure 2.2, where the depth of DO penetration in the sediment increased with increasing Reynolds numbers. With very high friction velocities in unamended sediment, there was no measurable uptake. Above this friction velocity, scour of the sediment

began to occur. This high velocity would inhibit nitrate uptake due to the low sediment-water contact time and potentially disrupting the bacterial community through scour and sediment transport (Tomasek et al., 2017).

Probable reasons for the differential response of nitrate uptake under variable fluid-flow conditions are solute mass transfer limitations to the sediment, and the diffusion of oxygen into the sediment. Under low friction velocities, oxygen penetration depth is shallow in the sediment, which is favorable for denitrification, but the lower turbulence-induced fluxes would also limit the diffusion of nitrate into the sediment. Nitrate mass transfer in this region may therefore limit nitrate uptake. For high friction velocities, oxygen penetration was deeper into the sediment, and the oxic conditions may have limited denitrification. While in this range there would be favorable solute mass-transfer, denitrification may have been limited by the presence of oxygen. For mid-range friction velocities, enhanced nitrate uptake could be due to a favorable balance between the availability of nitrate due to solute transfer, while having shallower oxygen penetrations than for high friction velocities. Most denitrifiers are facultative anaerobes (Van Rijn et al., 2006), due to the high energy yield of nitrate after oxygen (Schlesinger and Burnhardt, 2013). Oxygen diffusion in the sediment could stimulate aerobic processes such as respiration and decomposition, and once the oxygen is consumed for these processes, bacteria will begin using nitrate as an electron acceptor.

Gene abundance data suggests that bacteria were responding to fluid flow conditions. For unamended experiments with mid range shear velocities (0.75 and 1.04 cm s^{-1}), abundances of 16S rRNA, *nirS*, and *nirK* were all significantly lowest at the beginning of the experiment. Conversely, the low and high friction velocity experiments (0.51 and 1.31 cm s^{-1}, respectively) did not have significant increases in any gene abundances over the experimental duration. This potentially supports the hypothesis that optimal oxygen diffusion into the sediment stimulated the growth of bacteria that could denitrify in the absence of oxygen. Comparing denitrification rates as measured by assays (DeN and DEA) and by direct flux measurements from measuring flume nitrate concentrations over time (J_{NO3}) also suggests that mid-range shear velocities cause enhanced nitrate uptake. DeN and DEA rates can be compared to J_{NO3} rates since the

assays are normalized to areal rates and assumes that all denitrification occurs in the top 5 cm of sediment, and sediment depth in the flume was set at 5 cm. DeN and DEA rates were similar over the experiments for all unamended sediment, but the experiments with the low and high friction velocities had lower J_{NO3} rates. This suggests that even though all sediment had a similar potential to denitrify, the mid-range velocities had higher actual uptake due to the experimental conditions.

The acetylene block method is often reported to underestimate potential denitrification due to method limitations (Qin et al., 2013; Watts and Seitzinger, 2000; Woodward et al., 2009). Limitations of the acetylene block method that would cause an underestimation of denitrification rates include the inhibition of nitrification and nitrifier-denitrification, suppression of microbial respiration in the presence of C_2H_2, incomplete suppression of N_2O reductase, incomplete diffusion of C_2H_2 in sediment resulting in incomplete blockage of N_2O to N_2, and decomposition of C_2H_2 by microbes (Felber et al., 2012; Groffman et al., 2006; Seitzinger et al., 1993). However, in this study, DeN and DEA rates were approximately an order of magnitude greater than J_{NO3} rates. The DeN and DEA rates measured for sediment in this experiment were similar to those measured previously for sediment collected from the same site (Tomasek et al., 2017). In addition, J_{NO3} rates were comparable to those quantified in a similar flume experiment (O'Connor et al., 2006). One reason for the differences between J_{NO3} compared to DeN and DEA rates could be due to the redox conditions in the flume, where oxic conditions were present in the sediment, differing from the anoxic conditions of the assays (Bruesewitz et al., 2012), thereby causing increased denitrification rates for the assays. Also, the assays are maintained in slurried conditions, where all bacteria present in the sediment are able to denitrify nitrate in the water, and normalization to areal rates assume that the upper 5 cm of sediment has this same denitrification rate. Perhaps the sediment in the flume did not allow for nitrate to fully diffuse into the sediment, or denitrification was constrained to a narrow band below the oxygen penetration depth but within the nitrate diffusion depth.

2.5.2 Continuous Flume Experiments

DeN rates were similar among sediment types and appeared to increase with increasing velocity. DeN rates were much lower than DEA rates due to the very low nitrate concentrations at the end of the experimental runs. DEA rates were greatest at the mid-range velocity in the soy-amended sediment, appeared to increase with increasing velocity in the corn-amended, and were similar across velocities in the control sediment. From direct nitrate removal rates, the lowest velocities had the fastest rates. Since all sediment types were run concurrently at the same velocities, quantifying individual uptake rates for each sediment type via direct measurements were not possible.

Due to the experimental design, where the same sediment was used for each experimental run and experiments were run in order of increasing velocities, the differences seen due to differing velocities could have been due to experimental time. Results do show that amending sediment with carbon increases the potential of sediment to denitrify. Soybean meal has a much lower carbon to nitrogen ratio than corn stover (approximately 5 compared to 57) (USDA, 2011). Since the soybean meal is a higher quality of carbon, the bacteria would rapidly consume it for heterotrophic processes like denitrification. This may explain the differences in the patterns seen between corn and soy amended DEA rates, where rates for the soy-amended sediment continued up until after the 5 cm s^{-1} run, after which they started decreasing, possibly due to the decline in the readily useable carbon. The DEA rates of the corn-amended sediment increased over the entire duration of the experiment.

2.6 Conclusion

Friction velocities tested in the flume ranged from 0.51 to 1.53 cm s^{-1}. Friction velocity, an indication of turbulence levels and momentum flux from the water column to the sediment, mediated dissolved oxygen and nitrate uptake above the sediment-water interface. The thickness of the diffusive sublayer over which dissolved oxygen transport occurred at the sediment bed scaled inversely by the 7/5 power law of friction velocity and sediment roughness height. Maximum nitrate uptake was in the range of friction velocities from 0.75 to 1.1 cm s^{-1} (corresponding to Reynolds numbers from 2010 to

4700) for unamended sediment, and from 1.0 to 1.25 cm s^{-1} (corresponding to a Reynolds number of 5180 to 5380) for soy-amended sediment. Nitrate fluxes for soy-amended sediment experiments were nearly 100 times greater than for unamended sediment, indicating that adding labile carbon to sediments increases denitrification rates. However, assays revealed that the increased denitrification due to the carbon was largely as incomplete denitrification, where nitrous oxide is the terminal electron acceptor instead of fully completing the pathway to dinitrogen. Overall, maximum nitrate uptake occurred at mid-range friction velocities from 0.75 to 1.25 cm s^{-1} (corresponding to a Reynolds number from 2010 to 4320). High-friction velocities, larger than 1.5 cm s^{-1} (Reynolds number greater than 5000), and low-friction velocities, smaller than 0.50 cm s^{-1} (Reynolds number smaller than 1000), were found to minimize nitrate uptake by the sediment. Gene abundances for 16S rRNA, *nirS*, and *nosZ3* in unamended sediment significantly increased over the experimental duration for mid-range friction velocities, but not for low and high friction velocities. No gene abundances significantly increased over experimental duration in soy-amended sediment. Soy-amended sediment had significantly greater abundances of 16S rRNA and *nosZ3*, but not *nirS*. Excess nitrogen loading to surface waters in the agricultural Midwestern United States has several negative health and ecological effects, emphasizing the need for effective management strategies. The results of this study could provide guidance on management strategies to control fluid-flow conditions in streams in channels to maximize nitrate uptake in agricultural watersheds by the sediment. Promoting optimal turbulence conditions in headwater streams could facilitate sustained nitrate uptake and reduce nitrogen loading to higher-order streams.

3 Intermittent Flooding of Organic-Rich Soil Promotes the Formation of Denitrification Hot Moments and Hot Spots

3.1 Overview

Anthropogenic activity has altered the nitrogen cycle, necessitating management on the landscape level. Isolated time periods and areas, termed hot moments and hot spots, respectively, frequently account for a large percentage of nitrate removal in aquatic ecosystems. A series of experiments were conducted to determine the effect of hydrologic connectivity on denitrification rates, gene abundances, and nitrous oxide fluxes. Experimental areas were divided into flooded (always inundated), floodzone (intermittently inundated), and non-floodzone (not inundated) locations in low-organic and organic-rich soil. Our results demonstrated that intermittent flooding events enhanced denitrification rates from days to weeks after flooding, depending on the inundation period. Microbial analysis showed that short-term flood events did not lead to increases in denitrifying gene abundances or changes in community diversity. However, long-term hydrologic connectivity potentially led to differences in bacterial community composition. Enhanced denitrification rates did not have a corresponding increase in the ratio of incomplete to complete denitrification. Incomplete to complete denitrification ratios were high in always-inundated low-organic sandy soil, peaking at 40%. Results demonstrate that management strategies that promote hydrologic connectivity and intermittent flooding of organic-rich floodplain soils promote the formation of denitrification hot moments and hot spots, with relatively low incomplete denitrification rates (<3% of the total denitrification rates).

3.2 Introduction

Anthropogenic activity has greatly altered the nitrogen cycle in the past century. While the Haber-Bosch process has allowed for the modernization of agriculture and supports billions of people worldwide (Smil, 2002), the rate of anthropogenic nitrogen fixation is now nearly double the natural rate of terrestrial, bacterial-derived, fixation (Canfield et al., 2010). Nitrogen recovery by agricultural crops is typically less than 50% worldwide

(Fageria and Baligar, 2005), and approximately 25% of the nitrogen added to the biosphere is exported from rivers to oceans or inland basins (Mulholland et al., 2008). This inefficiency in crop nitrogen uptake and excess fertilizer applications in the intensively managed agricultural region of the Midwestern United States has caused negative impacts to human health (Powlson et al., 2008; Ward et al., 2010) and ecological consequences (Camargo and Alonso, 2006; Rabalais et al., 2007).

Complete denitrification is a stepwise microbial transformation pathway that reduces soluble nitrate to inert nitrogen gas. Denitrification is currently the only known natural microbial pathway to remove substantial amounts of nitrate from aquatic systems (Zhu et al., 2013). Isolated time periods and areas, termed hot moments and hot spots, respectively, frequently account for a large percentage of nitrate removal in aquatic ecosystems. (Groffman et al., 2009; McClain et al., 2003; O'Connor et al., 2006). Enhanced denitrification has been identified in hyporheic zones (Gomez-Velez et al., 2015), inundated floodplains (Forshay and Stanley, 2005; Scott et al., 2014; Shrestha et al., 2014), and restored floodplains (Kaushal et al., 2008; Roley et al., 2012a). Promoting the formation of these hot spots and hot moments can serve as a potential management strategy for nitrate removal. However, incomplete denitrification can have consequences through the release of nitrous oxide, a greenhouse gas with 300-times the global warming potential of CO_2 (Ravishankara et al., 2009). Nitrous oxide emissions are currently increasing by 0.7 parts per billion by volume per year, are responsible for 6% of the anthropogenic greenhouse effect, and contribute to stratospheric ozone depletion (Stehfest and Bouwman, 2006). Agriculture accounts for approximately 84% of the global anthropogenic nitrous oxide emissions (Smith et al., 2008b). Therefore, when evaluating denitrification, it is essential to consider how environmental conditions affect the nitrous oxide yield, or the proportion of denitrified nitrate that is incompletely converted to nitrous oxide as opposed to nitrogen gas (Beaulieu et al., 2011).

Periodic wetting and drying of soil alters denitrification rates. Initial wetting leads to pulsed release of nutrients (Baldwin and Mitchell, 2000; Corstanje and Reddy, 2004; Shenker et al., 2005), while wet-dry cycles lead to variations in redox conditions (Fiedler et al., 2007; Jones et al., 2014; Shenker et al., 2005), and can promote denitrification from

paired nitrification-denitrification (Baldwin and Mitchell, 2000; Dong et al., 2012; Shrestha et al., 2014). Fluctuating water levels create soils with a wide range of redox potentials, which leads to changes in nutrient dynamics and microbial community dynamics (Corstanje and Reddy, 2004; Fiedler et al., 2007). When wet soils begin to dry, oxygen diffuses into the soil and promotes nitrification, converting ammonium to nitrate. Rewetted soils often become anoxic, and the increased flux of nitrate leads to an increase in denitrification (Baldwin and Mitchell, 2000). While several studies have investigated the effects of flood events and increasing denitrification rates (Forshay and Stanley, 2005; Kaushal et al., 2008; Pinay et al., 2002), questions still remain as to how the duration and frequency of these events affect rates and how flooding affects the bacterial communities in floodplain soils.

While previous research has focused on identifying the formation of denitrification hot spots in a wide range of ecosystems (Jones et al., 2014; Mahl et al., 2015; Mulholland et al., 2008; Roley et al., 2012b), this study utilizes a controlled outdoor laboratory setting to investigate the effect of hydrologic connectivity on denitrification rates, microbial communities, and nitrous oxide fluxes. These relationships provide important information for the design and application of nitrogen management practices. Our previous research showed that site location along a transect of hydrologic connectivity affected the relationship between denitrification rates and microbial communities in a field setting (Tomasek et al., 2017) most likely due to differences in site inundation. We hypothesize that inundation will increase denitrification rates, and a longer duration of inundation will lead to sustained changes in denitrification rates as the microbial community has time to respond to the changing environmental conditions.

Here we report on results from two studies designed to investigate the effects of inundation on denitrification. One experiment utilized an outdoor experimental stream to simulate the effect of short-term (4 h) flooding events on the formation of denitrification hot moments in the stream channel and floodplain under two different nitrate concentrations. A DNA-based analysis was also used to quantify the abundances of genes for each step in the denitrification pathway, along with total bacterial abundance, for channel and floodplain locations. The second experiment utilized a flow-through basin

with a sloped soil surface to determine how longer duration flooding (7-14 days) and differences in inundation contribute to the formation of denitrification hot spots and nitrous oxide yield in two different types of soil under the same hydrologic conditions. The objectives of this study were to: (1) determine how short-term flooding events and inundation affect the formation of denitrification hot spots and hot moments, (2) determine if flooding alters the microbial community through qPCR and amplicon sequencing, and (3) investigate the impact of inundation on nitrous oxide emissions.

3.3 Materials and Methods

3.3.1 Experimental Site and Setup

Experiments were conducted in an experimental stream and a flow-through basin at the Outdoor StreamLab (OSL) at the St. Anthony Falls Laboratory (SAFL), University of Minnesota. Both the experimental stream and the flow-through basin receive water from the Mississippi River. The experimental stream is a sand-bed meandering stream with a vegetated floodplain (approximately 40 m by 20 m) receiving continuous flow since 2008 (Figure 3.1A). Mississippi River water is fed to the stream with an adjustable valve that allows for flow rate control. The stream is equipped with a sediment recirculation system, which collects sediment from a collection basin at the downstream end of the stream and transports it to a variable speed sediment feeder that dispenses the sediment directly into the stream. This ensures a controlled and continuous sediment feed. Subsurface inflow from outside the system is constrained by an impermeable layer underlying and surrounding the channel and floodplain. The flow-through basin is a 4.5 m × 4.5 m box with an impermeable membrane to prevent inflow and outflow to the surrounding area (Figure 3.1B). The basin's soil is sloped to allow for differential inundation across the basin area (Chapman et al., 2013).

Two floods were simulated in the OSL on 23 June and 8 July 2014. During the flood, the flow rate of Mississippi River water to the OSL was increased from approximately 25 L s^{-1} to approximately 900 L s^{-1}. The entire OSL floodplain was inundated with 5 cm of water for 4 hr. Five locations, two in the channel and three on the

floodplain, were sampled along a transect perpendicular to the middle meander bend (Figure 3.1A). Duplicate soil samples for measuring denitrification rates and triplicate soil cores to determine bulk density, soil water content, and soil organic matter were collected immediately before and immediately after flooding, and 1 and 3 days after flooding (1 h pre, 1 h post, 24 h post, and 72 h post, respectively). Triplicate soil samples for measuring denitrifying gene abundances were collected immediately before and after flooding, and 1 day after flooding.

The flow-through basin experiment was run from October to November 2015. Mississippi River water flowing through the basin was maintained at 0.44 L s^{-1} for the duration of the experiment. The water level in the basin is adjustable using standpipes of different heights at the outflow. Three zones of hydrologic connectivity were tested during the experiment: 1) always inundated (flooded), 2) periodically inundated (floodzone), and 3) never inundated (non-floodzone) (Figure 3.1B). Two soil types were used in the basin study, a sandy soil and an organic soil. The organic soil was the original one in the flow-through basin and the sandy soil was collected from a spillway in the OSL. The soil types were separated using PVC rings that were 5 cm deep and 25 cm in diameter. For the organic soil, the PVC rings were installed, and soil within all of the PVC rings designated for organic treatments was extracted, homogenized, and placed back into the rings. This was to ensure that the effects seen were purely from the variation in water level rather than differing soil. The collected sandy soil was homogenized, the PVC rings were installed, the organic soil within the ring was extracted, and the new sandy soil was placed into the ring.

Three rings of each type of soil were placed in each hydrologic zone (Figure 3.1B). The experiment began with the water height set between the flooded and floodzone boundary, such that the floodzone was not inundated. The water was kept at this boundary for one week, after which soil cores were collected. The water level was raised between the floodzone and non-floodzone boundary, inundating the floodzone, and kept at this height for one week. Soil cores were collected after the second one-week period. This water height adjustment and sample collection was repeated, with water

being maintained between the flooded and floodzone boundary for a week, followed by a height change to the boundary between the floodzone and non-floodzone for two weeks. The collected soil cores were analyzed to determine bulk density, soil water content, soil organic matter, denitrification potential, and nitrous oxide yield (Beaulieu et al., 2009).

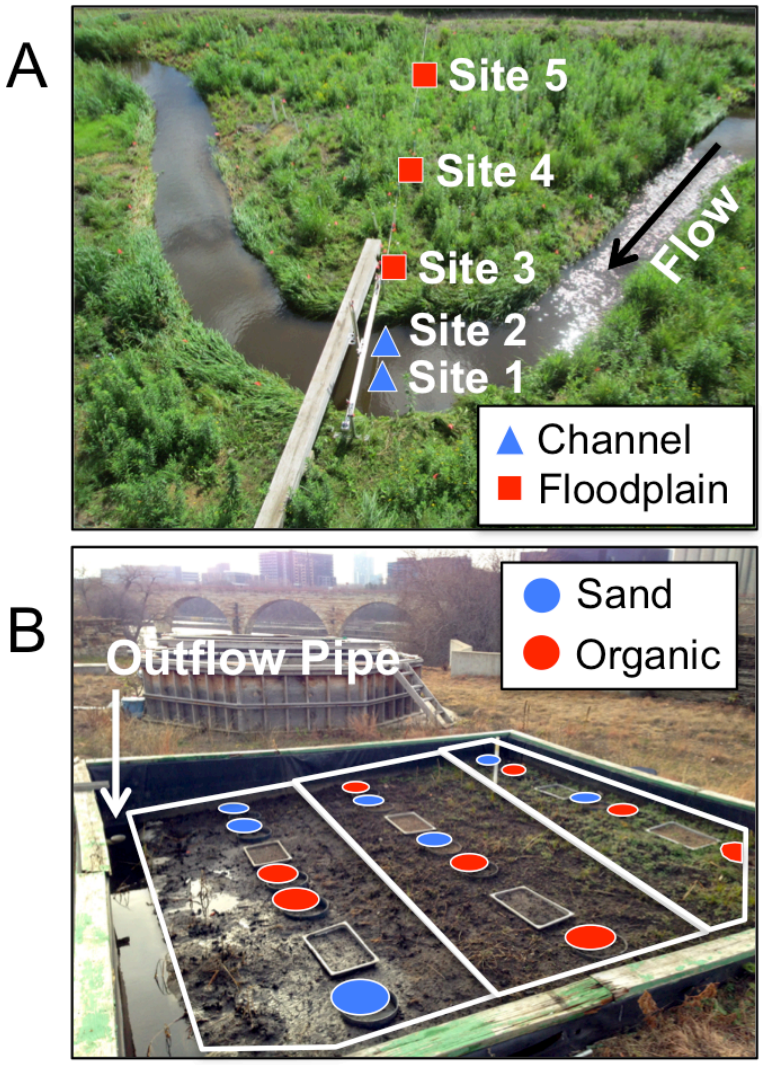

Figure 3.1. Schematics of the experimental setups in the Outdoor StreamLab (OSL). (A) Schematic of the experimental stream in the OSL with sample sites. Channel sites are shown as blue triangles and floodplain sites are shown as red squares under normal flow conditions. (B) Schematic of the flow-through basin in the OSL with sandy soil treatments in blue and organic in red. The white lines indicate the different divisions of the three hydrologic zones (flooded, floodzone, and non-floodzone from left to right).

3.3.2 Water and Soil Sampling

For the stream flooding experiment, water samples were collected immediately before and immediately after the flood, and 1 and 3 days after the flood from the stream channel. Water samples were also collected above the floodplain sampling locations during the flood. All water samples were collected in triplicate, filtered using pre-combusted 0.7 μm Whatman GF/F filters, and analyzed on a Lachat QC800 Autoanalyzer (Hach Company) to determine nitrate concentrations using the cadmium reduction method (Kazemzadeh and Ensafi, 2001). Water quality parameters (water temperature, specific conductivity, pH, and dissolved oxygen) were collected during the flooding experiments and in the flow-through basin using a Hydrolab Series 5 Datasonde (Hach Company, Loveland, CO).

Water velocity for the stream flooding experiment was measured in the channel immediately before and after the flood, and 1 and 3 days after the flood. Water velocities above the floodplain locations were collected during the flood. Channel velocity measurements were collected using an Acoustic Doppler Velocimeter (ADV) (Nortek Vectrino, Sandvika, Norway). Shear velocities (u_*) were calculated from velocities taken at several depths, and by using the logarithmic relationship between the time-averaged velocities and the corresponding log depth (Biron et al., 2004). Velocities over the floodplain locations were collected using a 2D handheld field ADV (SonTek Flowtracker).

Soil cores were collected from the experimental stream and the flow-through basin to determine bulk density, soil water content, soil organic matter, denitrification potential, and gene abundances. Soil samples for bulk density, soil moisture content, and organic matter were collected using a 35 mL syringe with the end cut off. Soil was collected in the syringe, the volume of the sample was recorded, the wet weight was measured, and the dried weight determined after drying the soil at 110°C for 1 day, or until the weight did not change. Dried soil was ground using a mortar and pestle, passed through a 2 mm sieve, and 5 g of the sieved soil was weighed into a crucible. The soil was combusted at 550°C for 4 h. The bulk density was determined by dividing the dry

weight of the soil by the volume of the collected sample. Volumetric soil water content was determined by subtracting the dry weight from the wet weight and normalizing by the soil volume (Gardner, 1986). Soil organic matter was determined by subtracting the combusted soil weight from the original dry soil weight in the crucible and dividing by the dry soil weight (Heiri et al., 2001). Maps of volumetric soil moisture (Figure 3.2) were created using a handheld soil moisture meter (FieldScout TDR 100, Spectrum Technologies) at georeferenced points in the OSL. Cores for determining denitrification potential were collected using 60 mL syringes with the ends cut off. Collected cores were transferred to a plastic bag and immediately transferred to a refrigerator at SAFL. Cores to determine gene abundances were collected using autoclaved 5 mL syringes with the ends cut off, and immediately transferred to a -20°C freezer.

Denitrification rates were determined using a modified acetylene block method (Groffman et al., 2009; Loken et al., 2016). Soil (40 g) and site-specific water (40 mL) were added to 125 mL Wheaton bottles. The bottles were flushed with helium to induce anoxic conditions and 10 mL of acetylene was injected to block denitrification at N_2O (Smith and Tiedje, 1979, Groffman et al., 2006). Site-specific water was used to determine denitrification under existing site conditions (DeN) and under non-limiting nutrient conditions (DEA). For both measurements, chloramphenicol (10 mg L^{-1}) was added to block *de novo* protein synthesis and to extend the linear period of N_2O accumulation (Tiedje et al., 1989). For DEA assays, nitrate (100 mg N L^{-1} as potassium nitrate), carbon (40 mg C L^{-1} as glucose), and phosphate (13.84 mg P L^{-1} as potassium dihydrogen phosphate) were added to the site water. N_2O accumulation over time was measured using a gas chromatograph (5890 series II, Hewlett-Packard) equipped with an electron capture headspace autosampler (Hewlett-Packard 7694), and rates were corrected using the Bunsen solubility coefficient (Tiedje, 1982). Denitrification rates were calculated as a function of bulk density, and converted to an areal rate by assuming that the majority of denitrification occurs in the top 5 cm (Arango et al., 2007, Inwood et al., 2007).

To determine N_2O formation due to incomplete denitrification, the same assays as described above were used, but without the addition of acetylene (Hunt et al., 2003). The

ratio between N_2O production rates from the assays without acetylene to the N_2O production rates with acetylene provides the ratio of incomplete to complete denitrification. Therefore, this ratio, referred to as the N_2O yield, represents the proportion of denitrified nitrate that is reduced to nitrous oxide as opposed to nitrogen gas (Beaulieu et al., 2011, Beaulieu et al., 2009). Assays to determine N_2O yield were performed on duplicate soil cores collected from the flow-through basin using non-amended water collected from the basin on the sample collection date.

3.3.3 Gene Abundances

Abundances of genes for each step in the denitrification pathway, *norB*, *narG*, *nirS*, *nirK*, *nosZ1*, and *nosZ3*, and total bacterial abundance, as measured by 16S rRNA, were determined for the June and July flood at the channel and floodplain locations in the experimental stream immediately before and after flooding, and 1 day post flooding. The DNeasy PowerSoil Kit (QIAGEN, Hilden, Germany) was used to extract DNA from 500 mg of soil. DNA concentrations were measured on a Qubit 2.0 fluorometer (Life Technologies), and quantitative PCR (qPCR) was used to determine the concentration of each gene in soil samples. The qPCR analysis was performed on a Roche Light Cycler 480 Real Time PCR (Roche Life Sciences, Indianapolis, IN). The specific primers used were U515F and U806R (BAC515F) for 16S rRNA (Wang and Qian, 2009), cnorB-BF and cnorBB-BR for *norB* (Dandie et al., 2007), narG-1960m2fE and narG2050m2R for *narG* (Kandeler et al., 2006; Lopez-Gutierrez et al., 2004), m-cd3AF and m-R3cd for *nirS*, nirK876F and nirK1040R for *nirK* (Bru et al., 2011; Petersen et al., 2012), nosZ_F and nosZ_1622R for *nosZ1* (Rosch et al., 2002), and nosZ2F and nosZ2R for *nosZ3* (Bru et al., 2011; Petersen et al., 2012). The qPCR standard curve r^2 values were all over 0.99 and the efficiencies ranged from 80-110%

3.3.4 Statistical Analysis

Statistical analyses were performed using JMP version 13.0 (SAS Institute Inc., Cary, NC). One-way ANOVA was used to determine the effect of sampling time on environmental parameters and denitrification rates during the June and July flood experiments, and to determine the differences between the two floods. If the ANOVA

was significant ($\alpha = 0.05$), a Tukey's post-hoc test was performed. For the flow-through basin, a similar approach was taken to compare the effects of sampling location on denitrification rates and differences over the course of the experiment. Mothur was used to calculate Shannon indices, Good's coverage, beta diversity [using analysis of similarity (ANOSIM)], and ordination plots. Bray-Curtis dissimilarity matrices were used to perform beta diversity analysis and ordination (Bray and Curtis, 1957). Ordination was performed by principal component analysis [PCoA (Anderson and Willis, 2003)], and all statistics were calculated at $\alpha = 0.05$.

3.4 Results

3.4.1 Short-term Flood Events in an Experimental Stream

Environmental conditions differed between the two flood events and between the channel and floodplain locations (Table 3.1). Nitrate concentrations of the Mississippi River water in the experimental stream were higher during the June flood than the July flood, with average concentrations of 0.94 and 0.51 mg $N\text{-}NO_3^- L^{-1}$, respectively. Floodplain locations had significantly greater ($p < 0.001$) organic matter than did channel locations for both floods. Floodplain locations were comprised of a sandy organic soil (average organic matter of 5.6%), whereas soil in the channel locations was coarse sand (average organic matter of 0.66%). Conditions also varied over the course of each flood. For the June flood, volumetric water content (VWC) of the floodplain locations significantly increased after the flood ($p = 0.002$), and remained elevated up to 1 day after the flood (Figure 3.2). For the July flood, VWC increased and remained elevated up to 3 days after the flood. VWC was statistically similar between the June and July flood at the floodplain locations for all sampling times except 3 days post flood, which was significantly greater ($p = 0.05$) during the July flood compared to the June flood. Shear velocities in the channel were much greater during flood-flow conditions than under normal-flow conditions for both floods (average shear velocities of 13 cm s^{-1} and 0.6 cm s^{-1}, respectively).

Table 3.1. Mean environmental parameters for the two flood events during the four sampling times. The channel location is the mean of the triplicate samples from Site 1 and Site 2, and the floodplain location is the mean of triplicate samples from Sites 3, 4, and 5. C_{NO3} is nitrate concentration in the experimental stream (Mississippi River water), OM is organic matter, VWC is volumetric water content, ρ_b is bulk density, DeN is denitrification under site conditions, and DEA is denitrification under non-nutrient limiting conditions.

	Date	Location	C_{NO3} (mg N-NO_3 L^{-1})	OM (%)	VWC (%)	ρ_b (g cm^{-3})	DeN (mg N m^{-2} h^{-1})	DEA (mg N m^{-2} h^{-1})
1 h Pre	6/23/14	Channel	0.97	0.63	30.9	1.54	0.24	0.82
1 h Post	6/23/14	Channel	0.92	0.9	28.1	1.62	0.13	0.16
24 h Post	6/24/14	Channel	0.92	0.64	32.2	1.59	0.01	0.04
72 h Post	6/25/14	Channel	1.03	0.75	27.9	1.71	0.04	0.06
1 h Pre	6/23/14	Floodplain	NA	5.60	30.1	1.07	4.84	11.7
1 h Post	6/23/14	Floodplain	NA	5.74	34.7	1.36	6.08	16.3
24 h Post	6/24/14	Floodplain	NA	5.42	33.9	1.42	8.03	17.9
72 h Post	6/25/14	Floodplain	NA	5.84	29.7	1.23	4.50	8.75
1 h Pre	7/08/14	Channel	0.49	0.70	33.1	1.61	0.25	0.25
1 h Post	7/08/14	Channel	0.45	0.67	31.2	1.48	0.08	0.02
24 h Post	7/09/14	Channel	0.48	0.75	30.9	1.65	0.09	0.03
72 h Post	7/10/14	Channel	0.49	0.76	30.8	1.59	0.00	0.01
1 h Pre	7/08/14	Floodplain	NA	4.53	31.2	1.81	3.84	10.5
1 h Post	7/08/14	Floodplain	NA	5.31	35.8	1.34	3.12	9.16
24 h Post	7/09/14	Floodplain	NA	5.22	34.3	1.46	3.50	6.02
72 h Post	7/10/14	Floodplain	NA	5.12	34.7	1.27	2.82	6.31

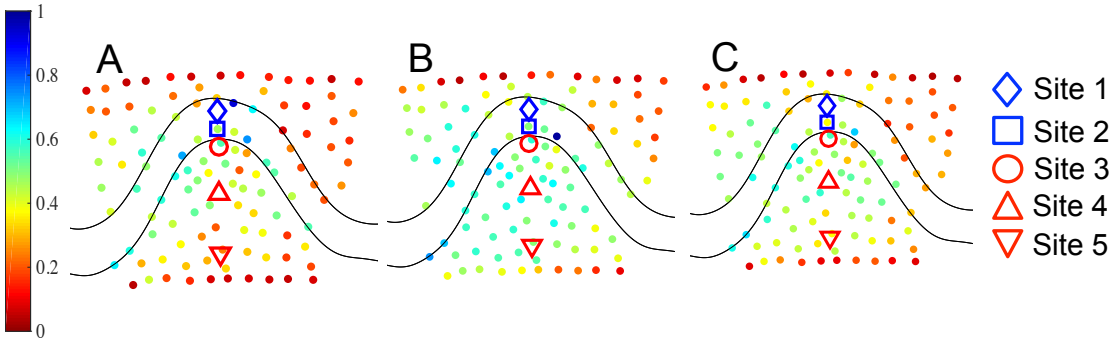

Figure 3.2. Map of volumetric water content for (A) 1 hour before the June flood (6/23/14), (B) 1 hour after the flood (6/23/14), and (C) 24 hours after the flood (6/24/14).

Correlations between environmental parameters and denitrification rates varied based on flood date and sampling location. There was a significant positive correlation between DeN and soil organic matter during the June and July floods ($p < 0.001$ and $r^2 = 0.67$ and 0.66, respectively). DEA and organic matter were also correlated for the June and July floods ($p < 0.001$ and $r^2 = 0.57$ and 0.45). There was a weak, but significant, correlation ($p = 0.05$, $r^2 = 0.17$) between VWC and DeN at the floodplain locations for the June flood, but no other correlations between water content and DeN or DEA were significant. Both the June and July floods had a negative correlation between DeN and bulk density ($p < 0.001$ and $r^2 = 0.26$, and $p = 0.02$ and $r^2 = 0.14$, respectively). DEA and bulk density were negatively correlated for the June ($p < 0.001$ and $r^2 = 0.26$) flood but not for the July flood.

Denitrification rates varied based on the flood date, sampling time, and sampling location. For both floods, non-amended (DeN) rates and amended (DEA) denitrification rates were significantly greater at floodplain locations than at channel locations when all sampling times were pooled ($p < 0.001$ for DeN and DEA for the June and July floods, Figure 3.3). DeN and DEA rates for floodplain locations significantly increased ($p = 0.001$ and $p = 0.03$ for DeN and DEA, respectively) up until 1 day post flooding during the June flood, and then returned back to pre-flood rates by 3 days post flood. The DeN rates significantly decreased ($p = 0.04$) in the channel locations after the June flood.

There was no significant effect of time on DeN or DEA rates for either floodplain or channel locations for the July flood.

Denitrification rates also varied at the different sampling times between floods. There was no significant difference ($\alpha = 0.05$) for DeN and DEA rates between samples collected immediately before the June and July floods at either the channel or floodplain locations. Immediately after the flood, the DeN and DEA rates were significantly greater ($p = 0.002$ and $p = 0.04$, respectively) for the June flood compared to the July flood at the floodplain locations. In contrast, there was no significant difference at the channel locations for either DeN or DEA rates. Similarly, for 1 day post flood, DeN and DEA rates were significantly greater ($p < 0.001$ for both) for the June flood compared to the July flood at the floodplain locations, but there was no difference at the channel locations. By 3 days after the flood, the June DeN rates were significantly different ($p = 0.05$) than the July rates at the floodplain location but there was no difference in DEA rates.

The difference between DeN and DEA rates varied between the sampling times for the two floods. During the June flood, DeN rates were significantly less than DEA rates immediately and 1 day post flood at the floodplain locations ($p = 0.04$ and $p < 0.001$, respectively). However, DeN and DEA rates were not significantly different immediately before the flood or 3 days after the flood. For the July flood, DeN rates were significantly less than DEA rates for all sampling times at the floodplain locations ($p = 0.01$, $p < 0.001$, $p = 0.02$, and $p = 0.004$ for immediately before, immediately after, 1 day after, and 3 days after the flood, respectively). DeN rates were only significantly less than DEA rates at channel locations 3 days after the flood for both flood events ($p = 0.04$ and $p = 0.01$ for June and July, respectively).

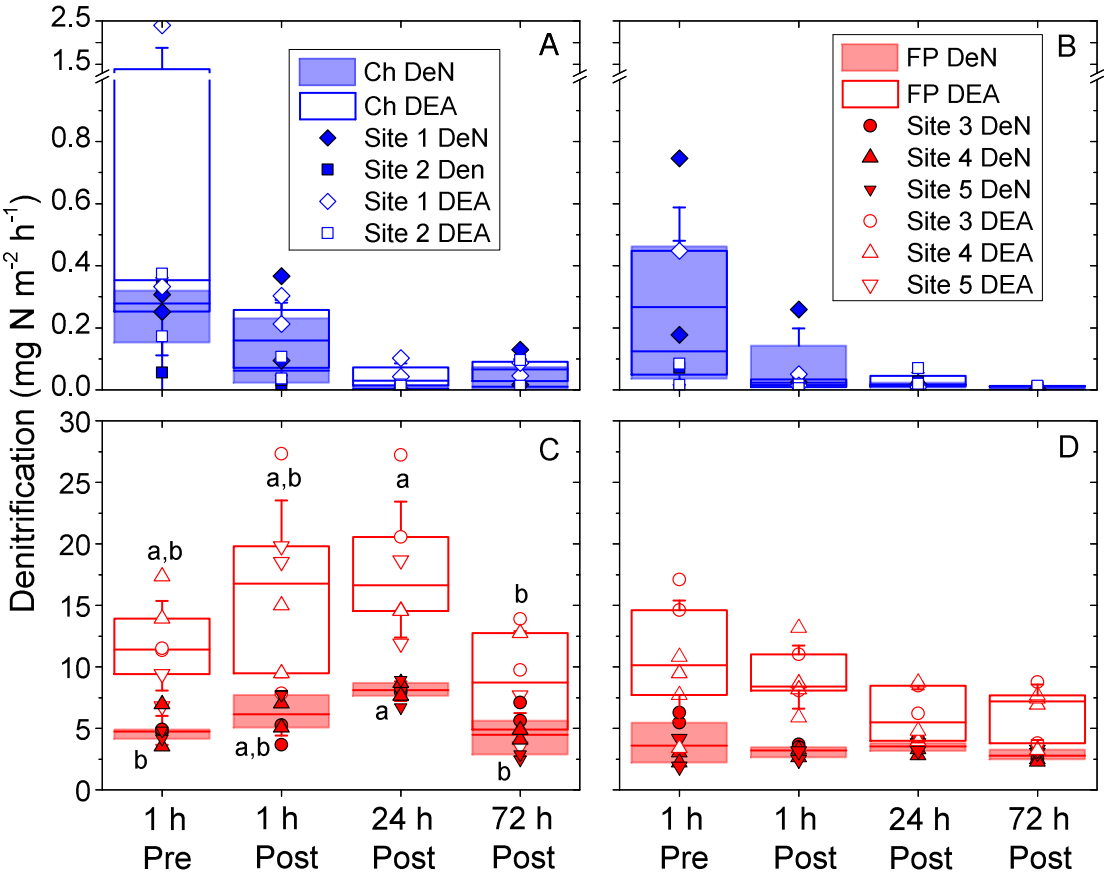

Figure 3.3. Denitrification rates under site conditions (DeN) and non-limiting nutrient conditions (DEA) at the channel locations (Ch) during the (A) June and (B) July flood, and at the floodplain locations (FP) for the (C) June flood and (D) July flood. Boxes represent the first and third quartile, the horizontal line across the box represents the median, and whiskers represent ± the standard deviation. One-way ANOVAs (α = 0.05) were conducted to determine the statistical significance of the effect of sampling time on denitrification rates, followed by a Tukey's post-hoc analysis on significant ANOVAs. Sampling times that are not connected by the same letter have significantly different denitrification rates as determined by the post-hoc analysis, and the letters are arranged according to decreasing DeN rates.

Bacterial abundances for 16S rRNA and denitrifying genes differed by location, sampling time, and flood date (Figure 3.4). For the June flood, several genes significantly decreased at the floodplain locations from after the flood, including 16S rRNA ($p < 0.001$), *narG* ($p < 0.001$), *norB* ($p = 0.05$), *nirK* ($p < 0.001$), and *nosZ1* ($p = 0.002$). For the channel locations during the same flood, 16S rRNA, *narG*, and *nirK* significantly decreased post flood ($p < 0.001$, $p < 0.001$, and $p = 0.002$, respectively). Other gene abundances remained nearly constant during all sampling periods with no significant difference in abundances between pre and post flood. Only the 16S rRNA and *nirK* genes significantly decreased ($p = 0.002$ and $p = 0.008$, respectively) at the floodplain locations over the sampling times during the July flood. At the channel locations during the July flood, 16S rRNA significantly decreased ($p = 0.03$), but four denitrifying genes also significantly increased after the flood ($p = 0.02$, $p = 0.01$, $p = 0.02$, and $p = 0.01$ for *narG*, *nirS*, *nosZ1*, and *nosZ3*, respectively). All other genes remained statistically similar over the sampling times during the July flood. For the June flood, 16S rRNA, *norB*, *nirK*, *nosZ1*, and *nosZ3* had significantly greater abundances at the floodplain locations compared to the channel locations when all sampling times were pooled ($p = 0.002$, $p = 0.001$, $p = 0.004$, $p < 0.001$, and $p < 0.001$, respectively). For the July flood, all abundances were greater at the floodplain locations compared to the channel locations when sampling times were pooled ($p = 0.007$, $p < 0.001$, $p = 0.001$, $p = 0.01$, $p < 0.001$, $p < 0.001$, and $p < 0.001$ for 16S rRNA, *narG*, *norB*, *nirS*, *nirK*, *nosZ1*, and *nosZ3*, respectively).

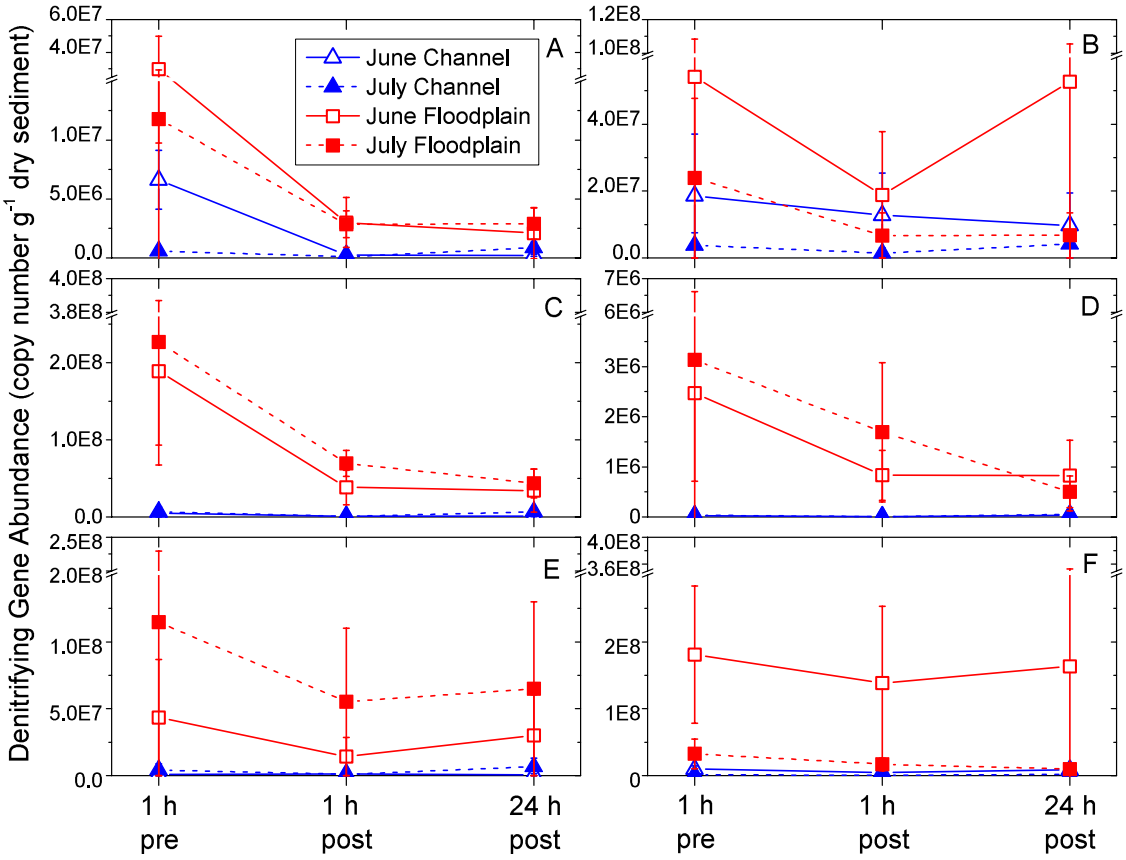

Figure 3.4. Mean denitrifying gene abundances of (A) *narG*, (B) *nirS,* (C) *nirK,* (D) *norB*, (E) *nosZ1,* and (F) *nosZ3* immediately before (1 h pre) and after (1 h post) the flood, and 1 day after (24 h post) the June and July 2014 floods. The mean for all genes was determined from the triplicate samples from Sites 1 and 2 (channel), and Sites 3, 4, and 5 (floodplain). Values are means ± the standard deviation.

3.4.2 Periodic Inundation in a Flow-through Basin

Nitrate concentrations varied in the flow-through basin over the course of the experiment (0.4 to 2.1 mg $N\text{-}NO_3^-$ L^{-1}). Nitrate concentration was 0.44, 1.02, 0.42, and 1.55 mg $N\text{-}NO_3^-$ L^{-1} for the October 8, October 15, October 22, and November 5 sampling date, respectively. The sandy soil had an organic matter of 1.1%, and the organic had an organic matter of 7.5%.

Denitrification (DeN) rates varied by sampling date, sampling location, and soil type (Figure 3.5). Overall, DeN rates for the organic soil were higher than that of the sandy soil, particularly at the floodzone location ($p < 0.001$, $p < 0.001$, $p = 0.002$, and $p < 0.001$ for October 8, October 15, October 22, and November 5, respectively). DeN rates for the organic and sandy soil were only statistically similar at the flooded location on October 22 and November 5. The DeN rates for the two soil types also exhibited different patterns. The DeN rates for the sandy soil were greatest at the flooded location and decreased to the non-floodzone location. DeN rates did not vary by location on the October 8 sampling date for the organic soil. This date was prior to water level being raised above the floodzone location. Rates at the floodzone location for the organic soil were significantly greater at the two dates when water was between the floodzone and non-floodzone locations ($p < 0.001$ for both October 15 and November 15). When water level was lowered to below the floodzone for 1 week, DeN rates of the organic soil were still greatest at the floodzone location The non-floodzone locations had statistically similar DeN rates ($\alpha = 0.05$) between all sampling dates for both the sandy and organic soil.

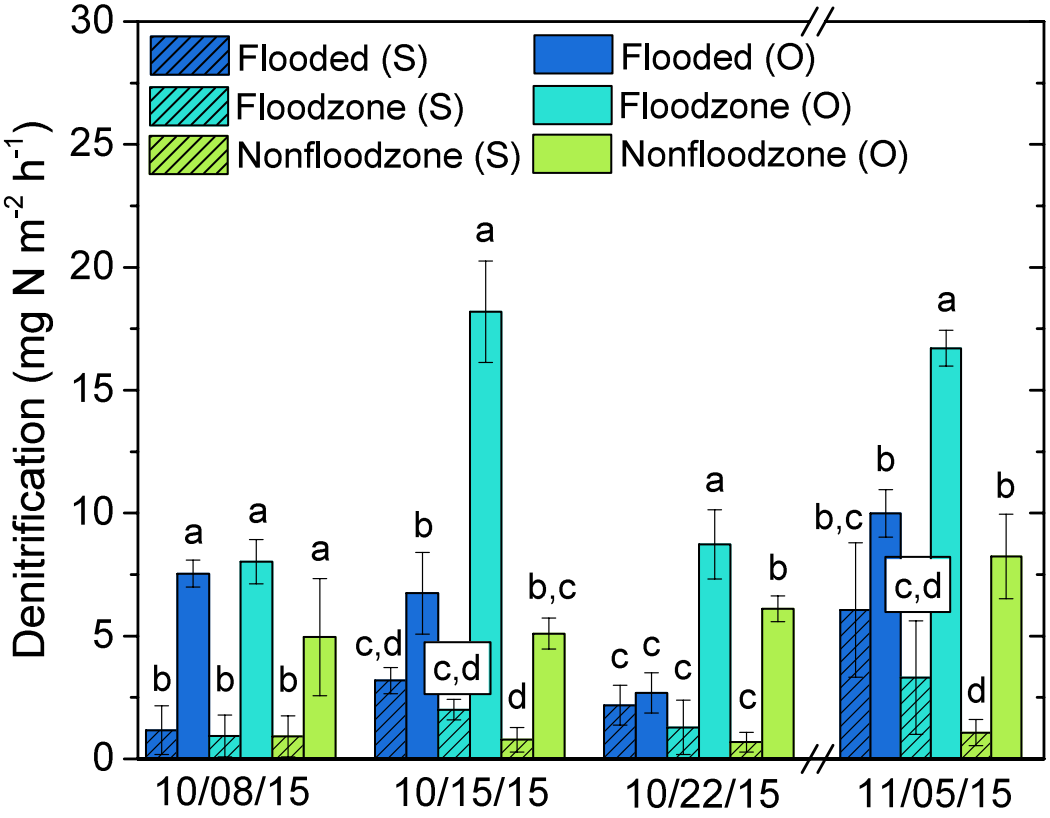

Figure 3.5. Denitrification rates under site conditions (DeN) for the sandy (S) and organic (O) soil at the three sampling locations on the four sampling dates. On October 14 and November 5, 2015, the floodzone was inundated with water. The error bars represent mean ± the standard deviation. One-way ANOVAs (α = 0.05) were conducted on each date independently to determine if the sampling location and sediment type had a significant effect on denitrification. Locations that are not connected by the same letter have significantly different DeN rates (each date compared independently) as determined by a Tukey's post-hoc analysis, and the letters are arranged according to decreasing DeN rates.

3.4.3 The Effect of Inundation and Organic Carbon on Nitrous Oxide Yield

Nitrous oxide fluxes varied by soil type and sampling location (Figure 3.6). For all four sampling dates, N_2O yield was greatest for the sandy soil in the flooded location. N_2O yield was slightly greater for the sandy soil compared to the organic soil at the floodzone location. Trends in N_2O yield for the organic soil differed for each sampling date.

Locations that had the greatest denitrification rates (organic soil at the floodzone location, Figure 3.5) had generally low N_2O yields.

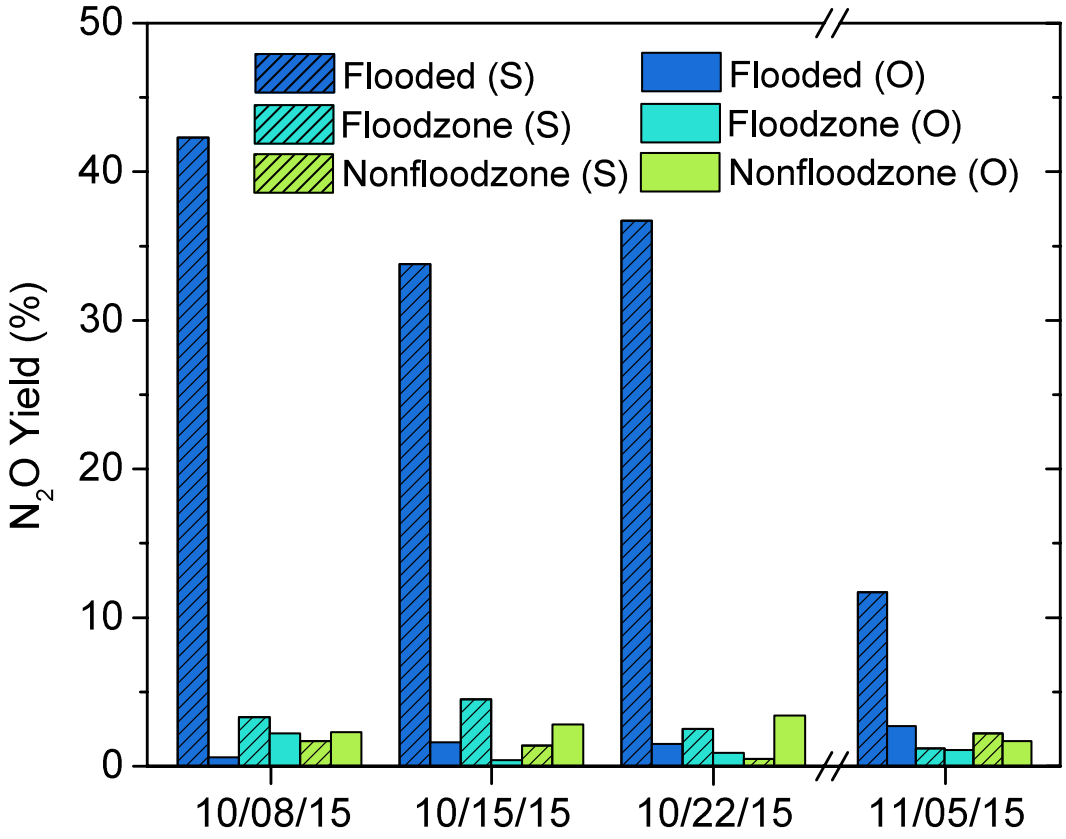

Figure 3.6. N_2O yield, or the proportion of denitrified nitrate that is converted to nitrous oxide as opposed to nitrogen gas (DeN without acetylene divided by DeN with acetylene), for the sandy (S) and organic (O) soil at the three sampling locations on the four sampling dates. On October 14 and November 5, 2015, the floodzone was inundated with water. Data was not statistically analyzed due to the limited number of samples.

3.4.4 Microbial Community Characterization

DNA from Sites 1 (channel), 3 (floodplain), and 5 (floodplain) and from immediately before and immediately after the June and July floods were sequenced and analyzed. Since this study focused on how short-term flooding affected denitrification rates and the

microbial community at channel and floodplain sites, Site 3 and 5 were combined for analysis. A mean Good's coverage of 99.6 ± 0.1% (mean ± standard deviation) was achieved among all samples, corresponding to a range of 637 to 1,207 operational taxonomic units (OTUs) observed within a single sample. Alpha diversity measured by the Shannon index did not significantly differ ($p = 0.44$) between the June and July flood (mean 4.10 ± 0.22 and 4.14 ± 0.27, respectively). However, diversity was significantly greater in channel samples compared to floodplain samples for all sampling periods except the June pre-flood. In addition, the diversity increased in channel samples following the June flood (Figure 3.7). No significant differences in Shannon indices were observed among the floodplain samples.

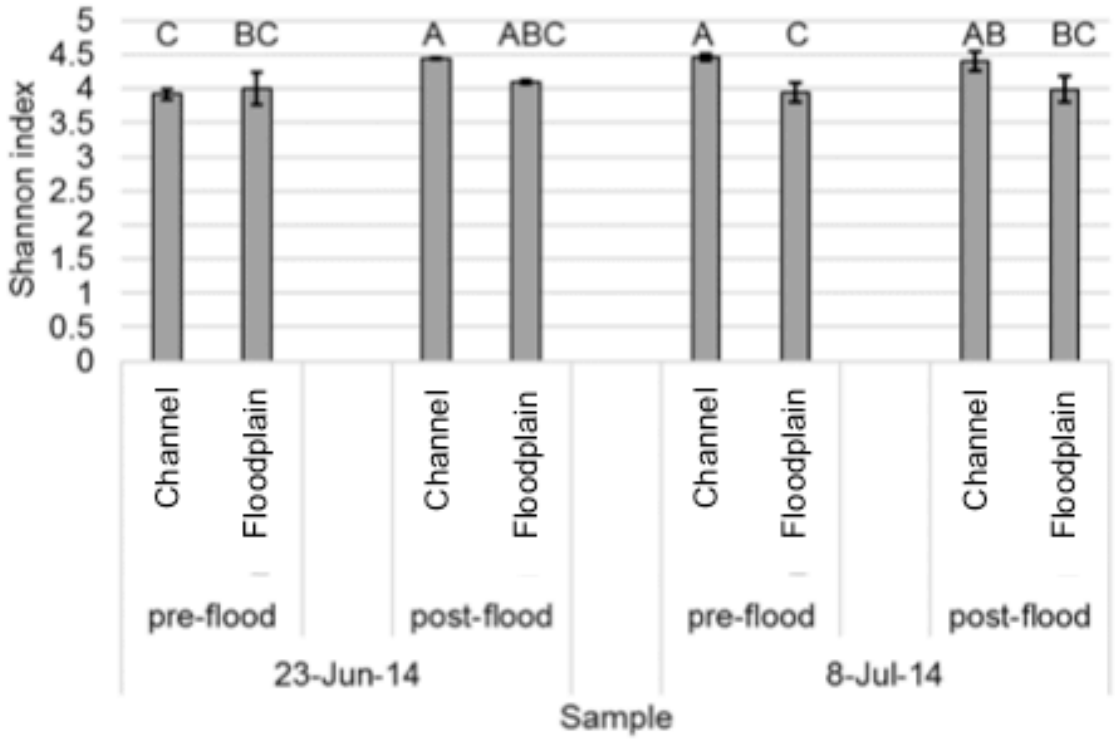

Figure 3.7. Shannon indices in samples collected prior to and following flooding during June and July floods. Error bars reflect standard deviations. Values sharing the same letter did not differ significantly by Tukey's post-hoc test ($p > 0.05$). Courtesy: Dr. Christopher Staley.

Microbial communities were predominantly comprised of members of the *Burkholderiaceae* and *Phyllobacteriaceae* family (Figure 3.8). Among the predominant families classified, the relative abundance of *Burkholderiaceae* was significantly greater during the June flood (Tukey's post-hoc $p = 0.031$). When grouped only by sampling position (channel v. floodplain), the abundances of *Burkholderiaceae*, *Planctomycetaceae*, and *Idiomarinaceae* were significantly greater in the channel ($p = 0.012$, < 0.0001, and 0.008, respectively). Conversely, the abundances of *Microbacteriaceae*, *Micromonosporaceae*, *Cytophagaceae*, and *Halobacteroidaceae* were greater in floodplain samples than in channel samples ($p = 0.002$, 0.049, < 0.0001, and 0.005). As a result of flooding, combining both sampling dates, the relative abundances of *Chitinophagaceae* decreased significantly in the channel ($p = 0.007$), but no other changes in family abundances were significantly altered in either channel or floodplain samples ($p > 0.05$).

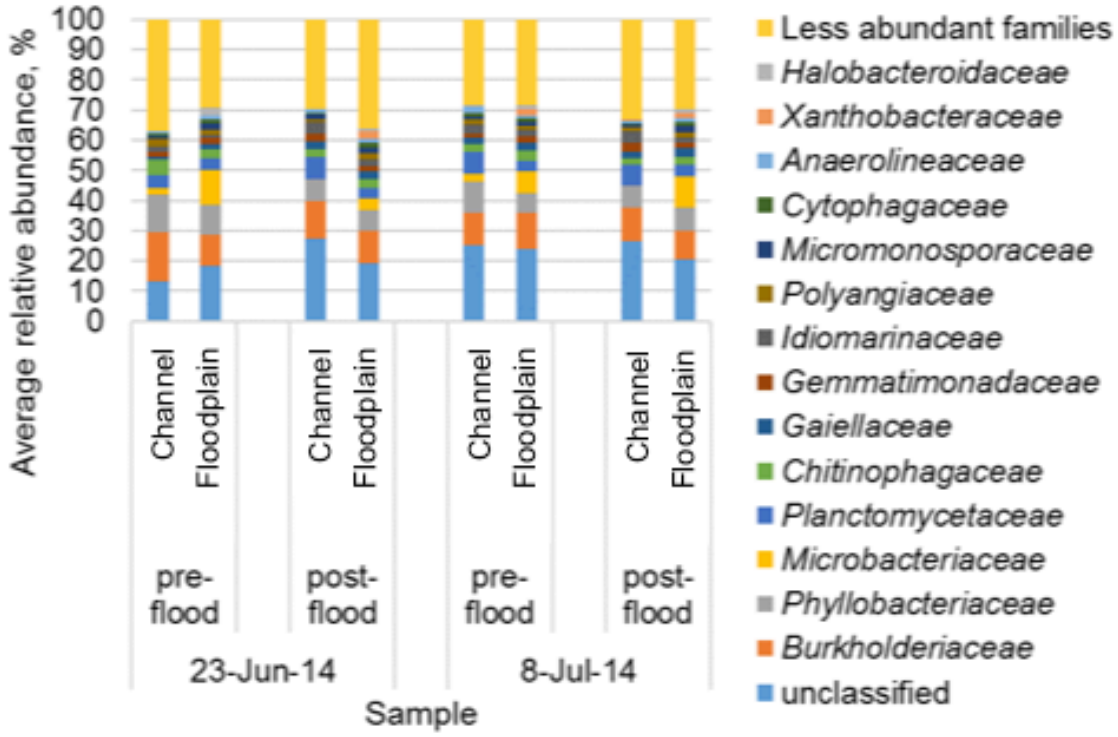

Figure 3.8. Distribution of abundant families in samples collected prior to and following the June and July flood. Courtesy: Dr. Christopher Staley.

Ordination of Bray-Curtis dissimilarity matrices among all samples (Figure 3.9) revealed significant separation of samples by site (analysis of similarity (ANOSIM) r = 0.70, $p < 0.001$). Community composition of samples collected during the June flood did not significantly differ from samples from the July flood event (ANSIM r = 0.00, $p = 0.42$). Composition also did not significantly differ (r = -0.03, $p = 0.63$) after flooding, taking both floods together. Similarly, when each site was considered individually, differences following flooding were not significant at Bonferroni corrected $a = 0.003$, correcting for multiple comparisons. The abundances of families that significantly affected ordination position showed similar to patterns found by ANOVA analysis. Site 1 had greater abundances of *Burkholderiaceae*, *Planctomycetaceae*, and *Anaerolinaceae*, while Site 5 had greater abundances of *Microbacteriaceae*, *Gaiellaceae*, *Micromonosporaceae*, and *Xanthobacteraceae* as well as *Chitinophagaceae*, *Cytophagaceae*, and *Bradyrhizobiaceae*. As a result of flooding (observed in relation to the y-axis), the abundances of *Phyllobacteriaceae* and *Polyangiaceae* tended to decrease while that of *Gemmatimonadaceae* tended to increase.

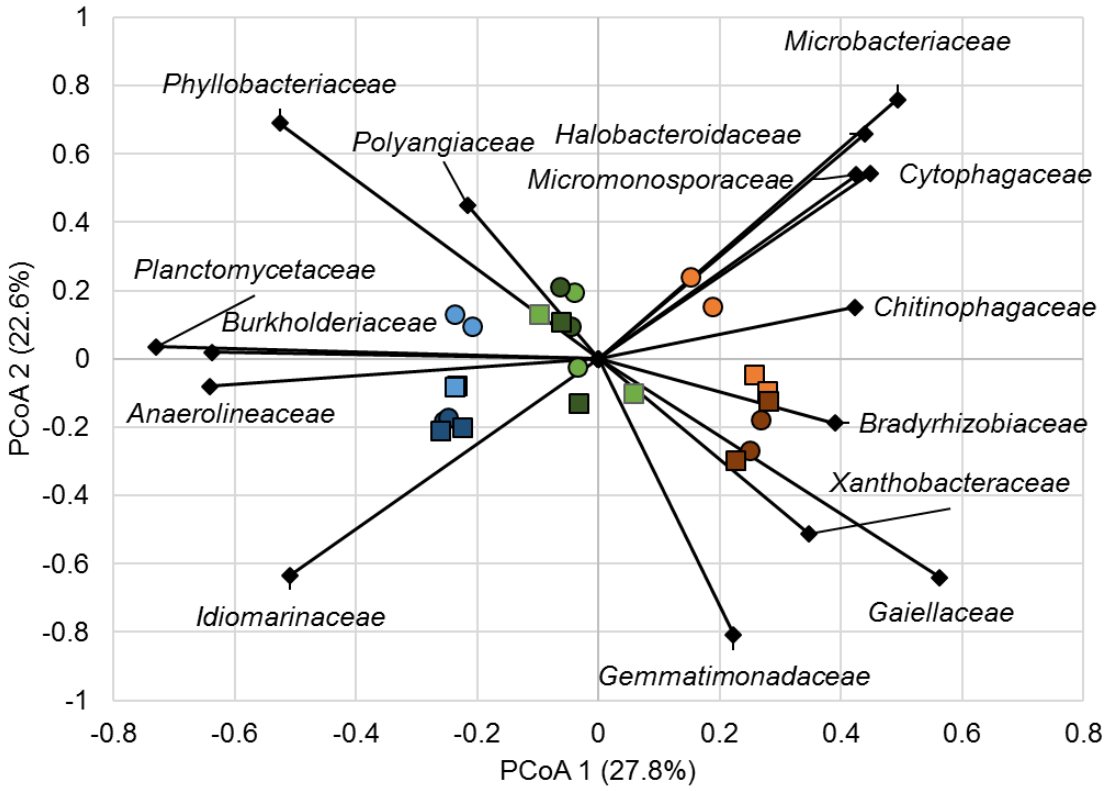

Figure 3.9. Principal coordinate analysis of Bray-Curtis dissimilarity matrices ($r^2 = 0.79$). Legend: June flood (○), July flood (□), channel (blue), flood zone (green), non-flood zone (orange), pre-flood (lighter), post-flood (darker). Abundances of families that significantly affected ordination position (among the 15 most abundant) are shown (Spearman correlations, $P < 0.05$). Courtesy: Dr. Christopher Staley.

3.5 Discussion

3.5.1 Formation of Hot Spots and Hot Moments

For both the June and July flood events in the experimental stream, denitrification rates at the channel locations decreased immediately after flooding, however this difference was only significant ($p = 0.04$) for the June flood. Water velocities and shear velocities (u_*) were much greater during the floods (average u_* of 13 cm s^{-1}) than under normal flow conditions (average u_* of 0.6 cm s^{-1}). Previous research has demonstrated that fast water velocities limit nitrate uptake (Alexander et al., 2009; Bukaveckas, 2007; O'Connor and

Hondzo, 2008b; O'Connor et al., 2012). Greater shear velocities also cause greater shear stresses on the bed sediment. This results in increased sediment transport, and during both floods, bedforms in the channel were visibly mobile. Decreases in gene abundances immediately after the June flood, along with decreased denitrification rates, suggest that increasing shear velocity, and therefore increasing bed mobilization, resulted in disruption of the microbial communities and decreases in denitrification rates. One potential mechanism is the washout of the communities with the sediment bed, indicated by the significant decrease in total bacterial abundance (16S rRNA). This implies that even if conditions were initially favorable for the formation of denitrification hot spots and hot moments, denitrification rates would decrease when shear velocities increase to the point where the sediment bed is mobilized.

For the experimental stream, denitrification rates were greater at the floodplain locations than at the channel locations for all sampling times. Floodplain locations had a much greater soil organic matter than did the sandy channel locations. Gene abundances were also much greater at the floodplain locations than at the channel locations. During the June flood, 16S rRNA and four of the denitrifying gene abundances (*norB*, *nirK*, *nosZ1*, and *nosZ3*) had significantly greater abundances at floodplain locations compared to channel, and during the July flood, 16S rRNA and all six of the denitrifying genes were significantly greater at the floodplain locations. In assays where nutrients were added to the site water, denitrification (DEA) rates were still significantly greater at the floodplain locations compared to the channel. This implies that even when nutrients are non-limiting, the lower abundances of denitrifying bacteria at these sandy locations may limit overall denitrification rates. Previous studies have also shown that sandy soils have less denitrification potential than more organic-rich soils (Deutsch et al. 2010; Gongol and Savage, 2016; Guentzel et al., 2014; Tomasek et al., 2017; Vance-Harris and Ingall, 2005). Therefore, connecting channels with their floodplains, particularly in low-organic sandy channels with limited denitrification capacity, should be targeted for the promotion of denitrification hot spots and hot moments.

We acknowledge that there are several potential limitations of the acetylene block method. These issues include not accounting for the activity from coupled nitrification-

denitrification (Seitzinger et al., 1993), and that acetylene may not completely inhibit the reduction of N_2O to N_2 (Yu et al., 2010), which would inflate the calculated N_2O yield using our methodology. However, for these experiments, this methodology was selected to compare how different sites and conditions affected relative denitrification rates as opposed to exact rates of in-situ denitrification. This method allows for a large number of samples to be run at once, and is appropriate when addressing the hot spot nature of denitrification (Groffman et al., 2006). Additionally, rates have been shown to be similar to other methods when incubating over a short time period and with the addition of chloramphenicol (Bernot et al., 2003; Roley et al., 2012a).

Differences between DeN and DEA rates during the June and July flood events suggest potential nutrient limitation at the floodplain locations. During the June flood, nitrate concentrations were higher than during the July flood (0.94 and 0.51 mg $N\text{-}NO_3^-$ L^{-1}, respectively). Since denitrification is dependent on several controlling environmental parameters, defining an exact concentration where nitrate becomes the limiting factor is difficult. Previous literature has found nitrate limitation in small streams at 0.4 mg $N\text{-}NO_3^-$ L^{-1} (Inwood et al., 2007), 0.7 mg $N\text{-}NO_3^-$ L^{-1} for a lake in Switzerland (Teranes and Bernasconi, 2000), and 0.9 mg $N\text{-}NO_3^-$ L^{-1} in a river-reservoir continuum (Wall et al., 2005). For the July flood event, denitrification rates increased with the addition of nutrients (DeN verse DEA rates) for all sampling times. In contrast, DEA rates only increased immediately after and 1 day after the June flood. If the differences in denitrification rates between the June and July flood can be solely attributed to nutrient limitation, it would be expected that there would not be a difference in DEA rates between the June and July floods for all sampling times. Instead, there was no significant difference in DEA rates between the June and July floods immediately before and 3 days after the floods, but DEA rates were significantly greater for the June flood immediately after and 1 day after the flood compared to the same sampling times for the July flood.

The increase seen in both DeN and DEA rates at the floodplain locations immediately after and 1 day after the June flood may indicate the formation of hot moments from short duration flood events. Pulse flood events can induce an initial release of nutrients from floodplain soil (Baldwin and Mitchell, 2000; Corstanje and

Reddy, 2004; Shenker et al., 2005), variation of soil redox potential (Du Laing et al., 2009; Kogel-Knabner et al., 2010; Lansdown et al., 2015; Niedermeier and Robinson, 2007), and short-term increases in denitrification rates (Austin et al, 2004; Fellows et al., 2011; Tockner et al., 1999; Wang et al., 2017). Perhaps during the June flood, this initial flush of nutrients, changing redox conditions, and higher nitrate conditions stimulated bacterial activity, inducing a physiological response and increasing denitrification rates. The increase in bacterial activity may also be reflected in the differences in DEA rates by sampling time. For the July flood, DEA rates were statistically similar across the sampling times. However, like DeN, DEA rates during the June flood are greatest 1 day after the flood, followed by immediately after the flood. Denitrification rates under site conditions (DeN) immediately before the June and July flood were statistically similar (p = 0.3). The short-term increase in denitrification rates after flooding suggests that remediation strategies that force pulse flows could increase nitrate uptake through the formation of denitrification hot moments.

The flow-through basin had differential denitrification rates at the three hydrologic zones and for the two soil types over the experimental duration. Similar to the flood experiments, DeN rates of the organic soil were much greater than the sandy soil. The greatest DeN rates were at the floodplain location on the sampling dates after it had been inundated with water (October 15 and November 5). Nitrate concentration was also greatest at these dates. However, if the increases in DeN rates were only due to higher nitrate concentrations, it would be expected that DeN rates would also be greatest at the flooded location on these dates. At the flooded location, DeN rates were significantly greater on November 5, but were statistically similar on the three other sampling dates.

Results from the flow-through basins suggest that periodically inundated sites lead to the formation of denitrification hot spots. DeN rates were greatest at the floodzone location after 7 and 14 days of inundation (October 15 and November 5, respectively), and increased DeN rates at the floodzone location were maintained even when the location had been dry for 7 days (October 22). Similarly, Sanchez-Andres et al. (Sanchez-Andres et al., 2010), found that inundation periods of greater than 7 days promoted denitrification, and Scott et al. (2014) (Scott et al., 2014) observed many biogeochemical

transformations within portions of the floodplains that frequently flooded after a record flood in the Atchafalaya River Basin. Alternating wet-dry cycles can potentially lead to increases in denitrification through paired nitrification-denitrification (Baldwin and Mitchell, 2000; Dong et al., 2012; Shrestha et al., 2014). When inundated areas dry, oxygen diffuses into the previously anoxic soil, promoting the growth of nitrifying bacteria and the conversion of ammonia to nitrite, which then oxidizes to nitrate. When the area is again inundated, the soil returns to anoxic conditions and the created nitrate is consumed by denitrifying bacteria. These conditions will favour facultative anaerobes, like denitrifiers.

3.5.2 Physiological or Population Response

Bacterial gene abundances were used to further investigate whether the differences in denitrification rates measured during the flood experiments were due to physiological or population responses. Physiological responses imply that favorable conditions lead to increased rates of bacterial activity per cell, whereas population response would be that conditions enhance the growth of bacteria, which would be detected by increases in gene abundances. During the June flood, denitrification rates were greatest one-day post flood, whereas rates were similar across sampling times during the July flood. Comparing the June and July floods, the June flood caused a greater reduction of gene abundances at the floodplain locations compared to the July flood (four denitrifying genes compared to one denitrifying gene); both experienced a reduction in total bacterial abundance (16S rRNA). If the increase seen in denitrification rates during the June flood was due to a population response, denitrifying gene abundances would likely have increased over the sampling times for the June flood and remained the same for the July flood. Therefore, the increased rates were not likely due to increasing abundances of denitrifying microbial communities. However, the physiological response of the bacterial community must be interpreted cautiously because measuring gene abundances may not accurately reflect gene expression.

Nitrate concentration is one of the main controlling parameters for denitrification (Inwood et al., 2007; Kemp and Dodds, 2002; Martin et al., 2001). As previously

mentioned, nitrate concentrations during the June flood were greater than during the July flood. The increase in denitrification rates under site conditions (DeN) and nutrient amended conditions (DEA) at the floodplain locations for all sampling times during the July flood confirm that denitrification was nutrient limited. If the differences between DeN rates at the floodplain locations for the June and July flood were purely from nutrient limitation, it would be expected that there would be no significant difference in DEA rates between the two floods. However, DEA rates between the June and July flood were not significantly different immediately before and 3 days after the flood, but they were immediately after and 1 day after the floods. This is also when DeN was greatest during the June flood. One possibility is that environmental conditions during the June flood stimulated bacterial activity at the transcription level, increasing the rates of denitrification that the bacteria were performing. Favorable environmental conditions, including higher nitrate concentrations and an initial pulse of water over long-term dried soils, could have increased activity, which was sustained 1 day after the flood but had declined by 3 days after. Similarly, previous studies have shown that denitrification increased after flooding and continued until nitrate was depleted (Forshay and Stanley, 2005), and that short-term flooding caused transient increases in denitrification rates that were uncorrelated with denitrifying gene abundances (Manis et al., 2014; Wang et al., 2017). Chen et al. (Chen et al., 2015) found that changing climatic conditions decreased the abundance of *norB* genes (DNA), but promoted the expression of *norB* (RNA). In order to confirm the hypothesized increases in denitrifier activity, future work should focus on the expression of denitrifying genes through RNA-based analyses.

Microbial community analysis was not performed for the flow-through basin experiment, but our results suggest that increases in denitrification rates measured at the floodzone location may be due to an increase in denitrifiers. While denitrification rates were lower than other sampling dates on October 22 (when water level was lowered below the floodzone), DeN rates were still greatest at the floodzone location compared to the flooded and never flooded zones. With longer periods of inundation, the microbial community would have time to adapt to the changing environmental conditions. Wang et al. (2017) (Wang et al., 2017) found that after inundation of one week or longer, the size

of the denitrifying microbial community increased. Also, inundation of soils that have denitrified recently (previously inundated soils) can have a stronger denitrification response due to the presence of denitrifying enzymes (Robertson and Groffman, 2015), and the denitrifying bacteria at locations that experience wet-dry cycling of soils may be more responsive to changing moisture conditions (Fellows et al., 2011).

3.5.3 N_2O Yields

N_2O yields, the ratio of N_2O production from incomplete to complete denitrification, was much greater in the sandy flooded soils than the organic flooded soils, and slightly larger in the floodzone sandy soils compared to the organic floodzone soils. Other studies have also shown high N_2O production in waterlogged sandy soils (Bandibas et al., 1994; Pihlatie et al., 2004). Pihlatie et al. (2004) (Pihlatie et al., 2004) also found that N_2O emission was high in sandy, waterlogged soils, but that this was due to nitrification rather than denitrification, indicating that these soils still remained at least partially aerobic even when inundated with water. The water in the flow-through basin remained oxic throughout the experimental duration. The large pore spaces of sandy soils could have allowed for more diffusion of oxygen into the soil. Nitrite could still be reduced to nitric oxide through denitrification by bacteria containing the *nirK* enzyme, however without *nosZ* expression, denitrification would stop at N_2O instead of N_2. Excluding the large N_2O yields determined in the flooded sandy soils, ranges of N_2O yields in this study (0.4 – 4.5%) were within the range found by Beaulieu et al. (2011) (Beaulieu et al., 2011) (0.04 – 5.6%) for streams and rivers. Future work is needed to determine how inundation effects the expression of denitrifying genes, and how this expression relates to differences seen in N_2O yields.

3.5.4 Inundation and the Microbial Community

Soil at the three sites sequenced (Site 1, 3, and 5) had varying moisture contents (Figure S1), and had significantly distinct community composition (Figure 6). Flooding did not affect the microbial community composition and the community did not vary between the June and July flood. Similarly, flooding did not affect diversity or familial abundances at

floodplain sites (Figure S2 and S3). This could indicate that the environmental conditions of a site, including soil moisture, strongly influences the community composition, and this is sustained during short-term flood events. Similar results were found by (Argiroff et al., 2017), where a long-term gradient of hydrologic connectivity was shown through metagenomic analyses to correspond to differences in the microbial communities. Disconnect between denitrification rates and gene abundances, denitrification rates, and alpha diversity (*e.g.* channel sites being more diverse but having lower rates), and the clear separation of sites based on their community composition, could suggest that the community composition has an effect on denitrification rates. Future work should investigate how short-term and sustained inundation effects community composition, and how this composition corresponds to denitrification rates.

3.5.5 Management Implications

Our results provide insight into the effect of inundation on denitrification rates and the potential mechanisms that drive the observed changes. The short-term flood event in the experimental stream stimulated denitrification in measurements taken immediately and 1 day after the flood, and this increase was most likely physiologically-based, where favourable environmental conditions stimulated denitrification rates among denitrifying bacteria. This transient increase in denitrification rates after a short-term flood event suggests that pulse flows potentially favour the formation of denitrification hot moments. Data comparison from the flow-through basin, with longer water retention durations than the short-term flood experiment, suggests that organic soils at locations that are periodically flooded have greater denitrification rates compared to locations that are always or never flooded. Increased denitrification rates were sustained at the periodically flooded location even when this area was not inundated. Also, nitrous oxide yield at these organic-rich, periodically flooded locations did not correspondingly increase with increased denitrification rates. The increased rates at the periodically flooded zone for the duration of the experiment suggest that a longer duration of inundation, along with wet-dry cycles, enhance denitrification. It can also be inferred that the bacterial community changes under these conditions, leading to the formation of denitrification hot spots.

Combining results collected from short-term flood events, longer inundation periods, and nitrous oxide release rates may provide useful information for potential remediation strategies. Our results suggest that strategies that promote periodical inundation and water retention on the floodplain would increase nitrate removal in an agricultural landscape without increases in nitrous oxide yields.

4 Environmental Drivers of Denitrification Rates and Denitrifying Gene Abundances in Channels and Riparian Areas

4.1 Overview

Intensive agriculture in the Midwestern United States contributes to excess nitrogen in surface water and groundwater, negatively affecting human health and aquatic ecosystems. Complete denitrification removes reactive nitrogen from aquatic environments and releases inert dinitrogen gas. We examined denitrification rates and the abundances of denitrifying genes and total bacteria at three sites in an agricultural watershed and in an experimental stream in Minnesota. Sampling was conducted along transects with a gradient from always inundated (in-channel), to periodically inundated, to non-inundated conditions to determine how denitrification rates and gene abundances varied from channels to riparian areas with different inundation histories. Results indicate a coupling between environmental parameters, gene abundances, and denitrification rates at the in-channel locations, and limited to no coupling at the periodically inundated and non-inundated locations, respectively. Nutrient-amended potential denitrification rates for the in-channel locations were significantly correlated ($\alpha = 0.05$) with five of six measured denitrifying gene abundances, whereas the periodically inundated and non-inundated locations were each only significantly correlated with the abundance of one denitrifying gene. These results suggest that DNA-based analysis of denitrifying gene abundances alone cannot predict functional responses (denitrification potential), especially in studies with varying hydrologic regimes. A scaling analysis was performed to develop a predictive functional relationship relating environmental parameters to denitrification rates for in-channel locations. This method could be applied to other geographic and climatic regions to predict the occurrence of denitrification hot spots.

4.2 Introduction

Anthropogenic activities have greatly altered the global nitrogen cycle, especially in the agriculturally dominated Midwestern United Sates, with severe consequences for human and aquatic health. The creation of synthetic nitrogen fertilizers through the Haber-Bosch process revolutionized modern agriculture and sustains approximately 40% of the world's population (Smil, 2002); however, this process contributes approximately 45% of the total fixed nitrogen produced annually, nearly double the natural rate of terrestrial nitrogen fixation (Canfield et al., 2010). The fixed nitrogen in synthetic fertilizers is most commonly in the ammonia or ammonium form, which when applied to fields is readily converted to nitrate in soils through nitrification (Robertson and Vitousek, 2009). Since most soils in the Midwest are negatively charged, nitrate is not adsorbed by soils, allowing nitrate to readily pass through soil (Di and Cameron, 2002), into tile drains, and directly to surface waters. Studies have reported that 50-70% of the fixed nitrogen applied to soils is lost through various hydrologic and gaseous pathways (Masclaux-Daubresse et al., 2010), and 20-25% of the nitrogen added to the biosphere is exported from rivers to oceans or inland basins (Mulholland et al., 2008). Excess nitrate in water has negative health (Powlson et al., 2008; Ward et al., 2010) and ecological impacts including eutrophication that leads to decreased dissolved oxygen concentrations in water (Rabalais et al., 2007). The Gulf of Mexico hypoxic (dead) zone is one of the largest in the world and is predominantly caused by nitrate export from the Mississippi River watershed (Turner et al., 2006).

Denitrification and anammox are currently the only two known natural microbiological pathways that remove substantial amounts of nitrogen from aquatic systems (Zhu et al., 2013). Anammox is the anaerobic oxidation of ammonium to dinitrogen gas (N_2) using nitrite as the electron acceptor, while denitrification is the step-wise microbiological reduction of nitrate to nitrite, nitric oxide, nitrous oxide, and ultimately to N_2 in complete denitrification. Denitrification is primarily an anaerobic process, but has also been reported to occur in microaerophilic and aerobic systems, and is performed by a diverse range of bacteria and fungi (Zumft, 1997). Denitrification and

dissimilatory nitrate reduction to ammonium (DNRA, also known as nitrate ammonification) provide the highest respiration energy yield after oxygen consumption and are, therefore, widespread across bacteria (Strohm et al., 2007). Small areas of active denitrification, denitrification hot spots, and short time periods, hot moments, frequently account for a great percentage of denitrification activity (Groffman et al., 2009; Guentzel et al., 2014; McClain et al., 2003; O'Connor et al., 2006). Several parameters, including organic carbon quality and concentration (Perryman et al., 2011; Pinay et al., 2000), sediment water content (Pinay et al., 2007), water velocity (Arnon et al., 2007a), sediment oxygen conditions, nitrate concentrations (Inwood et al., 2007), and floodplain location (Roley et al., 2012a), positively affect denitrification rates.

It is commonly assumed that biogeochemical process rates, such as denitrification, are positively correlated to the abundances of specific genes (Rocca et al., 2015). Most studies that consider both denitrification rates and microbial analysis target specific genes in the denitrification pathway, predominantly the nitrite reductase genes *nirS* and *nirK*, and the nitrous oxide reductase gene *nosZ* (Deslippe et al., 2014; Guentzel et al., 2014; Manis et al., 2014). These genes are targeted since the *nir* genes are unique to denitrifiers (Zumft, 1997), and the *nosZ* gene encodes for the final step in denitrification, the conversion of nitrous oxide (N_2O) to N_2, which has implications for greenhouse gas emission (Philippot et al., 2011). Previous studies have shown differing results between denitrification rates and denitrifying gene abundances. Positive correlations have been found between denitrification rates and *nirS* gene abundances in streams (Guentzel et al., 2014), and in estuaries (Smith et al., 2015). However, *Dandie et al.* (2011) found no significant correlations between denitrifying gene abundances (*nirS*, *nirK*, and *nosZ*) and potential denitrification rates across a range of soil conditions. Similarly, no correlation was found between *nirS* abundances and denitrification rates in a wetland with hydrologic pulsing (Song et al., 2010), nor in an urban estuary (Lindemann et al., 2016). Under certain conditions, denitrifying gene abundances appear to influence denitrification rates, but varying environmental conditions (such as pulsed inundations, varying moisture content, or carbon availability) can affect the correlations between genes and rates. Denitrification rates have been shown to vary with inundation

frequencies (Bettez and Groffman, 2012), and between channels and riparian areas in agricultural surface water systems (Mahl et al., 2015; Roley et al., 2012a), but the relationships between environmental and microbial drivers of denitrification rates in both channels and riparian areas remain unclear.

This research investigates the relationship between denitrification rates and gene abundances across channels and riparian areas to determine if environmental parameters, denitrification rates, and gene abundances are correlated under differing hydrologic conditions, and to use these correlations to develop a predictive functional relationship to identify hot spots and hot moments of denitrification activity. We collected soil and water samples from an agricultural watershed to determine variability in denitrification rates and denitrifying gene abundances along a reach and across ditch transects from channel to riparian areas. A scaling analysis was conducted to develop a predictive functional relationship between denitrification rates and environmental parameters for the always-inundated (in-channel) locations. Controlled flood experiments were performed in an outdoor experimental stream to incorporate high-velocity events into these predictive functional relationships. We used a DNA-based analysis to examine the abundances of denitrifying genes for each step in the denitrification pathway, along with total bacterial abundance, for all field sites. The objectives of this study were to: (1) quantify and correlate the driving environmental parameters of microbial denitrification and the differences in these relationships for in-channel and riparian locations in an agricultural watershed, (2) identify how denitrifying gene abundances, denitrification rates, and environmental parameters are related across transects from channels to riparian locations, and (3) develop and evaluate functional relationships between environmental parameters and denitrification rates.

4.3 Site Descriptions and Sampling

4.3.1 Seven Mile Creek Field Site

Sediment and water samples were collected from the Seven Mile Creek (SMC) watershed, an agricultural watershed in the Minnesota River basin in Southern Minnesota

(Figure 4.1). The SMC watershed is heavily tile-drained and land adjacent to SMC is predominantly in a corn-soybean rotation with animal production facilities in the upstream portion of the watershed. The SMC watershed transitions from agricultural ditched headwaters to a meandering trout stream in a county park before its confluence with the Minnesota River. Three sites along the length of SMC, two in the agriculturally dominated landscape (SMC-1 and SMC-2) and one in the county park (SMC-3), were sampled in 2014 (Table 4.1). Three locations along a transect perpendicular to the channel were sampled at SMC-1 and SMC-2. The in-channel location was located in the middle of the channel and was always inundated, the floodzone location was in an area that would periodically be inundated, and the non-floodzone location was within the ditch at an elevation that would not be inundated. The most upstream site, SMC-2, had a small, depositional floodplain at the floodzone location, whereas the floodzone location at SMC-1 had a trapezoidal channel geometry. The SMC-1 and SMC-2 sites had fine-grained sediment throughout the season, whereas sediment texture at the SMC-3 site varied from cobbles in June and October to a sandy organic substrate in August.

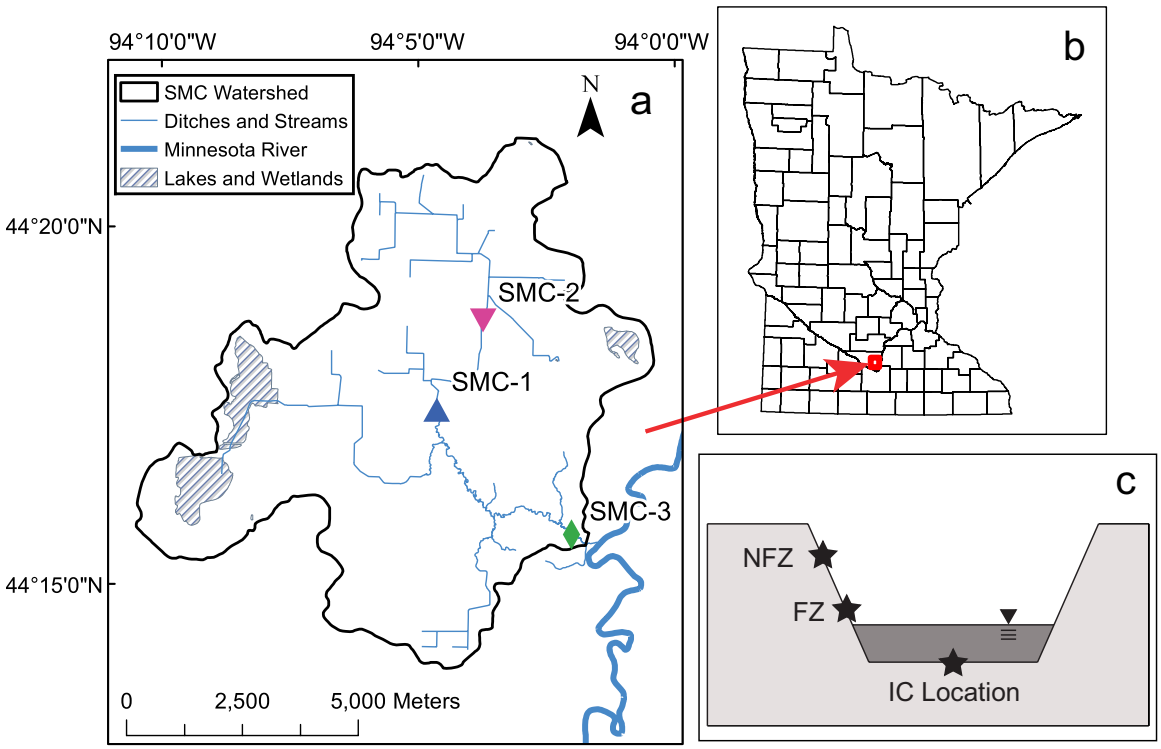

Figure 4.1. Seven Mile Creek (SMC) field sampling sites and (a) location of the sites where samples were collected in the SMC watershed, (b) location of SMC watershed, (c) cross-section schematic of the in-channel (IC), floodzone (FZ), and non-floodzone (NFZ) locations at the two upstream agricultural ditch sites (SCM-1 and SMC-2) in the SMC watershed.

Table 4.1. GPS coordinates of the Seven Mile Creek field sites.

Site	Coordinates
SMC-1	44.2925, -94.0759
SMC-2	44.3117, -94.0614
SMC-3	44.2634, -94.0319

Soil and water samples were collected from the SMC-1, SMC-2, and SMC-3 sites on 12 June, 20 August, and 20 October 2014. Measurements included: channel top width, water width and depth, soil water content, sediment bulk density, and sediment organic matter. Water velocity measurements were obtained using a Sontek Flowtracker (Xylem).

Water quality parameters (water temperature, pH, specific conductance, and dissolved oxygen) were collected using a Hydrolab Series 5 Datasonde (Hach Company, Loveland, CO). Water samples were analyzed for nitrate concentration as described below. Samples from all three sites were collected within an 8 h period on the same day to limit the effect of differing climatic conditions.

Sediment samples were collected at each location in SMC to quantify denitrification rates and the abundances of total bacteria and denitrifying genes. Since the microbial community can vary across small distances, triplicate locations were taken within 5 cm of each other, ensuring that sampling locations did not overlap. A modified 5 mL syringe (with the top removed) was used to collect sediment samples for DNA extraction. The syringes for DNA extraction were immediately placed on dry ice and were transferred to a -80°C freezer upon returning from the field. A modified 35 mL syringe was used to extract sediment for bulk density, water content, and organic matter. A modified 60 mL syringe was used to collect soil cores from the top 5 cm of sediment for quantification of denitrification rates, since most denitrification occurs within this depth (Arango et al., 2007; Inwood et al., 2007). The cores were transferred into a plastic bag, immediately placed on ice, transferred to a 4°C refrigerator at the end of the field day, and processed for potential denitrification rates within 2 days (Findlay et al., 2011).

4.3.2 Experimental Outdoor Stream

An experimental outdoor stream, the Outdoor StreamLab (OSL), located at the St. Anthony Falls Laboratory (SAFL), University of Minnesota, was used to conduct controlled flooding experiments during the summer of 2014. The OSL is a sand-bed, meandering stream with a vegetated floodplain (approximately 40 m by 20 m) that has been continuously running since 2008 and is fed under valve control from the Mississippi River (Guentzel et al., 2014). The OSL is equipped with a sediment feeder to maintain continuous bedload.

Two experimental floods were performed in the OSL, one in late June and one in early July 2014, to incorporate high velocity events into the predictive functional relationships. During the floods, the entire floodplain of the OSL was inundated with at

least 5 cm of Mississippi River water for 4 h. The total discharge during each flood was between 890 and 950 L s^{-1}; baseflow is maintained between 20 and 40 L s^{-1}. Two sites (25 cm apart) were sampled within the channel's middle meander of the OSL. Duplicate sediment samples for measuring denitrification rates were collected from each site immediately before, immediately after, 1 day after, and 3 days after flooding. During the flood, velocity measurements, water width and depth, and stream parameters were collected as was done in SMC. Soil samples used to determine the bulk density, water content, organic matter, and denitrification rates were collected as described above for the SMC.

4.4 Materials and Methods

4.4.1 Nitrate and Environmental Parameters

Triplicate water samples were collected from all in-channel SMC and OSL sites. Water samples were filtered using pre-combusted 0.7 μm Whatman GF/F filters. Nitrate concentrations were determined using the cadmium reduction method on a Lachat QC800 Autoanalyzer (Hach Company). Shear velocities were calculated by collecting velocities at several depths and using the logarithmic relationship between the shear velocity and the variation of time-averaged velocity with water depth (Biron et al., 2004; Schlicting, 1987).

Bulk density, water content, and organic matter were determined from collected sediment cores in duplicate. The volume and wet weight of the sediment cores were recorded, then dried for 24 h at 110°C, or until the weight no longer changed, to determine the sediment dry weight. Bulk density was determined by dividing the dry weight by the volume of sediment. The volumetric water content was determined by subtracting the dry weight from the wet weight and normalizing by the sediment volume and a sediment depth of 5 cm. Dried sediment was then ground and sieved through a 2 mm screen, approximately 5 g was weighed into a crucible, the sediment was dried again to remove introduced moisture and reweighed, and heated to 550°C for 4 h (loss on ignition method) (Heiri et al., 2001). The ash-free dry mass (AFDM) was quantified by

subtracting the ash weight from the dry weight, and the organic matter was determined by normalizing the AFDM in the same way as was done for water content.

Evapotranspiration (ET) was calculated for the floodzone and non-floodzone locations using a temperature-based method modified from Thornthwaite to determine the potential evapotranspiration (PET), and ET was calculated from PET using the relative water content (the ratio of the difference in current water content and the permanent wilting point to the difference in the field capacity of the soil and the permanent wilting point) (Thornthwaite, 1948, Dingman, 2008). Weather data from the Mankato, Minnesota airport (approximately 20 km away from the field site), were used for field weather conditions.

4.4.2 Denitrification and Denitrifying Enzyme Activity

Denitrification rates were determined using the acetylene block method modified from Groffman et al. (1999). In this method, acetylene (C_2H_2) is used to inhibit the reduction of N_2O to N_2 (Groffman et al, 2006; Smith and Tiedje, 1979). The accumulation of N_2O over time is easier to quantify than N_2 due to the high background atmospheric concentration of N_2. This method has several potential limitations. The acetylene block method can underestimate in situ denitrification rates since acetylene inhibits nitrification; therefore, the method does not account for the activity from coupled nitrification-denitrification (Seitzinger et al., 1993). Also, the acetylene block method may not completely inhibit the reduction of N_2O to N_2 (Yu et al., 2010). However, over short incubation times and with the addition of chloramphenicol, denitrification rates measured using the acetylene block method are similar to other methods (Bernot et al., 2003; Roley et al., 2012a). This method is appropriate when addressing denitrification hotspots and measuring potential denitrification for the comparison of sites (Groffman et al., 2006), and for using potential denitrification as an indirect measure of microbial functional diversity (Cavigelli and Robertson, 2000).

Denitrification rates were determined using non-amended site-specific water (referred to as DeN), and potential denitrification rates (referred to as DEA for denitrification enzyme activity) were determined using site-specific water amended with

nutrients. Both DeN and DEA assays were conducted using site-specific water with chloramphenicol added (10 mg L^{-1}) to block de novo protein synthesis and to extend the period of linear N_2O accumulation (Tiedje et al., 1989). Methods described in Loken et al. (2016) were used for both the DeN and DEA assays, with the exception that DEA assays were amended with nitrate (100 mg N L^{-1} as potassium nitrate), carbon (40 mg C L^{-1} as glucose), and phosphate (13.84 mg P L^{-1} as potassium dihydrogen phosphate). N_2O concentrations were analyzed on a gas chromatograph (5890 series II, Hewlett-Packard) equipped with an electron capture detector and a headspace autosampler (Hewlett-Packard 7694). N_2O production was measured as the accumulation of N_2O over the incubation time and was corrected using the Bunsen solubility coefficient (Tiedje, 1982). Denitrification rates (in mg N m^{-2} h^{-1}) were calculated as a function of bulk density and converted to an area rate by assuming that all denitrification occurs in the top 5 cm.

4.4.3 Quantification of Denitrifying Genes

We extracted DNA from 500 mg of sediment using MoBio PowerSoil DNA Isolation Kits (MoBio, Carlsbad, CA). Sediment was stored at -80°C until extraction. DNA was extracted as described by the manufacturer's protocol, except that the centrifuge time during the washing step was extended to 5 min and this step was performed twice to ensure that all DNA passed through the silica membrane filter. DNA concentrations were measured on a Qubit 2.0 fluorometer (Life Technologies).

Polymerase chain reaction (PCR), followed by gel electrophoresis, was used to determine the accuracy and efficiency of the DNA primers for each gene. The genes investigated in this project encompass the full pathway for complete denitrification, and included genes for nitrate reductase (*narG*), nitrite reductase (*nirS and nirK*), nitric oxide reductase (*norB*), and nitrous oxide reductase (*nosZ1* and *nosZ3*). Denitrifiers exist in two *nosZ* baring clades, *nosZ1* and *nosZ2* (Isobe and Ohte, 2014); *nosZ2* was excluded due to unreliable results. Instead *nosZ3*, which overlaps the two clades, was included to obtain better coverage of the final step of denitrification. The primers U515F and U806R (BAC515F) were used to quantify the total 16S rRNA genes in each sample. For all genes except *nirS*, gBlock Gene Fragments (Integrated DNA Technologies, Inc., USA)

were created from the primers for each selected gene. Plasmid standards were used for *nirS* due to the inability of the gBlock *nirS* to function reliably and efficiently with qPCR protocols.

Quantitative PCR (qPCR) was used to determine the concentration of each gene in sediment samples. The qPCR analysis used the SYBR Green Kit and was performed on a Roche Light Cycler 480 Real-Time PCR (Roche Life Sciences, Indianapolis, IN). The specific primers used were U515F and U806R for 16S rRNA (BAC515F), cnorB-BF and cnorB-BR for *norB* (Dandie et al., 2007), narG-1960m2fE and narG2050m2R for *narG* (Kandeler et al., 2006; Lopez-Gutierrez et al., 2004), nirK876F and nirK1040R for *nirK* (Bru et al., 2011, Petersen et al., 2012), m-cd3AF and m-R3cd for *nirS*, nosZ_F and nosZ_1622R for *nosZ1* (Rosch et al., 2002), and nosZ2F and nosZ2R for *nosZ3* (Bru et al., 2011; Petersen et al., 2012). Negative, no-template controls were included with each qPCR run. The qPCR efficiencies for all genes ranged from 80% to110%, with R^2 values over 0.99 for all calibration curves. Gene abundances were normalized per g dry soil for analysis.

4.4.4 Statistical and Scaling Analysis

Statistical analyses were performed to examine the spatial and temporal variability of environmental parameters (nitrate concentrations, soil water content, bulk density, and organic matter content), denitrification rates, and gene abundances (JMP, Version 11.0, SAS Institute Inc.). Multi-factor ANOVAs were used to determine the significance of season, site, and location. For factors that were statistically significant ($\alpha < 0.05$), a Tukey's post-hoc analysis was conducted to determine significant differences between subgroups.

The non-parametric Spearman's ρ, with $\alpha < 0.05$, was used to examine correlations for the denitrifying microbial community in each location (in-channel, floodzone, and non-floodzone). Correlations were determined between environmental parameters and the denitrifying microbial community. Similarly, significant correlations were identified between gene abundances and denitrification rates in each location using Spearman's ρ.

We used a scaling analysis to combine environmental parameters to quantify the overall influence of multiple parameters on denitrification. DeN rates were first compared to several environmental parameters to quantify individual regressions between the parameters and denitrification rates. Parameters were combined to form dimensionless groups using Buckingham's π theorem (Buckingham, 1914; Guentzel et al., 2014; O'Connor et al., 2006). These dimensionless groups are used to describe a process and establish a basis for similarity between the processes on different time and space scales (Warnaars et al., 2007). We formulated dimensionless groups to explain denitrification rates using environmental parameters. A multiple regression analysis was then conducted between the dependent dimensionless group and the independent dimensionless groups to determine the overall scaling relationship. While a multivariate regression using the environmental parameters could be performed, dimensional analysis reduces the number of independent variables and results in dimension-free parameters (Barnes et al., 2007). This method has previously been employed to determine the relationships between environmental parameters and denitrification (Guentzel et al., 2014; O'Connor et al., 2006), and other ecological relationships including cyanobacteria height (Barnes et al., 2007), caddisfly larval mass (Morris et al., 2011), and periphyton biomass (Warnaars et al., 2007). A predictive functional relationship was formulated for in-channel locations including both OSL and SMC sites.

4.5 Results

4.5.1 Nitrate and Environmental Parameters

Environmental parameters for SMC and the OSL are shown for the in-channel locations in Table 4.2, and for the floodzone and non-floodzone locations in Table 4.3. Maximum nitrate concentrations in SMC were very high since SMC drains primarily agricultural land. Nitrate concentrations in the stream varied temporally and spatially during the field season. From the multi-factor ANOVA, sites, dates, and the interaction between sites and dates had a significant effect on nitrate concentrations ($p < 0.001$, $p = 0.05$, and $p < 0.001$, respectively). In June, nitrate concentrations were greatest at SMC-1, but concentrations were much greater at SMC-3 than at SMC-1 and SMC-2 in August and

October. Nitrate concentrations were greatest in June (34 - 40 mg N L^{-1}) and much lower in August and October (<0.01 – 0.40 mg N L^{-1}) at the SMC-1 and SMC-2 sites. Nitrate concentrations at the SMC-3 site were also greatest in June, but remained relatively high (6 mg N L^{-1}) in August and October, likely due to groundwater inflow directly above this site. Groundwater inflow at SMC-3 also influenced the water temperature at this site, with June and October having warmer temperatures and August having cooler temperatures than the SMC-1 and SMC-2 sites. Water running through the OSL comes from the Mississippi River in Minneapolis, MN. Since the OSL lies above the confluence of the Minnesota River, nitrate concentrations were lower (0.45 - 1.0 mg N L^{-1}) than those seen around the same time at SMC.

Table 4.2. Mean[a] Environmental Parameters for In-Channel (IC) Seven Mile Creek (SMC) and Outdoor StreamLab (OSL) sites

Site	Month	C_{NO3} (mg N L^{-1})[b]	u_* (m s^{-1})	H (m)	ρ_b (g cm^{-3})	OM (g cm^{-2})	WC (g cm^{-2})	DO (mg L^{-1})	T (^oC)	DeN (mg N m^{-2} h^{-1})	DEA (mg N m^{-2} h^{-1})
SMC-1 IC	Jun	41	0.004	0.62	1.4	0.20	2.0	9.9	9.7	22.4	24.0
SMC-2 IC	Jun	34	0.008	0.62	1.1	0.22	2.7	6.3	7.6	10.7	24.6
SMC-3 IC	Jun	27	0.007	0.15	1.5	0.10	2.0	11	11	0.51	0.44
SMC-1 IC	Aug	0.01	0.004	0.58	1.4	0.11	1.8	3.6	22	0.36	4.96
SMC-2 IC	Aug	0.01	0.0002	0.23	1.1	0.23	2.7	1.8	23	1.28	38.0
SMC-3 IC	Aug	6.3	0.018	0.13	1.4	0.22	2.1	11	17	11.0	13.8
SMC-1 IC	Oct	0.02	0.004	0.50	1.5	0.18	2.2	9.9	9.7	0.34	15.6
SMC-2 IC	Oct	0.35	0.002	0.10	0.89	0.21	2.7	7.7	6.2	0.93	23.6
SMC-3 IC	Oct	5.8	0.030	0.11	1.6	0.04	1.7	11	11	2.44	2.46
OSL IC LD[c]	Jun	0.98	0.004	0.26	1.5	0.05	1.5	8.6	23	0.24	0.82
OSL IC HD[d]	Jun	0.92	0.098	0.68	1.6	0.07	1.4	8.6	23	0.13	0.16
OSL IC LD[c]	Jul	0.49	0.006	0.28	1.6	0.07	1.7	8.5	24	0.25	0.25
OSL IC HD[d]	Jul	0.45	0.096	0.71	1.8	0.06	1.6	8.5	24	0.08	0.03

[a]Mean is an average of triplicate replicates

[b]Minimum detection limit (MDL) of Lachat QC800 for nitrate analysis is 0.01 mg N L^{-1}

[c]Low discharge (LD)

[d]High discharge (HD)

Table 4.3. Mean Environmental Parameters for Floodzone (FZ) and Non-Floodzone (NFZ) Seven Mile Creek (SMC) site locations.

Site	Month	ρ_b (g cm^{-3})	OM (g cm^{-2})	WC (g cm^{-2})	DeN (mg N m^{-2} h^{-1})	DEA (mg N m^{-2} h^{-1})
SMC-1 FZ	Jun	0.82	0.49	2.6	7.26	41.4
SMC-1 NFZ	Jun	0.64	0.63	1.5	7.68	24.5
SMC-2 FZ	Jun	0.87	0.65	2.0	15.6	49.3
SMC-2 NFZ	Jun	0.70	0.55	1.6	7.97	18.4
SMC-1 FZ	Aug	0.79	0.37	2.4	9.33	26.4
SMC-1 NFZ	Aug	0.64	0.64	2.0	5.69	15.1
SMC-2 FZ	Aug	0.65	0.37	3.1	5.04	42.2
SMC-2 NFZ	Aug	0.69	0.48	0.9	6.55	12.8
SMC-1 FZ	Oct	0.85	0.46	1.3	7.17	22.3
SMC-1 NFZ	Oct	0.85	0.56	1.5	9.09	26.0
SMC-2 FZ	Oct	0.71	0.30	2.5	4.02	14.7
SMC-2 NFZ	Oct	0.82	0.44	1.5	7.37	16.4

Water content, bulk density, and organic matter also varied spatially and temporally between SMC-1 and SMC-2. Date, location, site, and the interactions between date and location, location and site, and date and location and site all had a significant effect on sediment water content (p =0.01, $p < 0.001$, $p < 0.001$, $p < 0.001$, $p = 0.005$, and $p < 0.001$, respectively). Location, site, and the interactions between date and location, date and site, and location and site all had a significant effect on bulk density ($p < 0.001$ for all). Date, location, and the interactions between date and location, date and site, location and site, and date and location and site all had a significant effect on benthic organic matter ($p < 0.001$, $p < 0.001$, $p < 0.001$, $p = 0.005$, $p < 0.001$, and $p = 0.002$, respectively). Comparing channel and riparian areas, the in-channel and floodzone location had similar sediment water content, but both had significantly greater water content than did the non-floodzone location (Tukey's post-hoc, $p < 0.001$). Bulk density was similar at the floodzone and non-floodzone locations, but was much greater ($p <$

0.001) at the in-channel location. Sediment organic matter was greatest at the non-floodzone location, and the in-channel location had the lowest organic matter ($p < 0.001$).

The in-channel conditions at the SMC-1, SMC-2, and SMC-3 sites varied from June to October. In June, water velocities were faster than in August and October, when both SMC-1 and SMC-2 were near stagnant and the SMC-3 site had transitioned from a flowing stream into slow-moving, shallow pools. The organic matter at the SMC-3 site varied temporally and was greater in August than in June and October (Tukey's post-hoc, $p = 0.03$, $p = 0.004$, respectively). In June, the substrate was primarily large cobbles with small, sandy areas near the banks, and the organic matter was 0.09 g cm^{-2}. Extensive flooding occurred across Minnesota between the June and August sampling dates, changing the channel morphology. In August, the dominant bed material was sand and the benthic organic matter was higher than that seen during other field dates (0.22 g cm^{-2}), likely due to the flooding and the delivery of organic-rich sediment from the upstream ditches to the site. The in-channel SMC-3 and OSL sites, which both had sandy substrates and fast velocities, were both very different from the silty sediments and slow velocities at the in-channel SMC-1 and SMC-2 sites. In-channel shear velocity in SMC was significantly different by site (ANOVA, $p < 0.001$), and was much greater at SMC-3 than at both SMC-1 and SMC-2 (Tukey's post-hoc, $p < 0.001$ for both). In-channel OSL locations in the mobile sandy bed had low organic matter content (0.06 g cm^{-2}).

4.5.2 Spatial and Temporal Variability in Denitrification

All sites exhibited denitrification activity as measured by the acetylene block assays, except for DeN at an OSL site 1 day after the June flood. DeN ranged from 0.0 to 22 mg N m^{-2} h^{-1}. In SMC, DeN varied seasonally and spatially (Figure 4.2). Date, location, and the interactions between date and location, and date and location and site all had a significant effect on DeN ($p < 0.001$, $p = 0.05$, $p = 0.005$, and $p = 0.05$, respectively). The in-channel DeN rates were highest in June at both the SMC-1 and SMC-2 sites (22 and 7.3 mg N m^{-2} hr^{-1}, respectively), and decreased to below 1 mg N m^{-2} hr^{-1} in August and October. The SMC-3 site had greater DeN in August (11 m^{-2} hr^{-1}) compared to the low rates in June and October (0.5 and 2.4 mg N m^{-2} hr^{-1}, respectively). The SMC-1 and SMC-2 floodzone and non-floodzone locations had statistically similar DeN rates

throughout the season, except for significantly greater (Tukey's post-hoc, $p < 0.001$) DeN at the floodzone SMC-2 location in June.

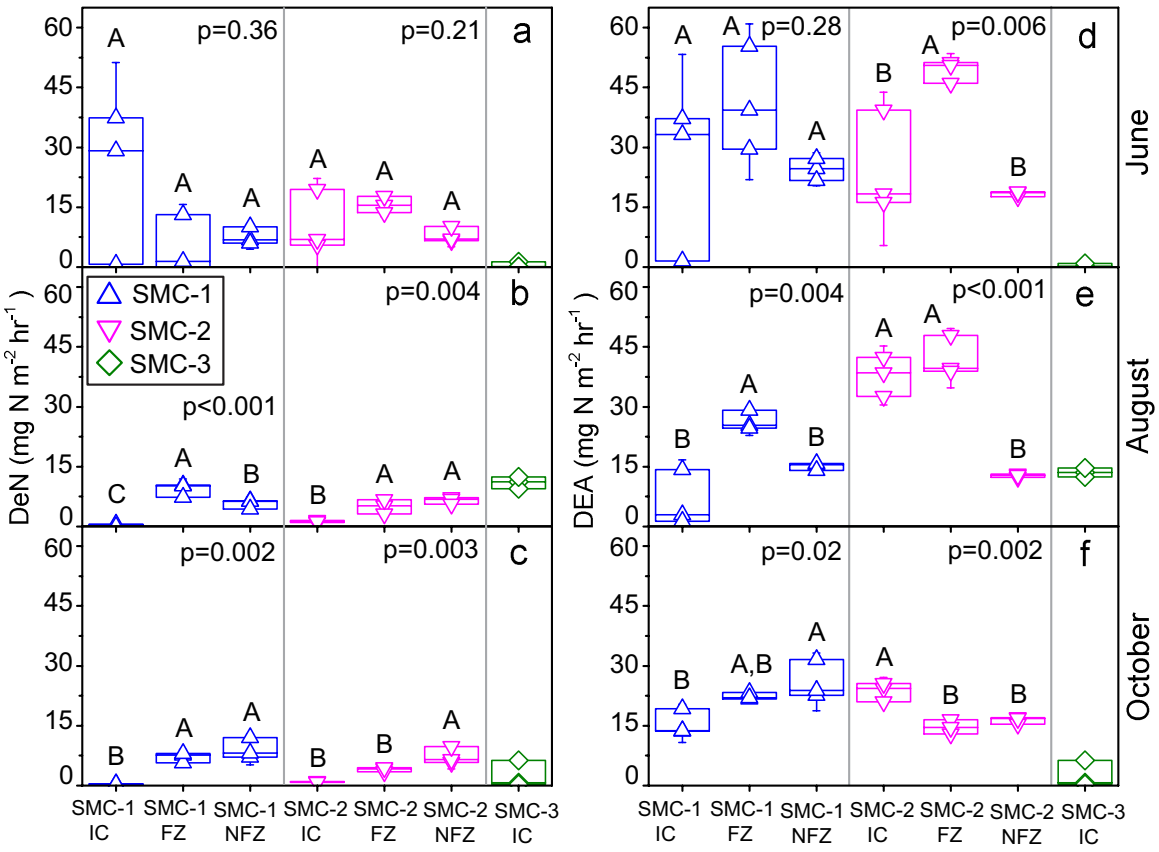

Figure 4.2. Denitrification rates for in-channel (IC), floodzone (FZ), and non-floodzone (NFZ) locations at the SMC-1, SMC-2, and SMC-3 sites in the Seven Mile Creek (SMC) watershed under site conditions (DeN) on the (a) June, (b) August, and (c) October field sampling dates, and non-limiting nutrient conditions (DEA) on the (d) June, (e) August, and (f) October field sampling dates. The p-values represent the statistical significance (one-way ANOVA, $\alpha < 0.05$) of the effect of location (in-channel, floodzone, and non-floodzone) on DeN and DEA rates in SMC-1 and SMC-2 independently for the June, August, and October 2014 sampling dates. Locations that are not connected by the same letter have significantly different denitrification rates than the other locations at each site (SMC-1 and SMC-2 separately) as determined by a Tukey's test. The letters are arranged according to decreasing means. Boxes represent the first and third quartile and whiskers represent ±1.5 of the standard deviation.

The DEA trends also varied seasonally and rates ranged from 0.0 to 49 mg N m^{-2} h^{-1}. Date, location, site, and the interactions between date and location, date and site, location and site, and date and location and site all had a significant effect on DEA ($p < 0.001$, $p < 0.001$, $p = 0.03$, $p < 0.001$, $p < 0.001$, $p < 0.001$, $p = 0.05$, respectively). The SMC-1 site had the greatest DEA at the floodzone location in June. However, the rate was not significantly different from the rate at the other two site locations. In August, the SMC-1 site had the greatest DEA at the floodzone location. In October, the greatest DEA was at the non-floodzone location; however, it was statistically similar to the floodzone location (Tukey's post-hoc, $p = 0.43$). In June and August, the SMC-2 site had the greatest DEA at the floodzone location; in October, the DEA rate was greatest at the in-channel location.

The DEA rates were compared for all field dates based on site and location (comparison between SMC-1 in-channel, floodzone, or non-floodzone locations separately from SMC-2 in-channel, floodzone, or non-floodzone locations). The findings showed that the floodzone location at both SMC-1 and SMC-2 had the highest denitrification enzyme activities. When DEA for all dates and locations were compared between the sites (in-channel, floodzone, and non-floodzone locations combined for each site), site SMC-2 had higher rates than did SMC-1, but they were statistically similar. The rates for both sites, however, were much greater than the rate for SMC-3. When only in-channel locations were compared between sites, the sites were significantly different (ANOVA, $p < 0.001$) and SMC-2 was significantly greater than SMC-1 and SMC-3 (Tukey's post-hoc, $p = 0.02$ and $p < 0.001$, respectively); both SMC-1 and SMC-3 were statistically similar. The ratio between DEA and DeN was significantly different on a seasonal basis ($p = 0.002$) at in-channel locations at SMC-2, with a much higher ratio when nitrate concentrations were low in August and October. Similarly, the DEA to DeN ratio at SMC-1 was seasonally different ($p = 0.05$), with higher ratios in October; while August had low nitrate concentrations, benthic organic matter was significantly less (Tukey's post-hoc, $p = 0.02$) in August at SMC-1 than in June and October.

4.5.3 Denitrifying Gene Abundance

The abundances of denitrifying genes (for *norB*, *narG*, *nirS*, *nirK*, *nosZ1*, and *nosZ3*), along with the total bacterial abundance (using the 16S rRNA gene), were determined for all SMC sites and all locations (in-channel, floodzone, and non-floodzone). The SMC sites contained 10^8 to 10^9 16S rRNA copy numbers per gram dry weight of sediment, a value that is within the range for other agricultural soils (Deslippe et al., 2014). Gene abundances varied by site and location (Figure 4.3 and Table 4.4), with 16s rRNA and four of the six denitrifying genes being significantly different by site and location (ANOVA, p = 0.006 and 0.007, p = 0.04 and <0.001, p = 0.02 and 0.001, and p = 0.02 and 0.002 for *norB*, *nirS*, *nosZ1*, and *nosZ3* at SMC-1 and SMC-2, respectively).

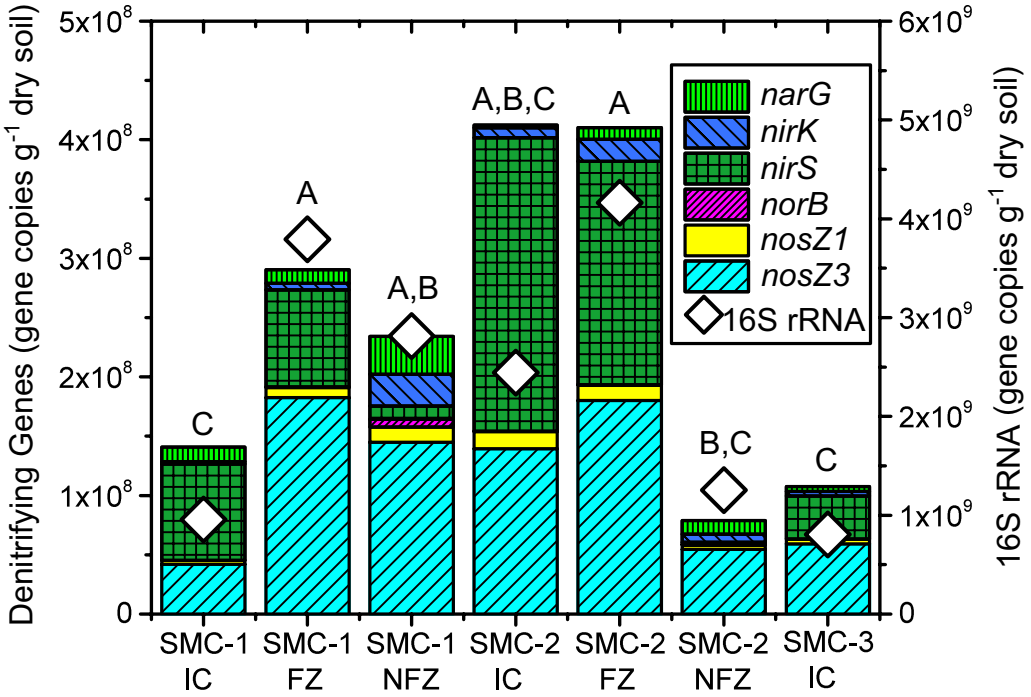

Figure 4.3. Mean denitrifying gene abundances at the in-channel (IC), floodzone (FZ), and non-floodzone (NFZ) locations at the SMC-1, SMC-2, and SMC-3 sites in the Seven Mile Creek (SMC) watershed from June, August, and October. The mean for all genes was determined from the triplicate samples for each date and location. Open diamonds represent the mean abundances of 16S rRNA. The p value represents the statistical significance (one-way ANOVA, $\alpha < 0.05$) of the effect of sites and location on 16S rRNA abundances. Locations that are not connected by the same letter have significantly different 16S rRNA abundances as determined by a Tukey's post-hoc analysis, and the letters are arranged according to decreasing means.

Table 4.4. Mean abundances of 16S rRNA and denitrifying genes expressed as gene copies per gram of dry soil at the in-channel (IC), floodzone (FZ), and non-floodzone (NFZ) locations at the three sites in the Seven Mile Creek (SMC) watershed. The mean was determined from the triplicate samples for each date and location.

Site	16S rRNA	*norB*	*narG*	*nirS*	*nirK*	*nosZ1*	*nosZ3*
SMC-1 IC	9.55E8	7.04E4	1.24E7	8.15E7	1.84E6	3.24E6	4.19E7
SMC-1 FZ	3.79E9	5.22E5	1.16E7	8.17E7	5.35E6	8.69E6	1.82E8
SMC-1 NFZ	2.81E9	6.52E6	3.82E7	1.12E7	2.67E7	1.29E7	1.45E8
SMC-2 IC	2.44E9	1.38E5	2.11E6	2.48E8	8.50E6	1.44E7	1.40E8
SMC-2 FZ	4.16E9	4.68E5	9.82E6	1.88E8	1.86E7	1.31E7	1.80E8
SMC-2 NFZ	1.26E9	2.26E5	1.27E7	2.16E6	6.66E6	3.82E6	5.45E7
SMC-3	8.07E8	3.98E4	3.94E6	3.63E7	3.92E6	3.98E6	5.93E7

Total bacterial abundance, as determined from 16S rRNA, was significantly different by site and location (ANOVA, $p < 0.001$). The abundance of 16S rRNA was greatest at the floodzone locations of SMC-1 and SMC-2, and the lowest at the in-channel locations at SMC-1 and SMC-3 (Figure 3). The non-floodzone locations at both SMC-1 and SMC-2 had a different denitrifying gene abundance profile than did the floodzone and in-channel locations, most notably the smallest abundance of *nirS*. The abundances of *nirS* were statistically similar ($\alpha = 0.05$) at SMC-3 and the non-floodzone locations of SMC-1 and SMC-2, and these abundances were less than those found at all other sites and locations.

Correlations between denitrification rates and environmental parameters to gene abundances were quantified separately for the in-channel, floodzone, and non-floodzone locations using a Spearman's ρ correlation (Table 4.5, Table 4.6, and

Table 4.7). DeN was only significantly ($\alpha = 0.05$) correlated with 16S rRNA at the in-channel location, and with *norB* at the floodzone location; there were no significant correlations between DeN and genes at the non-floodzone location. The in-channel location had the greatest number of significant correlations between gene copy numbers,

environmental parameters, and DEA rates. Five of the six denitrifying genes were significantly positively correlated with DEA at the in-channel location, whereas the floodzone and non-floodzone locations were each only significantly correlated with the abundance of one denitrifying gene (positively correlated with *narG* and negatively correlated with *nirK*, respectively).

Table 4.5. Correlations between gene copy numbers per gram dry soil, organic matter (OM), water content (WC), bulk density (ρ_b), nitrate concentration (C_{NO3}), DeN rates, and DEA rates for in-channel locations in Seven Mile Creek (SMC) represented with Spearman's ρ and the significance (p). Only significant correlations ($\alpha > 0.05$) are shown.

	16S rRNA		*norB*		*narG*		*nirS*		*nirK*		*nosZ1*		*nosZ3*	
	ρ	p	ρ	p	ρ	p	ρ	p	ρ	p	ρ	p	ρ	p
OM	.76	<.01	.55	<.01			.64	<.01	.68	<.01	.67	<.01	.69	<.01
WC	.70	<.01	.59	<.01			.71	<.01	.56	<.01	.60	<.01	.68	<.01
ρ_b	-.73	<.01	-.53	<.01			-.63	<.01	-.45	.02	-.49	.01	-.63	<.01
C_{NO3}			-.40	.04					-.41	.03				
DeN	.44	.02												
DEA	.73	<.01	.58	<.01			.74	<.01	.50	<.01	.55	<.01	.60	<.01

Table 4.6. Correlations between gene copy numbers per gram dry soil, organic matter (OM), water content (WC), bulk density (ρ_b), DeN rates, and DEA rates for floodzone locations in Seven Mile Creek (SMC) represented with Spearman's ρ and the significance (p). Only significant correlations ($\alpha > 0.05$) are shown.

	16S rRNA		*norB*		*narG*		*nirS*		*nirK*		*nosZ1*		*nosZ3*	
	ρ	p	ρ	p	ρ	p	ρ	p	ρ	p	ρ	p	ρ	p
OM							-.68	<.01					-.54	.02
WC					.57	.01	.62	<.01	.49	<.01				
ρ_b							-.55	.02						
DeN			.56	.02										
DEA					.49	.04								

Table 4.7. Correlations between gene copy numbers per gram dry soil, organic matter (OM), water content (WC), bulk density (ρ_b), DeN rates, and DEA rates for non-floodzone locations in Seven Mile Creek (SMC) represented with Spearman's ρ and the significance (p). Only significant correlations ($\alpha > 0.05$) are shown.

	16S rRNA		*norB*		*narG*		*nirS*		*nirK*		*nosZ1*		*nosZ3*	
	ρ	p	ρ	p	ρ	p	ρ	p	ρ	p	ρ	p	ρ	p
OM			.57	.02										
WC									-.64	<.01				
ρ_b														
DeN														
DEA									-.61	<.01				

4.5.4 Scaling Analysis

DeN rates were compared with several controlling environmental parameters. For the in-channel locations (Figure 4.4), DeN was negatively related to increasing shear stress velocity at the sediment-water interface (u_*), increasing water depth (H), and soil bulk density (ρ_B). DeN was positively related to organic matter (OM), water content (WC), and nitrate concentration (C_{NO3}). However, only the trends for bulk density, organic matter, and water content were significant (regression analysis, $p = 0.005$, $p < 0.001$, and $p < 0.001$, respectively). Trends for the floodzone and non-floodzone locations were considered separately from the in-channel locations since our analysis revealed differential responses between denitrification rates, environmental parameters, and gene abundances based on location (Figure 4.2, Figure 4.3, Table 4.5, Table 4.6, and Table 4.7). DeN for SMC floodzone and non-floodzone locations were significantly positively correlated with bulk density and organic matter (regression analysis, $p = 0.04$ for both), with no significant relationship between DeN and water content (Figure 4.5).

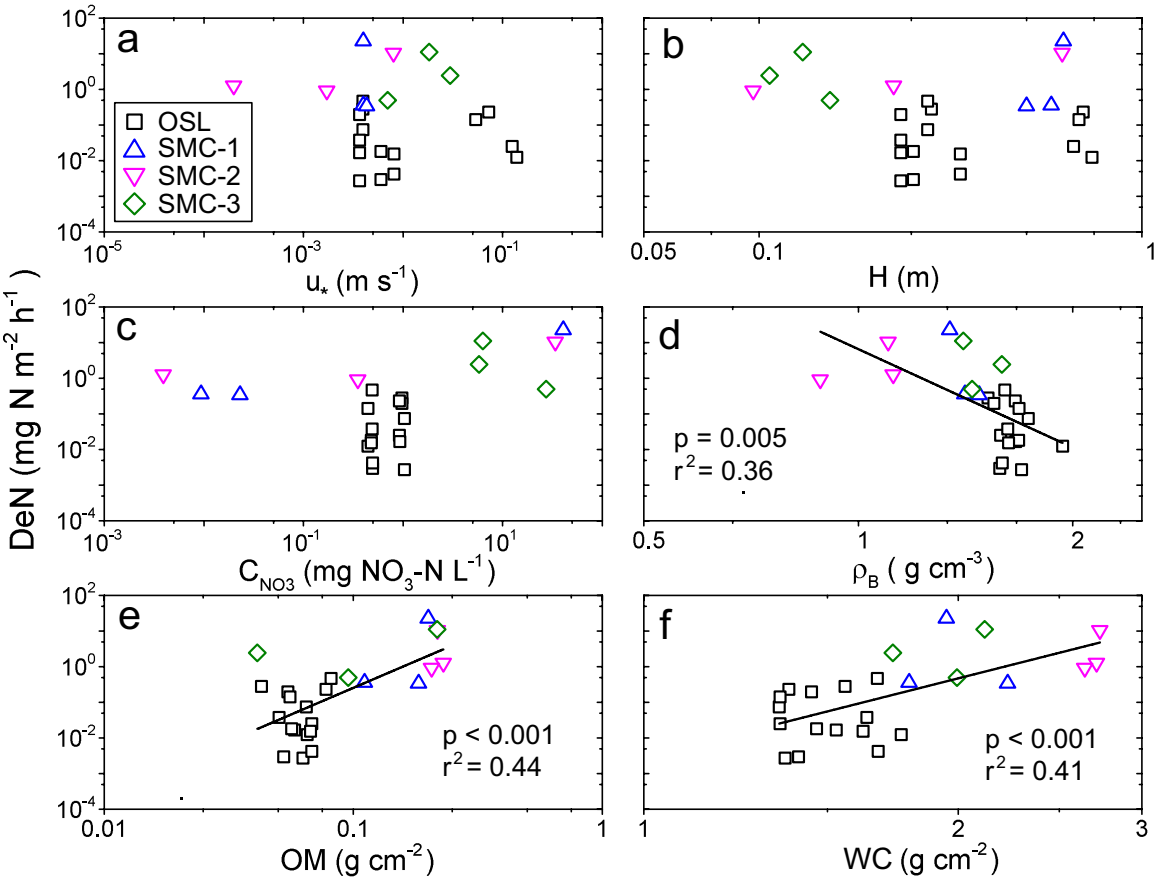

Figure 4.4. DeN as a function of individual parameters including (a) stream shear velocity (u_*), (b) water depth (H), (c) water nitrate concentration (C_{NO3}), (d) bulk density (ρ_b), (e) organic matter (OM), and (f) sediment water content (WC) for in-channel locations in the Seven Mile Creek (SMC) watershed and the Outdoor StreamLab (OSL). The *p* values represent the statistical significance of the regressions ($\alpha < 0.05$) between environmental parameters and denitrification rates.

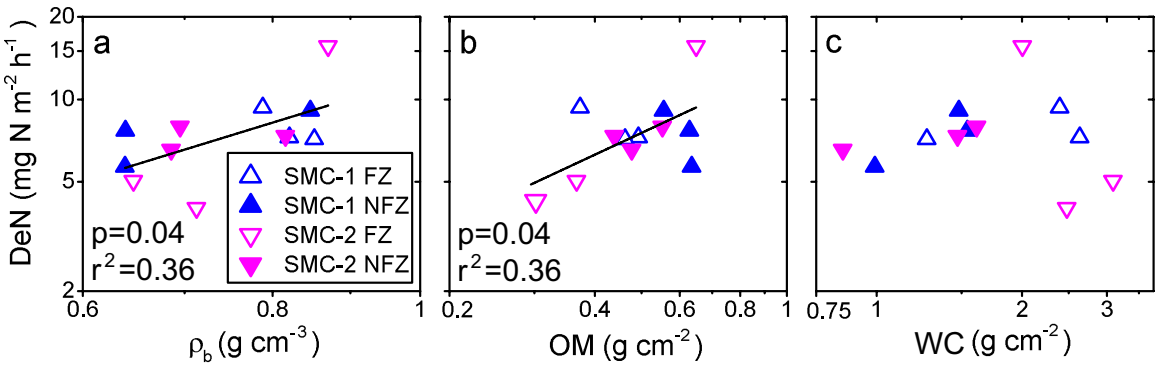

Figure 4.5. DeN as a function of individual parameters including (a) bulk density (ρ_b), (b) organic matter (OM), and (c) sediment water content (WC) for floodzone (FZ) and non-floodzone (NFZ) locations in the Seven Mile Creek (SMC) watershed. The *p* values represent the statistical significance of the regressions ($\alpha < 0.05$) between environmental parameters and denitrification rates.

The parameters were combined to form dimensionless groups and overall dimensionless functional relationships were developed, one for in-channel locations and one for floodzone and non-floodzone locations. For the following dimensionless groups, parameters are described above with the addition of υ, which represents the viscosity of water, ET that represents evapotranspiration, and w is channel top width. For in-channel locations, the dimensionless nitrate uptake $\left\langle \frac{DeN}{u_* C_{NO3}} \right\rangle$ was the dependent group and was analyzed against the independent dimensionless groups including Reynolds number $\left\langle \frac{u_* H}{\nu} \right\rangle$, organic carbon ratio $\left\langle \frac{OM}{WC} \right\rangle$, and interstitial space $\left\langle \frac{\rho_b}{C_{NO3}} \right\rangle$ individually to explore a power law scaling between the dependent and independent groups (Figure 4.6 and Figure 4.7). The proposed scaling explained 71% of the variation for in-channel dimensionless nitrate uptake. To expand on the robustness of the proposed scaling, additional data were added to the SMC and OSL data sets, including field data from SMC in 2015 and from multiple sand-bed streams across Minnesota (Guentzel et al., 2014) (Figure 4.8). The overall scaling relationship (Equation 4.1) was determined by a multiple regression analyses between the dependent versus independent groups,

explained 59% of the variation for in-channel dimensionless nitrate uptake. The resulting scaling relationship for nitrate uptake is as follows:

$$\left\langle \frac{DeN}{u_* C_{NO3}} \right\rangle = 10^{-5/2} \left\langle \frac{u_* H}{\nu} \right\rangle^{-5/6} \left\langle \frac{OM}{WC} \right\rangle^{7/4} \left\langle \frac{\rho_b}{C_{NO3}} \right\rangle^{1/2} \qquad \text{(Equation 4.1)}$$

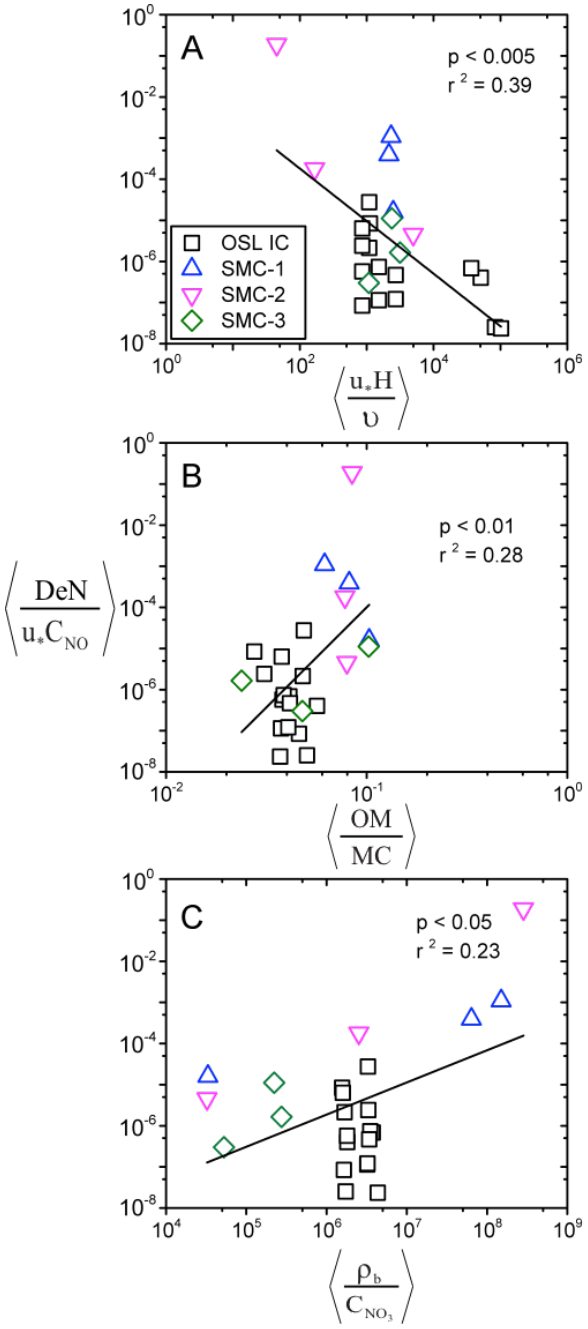

Figure 4.6. Dimensionless nitrate uptake $\left\langle \frac{DeN}{u_* C_{NO3}} \right\rangle$ verses (a) dimensionless shear Reynolds number $\left\langle \frac{u_* H}{\nu} \right\rangle$, (b) dimensionless carbon ratio $\left\langle \frac{OM}{WC} \right\rangle$, and (c) dimensionless interstitial space $\left\langle \frac{\rho_b}{C_{NO3}} \right\rangle$ across all IC locations for the 2014 field season. Each symbol represents the average of three samples.

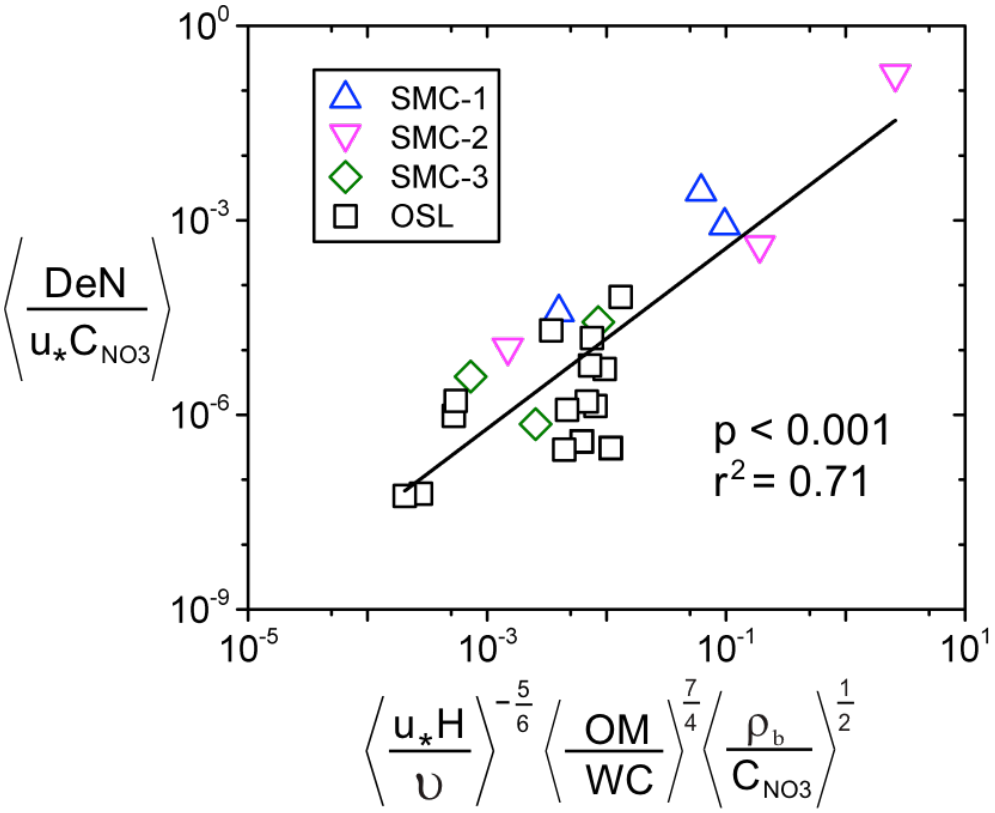

Figure 4.7. Relationship between dimensionless nitrate uptake, Reynolds number, dimensionless carbon ratio, and dimensionless interstitial space for in-channel locations in the Seven Mile Creek (SMC) watershed and the Outdoor StreamLab (OSL) in 2014. The *p* value represents the statistical significance ($\alpha < 0.05$) of the regression analysis of the scaling relationship between dimensionless nitrate uptake and the dimensionless groups.

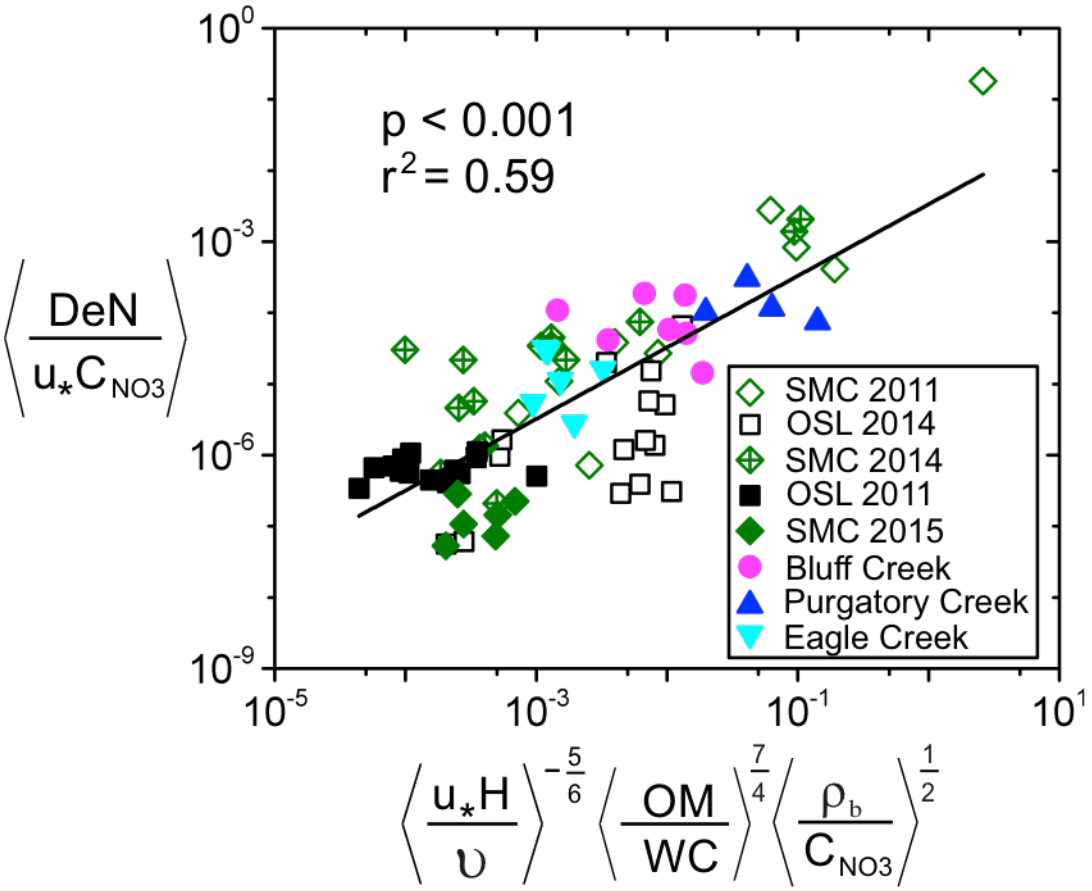

Figure 4.8. The relationship between dimensionless nitrate uptake, Reynolds number, dimensionless carbon ratio, and dimensionless interstitial space for data presented in this paper, along with data from SMC-1, SMC-2, and SMC-3 in 2015, and various streams across Minnesota (Guentzel et al., 2014). The *p* value represents the statistical significance ($\alpha < 0.05$) of the regression analysis of the scaling relationship between dimensionless nitrate uptake and the dimensionless groups.

The same approach was taken when creating the floodzone and non-floodzone functional relationship. The dimensionless NO_3^- uptake $\left\langle \frac{DeN}{ET\,\rho_b} \right\rangle$ was plotted against dimensionless evapotranspiration $\left\langle \frac{ET\,w}{\nu} \right\rangle$, and the dimensionless carbon ratio $\left\langle \frac{OM}{WC} \right\rangle$ to determine the exponents for the relationship (Figure 4.9). Using 2014 field data, the dimensionless relationship plotted on a log-log plot described 90% of the variation for the

floodzone and non-floodzone locations (Figure 4.10). However, when 2015 field data was added to the equation, the relationship was not statistically significant ($\alpha < 0.05$) (Figure 4.11), and the predictive functional relationship was less correlated to nitrate uptake than individual environmental parameters (Figure 4.5).

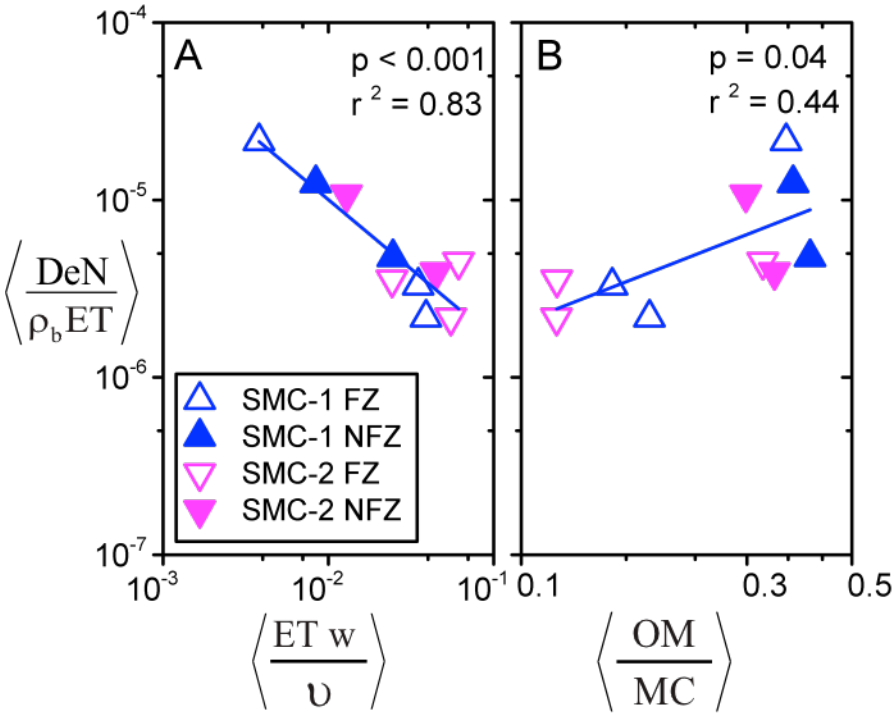

Figure 4.9. Dimensionless nitrate uptake $\left\langle \frac{DeN}{ET\,\rho_b} \right\rangle$ verses (a) dimensionless evapotranspiration $\left\langle \frac{ET\,w}{\nu} \right\rangle$, and (b) dimensionless carbon ratio $\left\langle \frac{OM}{WC} \right\rangle$ for FZ and NFZ locations at the SMC field sties in 2014. Each symbol represents the average of three samples.

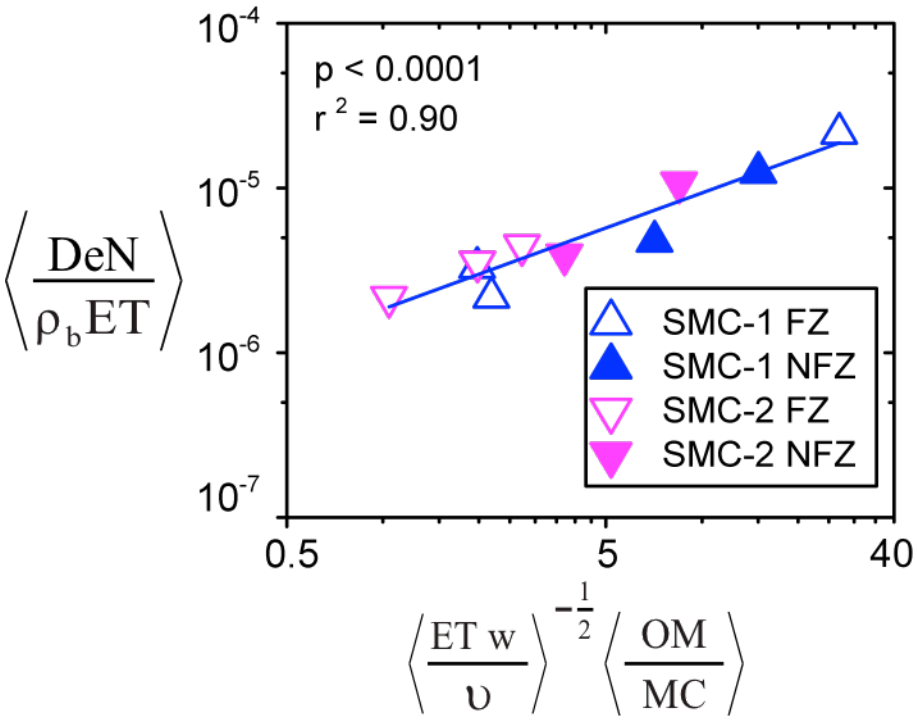

Figure 4.10. The relationship between dimensionless NO_3^- uptake and other dimensionless groupings for Seven Mile Creek (SMC) floodzone (FZ) and non-floodzone (NFZ) locations in 2014. Each symbol represents the average of three samples.

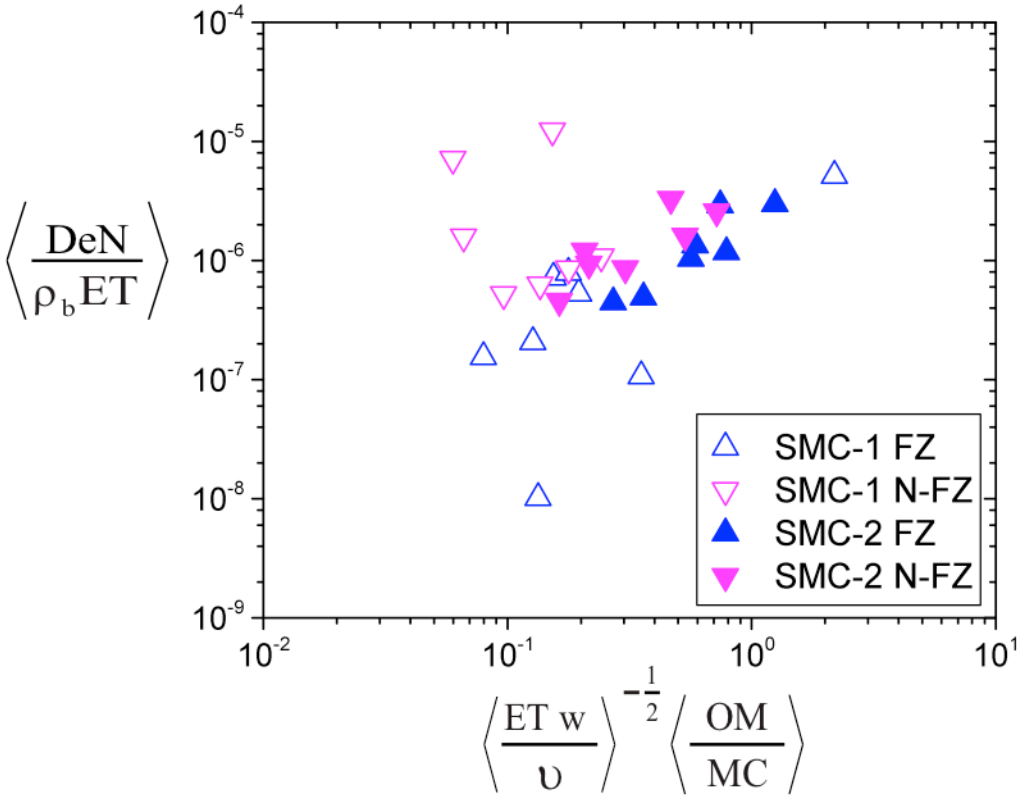

Figure 4.11. The relationship between dimensionless NO_3^- uptake and other dimensionless groupings for Seven Mile Creek (SMC) floodzone (FZ) and non-floodzone (NFZ) locations for both 2014 and 2015. Each symbol represents the average of three samples.

4.6 Discussion

4.6.1 Environmental Parameters and Denitrification Rates

Both DeN and DEA rates varied temporally and spatially. In this study, the DeN rates were within the range reported for agricultural systems (Mahl et al., 2015; Pina-Ochoa and Alvarez-Cobelas, 2006; Roley et al., 2012a). Also, DeN rates measured in this study were similar to those from published data using multiple methods and were dependent on nitrate concentrations (Roley et al., 2012a). One explanation for the variation of DeN rates for in-channel locations is the large seasonal fluctuations in nitrate concentration at

the SMC sites. Nitrate concentrations were very high in June and much lower in August and October. This seasonal pattern of nitrate concentrations is typical of agricultural systems, with high nitrate loads in late fall, winter, and early spring, and lower concentrations in the summer (Johnson et al., 1997; Quinn et al., 1997; Schaller et al., 2004). Nitrate acts as an electron acceptor in denitrification and under limiting nitrate conditions denitrification rates are reduced. Nitrate limitation was previously reported in small streams at 0.4 mg NO_3-N L^{-1} (Inwood et al., 2007) and 0.9 NO_3-N L^{-1} in a river-reservoir continuum (Wall et al., 2005), although this concentration could be as great as 5 NO_3-N L^{-1} in agricultural systems (Mahl et al., 2015). The low nitrate concentrations later in the year at the SMC-1 and SMC-2 sites most likely explain the decrease in in-channel denitrification rates at these locations and the greater difference between DeN and DEA. A large ratio between DEA and DeN could indicate a nutrient limitation, where bacteria could denitrify more but are limited under current site conditions. This relationship is shown in Figure 4.12a, where low nitrate concentrations resulted in high ratios between DEA to DeN. The increase in the DEA to DeN ratio was not seen at the OSL sites where benthic organic matter was very low. A power law was fitted to the SMC data, excluding the OSL sites, and the resulting trend explained 79% of the variation of the DEA to DeN ratio. When OSL data were included, the resulting trend explained 33% of the DEA to DeN ratio. SMC-3 maintained a high nitrate concentration throughout the year, most likely due to the groundwater inflow above the site, and did not experience the seasonal differences between DEA and DeN rates.

Organic carbon availability also has a large effect on DeN rates. The SMC-3 site in June and October and the OSL sites had sandy sediments with low organic carbon and low DeN rates. DeN rates were greater in August than at the other dates at SMC-3 when sediment organic matter was greater. DeN rates at SMC-3 and the OSL were similar to DEA rates for all sampling dates, suggesting that these sites were expressing almost their full potential of denitrification and that these sites are potentially limited in even forming an established denitrifying bacterial community. This could be due to the characteristics of the sandy sediment, or with higher stream velocities and a mobile sand bed, the sediment microbial communities were disrupted and bacterial growth was inhibited. This suggestion is supported by the microbial data at SMC-3, where overall bacterial

abundance and denitrifying gene abundances were regularly in the lowest quantile for all sites and locations. Figure 4.12b shows the effect of benthic organic matter verses the ratio of DEA to DeN. At the OSL sites, which had low organic matter and low nitrate concentrations, denitrification rates did not increase by adding nutrients. However, at sites with benthic organic matter >0.1 g cm^{-2} and with nitrate concentrations <5 mg NO_3-N L^{-1}, denitrification rates increased when nutrients were added. This relationship combined with that shown in Figure 4.12a suggests a co-limitation between sediment benthic organic matter and water nitrate concentrations.

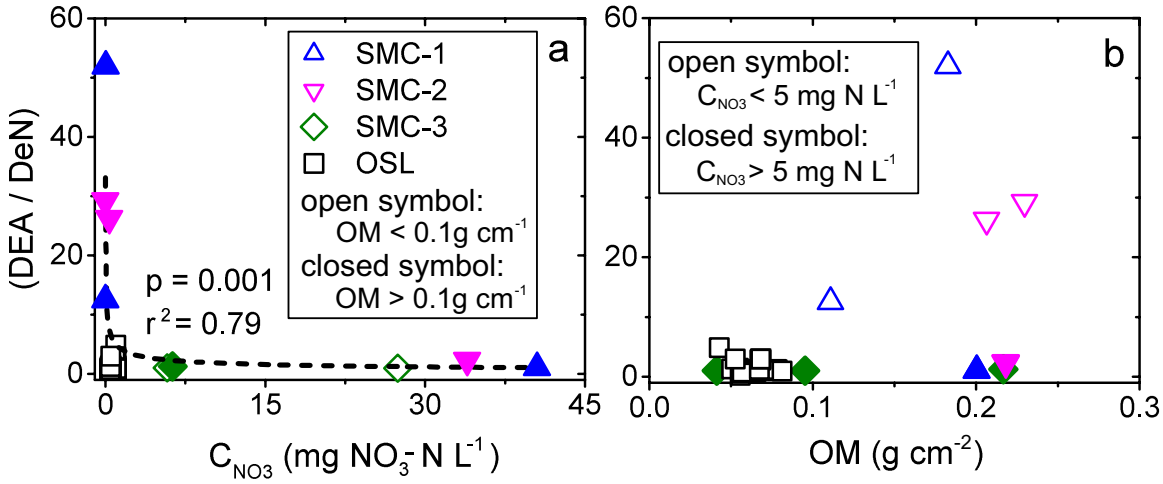

Figure 4.12. Ratio between in-channel denitrification rates using site-specific water as collected (DeN), and amended with phosphate, nitrate, and carbon (DEA) relative to (a) site water nitrate concentration, and (b) benthic organic matter of the sediment for in-channel locations in the Seven Mile Creek (SMC) watershed and the Outdoor StreamLab (OSL). In (a), open symbols represent sites with benthic organic matter <0.1 g cm-2, and in (b), open symbols represent sites where water nitrate concentration was <5 mg NO3-N L-1. The dotted line in (a) represents the power law fitted to the SMC data, excluding the OSL sites, and the p-value represents the significance ($\alpha < 0.05$) of the fitted power law equation.

Site inundation and agricultural ditch geometry can affect nitrate uptake rates. Ditch sites in this study had differing geometry. The SMC-2 site had an inset depositional floodplain at the floodzone location, whereas the SMC-1 site is trapezoidal with relatively steep banks. Several studies have shown that periodic inundation can increase

denitrification rates, due in large part to factors such as coupled nitrification-denitrification, increases in organic carbon, and changes in nutrient availability (Capps et al., 2014; Shrestha et al., 2014; Woodward et al., 2015). DeN rates at both the SMC-1 and SMC-2 floodzone locations were greater than rates for the in-channel locations in August and October, and DEA rates at both floodzone locations were greater in June and August. Sites with floodplain benches, like the floodzone location at SMC-2, provide additional benefits for nitrate uptake through denitrification by providing increased bioreactive surface area, increases in water residence time, slower water velocities and reduced shear stress, and increases in sediment deposition (Mahl et al., 2015; Roley et al., 2012a; Roley et al., 2012b). Mahl et al. (2015) documented increased nitrogen removal when floodplain benches were inundated (3-fold to 24-fold increase), and sites with more frequent flooding events experienced higher annual nitrogen removal. In this study, the floodzone location within the depositional floodplain of SMC-2 had a higher DeN rate than the SMC-1 floodzone location in June; DEA rates were higher at the floodzone SMC-2 location than at the floodzone location at SMC-1 in June and August. Remediation strategies that create sites that periodically flood, and especially strategies that include constructed floodplains, have the potential to increase nitrate uptake in agricultural ditches.

4.6.2 Scaling Relationship

Due to variability and multiple controlling biotic and abiotic factors, denitrification is an especially difficult process to predict (Groffman et al., 2006). Using a scaling analysis, denitrification rates and environmental parameters were combined to form dimensionless groups, and these assemblages were analyzed to develop a functional relationship for denitrification rates at in-channel locations. An important aspect of the dimensionless analysis is that the by forming dimensionless groups, trends for the entire group of parameters are considered, rather than trends for individual parameters. We designated the dimensionless nitrate uptake as the dependent group $\left\langle \frac{\mathrm{DeN}}{u_* C_{NO3}} \right\rangle$, which represents the ratio between potential microbiological nitrate removal rate by denitrifying bacteria in the sediment $\left(\mathrm{DeN}\right)$ and the convective nitrate flux that is delivered to the sediment by the

turbulent vertical fluid flow momentum flux $\left(u_* C_{NO3}\right)$. This ratio is much less than 1 ($\left\langle \frac{DeN}{u_* C_{NO3}} \right\rangle << 1$, Figure 6 and Figure 7), indicating that the overall nitrate removal rate is controlled by the denitrifying activity of the bacteria in the sediment. The proposed scaling relationship (Equation 1) suggests that the dimensionless nitrate uptake is inversely related to the Reynolds number $\left\langle \frac{u_* H}{\nu} \right\rangle^{-5/6}$, and related to the dimensionless carbon ratio $\left\langle \frac{OM}{WC} \right\rangle^{7/4}$ and interstitial space $\left\langle \frac{\rho_b}{C_{NO3}} \right\rangle^{1/2}$. Thus, as the Reynolds number increases, there is: (1) less sediment-water contact time, (2) inhibited denitrification due to the increased convective flux of oxygen into the sediment, and (3) increased turbulence causing sediment bed mobility, thereby disrupting the bacterial community. The dimensionless carbon ratio provides an indication of the amount of available carbon in the sediment for a given water content. Since denitrification is a heterotrophic process and positively related to organic carbon (Figure 4.4e), it is logical that the trend with dimensionless nitrate uptake is positive. The positive trend between interstitial space and dimensionless nitrate uptake could indicate that increasing interstitial space leads to increased area for denitrifying bacteria (Solomon et al., 2009). However, very high interstitial space, indicating sediments with very high porosity, could cause more oxygen to diffuse into the sediment, leading to decreased denitrification.

The proposed scaling relationship was validated by adding an additional year of data (2015) from Seven Mile Creek and including data from multiple watersheds over additional years (Guentzel et al., 2014) (Figure 4.8). This relationship for in-channel locations (Equation 1) enables the prediction of denitrification rates from measureable environmental parameters and can facilitate the prediction of denitrification hot spots. The scaling approach to predict nitrate uptake in floodzone and non-floodzone areas described 90% of the variation in the 2014 SMC data, but was not significant when 2015 field data was added. This may be due to the fact that 2015 was a much wetter year than was 2014, causing the floodzone locations to undergo more frequent wetting-drying

cycles. This change in hydrologic variability likely caused the differences in the relationship between environmental parameters and denitrification rates (Banerjee et al., 2016). Wetting and drying cycles cause paired nitrification-denitrification (Baldwin and Mitchell, 2000; Xiang et al., 2008), which could increase bacterial abundances and denitrification activities. Therefore, the inclusion of inundation frequency and history with the variability of water content, which is not available in our study, could provide a more robust scaling analysis for the floodzone.

4.6.3 Coupling Between Denitrifying Gene Abundances, Denitrification Rates, and Environmental Parameters

Investigating the relationships between denitrifying gene abundances, denitrification rates, and environmental parameters addresses the question of whether increased denitrification rates in a landscape is a physiological response, in which rates increase due to favorable environmental conditions, or a population response, in which rates increase due to an increase in denitrifiers. The differences in denitrifying gene abundances at the in-channel, floodzone, and non-floodzone locations, along with differing rates of denitrification, suggest that the correlation between environmental parameters, denitrification rates and denitrifying microbial community at these locations are differentially coupled. The in-channel locations had multiple significant relationships between environmental parameters, denitrification rates, and gene abundances, while the floodzone locations had fewer significant correlations, and the non-floodzone locations had only three significant correlations (Table 4.5, Table 4.6, and Table 4.7). Both DeN and DEA rates at the in-channel and floodzone locations varied from June to October, whereas the non-floodzone had similar DeN and DEA rates throughout the season. The denitrifying gene abundance profiles at the in-channel and floodzone sites were more similar than those at the non-floodzone location, most notably with *nirS* abundances. The abundances of *nirS* were similar between the non-floodzone locations at SMC-1 and SMC-2, but were different from every other site and location. Previous research showed that *nirS* gene fragments could be amplified from marsh soil but not from forested upland soils (Prieme et al., 2002).

Guentzel et al. (2014) previously reported that *nirS* gene copy numbers per gram soil were positively related to DEA rates for in-channel locations, but other site locations were not investigated. The positive relationship between DEA and several denitrifying genes seen in in-channel locations, but not at the floodzone or non-floodzone locations, indicates that DNA-based gene abundances alone are not a complete indicator for DEA at all site locations. DNA-based measurements of gene abundances provide a picture of what denitrifying genes are present in a soil sample; however, these measurements do not show whether genes are actively transcribed. A recent review of several studies tying biogeochemical process rates to gene abundances found a broad positive relationship between the two, but suggested that the variation in correlation strength indicates that gene abundances cannot be used blindly as a proxy for process rates. Instead, the relationship must be investigated at the site-scale before abundances can be used to infer rates (Rocca et al., 2015). Our results confirm this finding and suggest that the relationship between biogeochemical processes and gene abundances varies not only between sites, but also between small distances at the same site under different environmental conditions.

Determining whether the differences seen in denitrification rates are due to a metabolic or population response is not straightforward and depends on location. For in-channel sites, where there were several positive significant relationships between gene abundances and denitrification rates, differential rates seen across the season could be due to changes in microbial populations, with higher abundances leading to higher rates. However, at the non-floodzone sites, where there were no significant positive relationships between denitrification rates and denitrifying gene abundances, population increases in denitrifying bacteria may have had no effect on rates. Our findings suggest that the hydrologic regime of a site must be considered when trying to understand nitrogen dynamics at a site and when planning for potential management strategies.

4.7 Conclusion

Denitrification rates in an agricultural landscape varied temporally, spatially, and across transects from channels to riparian areas with different inundation frequencies. Locations that were periodically inundated were found to have equal, and occasionally greater,

denitrification rates than always inundated locations. This finding has implications for agricultural remediation strategies such as constructed floodplain benches, in which nitrogen uptake would be increased if the bioreactive surface area was increased and high nitrate water was delivered to the floodplain bench. Denitrifying gene abundances, denitrification rates, and environmental parameters were closely coupled at locations that were always inundated, but little to no coupling was seen at the periodically and non-inundated locations, respectively. This finding suggests that DNA-based analysis of denitrifying gene abundances alone cannot predict functional responses (denitrification potential), especially in studies with varying hydrologic regimes. Denitrification rates and environmental parameters were combined to formulate dimensionless groups and ultimately a predictive scaling relationship that can be used to estimate nitrate removal on agricultural landscapes. This method could be applied to other geographic and climatic regions to predict the occurrence of denitrification hot spots.

5 The Effect of Varying Hydrologic Connectivity on Denitrification Rates and Microbial Community Composition

5.1 Overview

While modern developments in agriculture have allowed for increases in crop yields and rapid human population growth, they have also drastically altered biogeochemical cycles, including the biotransformation of nitrogen. Denitrification is a critical process performed by bacteria and fungi that removes nitrate in surface waters, therefore serving as a potential natural remediation strategy. In Chapter 4, it was found that constant inundation resulted in a coupling of denitrification gene abundances, environmental parameters, and denitrification rates, however these relationships were not maintained in periodically-inundated and non-inundated regions. This chapter combines data from two years, a normal precipitation year and an above-average year, to further understand the effect that legacy hydrologic connectivity has on the relationships between environmental parameters, denitrification rates, and gene abundances. In addition, Illumina next-generation sequencing, performed by Christopher Staley and Ping Wang at the University of Minnesota BioTechnology Institute, was utilized to further explain how the microbial community is shaped by this connectivity, and how this community relates to denitrification rates in an agricultural watershed. Within the same year, we found that hydrologic connectivity of a location had a significantly greater ($p = 0.01$) effect on denitrification rates, denitrifying gene abundances ($p < 0.001$), and the microbial community ($p < 0.001$) than did the location along the creek or sampling month. These relationships were significantly different by year ($p < 0.001$). In 2015, the wetter year with more frequent inundation, denitrification rates, gene abundances, and environmental parameters were more coupled at the periodically inundated site than they were in 2014. However, at the non-inundated site, these relationships were uncoupled in 2014 and 2015. Results showed that the hydrologic connectivity had a strong effect on the prokaryotic community, where inundation was associated with shifts favoring increased denitrification potential. This work also emphasizes that understanding the linkages

between hydrologic connectivity, microbial community composition, and genetic potential for biogeochemical cycling is a necessary and promising avenue to explore for future remediation strategies.

5.2 Introduction

The expansion of modern agricultural practices and the use of synthetic nitrogen (N) fertilizers have resulted in several environmental and ecological consequences. Approximately 45% of total fixed nitrogen (as ammonia, NH_3) produced annually originates from chemical fertilizers (Canfield et al., 2010), and 50-70% of the fixed nitrogen applied to soils is lost to the atmosphere or through soil leaching (Masclaux-Daubresse et al., 2010). Fixed nitrogen in soils is converted to nitrate (NO_3^-) by nitrification, and in tile-drained systems, such as those in the Midwestern United States, the leached NO_3^- is transported directly to water bodies via tile or field drainage. Nitrate loading leads to eutrophication, decreased dissolved oxygen levels, and negative ecological and health effects (Powlson et al., 2008; Rabalais et al., 2007). Anthropogenic alteration of the nitrogen cycle also leads to increased emissions of the greenhouse gas nitrous oxide (N_2O) through incomplete denitrification (Davidson, 2009; Venterea et al., 2012). While only a small fraction (3 to 5%) of N applied in fertilizers is lost as N_2O (Crutzen et al., 2008), this still accounts for 50-60% of global N_2O emissions (USEPA, 2010). Nitrous oxide gas has a considerably greater global warming potential than other greenhouse gases (Ravishankara et al., 2009).

Nitrate is removed from ecosystems through assimilation into biomass by plants and algae, or through anaerobic oxidation of ammonia (anammox) processes and microbiologically-driven denitrification. Anammox involves the anaerobic oxidation of ammonium (NH_4^+) to nitrogen gas (N_2), and is carried out by a diverse group of bacteria within the phylum *Planctomycetes* (Humbert et al., 2010; Kuenen, 2008). Denitrification is the step-wise reduction of nitrate to nitrite (NO_2^-), nitric oxide (NO), N_2O, and finally to N_2. Due to its high reduction potential, denitrification is performed by a broad range of prokaryotic species and fungi, and while it is primarily an anaerobic process, it has also been observed in microaerophilic and aerobic environments (Zumft, 1997).

Riparian areas, or the interfaces between terrestrial and aquatic ecosystems, often experience increased rates of biogeochemical cycling (Hefting et al., 2006; McClain et al., 2003). Previous research suggests that these interfaces can lead to the formation of small areas and short time periods, termed hot spots and hot moments respectively, of enhanced denitrification (Mahl et al., 2015; Roley et al., 2012a; Roley et al., 2012b). Denitrification rates are influenced by several environmental parameters including organic carbon, bulk density, soil water content, water nitrate concentration, and water velocity, and we previously employed dimensionless analysis to develop predictive functional relationships to correlate all parameters in a single equation in always inundated locations (Tomasek et al., 2017). An equation was created for periodically inundated and never inundated locations, however the trend was inconsistent between a normal and wet year. Questions remain as to how the inundation history of a site affects the correlation between environmental parameters, denitrification rates, and the microbial community under different inundation regimes.

Previous studies have measured the relationship between environmental parameters, denitrification rates, and bacterial community structure (Cao et al., 2008, Harvey et al., 2013; Shrewsbury et al., 2016; Tatariw et al., 2013). However, these studies usually targeted only few genes in the denitrification pathway, primarily the gene encoding for nitrite reductase (*nirS* or *nirK*) due to it being specific to denitrifiers (Zumft, 1997), or the gene encoding for nitrous oxide reductase (*nosZ)* due to its importance for nitrous oxide production (Domeignoz-Horta et al., 2016; Philippot et al., 2011). Inconsistent trends have been observed relating abundances of denitrification genes with actual process rates (Guentzel et al., 2014; Song et al., 2010; Tomasek et al., 2017), and a broader meta-analysis revealed only a weak correlation between gene abundances and process rates when both were measured (Rocca et al., 2015).

Advances in next-generation sequencing have allowed for more thorough characterization of bacterial communities in the environment (Staley and Sadowsky, 2016). However, due to large diversity and species richness in soil and sediment communities, as well as microscale variation in community composition, using a community profile to assess functionally relevant shifts due to changing environmental conditions remains challenging (Blackwood et al., 2006; Robertson et al., 1997; Schmidt

and Waldron, 2015). Therefore, in order to determine how community-level variation is related to environmental conditions, process rates, and functional gene abundances, the four components must be measured simultaneously. We previously reported a relationship between gene abundances and denitrification rates at samples collected from in-channel locations of an agricultural watershed, containing Seven Mile creek, located in the Minnesota River Basin (Tomasek et al., 2017). In contrast, we found limited to no coupling between process rates and gene abundances at intermittently-inundated or never-inundated hydrologic regimes.

In the current study, we expand upon our previous studies relating denitrification rates, physicochemical parameters, and denitrification gene abundances by incorporating prokaryotic community compositions, determined using Illumina next-generation sequencing of the V4 hypervariable region of the 16S rRNA gene. Samples were collected from three sites in the agriculturally-dominated Seven Mile Creek (SMC) watershed over two years. The hydrologic connectivity of sampling locations ranged from constantly inundated to never inundated. We hypothesized that the hydrologic connectivity of a sampling location would have a greater influence on denitrification rates, gene abundances, and bacterial communities than variation in sampling date and site location in SMC. Furthermore, we suspected that community composition would be associated with denitrification rates due to the relatively broad distribution of denitrification genes. Results of this study reveal how varying hydrologic connectivity affects denitrification rates and further provide novel information regarding the interaction and influence of the prokaryotic community at large on denitrification rates resulting from these hydrologic conditions.

5.3 Methods

5.3.1 Site description and sampling

Field data was collected from three sites in the agriculturally dominated Seven Mile Creek Watershed (SMC). Two sites were located in the upstream ditched agricultural headwaters and one site was downstream in an unditched, forested area in a county park directly above the confluence with the Minnesota River. Three locations were sampled

from the two upstream agricultural sites across a transect of differing hydrologic regimes, from always inundated, to periodically inundated, to never inundated. A schematic of the field sites and sampling locations is shown in Figure 4.1. SMC-2 had a small, natural inset floodplain at the floodzone location, compared to the traditional trapezoidal ditch geometry at SMC-1 (Figure 5.1).

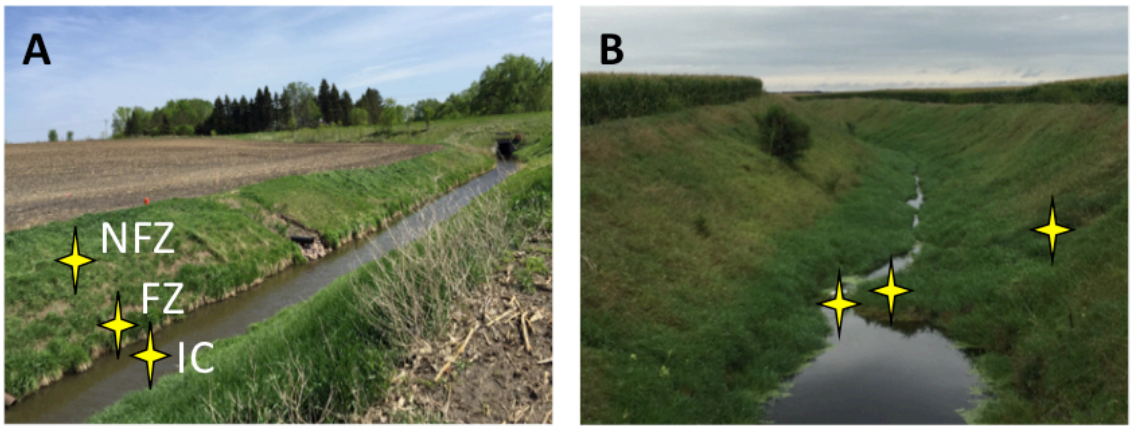

Figure 5.1. In-channel (IC), floodzone (FZ), and non-floodzone sampling locations at (A) SMC-1 and (B) SMC-2.

Water and soil samples were collected on June 12, August 20, and October 20 in 2014, and May 12, June 15, July 27, August 18, and November 9 in 2015. Measurements included: channel width and depth, water nitrate concentrations, soil nitrate concentrations, soil bulk density, soil water content, soil organic matter, and water velocity. General water characteristics (water temperature, specific conductivity, pH, and dissolved oxygen) were collected at each site using a Hydrolab Series 5 Datasonde (Hach Company, Loveland, CO).

Soil cores were collected and analyzed for denitrification potential, denitrifying gene abundances, bacterial communities using metagenomics, and soil characteristics including bulk density, volumetric water content, and organic matter. For gene abundances and metagenomics, samples were collected concurrently with soil cores for denitrification rates except for the November 2015 sampling date, when samples were

collected on October 20, 2015. Triplicate soil cores were collected for DNA extraction, within 5 cm of each other, using an autoclaved 5 mL syringe with the end removed. After collection, samples were immediately placed on ice and held at -80°C prior to extraction. Triplicate soil cores were collected for soil characteristics using a 35 mL syringe with the end removed. Triplicate soil cores for quantification of the denitrification potential were collected using a 60 mL syringe with the ends removed.

5.3.2 Quantifying Environmental Parameters

Nitrate concentration in water samples was quantified from sites in triplicate in 2014 and 2015, along with total dissolved nitrogen (TDN) and dissolved organic carbon (DOC) in 2015. Water was filtered through pre-combusted 0.7 µm GF/F filters (Whatman, USA) for all analysis. Nitrate concentrations were determined on a Lachat QC800 Autoanalyzer (Hach Company, USA) using the cadmium reduction method. TDN and DOC concentrations were determined by a TOC analyzer with a total N module (TOC-V CSH, Shimadzu).

Soil parameters were determined all collected samples. Soil cores were collected, the volume was recorded, the sample was dried for 24 h at 110°C, and the dry weight was recorded. Volumetric water content was determined by normalizing the difference between the wet weight and dry weight by the soil volume. Bulk density was determined by normalizing the dry weight by the soil volume. The soil organic matter was determine using the loss on ignition (LOI) method (Heiri et al., 2001), where dry soil was ground with a mortar and pestle, passed through a 2 mm sieve and approximately 5 g was burned at 550°C for 4 h. The difference between the dry weight and the burned weight, normalized by the dry weight provides the LOI percent. Soil nitrate was measured through water extractions, the nitrate concentration of the extracted water was measured as described above, and the concentration was normalized by the dry weight of the sample.

5.3.3 Denitrification Potential, Gene Abundances, and Bioinformatics

Soil cores were also collected to determine denitrification potential under both site (DeN) and non-nutrient limiting (DEA) conditions, denitrifying gene abundances, and

characterization of the bacterial communities using metagenomics. DeN and DEA rates were determined using the same methods as described in Chapter 4.4.2, and gene abundances were determined using the same methods as described in Chapter 4.4.3. Metagenomic analysis was run using the same sample DNA that was extracted from soil for qPCR gene quantification.

The V4 hypervariable region of 16S rRNA was amplified using the 515F/806R primer set (Caporaso et al., 2012) and sequenced using the dual index method by the University of Minnesota Genomics Center (UMGC, MN, USA) (Gohl et al., 2016). Samples from 2014 were paired-end sequenced on the Illumina HiSeq2500 (Illumina, Inc,, CA, USA) at a read length of 150 nucleotides (nt) and samples from 2015 were paired-end sequenced on the Illumina MiSeq at a read length of 300 nt. Raw data was deposited in the Sequence Read Archive of the National Center for Biotechnology Information under BioProject accession number SRP113317.

Mothur version 1.35.1 was used to process and analyze the sequence data (Schloss et al., 2009). Samples were trimmed to 150 nt for quality based on quality score (>35 over a 50 nt window), ambiguous bases (0), homopolymer length (≤ 8), and primer mismatches (≤ 2), and were paired-end joined using fastq-join software (Aronesty, 2013). High quality sequences were aligned against the SILVA database version 123 (Pruesse et al., 2007), subjected to a 2% pre-cluster (Huse et al., 2010), and UCHIME was used to remove chimeric sequences (Edgar et al., 2011). Complete-linkage clustering with a 97% similarity was used to assign operational taxonomic units (OTUs), and the Ribosomal Database Project, version 14 (Cole et al., 2009) was used to assign taxonomic classifications.

5.3.4 Statistical Analysis

JMP (Version 11.0, SAS Institute Inc) was used for ANOVAs and the non-parametric Spearman's ρ. Multi-factor ANOVAs ($\alpha < 0.05$) were used to examine the effect of season, site, and location on the spatial and temporal variability of environmental parameters, denitrification rates, and gene abundances. When factors were significant, a Tukey's *post-hoc* analysis was performed to determine the statistical differences between subgroups. Spearman's ρ ($\alpha < 0.05$) was used to determine correlations between

environmental parameters, denitrification rates, and gene abundances in each location (in-channel, floodzone, and non-floodzone).

Canonical correspondence analysis was performed using XLSTAT version 2015.6 (Addinsoft, MA, USA). Shannon indices, beta diversity calculations, and ordination plots were calculated using mothur. Beta diversity analysis and ordination were performed using Bray-Curtis dissimilarity matrices (Bray and Curtis, 1957). Analysis of molecular variance (ANOSIM) (Clarke, 1993) was used to examine differences in the community composition between season, sites, and locations, and the analysis of molecular variance (AMOVA) (Excoffier et al., 1992) was used to evaluate sample clustering. Ordination was performed by principal component analysis (PCoA) (Anderson and Willis, 2003) and Spearman correlations of family abundances associated with ordination were calculated using the corr.axes command in mothur. Partial redundancy analysis was performed by variance partitioning from the vegan package in R (Borcard et al., 1992; Oksanen et al., 2015).

5.4 Results

5.4.1 Annual Variation of Hydrologic and Environmental Parameters

Precipitation and discharge varied between 2014 and 2015 in the Seven Mile Creek (SMC) Watershed (Figure 5.2). Minnesota experienced heavy precipitation statewide on June 19, 2014, causing extensive flooding and fast discharge. However, after this event, precipitation was low and discharge remained very low in SMC. In 2015, precipitation events were more spread out across the year, resulting in more variation in discharge. Average discharge in SMC in 2015 was 0.89 ± 1.1 $m^3 s^{-1}$, and in 2014 was 0.28 ± 0.37 $m^3 s^{-1}$.

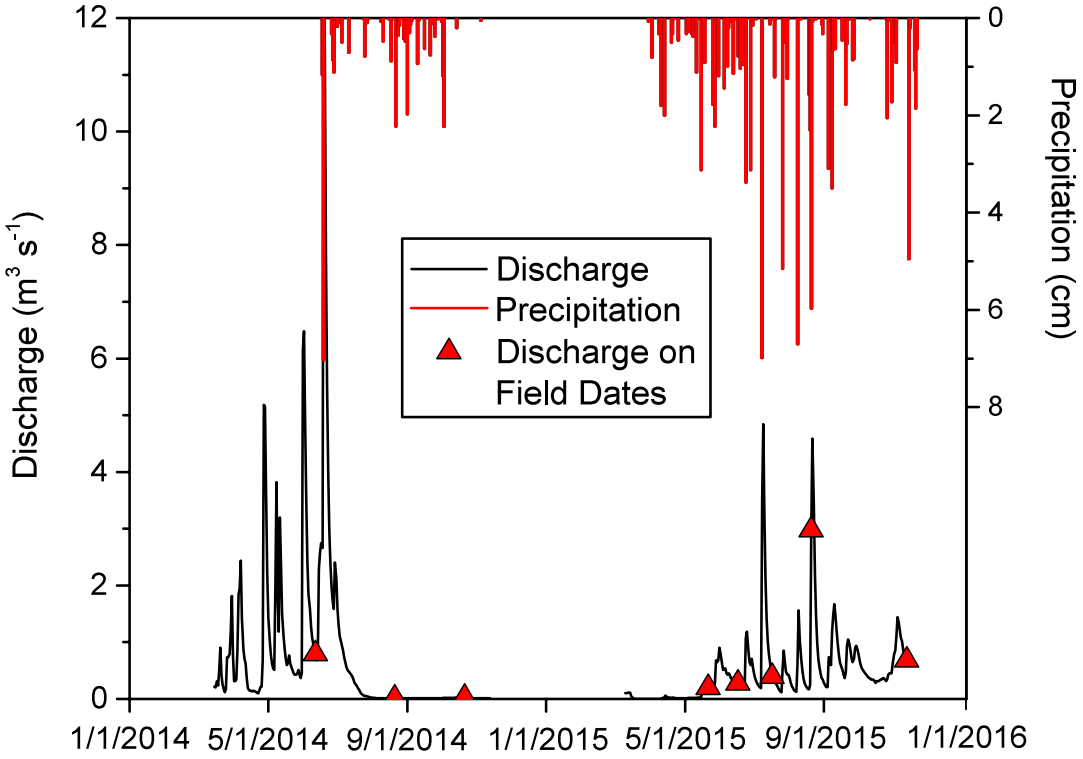

Figure 5.2 Discharge (black) and precipitation (red) recorded at SMC-3 in the Seven Mile Creek (SMC) Watershed over the duration of the study period. Red triangles represent the discharge on the sampling dates.

Seasonal and annual variations in discharge led to differential inundation at SMC locations. Average water depth was greater in 2015 (0.45 ± 0.24 m) compared to average depth in 2014 (0.34 ± 0.23). Figure 5.3, Figure 5.4, and Figure 5.5 show SMC-1, SMC-2, and SMC-3, respectively, over the sampling duration. This was particularly evident in 2015, where the floodzone location at SMC-2 had some standing water in June, July, August, and October (Figure 5.4). In October of 2015, the inset floodplain isn't even visible due to the high water depth.

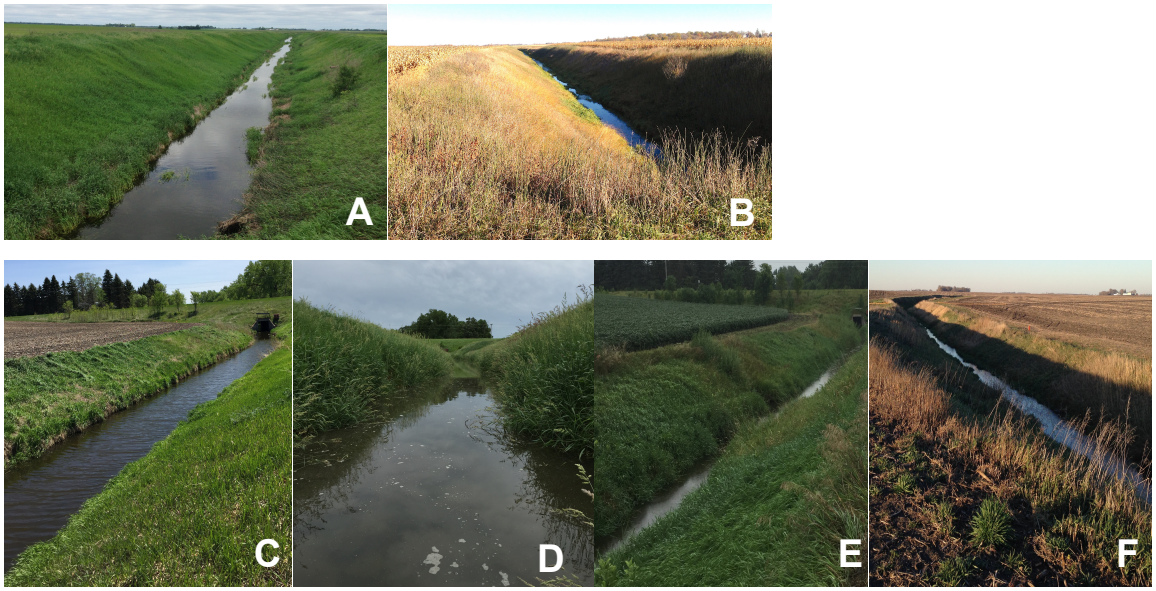

Figure 5.3. SMC-1 in (A) June 2014, (B) October 2014, (C) May 2015, (D) June 2015, (E) August 2015, and (F) October 2015.

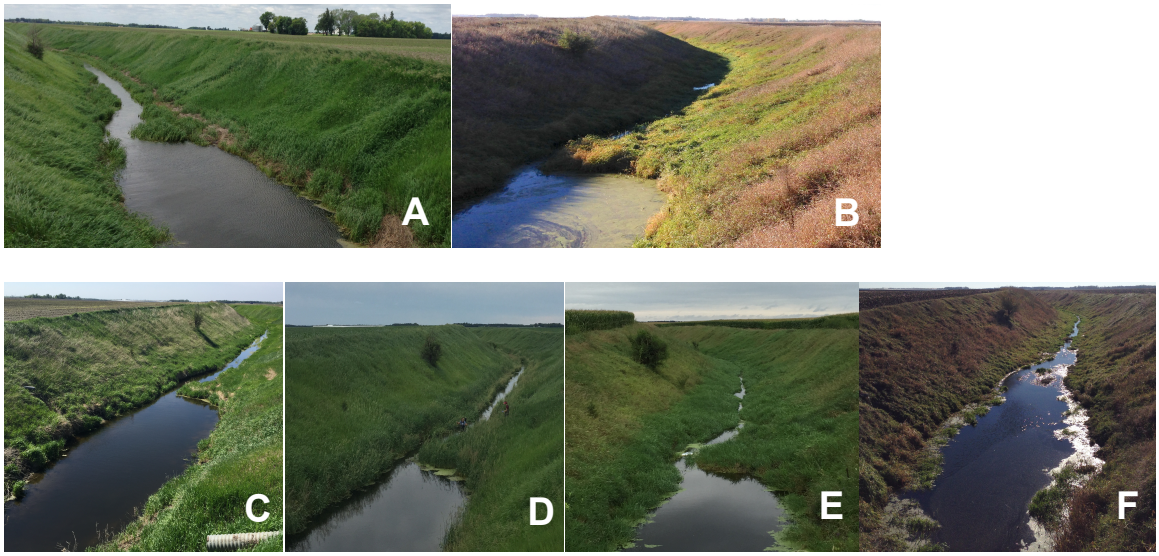

Figure 5.4. SMC-2 in (A) June 2014, (B) October 2014, (C) May 2015, (D) June 2015, (E) August 2015, and (F) October 2015.

Figure 5.5. SMC-3 in (A) June 2014, (B) October 2014, (C) June 2015, (D) August 2015, and (E) October 2015

5.4.2 Environmental Parameters

Environmental parameters at field sampling locations in Seven Mile Creek (SMC) Watershed in 2015 are shown in Table 5.1, Table 5.2, and Table 5.3. Parameters for 2014 are shown in Table 4.2 and Table 4.3. Organic matter was the greatest at the non-floodzone locations. Organic matter at the floodzone location at SMC-1 decreased throughout the sampling season in 2015, whereas it stayed relatively constant at SMC-2. Average shear stress was greater in 2015 (0.024 ± 0.21 m s^{-1}) compared to 2014 (0.009 ± 0.009 m s^{-1}), especially at SMC-1 and SMC-2. Volumetric water content was greater at the floodzone locations compared to the non-floodzone locations, and in 2015 for all sampling dates besides August, volumetric water content was greater at the floodzone location of SMC-2 compared to SMC-1.

Table 5.1. Mean[a] environmental parameters for in-channel (IC) locations in Seven Mile Creek (SMC) Watershed in 2015.

Site	Month	Water C_{NO3} (mg N L^{-1})[b]	Sediment C_{NO3} (mg N kg^{-1})[a]	u_* (m s^{-1})	H (m)	ρ_b (g cm^{-3})	OM (%)	VWC (%)	DO (mg L^{-1})	T (^oC)	DeN (mg N m^{-2} h^{-1})	DEA (mg N m^{-2} h^{-1})
SMC-1 IC	May	0.08	0.10	0.001	0.64	1.28	3.47	50.4	8.01	16.6	0.62	18.4
SMC-2 IC	May	0.01	0.19	0.009	0.20	0.85	6.21	59.9	4.31	12.3	0.64	16.3
SMC-3 IC	May	5.5	0.11	0.006	0.22	1.52	1.69	40.8	11.5	14.5	8.78	11.0
SMC-1 IC	June	23.8	0.25	0.011	0.56	1.23	3.07	51.1	9.37	19.8	31.6	42.3
SMC-2 IC	June	26.1	0.41	0.007	0.60	1.02	5.05	57.5	5.56	17.7	14.5	19.8
SMC-3 IC	June	17.0	0.31	0.060	0.28	1.72	0.65	30.5	10.9	19.4	2.06	1.29
SMC-1 IC	July	18.4	0.16	0.012	0.69	1.29	1.61	50.7	6.48	21.2	4.52	22.0
SMC-2 IC	July	18.9	NA	0.030	0.81	0.42	7.82	65.4	2.55	19.0	61.5	103
SMC-3 IC	July	15.5	3.11	0.035	0.16	1.64	0.59	24.8	8.81	22.1	0.41	1.26
SMC-1 IC	Aug	12.7	0.24	0.010	0.57	1.43	1.76	38.6	5.70	18.2	19.9	26.4
SMC-2 IC	Aug	12.6	0.13	0.014	0.33	1.04	3.07	50.1	3.61	17.5	22.6	27.9
SMC-3 IC	Aug	11.3	0.06	0.036	0.15	1.35	1.00	41.0	9.94	18.4	2.01	1.73
SMC-1 IC	Nov	30.9	1.90	0.028	0.75	1.23	2.81	54.3	10.5	10.5	14.6	13.3
SMC-2 IC	Nov	31.2	0.77	0.021	0.67	0.76	5.43	62.8	7.02	9.92	51.5	71.8
SMC-3 IC	Nov	20.7	0.68	0.077	0.10	1.59	0.85	34.0	10.1	11.9	7.22	11.2

[a]Mean is an average of triplicate replicates
[b]Minimum detection limit (MDL) of Lachat QC800 for nitrate analysis is 0.01 mg N L^{-1}

Table 5.2. Mean environmental parameters for floodzone (FZ) locations in Seven Mile Creek (SMC) Watershed in 2015.

Site	Month	Sediment C_{NO3} (mg N kg^{-1})	ρ_b (g cm^{-3})	OM (%)	VWC (%)	DeN (mg N m^{-2} h^{-1})	DEA (mg N m^{-2} h^{-1})
SMC-1 FZ	May	13.84	1.11	7.00	43.6	0.86	3.11
SMC-2 FZ	May	0.18	0.66	9.47	69.1	3.00	27.0
SMC-1 FZ	June	3.75	1.04	6.79	60.3	3.28	8.04
SMC-2 FZ	June	0.47	0.64	8.99	71.6	15.4	18.1
SMC-1 FZ	July	6.19	1.23	4.95	40.3	0.24	3.29
SMC-2 FZ	July	0.31	0.62	NA	80.8	31.6	45.4
SMC-1 FZ	Aug	1.22	1.17	2.53	50.3	2.18	6.27
SMC-2 FZ	Aug	0.22	0.50	9.65	43.3	42.4	64.8
SMC-1 FZ	Nov	8.68	1.22	2.61	53.1	4.61	4.50
SMC-2 FZ	Nov	0.78	0.59	10.5	73.1	42.4	64.8

Table 5.3. Mean environmental parameters for non-floodzone (NFZ) locations in Seven Mile Creek (SMC) Watershed in 2015.

Site	Month	Sediment C_{NO3} (mg N kg^{-1})[a]	ρ_b (g cm^{-3})	OM (%)	VWC (%)	DeN (mg N m^{-2} h^{-1})	DEA (mg N m^{-2} h^{-1})
SMC-1 NFZ	May	9.71	0.78	19.4	38.9	6.69	21.4
SMC-2 NFZ	May	8.34	0.87	18.6	43.0	10.2	16.7
SMC-1 NFZ	June	19.4	0.71	18.8	32.6	10.9	22.2
SMC-2 NFZ	June	6.84	0.93	13.9	51.5	17.0	23.7
SMC-1 NFZ	July	25.0	0.69	16.2	40.3	5.8	21.5
SMC-2 NFZ	July	9.67	0.75	12.9	38.6	6.44	18.3
SMC-1 NFZ	Aug	32.8	0.70	13.8	37.2	4.16	20.9
SMC-2 NFZ	Aug	23.8	0.77	12.3	43.3	8.74	18.7
SMC-1 NFZ	Nov	33.9	0.75	15.0	39.3	11.5	35.9
SMC-2 NFZ	Nov	1.53	0.81	12.7	40.6	14.0	33.1

Water nitrate concentrations varied widely over the field sampling duration (Figure 5.6). Nitrate concentrations ranged from 0.01 to 40.5, 0.01 to 33.9, and 5.5 to 27.4 mg $N\text{-}NO_3^-$ L^{-1} at SMC-1, SMC-2, and SMC-3, respectively. Average concentrations were 15.8, 15.4, and 13.7 mg $N\text{-}NO_3^-$ L^{-1} at SMC-1, SMC-2, and SMC-3, respectively. In August and October 2014, and May 2015, nitrate at SMC-1 and SMC-2 was below the minimum detection limit (0.01 mg $N\text{-}NO_3^-$ L^{-1}). Nitrate concentrations at SMC-3 were never below 5 mg $N\text{-}NO_3^-$ L^{-1}, most likely due to the inflow of groundwater just upstream of this site; groundwater was also most likely responsible for the lower concentrations at SMC-3 compared to SMC-1 and SMC-2 when surface water concentrations were high.

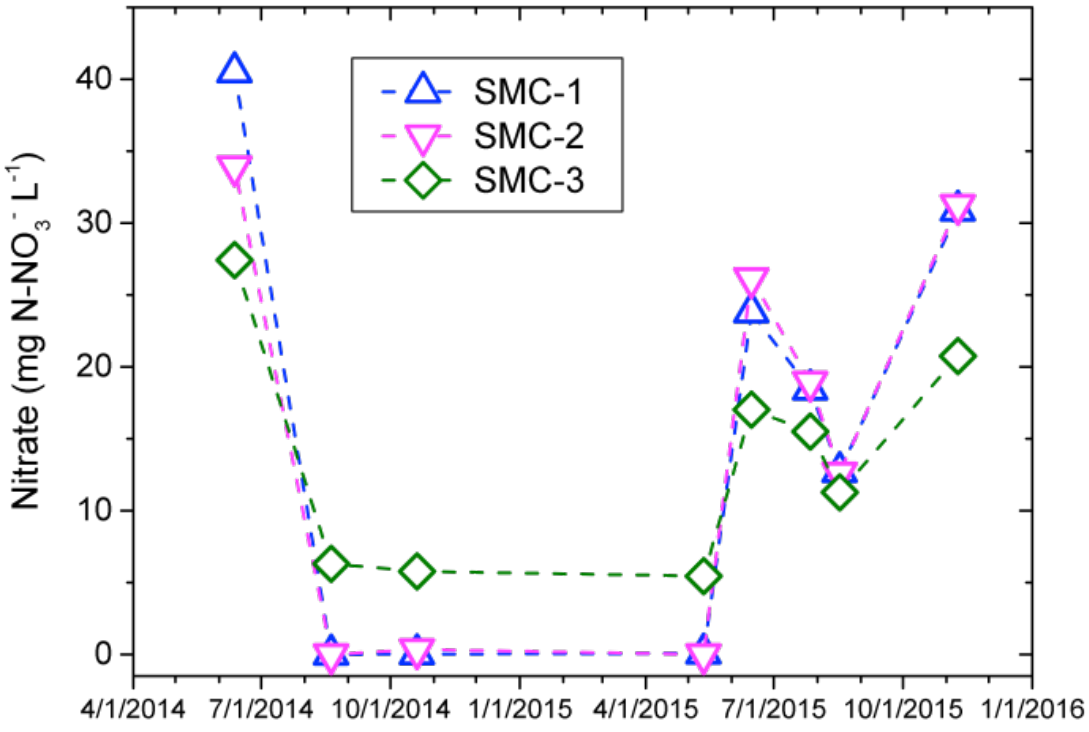

Figure 5.6. Nitrate concentrations at SMC-1, SMC-2, and SMC-3 in the Seven Mile Creek Watershed (SMC) over the field sampling duration.

Sediment nitrate concentrations also varied based on location, site, and season. For channel locations, concentrations ranged from 0.1 to 1.9, 0.13 to 0.77, and 0.06 to 3.11 mg $N\text{-}NO_3^-$ kg dry $soil^{-1}$ at SMC-1, SMC-2, and SMC-3, respectively. For floodzone locations, concentrations ranged from 1.22 to 13.8 and 0.18 to 0.78 mg $N\text{-}NO_3^-$ kg dry $soil^{-1}$ at SMC-1 and SMC-2, respectively. For non-floodzone locations, concentrations ranged from 5.10 to 33.9 and 1.53 to 23.8 mg $N\text{-}NO_3^-$ kg dry $soil^{-1}$ at SMC-1 and SMC-2, respectively. At the non-floodzone location of SMC-1, sediment nitrate concentrations increased over the sampling season in 2015.

5.4.3 Correlation Between Denitrification Rates and Environmental Parameters

Denitrification rates varied temporally and spatially. DeN rates were significantly greater in 2015 than in 2014 (Tukey's post-hoc $p < 0.001$), greater among channel samples than samples collected in the non-floodzone ($p = 0.01$), and greater at SMC-2 than the other sites ($p < 0.001$). DEA was greater in 2015 ($p = 0.005$), greater among channel samples than those in the non-floodzone ($p = 0.028$), and significantly different among sites, with SMC-2 > SMC-1 > SMC-3 ($p < 0.001$). In-channel rates of DeN at SMC-1 and SMC-2 were lowest in August and October 2014, and May 2015. This is also when nitrate concentrations were the lowest (Figure 5.6). When nutrients were added (DEA assays), denitrification rates during these sampling times increased. Denitrification rates (both DeN and DEA) were greatest at SMC-2 in July and November 2015. Both DeN and DEA rates at SMC-3 were low during all sampling dates.

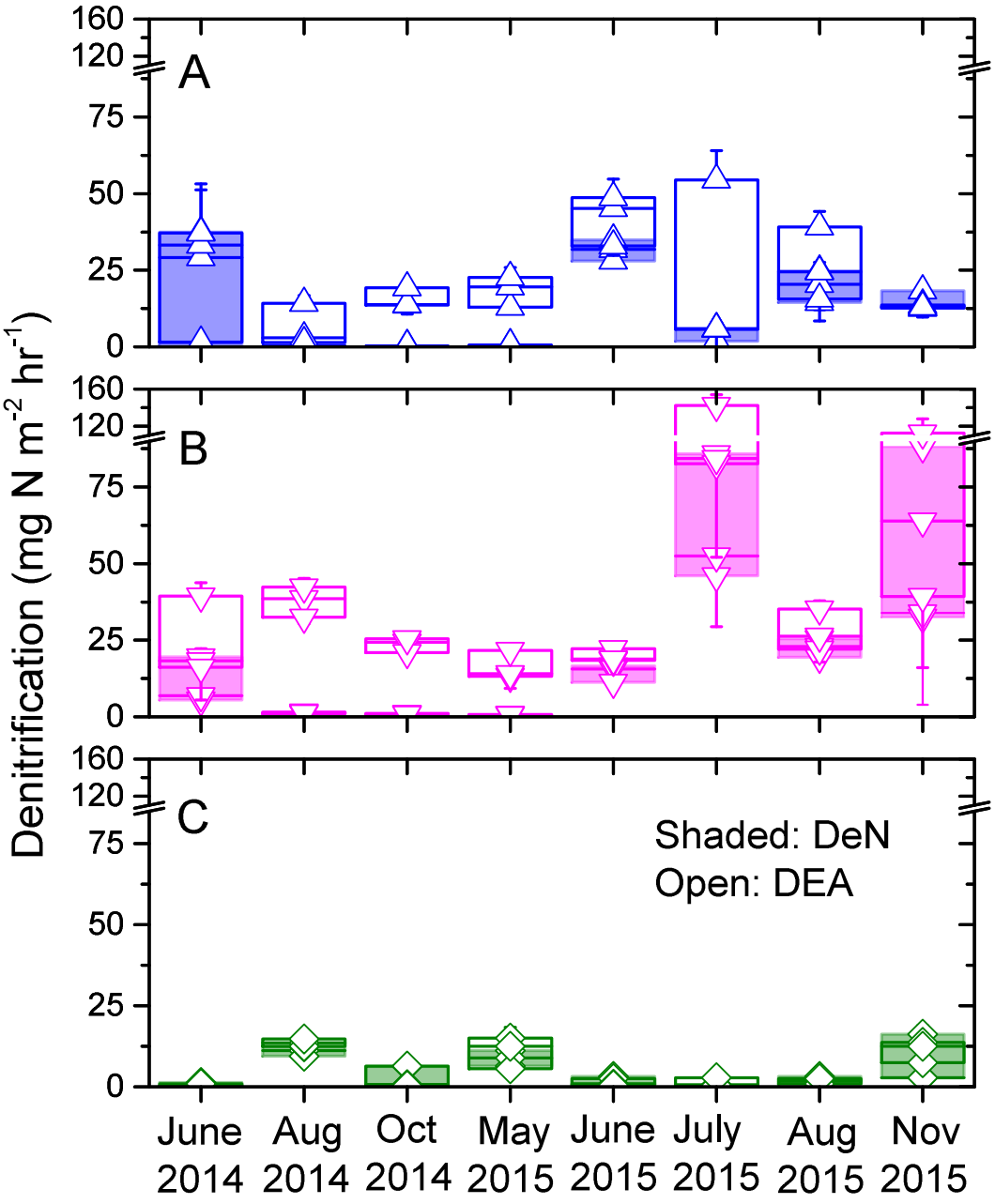

Figure 5.7. In-channel denitrification rates under site conditions (DeN) and non-nutrient limiting conditions (DEA) at (A) SMC-1, (B) SMC-2, and (C) SMC-3 over the field sampling duration. Boxes represent the first and third quartile and whiskers represent ±1.5 of the standard deviation. Shaded boxes represent DeN rates and open represents DEA rates.

Denitrification rates also varied temporally at the floodzone and non-floodzone locations (Figure 5.8). DeN rates at the floodzone location of SMC-1 (Figure 5.8A) were similar throughout the sampling dates. However, DEA rates decreased seemingly exponentially, with highest rates in June 2014. DeN rates at the floodzone location of SMC-2 were higher in 2015 than 2014, and both DeN and DEA varied across the sampling dates. However, the ratio of DEA to DeN (a representation of the amount of nutrient limitation) was greater in 2014 and May of 2015 compared to the rest of the 2015 sampling dates. DeN and DEA rates at the non-floodzone location of SMC-1 and SMC-2 were similar across sampling dates, although adding nutrients did increase denitrification rates for all sampling dates. DeN rates for non-floodzone locations separated by site (SMC-1 and SMC-2 separately) were not significantly different over the sampling duration (Tukey's post-hoc > 0.05). DeA rates at the non-floodzone locations separated by site were significantly greater at the November 2015 date for both sites, and significantly less than other dates in August 2014, but were statistically similar at all other dates. The DEA to DeN ratio was greater at SMC-1 compared to SMC-2 for all sampling dates besides November 2015 when the ratio was the same at the two locations.

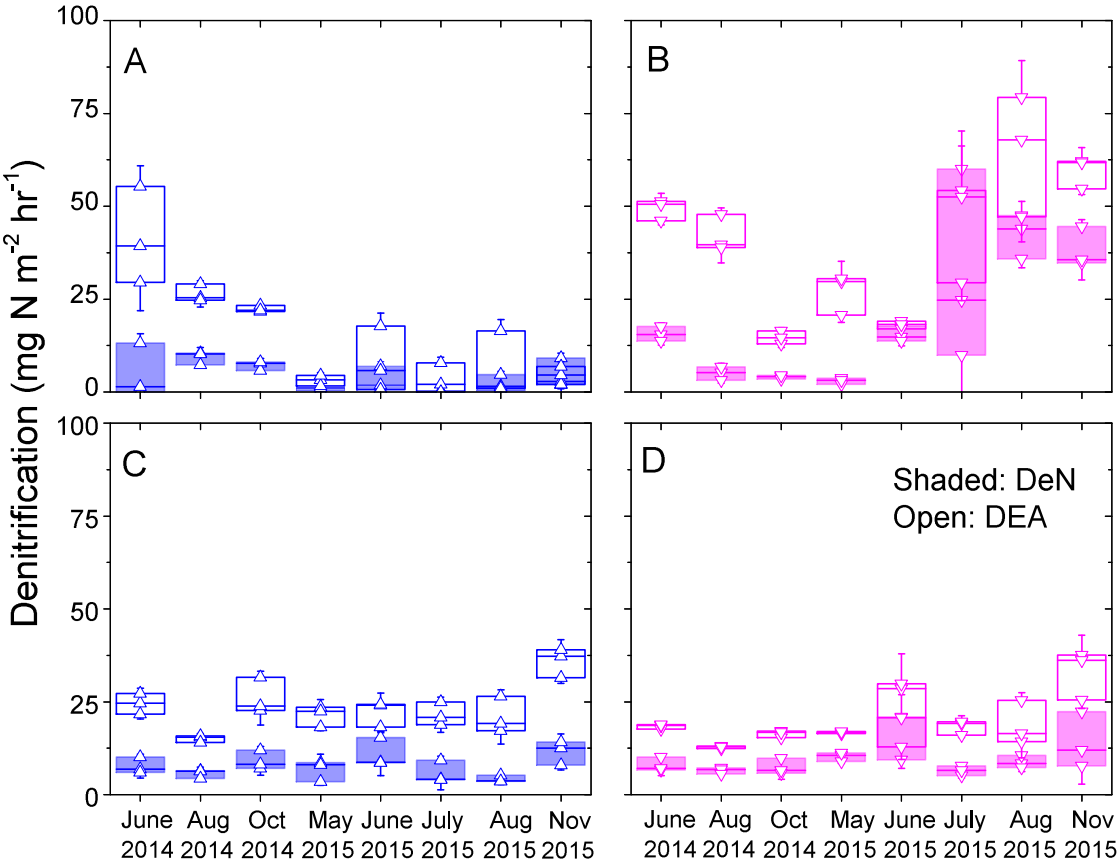

Figure 5.8. Denitrification rates under site conditions (DeN) and non-nutrient limiting conditions (DEA) at (A) the floodzone location at SMC-1, (B) the floodzone location at SMC-2, (C) the non-floodzone location at SMC-1, and (D) the non-floodzone location at SMC-2 over the field sampling duration. Blue represents SMC-1 and magenta represents SMC-2. Boxes represent the first and third quartile and whiskers represent ±1.5 of the standard deviation. Shaded boxes represent DeN rates and open represents DEA rates.

DeN and DEA rates at the non-floodzone location had less variability compared to in-channel and floodzone locations. Figure 5.9 and Figure 5.10 show the normalized histograms of DeN and DEA rates, respectively, over the entire experimental duration at the three locations. The histograms are binned into 5 mg N m^{-2} h^{-1}. The non-floodzone locations have fewer bins for both DeN and DEA, and a higher normalized frequency for these bins, compared to the in-channel and floodzone locations. Therefore, denitrification rates under site conditions and non-nutrient limiting conditions are similar and consistent

across the field study duration. The bins for the floodzone locations (Figure 5.9B) above 30 mg N m^{-2} h^{-1} are from SMC-2.

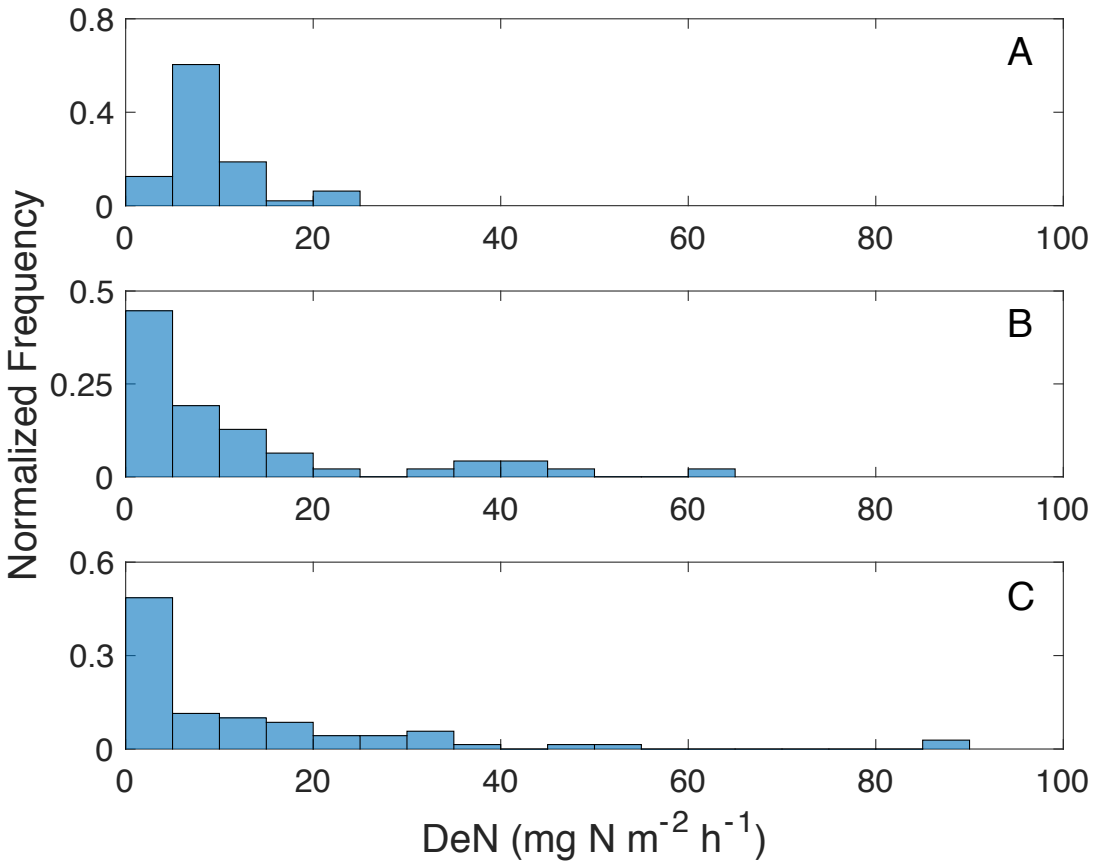

Figure 5.9. Normalized histogram of DeN rates at (A) non-floodzone, (B) in-channel, and (C) in-channel locations in the Seven Mile Creek Watershed over the experimental duration. The histogram bin width is 5 (mg N m^{-2} hr^{-1}).

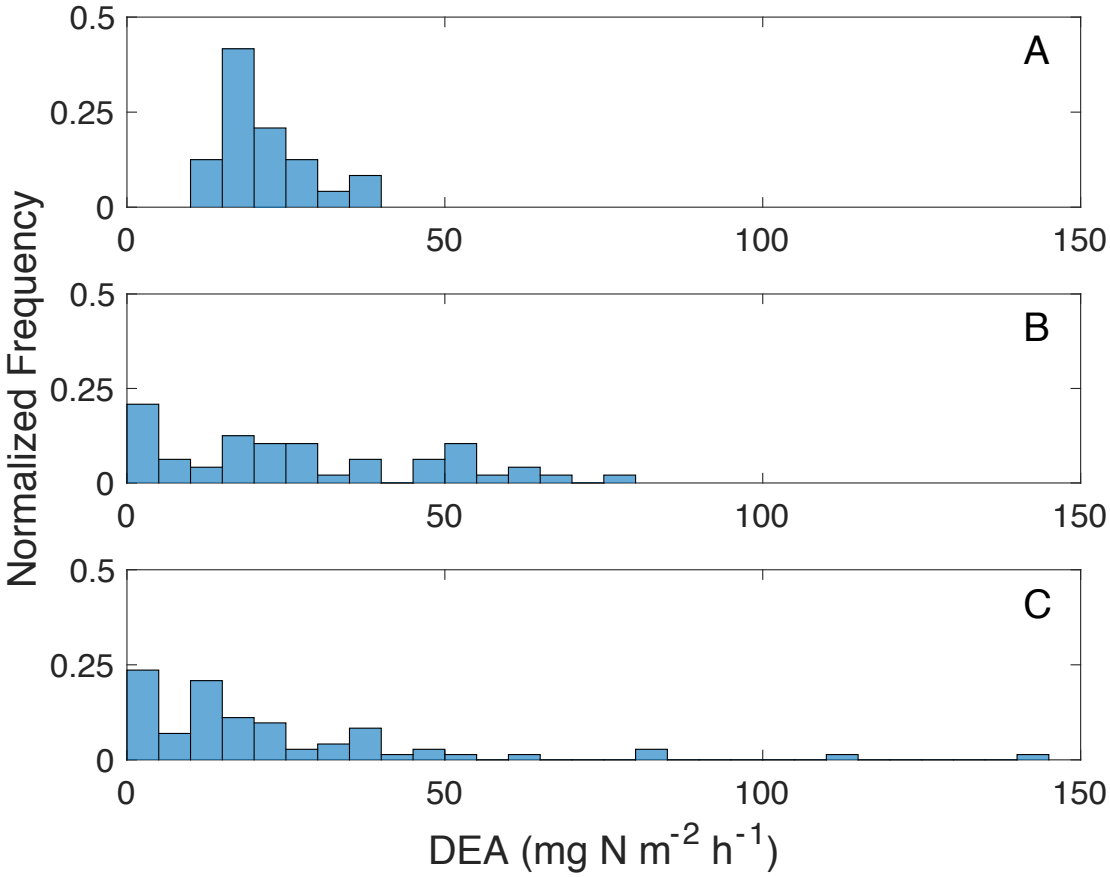

Figure 5.10. Normalized histogram of DEA rates at (A) non-floodzone, (B) in-channel, and (C) in-channel locations in the Seven Mile Creek Watershed over the experimental duration. The histogram bin width is 10 (mg N m^{-2} hr^{-1}).

Significant trends ($\alpha = 0.05$) were found for in-channel locations between DeN rates and environmental parameters (Figure 5.11). Positive relationships were found between DeN and water depth, water nitrate concentration, sediment organic matter, and soil moisture. DeN and bulk density were negatively related. All correlations were relatively weak, with the largest r^2 of 0.3 between bulk density and DeN.

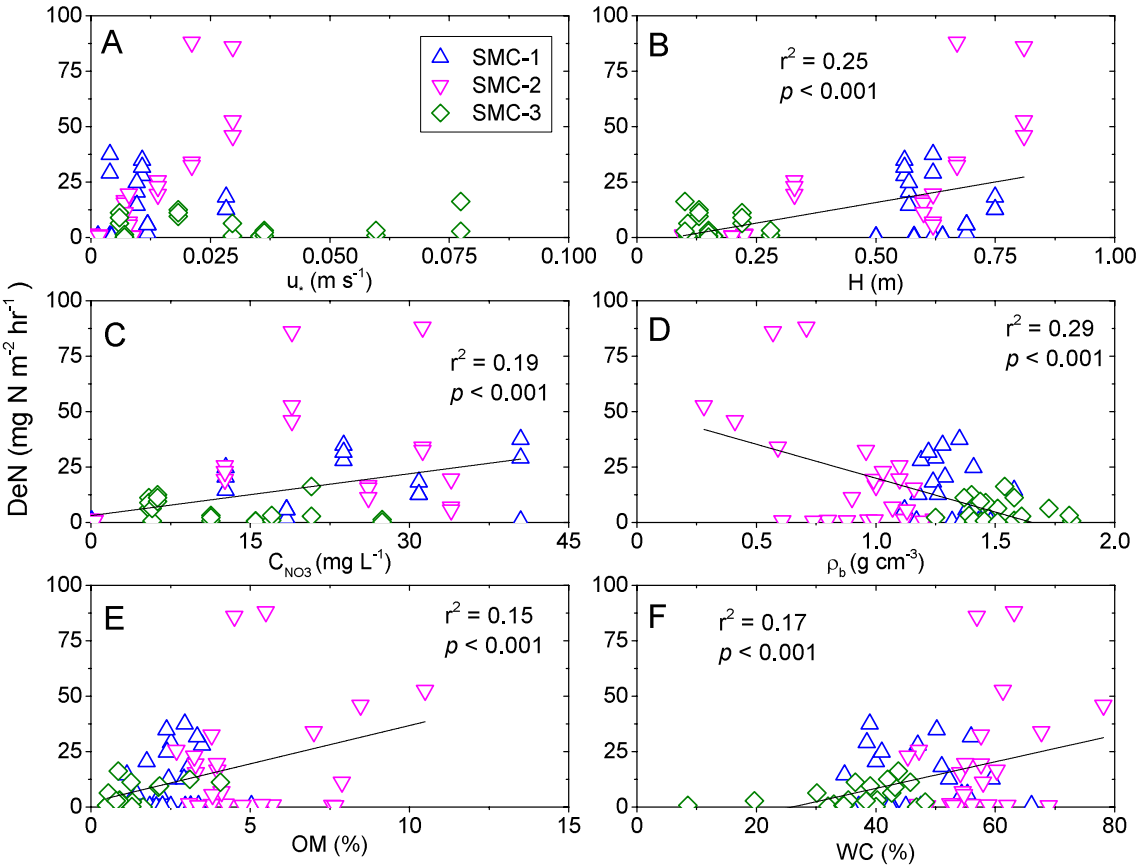

Figure 5.11. DeN as a function of individual parameters including (A) stream shear velocity (u_*), (B) water depth (H), (C) water nitrate concentration (C_{NO3}), (D) bulk density (ρ_b), (E) organic matter (OM), and (F) sediment water content (WC) for in-channel locations in the SMC in 2014 and 2015.

Since nitrate is one of the main parameters that drives denitrification rates, the trend we determined between DeN and water nitrate concentrations was compared to previous studies (Figure 5.12). The black line in the graph represents the predicted denitrification rate from nitrate concentrations at SMC sites using a fitted line for denitrification rates and nitrate concentrations across the U.S. with variable land uses (including LINX2 data for reference, urban, and agricultural streams), and using multiple methods (whole stream isotopic methods, membrane inlet mass spectrometry, *in situ* chamber techniques, and the acetylene block) (Mahl et al., 2015; Roley et al., 2012a). The slope found for our data (0.627) was very similar to that found for literature values

(0.669). The intercept for our data was higher than for literature values, however this is probably due to the very high nitrate concentrations in our system. Since there should be no denitrification occurring when no nitrate is present, we forced the SMC regressed line through the literature intercept (0.223, light red line).

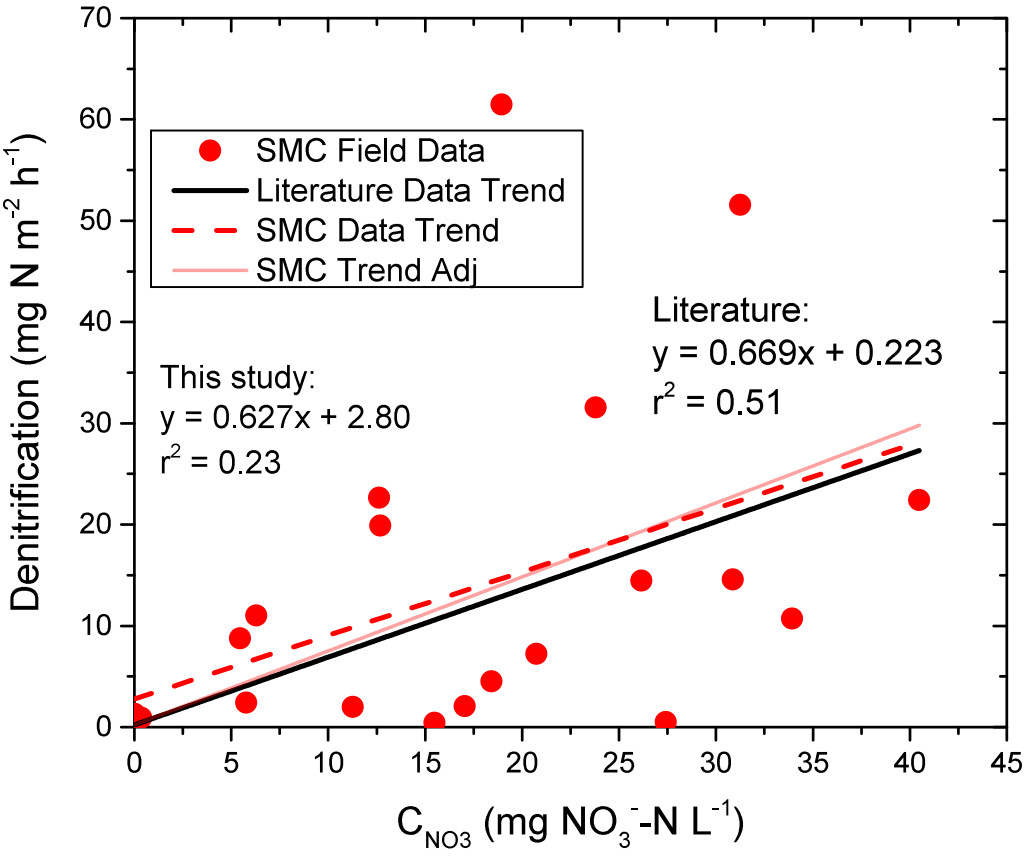

Figure 5.12. DeN as a function of nitrate concentration (C_{NO3}) for Seven Mile Creek (SMC) sites over the field sampling duration in relation to previous data. The red circles are the mean of the triplicate DeN and nitrate concentrations for SMC sites. The red dotted line is the fitted linear trend for data in this study. The black line represents the fitted equation between DeN and nitrate from previous studies and LINX2 reference, urban, and agricultural streams, using multiple methods (Mahl et al., 2015, Roley et al., 2012a). The light red solid line is the red dotted line forced through the intercept of the literature equation (0.223).

Figure 5.13 shows the effect of nitrate and benthic organic matter on denitrification for Seven Mile Creek sites. In the graph, nitrate concentration (A) and benthic organic matter (B) is plotted against DEA normalized by DeN rates. When nitrate concentrations are low, denitrification rates are low, but adding nutrients greatly increases rates (DEA). When nitrate concentrations are high, the DEA to DeN ratio is low, meaning that adding nutrient concentrations has little effect on denitrification rates. Benthic organic matter did not seem to have an effect on the DEA to DeN ratio. DEA to DeN ratio only increased in low nitrate sites. However, for these field sites, there were no low organic matter sites with low nitrate concentrations. SMC-3 had low organic matter but high nitrate concentrations, and SMC-1 and SMC-2 both had larger organic matter content.

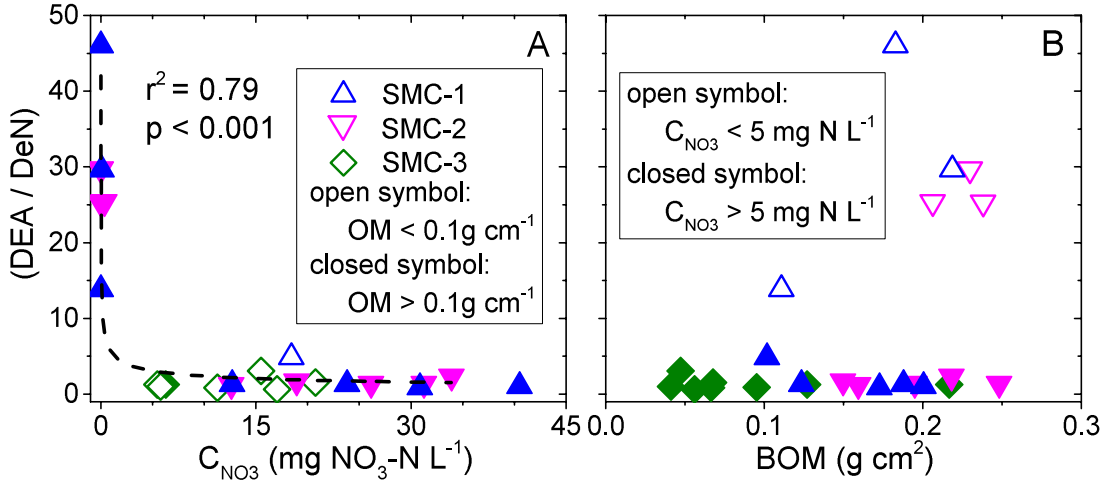

Figure 5.13. The ratio between in-channel denitrification rates using site-specific water as collected (DeN), and amended with phosphate, nitrate, and carbon (DEA) relative to (A) site water nitrate concentration, and (B) benthic organic matter of the sediment for in-channel locations in the Seven Mile Creek (SMC) watershed for 2014 and 2015. In (a), open symbols represent sites with benthic organic matter <0.1 g cm-2, and in (b), open symbols represent sites where water nitrate concentration was <5 mg NO3-N L-1. The dotted line in (a) represents the power law fitted to the data, and the p-value represents the significance ($\alpha < 0.05$) of the fitted power law equation.

Denitrification was significantly (α) related to sediment nitrate concentration, bulk density, sediment organic matter, and water content at floodzone locations at Seven Mile Creek. Denitrification rates exponentially decreased with sediment nitrate concentrations, and sediment nitrate concentrations were much lower at SMC-2 than SMC-1. SMC-2 had lower bulk density than did SMC-1, and denitrification was negatively related to bulk density. Organic matter and water content are both positively related to denitrification rates, and in general, SMC-2 had both greater organic matter and greater water content.

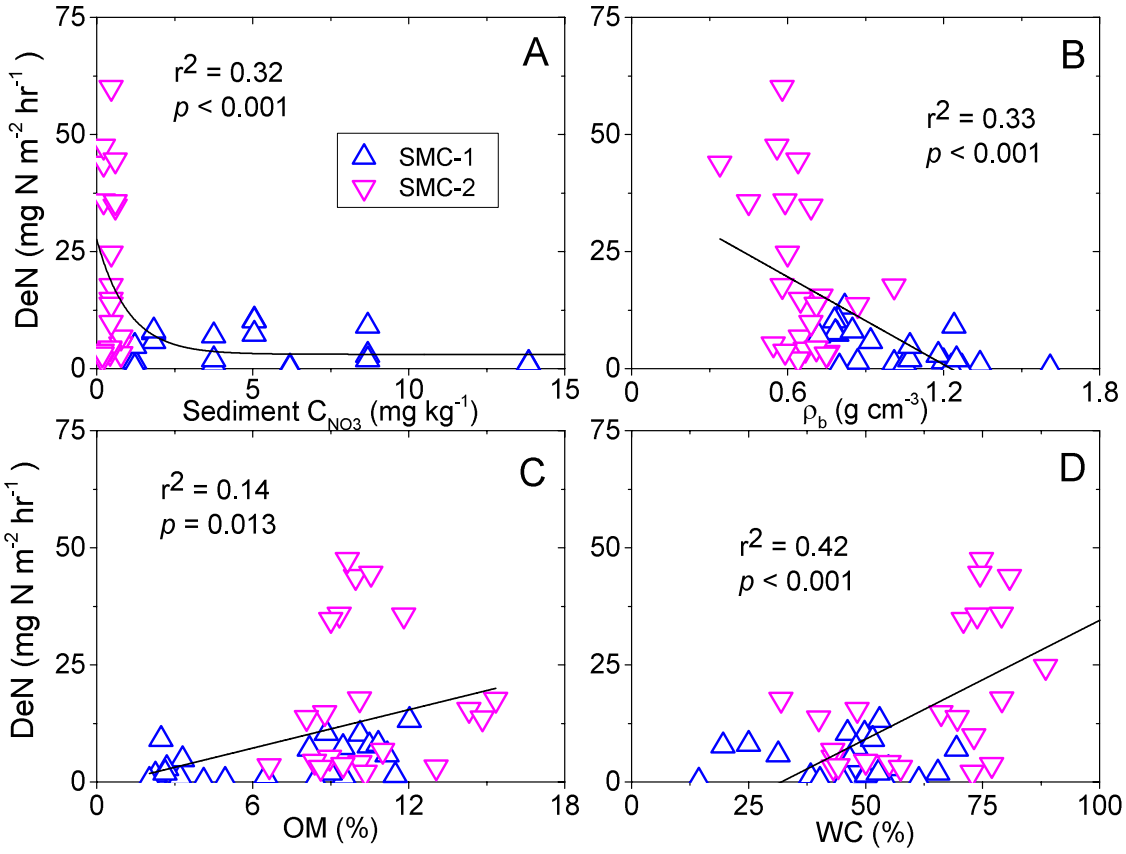

Figure 5.14. DeN as a function of individual parameters including (A) sediment nitrate concentration, (B) bulk density (ρ_b), (C) organic matter (OM), and (D) sediment water content (WC) for floodzone locations in the SMC in 2014 and 2015.

Denitrification was significantly (α) related to bulk density and water content at the non-floodzone locations of SMC. Denitrification at the channel and floodzone locations was negatively related to bulk density, whereas for the non-floodzone locations, it is positively related. At the non-floodzone location, increasing bulk density was significantly positively ($r^2 = 0.37$, $p < 0.001$) related to water content, whereas the channel and floodzone were negatively related ($r^2 = 0.72$, $p < 0.001$; $r^2 = 0.33$, $p < 0.001$ for channel and floodzone, respectively). Similarly, while bulk density and sediment organic matter were significantly correlated at the channel and floodzone locations ($r^2 = 0.81$, $p < 0.001$; $r^2 = 0.43$, $p < 0.001$ for channel and floodzone, respectively), non-floodzone locations were only weakly correlated ($r^2 = 0.10$, $p = 0.04$). Non-floodzone locations had the highest sediment nitrate concentrations, and denitrification was not related to the concentration.

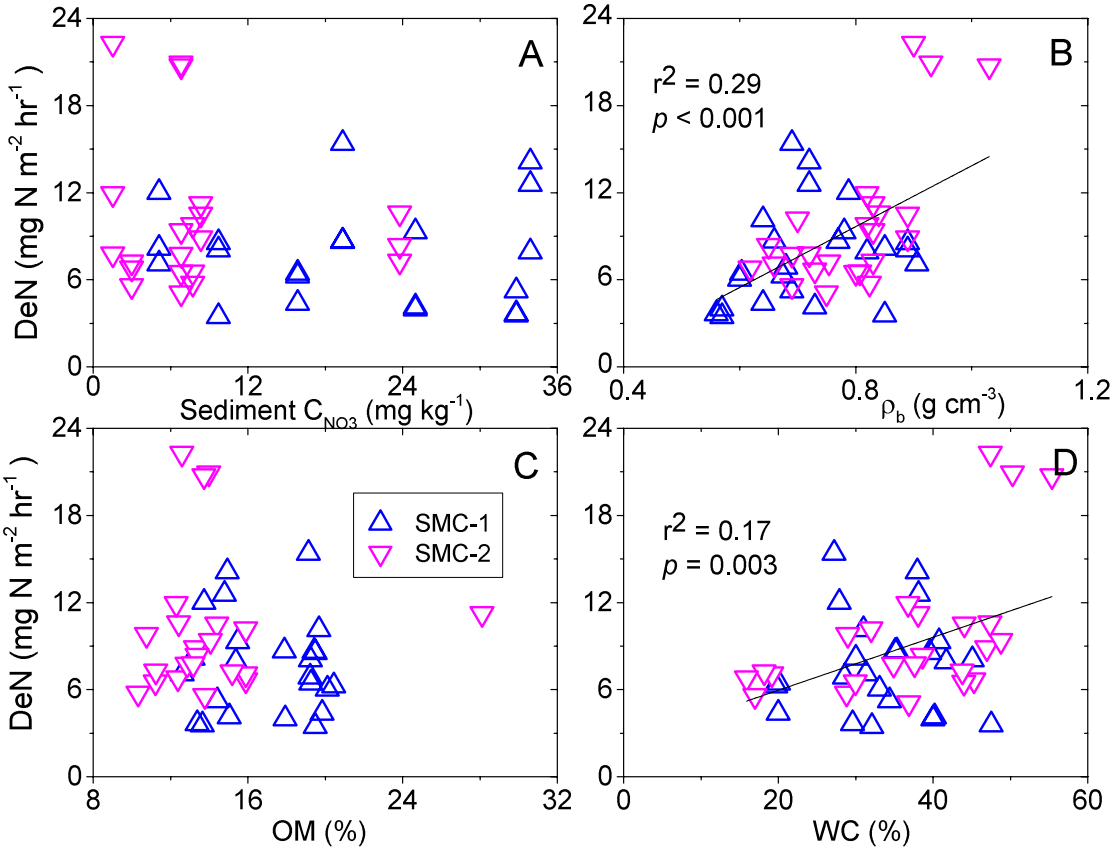

Figure 5.15. DeN as a function of individual parameters including (A) sediment nitrate concentration, (B) bulk density (ρ_b), (C) organic matter (OM), and (D) sediment water content (WC) for non-floodzone locations in the SMC in 2014 and 2015.

5.4.4 Denitrifying Gene Abundances

Gene abundances quantified by qPCR (Figure 5.16, Figure 5.17, and Table 5.4) were significantly different by year, site, and location. The 16S rRNA gene abundances were significantly greater in 2014 compared to 2015 ($p < 0.001$), at the floodzone location compared to the in-channel and non-floodzone locations ($p < 0.001$), and significantly smallest at SMC-3 ($p < 0.001$). Generally, floodzone locations had the greatest gene abundances, and by site, SMC-2 had the greatest and SMC-3 had the least abundance (Table 5.4).

In-channel, floodzone, and non-floodzone gene abundances varied seasonally and by site (Figure 5.16). SMC-2 had both the greatest gene abundances and the greatest variability in abundances across the sampling period. SMC-2 had greater in-channel gene abundances compared to SMC-1 and SMC-3. SMC-1 had similar in-channel abundances throughout the sampling period, while greatest denitrifying gene abundances occurred in July 2015 at SMC-2 and in August 2014 at SMC-3. Floodzone denitrifying gene abundances seemed to exponentially decrease over the sampling period at SMC-1 (Figure 5.17A), while abundances at the floodzone location were greater in 2015 than 2014 at SMC-2 and were much greater than the other sites and locations. For the non-floodzone locations, gene abundances were very low in June and July of 2015 at SMC-1 and were low in June of 2014 and July and August of 2015 at SMC-2.

Correlations between gene abundances to denitrification rates and environmental parameters varied between locations and between years. Table 5.5, Table 5.6, and Table 5.7 show correlations at in-channel, floodzone, and non-floodzone sites, respectively, for 2015, and Table 4.5, Table 4.6, and Table 4.7 show correlations for 2014. Compared to 2014, the floodzone location had many more correlations in 2015 (8 compared to 35). Similar to 2014, the non-floodzone location had very few correlations in 2015.

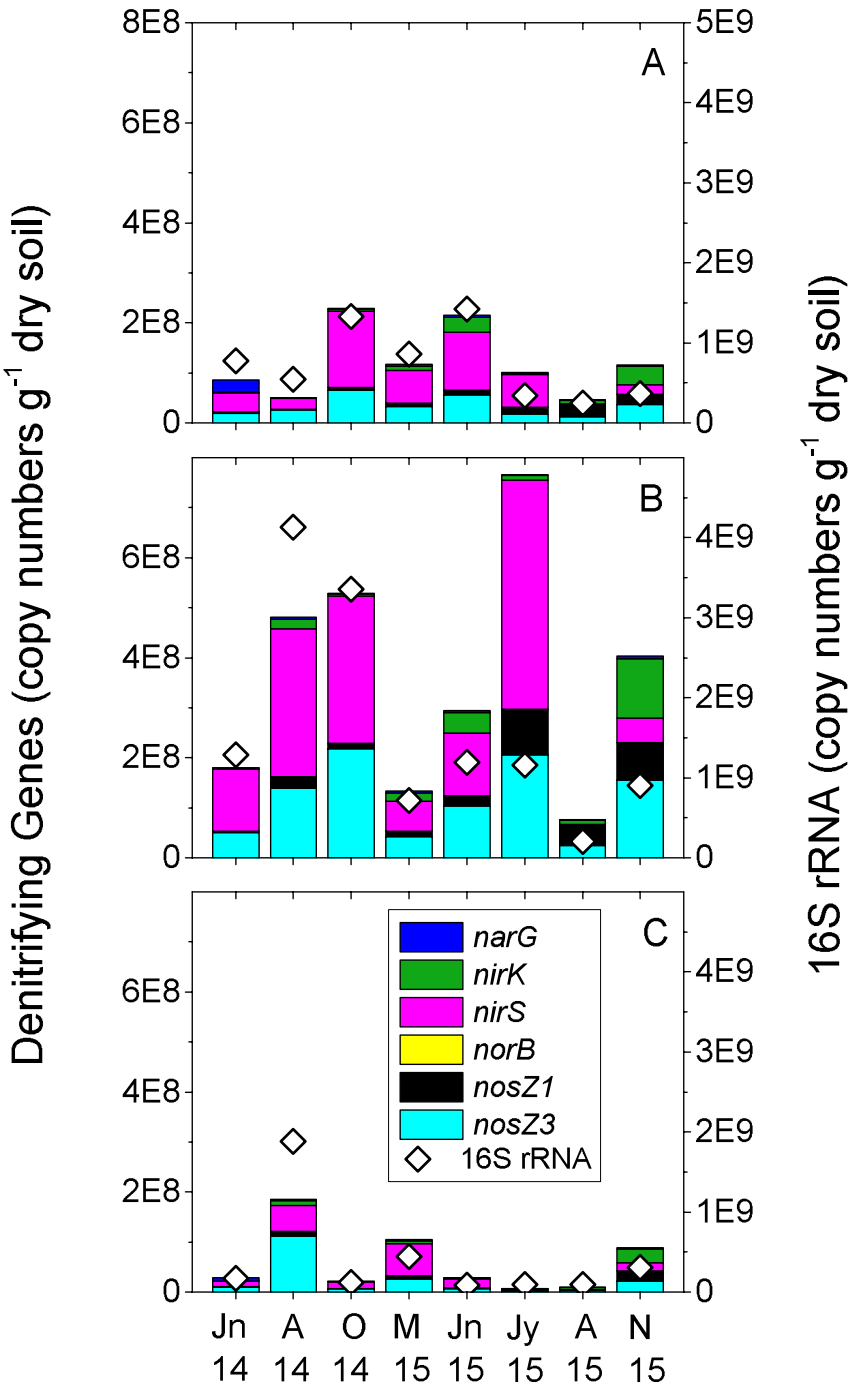

Figure 5.16. Mean denitrifying gene abundances at the in-channel (IC) locations at (A) SMC-1, (B) SMC-2, and (C) SMC-3 over the field sampling duration. The mean for each genes was determined from the triplicate samples for each date. Colored bars represent different denitrifying genes and open diamonds represent the mean abundances of 16S rRNA.

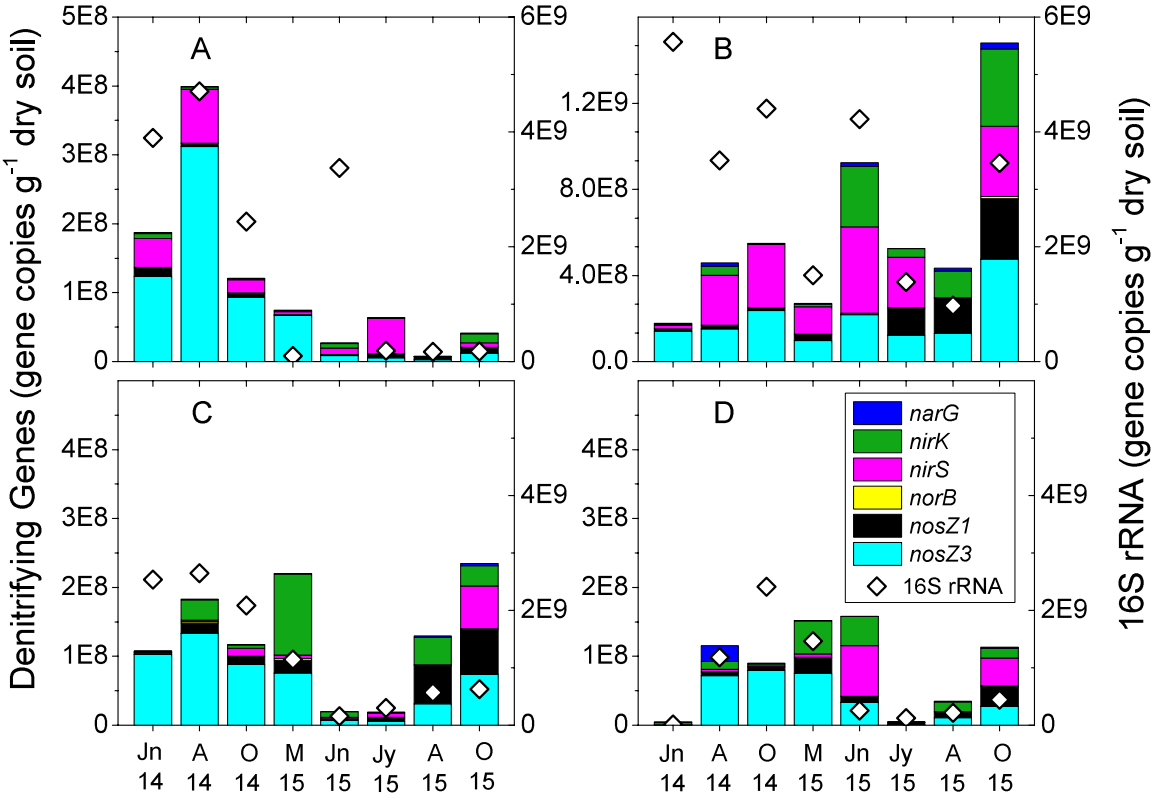

Figure 5.17. Mean denitrifying gene abundances at (A) the floodzone location of SMC-1, (B) the floodzone location of SMC-2, (C) the non-floodzone location of SMC-1, and (D) the non-floodzone location of SMC-2 over the field sampling duration. The mean for each genes was determined from the triplicate samples for each date. Colored bars represent different denitrifying genes and open diamonds represent the mean abundances of 16S rRNA.

Table 5.4. Differences in gene abundances due to year, site, and location at Seven Mile Creek sites. Significant ($\alpha = 0.05$) correlations are shown with Tukey's post-hoc *p* values in parenthesis.

Gene	Year	Location	Site
16S rRNA	2014 > 2015 (<0.001)	floodzone > others (<0.001)	SMC3 < others (<0.001)
cnorB	2015 > 2014 (0.005)	channel < others (0.002)	SMC3 < others (<0.001)
narG			
nirS		non-floodzone < others (0.007)	SMC2 > others (<0.001)
nirK	2015 > 2014 (0.001)	channel < non-floodzone < foodzone (0.003)	SMC2 > others (0.001)
nosZ1	2015 > 2014 (<0.001)	floodzone > others (0.004)	SMC2 > others (<0.001)
nosZ3	2014 > 2015 (0.002)	floodzone > others (<0.001)	SMC3 < others (<0.001)

Table 5.5. Correlations between gene copy numbers per gram dry soil, organic matter (OM), water content (WC), bulk density (ρ_b), nitrate concentration (C_{NO3}), DeN rates, and DEA rates for channel locations in Seven Mile Creek (SMC) in 2015 represented with Spearman's ρ and the significance (p). Only significant correlations ($\alpha > 0.05$) are shown.

	16S rRNA		*norB*		*narG*		*nirS*		*nirK*		*nosZ1*		*nosZ3*	
	ρ	p	ρ	p	ρ	p	ρ	p	ρ	p	ρ	p	ρ	p
OM	0.82	<0.001	0.48	0.001	0.57	<0.001	0.56	<0.001	0.54	<0.001	0.62	<0.001	0.83	<0.001
WC	0.72	<0.001	0.51	<0.001	0.51	0.003	0.50	<0.001	0.60	<0.001	0.64	<0.001	0.80	<0.001
ρ_b	-0.66	<0.001	-0.48	<0.001	-0.38	0.010	-0.43	0.004	-0.51	<0.001	-0.68	<0.001	-0.75	<0.001
C_{NO3}							0.30	0.045	0.56	<0.001	0.46	0.002	0.43	0.003
DeN	0.36	0.018	0.40	0.009					0.43	0.004	0.66	<0.001	066	<0.001
DEA	0.65	<0.001	0.41	0.006	0.41	0.005	0.40	0.007	0.47	0.001	0.64	<0.001	0.68	<0.001

Table 5.6. Correlations between gene copy numbers per gram dry soil, organic matter (OM), water content (WC), bulk density (ρ_b), DeN rates, and DEA rates for floodzone locations in Seven Mile Creek (SMC) in 2015 represented with Spearman's ρ and the significance (p). Only significant correlations ($\alpha > 0.05$) are shown.

	16S rRNA		*norB*		*narG*		*nirS*		*nirK*		*nosZ1*		*nosZ3*	
	ρ	p	ρ	p	ρ	p	ρ	p	ρ	p	ρ	p	ρ	p
OM	0.70	<0.001	0.74	<0.001	0.73	<0.001	0.49	0.010	0.66	<0.001	0.68	<0.001	0.84	<0.001
WC	0.69	<0.001	0.82	<0.001	0.65	<0.001	0.46	0.011	0.76	<0.001	0.78	<0.001	0.72	<0.001
ρ_b	-0.67	<0.001	-0.82	<0.001	-0.70	<0.001	-0.42	0.022	-0.76	<0.001	-0.77	<0.001	-0.80	<0.001
DeN	0.64	0.003	0.82	<0.001	0.70	<0.001	0.37	0.046	0.85	<0.001	0.76	<0.001	0.75	<0.001
DEA	0.65	0.002	0.89	<0.001	0.73	<0.001	0.43	0.017	0.76	<0.001	0.82	<0.001	0.78	<0.001

Table 5.7. Correlations between gene copy numbers per gram dry soil, organic matter (OM), water content (WC), bulk density (ρ_b), DeN rates, and DEA rates for non-floodzone locations in Seven Mile Creek (SMC) in 2015 represented with Spearman's ρ and the significance (p). Only significant correlations ($\alpha > 0.05$) are shown.

	16S rRNA		*norB*		*narG*		*nirS*		*nirK*		*nosZ1*		*nosZ3*	
	ρ	p	ρ	p	ρ	p	ρ	p	ρ	p	ρ	p	ρ	p
OM														
WC														
ρ_b														
DeN							0.38	0.037						
DEA							0.47	0.008						

5.4.5 Microbial Community Analysis

Operational taxonomic units (OTUs) ranged from 385 to 8,160, with a mean Good's coverage of 96.3 ± 0.3% (mean ± standard deviation). Alpha diversity, referring to the species richness (Jost, 2007) as measured by Shannon indices, was significantly greater for 2015 samples compared to 2014 (7.26 ± 0.40 and 4.07 ± 0.23, respectively, $p < 0.001$) (Figure 5.18). For 2014 samples, diversity decreased by position as: channel > floodzone > non-floodzone ($p \leq 0.002$), but there was no significant difference in diversity between sampling months. In 2015, there was no significant difference in diversity between channel and floodzone locations, but both locations were significantly greater than the diversity at the non-floodzone locations (Figure 5.18B). Also, diversity varied by sampling month in 2015, with July ($p = 0.014$) and August ($p = 0.018$) having significantly greater diversity than in May.

The prokaryotic community composition, or beta diversity, among samples was significantly different between years (ANOSIM R = 1, $p < 0.001$). Sample location had a greater influence on beta diversity (R = 0.271, post-hoc $p < 0.01$) than did sample site (R = 0.066, $p \leq 0.013$) for the entire sampling duration. When separated by year, this trend was maintained, except community composition between in-channel locations at SMC-2 and SMC-3 were not significantly different in 2014. The community composition also did not significantly vary by month for either year. Ordination of Bray-Curtis dissimilarities matrices using PCoA showed distinct separation by sample location, particularly in 2014 (Figure 5.19 showing the 15 most abundant families in each year). Analysis relating family abundances to ordination position using a Spearman correlation analysis showed similar trends for both years ($p \leq 0.006$). Specifically, abundances of member of the family *Anaerolineaceae* were related to in-channel samples, members of *Cytophagaceae*, *Gemmatimonadaceae*, and *Xanthomonadaceae* were related to floodzone samples, and members of *Gaiellaceae* were found at greater abundances in non-floodzone samples.

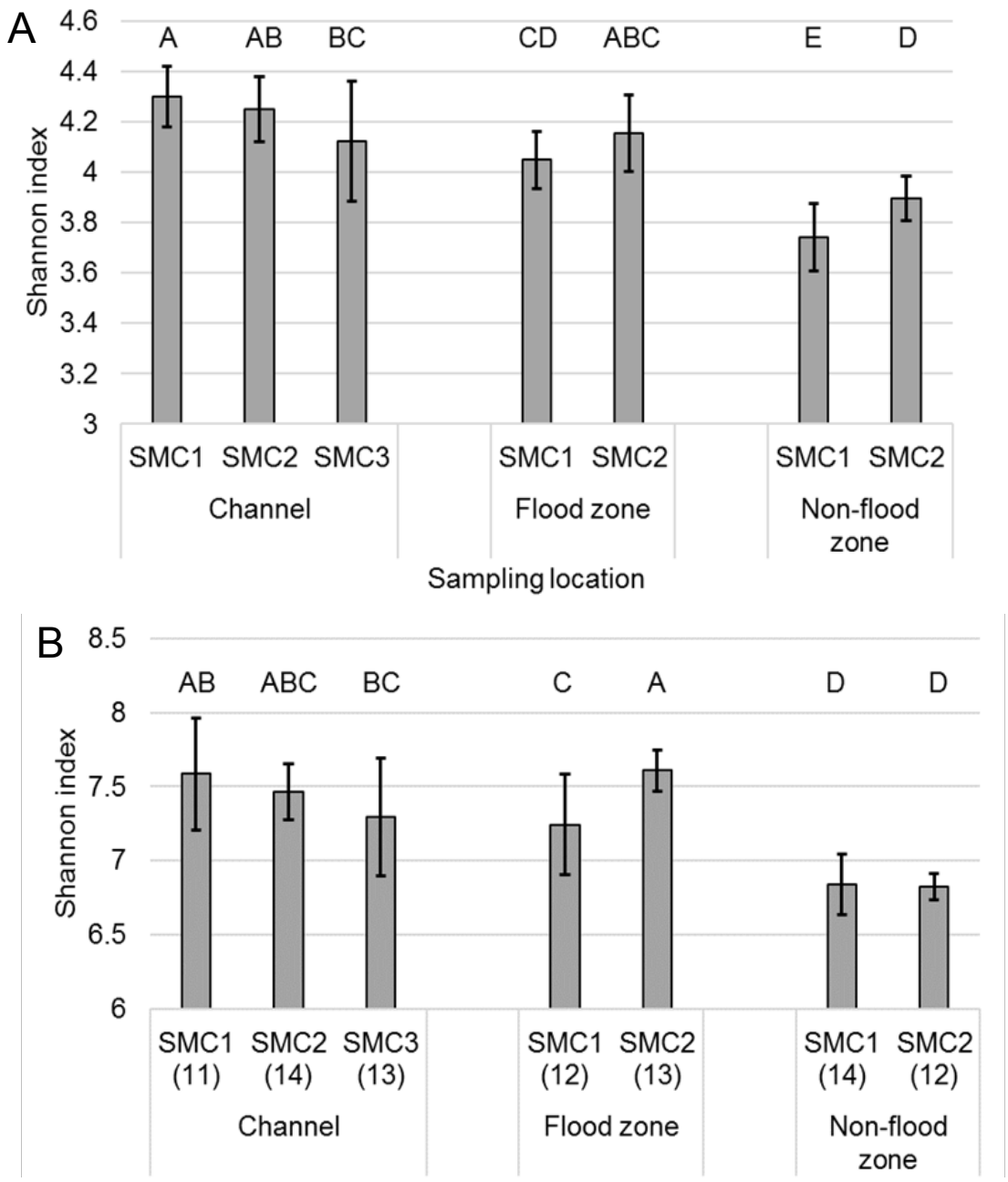

Figure 5.18. Shannon indices of sites and locations from (A) 2014 and (B) 2015. The error bars represent the standard deviation. In 2017, n = 9 for all groups, and in 2015, n is shown in parenthesis. Letters represent differences as determined by a Tukey's post-hoc analysis. Sites that are not connected by the same letter have significantly different Shannon indices, and the letters are arranged according to decreasing indices. Courtesy: Dr. Christopher Staley.

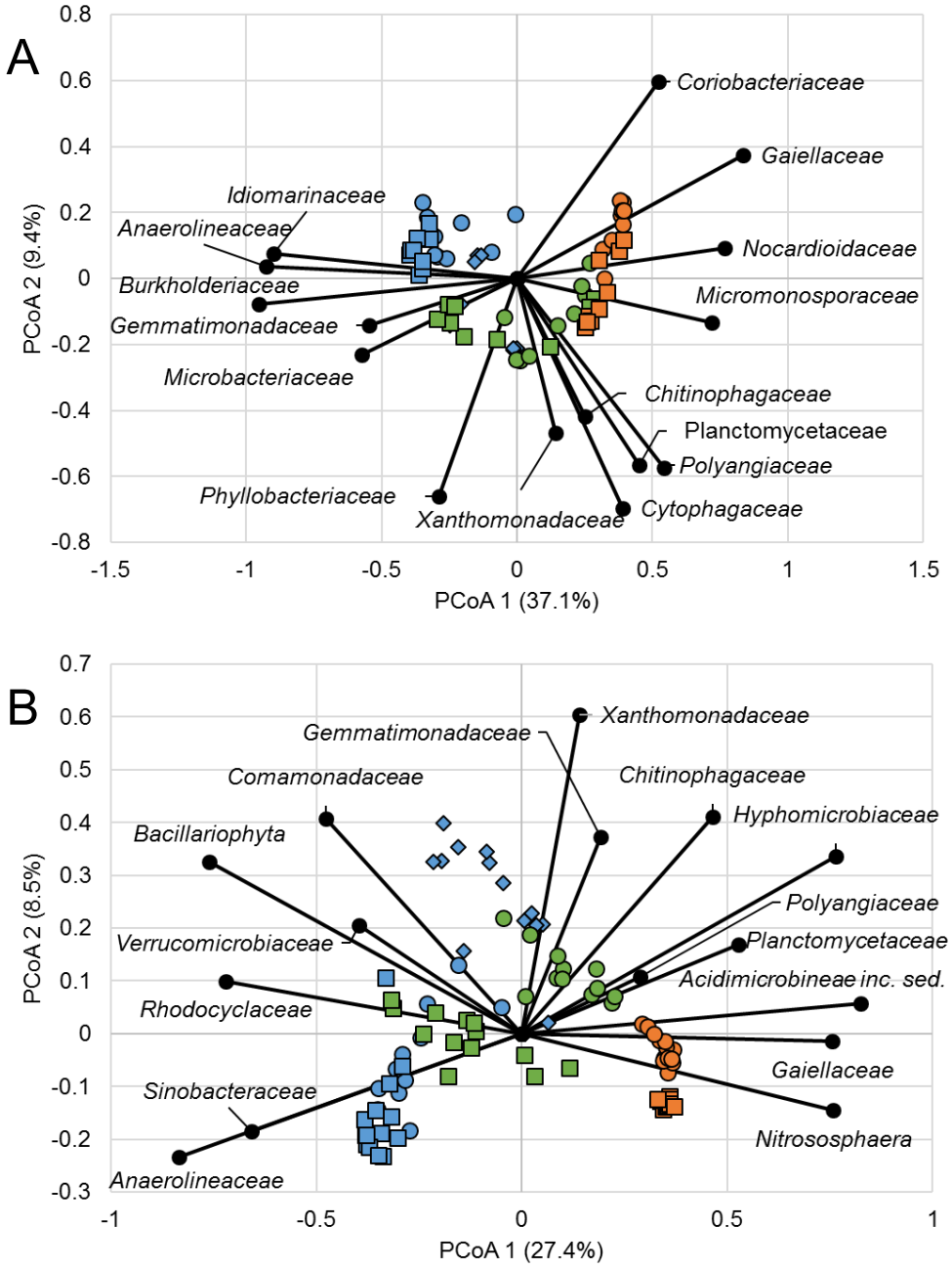

Figure 5.19. Principal coordinate analysis of Bray-Curtis dissimilarity matrices from soil samples collected in (A) 2014 ($r^2 = 0.82$) and (B) 2015 ($r^2 = 0.73$). Relative abundances of the 15 most abundance families were significantly correlated with ordination position ($p < 0.05$). Legend: SMC1 (●), SMC2 (■), SMC3 (♦), channel (blue), flood zone (green), non-flood zone (orange). Courtesy: Dr. Christopher Staley.

To determine the effects of community composition, denitrifying gene abundances, spatial and temporal variability, and environmental parameters on DeN and DEA rates, a constrained redundancy analysis was used for variance partitioning. Community composition as measured by the abundances of the predominant families (mean ≥1.0% of sequence reads) alone accounted for 21.8% of the variation in denitrification rates. Non-community factors accounted for 37.1% of the variation in denitrification rates, and interactions between all parameters accounted for 41.1%.

A canonical correspondence analysis (CCA) was used to investigate the relationships between all parameters and the microbial community (Figure 5.20). Denitrification genes were closely clustered, and were significantly positively correlated with one another according to Spearman's correlation (ρ = 0.221 to 0.826, $p \leq 0.004$). Similar to the PCoA analysis, channel and non-floodzone locations were found to associate with bacterial families. However, floodzone locations showed inconsistent relationships between PCoA and CCA. There were no consistent correlations between family abudnances and denitrification genes. DeN rates were positively correlated to the abundances of families *Burkholderiaceae*, *Anaerolinaceae*, *Acidimicrobineae incertae sedis*, *Cytophagaceae*, and *Hyphomicrobiaceae* (arranged according to increasing abundances) (ρ = 0.169 to 0.251, $p \leq 0.041$), while families of *Gaiellaceae*, *Comamonadaceae*, and *Sinobacteraceae* were negatively correlated (ρ = -0.291 to -0.168, $P \leq 0.042$).

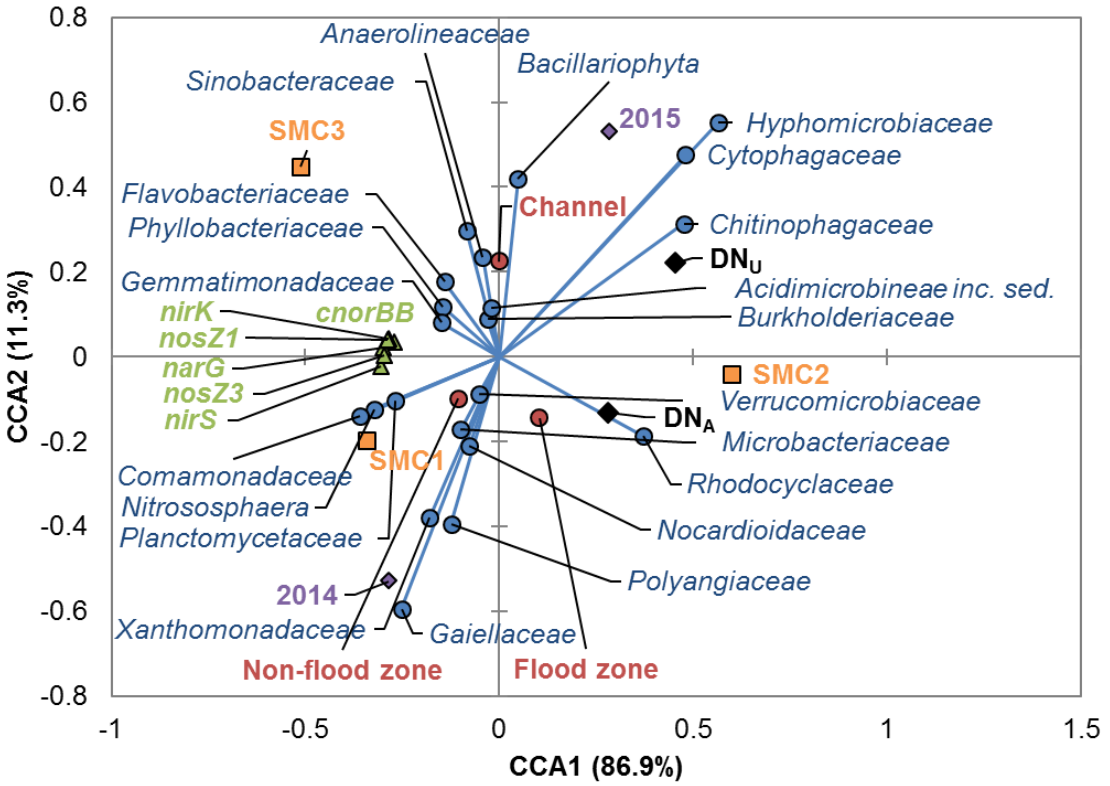

Figure 5.20. Conical correspondence analysis of sampling sites, years, and locations; denitrification rates; denitrification gene abundances; and family abundances (from the 15 most abundant families). Legend: sampling sites (■), years (♦), positions (●), denitrification rates (■), denitrification genes (▲), and prokaryotic families (●). Courtesy: Dr. Christopher Staley.

5.5 Discussion

5.5.1 Influence of Environmental Parameters on Denitrification

Denitrification rates under site conditions (DeN) and non-nutrient limiting conditions (DEA) varied in response to sampling location (hydrologic connectivity of a site) and environmental parameters. Precipitation greatly affects nitrate loading, with loads increasing by 51% in wet years, and nitrate varies by season, with concentrations generally being greatest in spring, followed by summer, and lowest in the fall (MPCA, 2013). In August and October 2014, and May 2015, when nitrate concentrations were lowest, the low DeN rates and the large differences between DeN and DEA implied that

channel locations at SMC-1 and SMC-2 were likely nitrate limited on these dates. Nitrate concentrations were high throughout the 2015 sampling period, except in May, potentially due to the higher precipitation.

Nitrate is one of the main controlling factors in denitrification. In this study, there was a weak significant correlation between denitrification and stream nitrate concentrations (Figure 5.11C). When looking further at this figure, there is a line of pink triangles (SMC-2) along the x-axis in the bulk density (D), organic matter (E), and water content (F) graphs, indicating very low DeN rates where the trends for these parameters predict higher rates. This can be explained by the low nitrate concentrations during these sampling times. The relationship we found between DeN and nitrate in this study was similar to a relationship developed using previous studies from reference, agricultural, and urban streams using multiple methods (Figure 5.12). Figure 5.13 reinforces the effect of nitrate concentrations on denitrification. When nitrate concentrations are high (>5 mg $N\text{-}NO_3^-$ L^{-1}), adding nutrients (carbon, phosphate, nitrate) has a much smaller affect on denitrification rates compared to when nitrate concentrations are low.

Besides stream nitrate, other environmental parameters that are significantly correlated with DeN rates at in-channel locations include water depth, bulk density, soil organic matter, and soil water content ($p < 0.001$ for all parameters), however all trends were relatively weak (greatest r^2 of 0.29). Denitrification is not universally controlled by a single parameter, but instead is better predicted by including several parameters (Chapter 4.6.2). At SMC sites, there were no sampling points where nitrate concentration was low and sediment organic matter was high (Figure 5.13). SMC-3 had low organic matter, but had high nitrate concentrations due to the groundwater inflow directly upstream of the site. This graph was presented previously with only 2014 data but with the inclusion of OSL sites (Figure 4.12), where OSL sites had low organic matter and low nitrate. While adding nitrate to theses samples with low organic matter, the DEA to DeN ratio remained low, whereas in the higher organic matter SMC samples, the DEA to DeN ratio greatly increased, again emphasizing the inter-connectedness between environmental parameters.

Denitrification rates at the floodzone locations were significantly negatively related to soil nitrate concentration and bulk density, and positively related to sediment

organic matter and soil water content. As discussed above, increasing stream nitrate concentrations were positively related to denitrification rates, which is expected since nitrate serves as an electron accepter in denitrification. Soil nitrate concentrations were much lower at SMC-2 than at SMC-1, and denitrification rates were higher at SMC-2 compared to SMC-1. The floodzone location of SMC-2 was inundated more frequently than SMC-1, therefore one possibility is that the inundation led to anoxic conditions and therefore denitrification at SMC-2, reducing the soil nitrate condition. If SMC-1 was not inundated, oxygen could have more readily diffused into the sediment, thereby inhibiting denitrification, and potentially increasing nitrification rates and the production of nitrate from ammonia, resulting in higher soil nitrate concentrations. Since soil water extractions solely for nitrate were used, it is impossible to tell how the ammonia concentration (as an indication for nitrification) was changing over time.

At the non-floodzone location, denitrification rates were only significantly related to bulk density and water content. Unlike the other locations where bulk density and denitrification were negatively related, increasing bulk density was positively related to denitrification rates. This is probably due to the positive correlation between bulk density and water content at the non-floodzone locations, whereas at in-channel and floodzone locations, bulk density and water content are negatively correlated. Soil nitrate concentrations at non-floodzone locations were greater than in-channel and floodzone locations, most likely due to similar reasons as described above. Denitrification is inhibited in oxygenic environments, and non-floodzone locations were never inundated. Therefore, there would be more oxygen into the sediment, less denitrification, and greater soil nitrate.

5.5.2 The Effect of Hydrologic Connectivity on Denitrification

In-channel denitrification was very different at SMC-3 compared to SMC-1 and SMC-2. SMC-3 had much lower DeN and DEA rates compared to SMC-1 and SMC-2, which may be due to site characteristics including sandy sediment and greater shear velocities, leading to a potentially less stable microbial community due to increased bedload transport (Arnon et al., 2007a; Tomasek et al., 2017). Both DeN and DEA for in-channel locations at SMC-2 was significantly greater ($p = 0.009$ and $p < 0.001$, respectively) than

at SMC-1 and SMC-3. SMC-2 generally had the lowest bulk density, greatest organic matter, and lowest dissolved oxygen (Table 5.1), all conditions that favor denitrification.

Previous research has shown that reconnecting channels with riparian areas can enhance denitrification (Kaushal et al., 2008; Klocker et al., 2009; Mahl et al., 2015; Roley et al., 2012a). The two agricultural sites in this study, SMC-1 and SMC-2, had differing ditch geometry. SMC-1 had a traditional trapezoidal configuration (Figure 5.3), whereas SMC-2 had an inset depositional floodplain at the floodzone location (Figure 5.4). Therefore, the floodzone location at SMC-2 would have a larger reactive surface area, more sediment-water contact time, a larger hyporheic zone, and would likely favor greater rates of nitrogen cycling (Hefting et al., 2006; McClain et al., 2003; Wang et al., 2012; Woodward et al., 2015). Precipitation during the summer of 2014 occurred largely in one rain event in late June, whereas the rest of the summer was relatively dry. In comparison, precipitation was greater and occurred more frequently throughout the summer in 2015. The increased precipitation in 2015 caused inundation at the floodzone location, particularly at SMC-2. This potentially caused the differential correlations between denitrification rates, environmental parameters, and gene abundances in 2015 compared to 2014 at floodzone locations (Table 5.6 compared to Table 4.6). The floodzone location at SMC-2 had significantly greater soil moisture content and DeN in 2015 than in 2014. However, there was no significant difference between 2015 and 2014 in soil water content or DeN at the floodzone location of SMC-1. Denitrifying gene abundances were also significantly greater at the floodzone location of SMC-2 compared to SMC-1 in 2015.

DeN and DEA rates at the non-floodzone locations of SMC-1 and SMC-2 remained relatively constant throughout the study period. DeN rates at non-floodzone locations at both sites were statistically similar over the study period. Similarly, DEA rates were significantly greatest in November 2015 at both sites, and were the lowest at SMC-1 in August 2014, but were otherwise statistically similar over the period. From the normalized histograms of DeN and DEA rates (Figure 5.9 and Figure 5.10), non-floodzone locations had the smallest range of denitrification rates, consistent rates on all dates (fewest number of bins for the different locations), and no extreme values.

5.5.3 Denitrification Rates and the Microbial Community

Similar temporal patterns were also observed between denitrification rates and gene abundances. For in-channel sites, denitrifying gene abundances were greatest in July 2015 at SMC-2 and August 2014 at SMC-3. These dates also had high denitrification rates relative to other sampling dates. At the SMC-1 floodzone locations, DEA rates appeared to decrease exponentially (Figure 5.8), and denitrifying gene abundances followed a similar pattern (Figure 5.17).

Abundances of all genes except *nirS* were significantly and positively correlated to DeN, and all abundances were correlated to DEA when all locations are considered together. This suggests that in Seven Mile Creek sites, denitrification is related to active transcription and the abundances of denitrifying bacteria at sites (Rocca et al., 2015). When separated by location, correlations between rates and abundances differ. We previously reported that in 2014, denitrifying gene abundances were coupled with DEA rates only at in-channel locations (Tomasek et al., 2017) (Chapter 4.6.3). When data from both years is considered, abundances of all genes are correlated with DEA at both in-channel and floodzone locations, and now, DeN is also correlated with gene abundances, with the exception of *narG* and *nirS*. In 2014, in-channel nitrate concentrations were low, so even if denitrifiers were present, without nitrate, no denitrification would occur, therefore a correlation between gene abundances and DeN is not expected. In 2014, denitrification was not positively correlated with any gene abundances at non-floodzone locations, and in 2015, it was only correlated with *nirS* abundances.

The lack of correlation between denitrification rates and gene abundances may explain why similar denitrification rates with a small range in potential values were observed across sampling dates at the non-floodzone locations, where unfavorable environmental conditions limit denitrification rates, even when denitrifying bacteria are present. Our data may suggest that inundation is one method that may induce a denitrification response, and the potential formation of hot spots and hot moments, by providing more favorable environmental conditions. In 2014, when precipitation was lower and the floodzone was not inundated, floodzone locations had few correlations between environmental parameters, rates, and abundances, similar to the non-floodzone locations. However, in 2015, when the floodzone location was periodically inundated,

correlations between parameters, rates, and abundances were much stronger, similar to the in-channel locations. This suggests that by inundating a previously dry area, denitrification rates may be stimulated. Similarly, a previous study suggested that flooding induced a physiological response among denitrifiers (Manis et al., 2014).

Metagenomic analysis provides further information on how hydrologic connectivity affects microbial community structure and the relationship between the bacterial community and denitrification rates. Soil microbial communities have previously been shown to vary more as a result of site than specific treatments (Fernandez et al., 2016a; Fernandez et al., 2016b). Community composition differed between sampling years and sites, but hydrologic connectivity was shown to more strongly drive differences in composition than annual or geographic variation. Family-level abundances and functional genes significantly separated by hydrologic regime, with increasing connectivity corresponding to an increase in the abundances of Proteobacteria, similar to a previous report by Agarioff et al. (2017). Increasing hydrologic connectivity favored more highly anaerobic communities, but denitrification genes were evenly spread across the three locations. There were few correlations between family-level abundances and either denitrification rates or gene abundances, potentially due to the functional redundancy resulting from the wide distribution of these genes (Shapleigh, 2006; Zumft, 1997). Prokaryotic community composition and its interaction with other environmental parameters caused a considerable amount of variation in denitrification rates. Several of the families correlated with denitrification rate were significantly associated with inundation, such as *Anaerolinaceae* and *Microbacteriaceae*, suggesting these families potentially play an important role in denitrification.

The community diversity also shows trends similar to denitrification rates. For in-channel locations, SMC-3 had significantly lower alpha diversity compared to SMC-1 and SMC-2 in both 2014 and 2015, and both DeN and DEA were also much lower at this site. At floodzone locations, SMC-2 had significantly greater diversity than SMC-1, and DeN and DEA were both much greater at SMC-2. Non-floodzone locations had much lower diversity than either in-channel or floodzone locations, which may also have led to the lower denitrification rates at this location. With smaller diversity, there is less redundancy in the community, meaning the location is less adaptable to unfavorable

environmental conditions, like the high-oxygen, low-moisture conditions at the non-floodzone locations.

5.6 Conclusions

Results of this study reveal how varying hydrologic regimes associated with differences in hydrologic connectivity influence both denitrification rates as well as prokaryotic community composition. Frequent inundation increases both denitrification gene abundances and denitrification rates, and indirectly influences the composition of the microbial community. Non-inundated locations had consistent denitrification rates across the sampling duration, along with significantly lower diversity than in-channel and floodzone locations. Also, family-level abundances and functional genes significantly separated by hydrologic regime. Further study is necessary to determine which environmental parameters are most likely to shift microbial communities to stimulate biogeochemical processes including denitrification. However, this study provides novel evidence that inundation drives shifts in the microbial community that increase denitrification rates. Thus, changing patterns of hydrologic connectivity may serve as an effective management strategy to remediate nitrate pollution by causing corresponding shifts in the microbial community.

6 Conclusions

6.1 Summary of Thesis

Anthropogenic alteration of the nitrogen cycle has resulted in increased nitrate loading to surface and groundwater in the Midwestern United States. Denitrification, the microbial reduction of nitrate to nitrogen gas, can be viewed as a net sink for reactive nitrogen in aquatic systems. Understanding the mechanisms that mediate and enhance denitrification can better inform the design and implementation of management strategies. Research presented in this dissertation focused on identifying the environmental drivers of denitrification rates and the microbial community using a range of scales, from small-scale laboratory experiments, to larger-scale outdoor experiments, to field-scale investigations.

A recirculating laboratory flume was used to determine the effect of small-scale turbulence and sediment organic carbon on denitrification. Sediment for the flume experiment was collected from an agricultural ditch, and was used either as-collected or amended with soybean meal. Results showed that nitrate uptake was mediated by turbulence levels above the sediment-water interface, and maximum nitrate uptake for unamended and carbon-amended occurred when friction velocities were between 0.75 and 1.25 cm s^{-1}. Carbon-amended sediment had faster uptake rates than as-collected sediment. For experiments using as-collected sediment, gene abundances significantly increased over the course of the experiments for mid-range friction velocities, but increases were not observed for low and high friction velocities. Results from this experiment could provide guidance in promoting fluid-flow conditions in streams and channels to maximum nitrate uptake in agricultural watersheds.

The effect of short-term inundation in an outdoor experimental stream and longer duration inundation for different soil carbon contents in a flow-through basin were explored in the Outdoor StreamLab. Results showed that short-term flood events in the experimental stream and floodplain enhanced denitrification rates up to one-day post inundation, but that short-term flood events did not lead to increases in denitrifying gene abundances of changes in community diversity. Longer duration inundation in the flow-

through basin led to sustained increases in denitrification rates. These results suggest that management strategies that promote hydrologic connectivity and intermittent flooding could enhance the formation of denitrification hot spots and hot moments.

Field sampling was used to further explore the drivers of denitrification, and to investigate the effect of hydrologic connectivity on denitrification rates and the microbial community. Samples were collected from a site in Southern Minnesota in 2014 and 2015. Since more than a single environmental parameter influences denitrification, a scaling relationship was performed to develop a predictive functional relationship for in-channel denitrification rates. A functional relationship was developed for floodzone and non-floodzone locations for 2014, but the relationship failed to be significant in 2015, possibly due to the higher rainfall intensity. Results showed that for both 2014 and 2015, environmental parameters, denitrification rates, and denitrifying gene abundances were strongly correlated for in-channel locations, and but there was little to no correlation for non-floodzone locations. However, for floodzone sites, there were few correlations between parameters, rates, and abundances in 2014, but for 2015, when the floodzone was inundated at a greater frequency than 2014, they were strongly correlated. Metagenomic analysis revealed that hydrologic connectivity had a large effect on the prokaryotic community. These results suggest that reconnecting channels with their floodplains, and allowing for increased hydrologic connectivity could cause a shift in the prokaryotic community and result in increased denitrification rates.

Nitrate concentrations in the agricultural Midwest continue to exceed surface water standards, with negative implications for human health and aquatic ecosystems, emphasizing the need for effective management strategies. Based on the research presented in this dissertation, managing channels to maintain optimal friction velocities, creating periodic pulse-flows to deliver water to riparian areas, and increasing hydrologic connectivity of agricultural streams could increase denitrification in agricultural watersheds. Therefore, management strategies that promote these findings could facilitate sustained increases in nitrate uptake, and reduce nitrogen loading to higher-order streams.

6.2 Overall Conclusions

This dissertation investigated the effects of environmental parameters and inundation on denitrification rates and the microbiological communities in an agricultural landscape. Turbulence and organic carbon were discovered to mediate nitrate uptake, with carbon-amended sediment having greater rates than unamended sediment, and both types of sediment having optimal uptake at mid-range shear stress velocities above the sediment-water interface. Short-term inundation stimulated transient increases in denitrification rates, while longer duration inundation caused sustained increases in denitrification rates, indicating the potential formation of denitrification hot moments and hot spots, respectively.

6.3 Recommendations

Results discussed in this dissertation provide four recommendations for the promotion of denitrification in agricultural channels. One: control fluid flow in channels and target mid-range shear velocities for optimal denitrification rates. Two: design channels for inundation since both pulse flows and longer inundation periods enhance denitrification rates. Three: reconnect channels with riparian areas. This has several benefits including slower water flows in the channel, increased organic matter, and more reactive surface area leading to greater sediment-water contact time and therefore greater denitrification. Four: use a combination of management practices including on-field management strategies. Denitrification in channels and riparian areas alone is not enough to reduce the extremely high loads of nitrate in agricultural surface waters to acceptable levels, even with optimized rates.

6.4 Future Work

Flume experiments showed that amending sediment with soybean meal increased nitrate uptake, but most of this denitrification was as incomplete denitrification, which has negative implications for greenhouse gas emissions. Future work should investigate the effect of amending sediment with various qualities of carbon to determine the optimal type of carbon amendment with enhanced uptake rates but reduced N_2O yields. Flood experiments in the outdoor experimental stream showed short-term increases in

denitrification rates with no affect on denitrifying gene abundances. We inferred that favorable environmental conditions stimulated the activity of denitrifying bacteria, thereby increasing nitrate uptake rates. However, DNA-based methods can only determine whether a gene is present, not whether the gene is active. Therefore, future work should incorporate RNA-based methods to determine how inundation affects the expression of denitrifying genes. Longer duration inundations lead to sustained increases in denitrification rates, however microbiological analysis was not performed for this experiment. Future work should investigate how inundation affects both gene abundances and expression of these genes, and should investigate how different periods of inundation frequency affect denitrification rates to design optimal management strategies. Since denitrification rates in the floodzone location were discovered to be highly dependent on inundation history, future work should add a variable to the functional relationship that incorporates inundation frequency and duration in the riparian zone.

7 References

Alexander, R. B., Bohlke, J. K., Boyer, E. W., David, M. B., Harvey, J. W., Mulholland, P. J., Seitzinger, S. P., Tobias, C. R., Tonitto, C. and Wollheim, W. M. (2009), Dynamic modeling of nitrogen losses in river networks unravels the coupled effects of hydrological and biogeochemical processes, *Biogeochemistry,* 93, 91-116.

Anderson, M. J. and Willis, T. J. (2003), Canonical analysis of principal coordinates: A useful method of constrained ordination for ecology, *Ecology,* 84(2), 511-525.

Arango, C. P., Tank, J. L., Schaller, J. L., Royer, T. V., Bernot, M. J. and David, M. B. (2007), Benthic organic carbon influences denitrification in streams with high nitrate concentration, *Freshwater Biology,* 52(7), 1210-1222.

Arat, S., Bullerjahn, G. S. and Laubenbacher, R. (2015), A Network Biology Approach to Denitrification in Pseudomonas aeruginosa, *Plos One,* 10(2), 12.

Argiroff, W. A., Zak, D. R., Lanser, C. M. and Wiley, M. J. (2017), Microbial Community Functional Potential and Composition Are Shaped by Hydrologic Connectivity in Riverine Floodplain Soils, *Microbial Ecology,* 73(3), 630-644.

Arnon, S., Gray, K. A. and Packman, A. I. (2007a), Biophysicochemical process coupling controls nitrate use by benthic biofilms, *Limnology and Oceanography,* 52(4), 1665-1671.

Arnon, S., Peterson, C. G., Gray, K. A. and Packman, A. I. (2007b), Influence of flow conditions and system geometry on nitrate use by benthic biofilms: Implications for nutrient mitigation, *Environmental Science & Technology,* 41(23), 8142-8148.

Aronesty, E. (2013), Comparison of Sequencing Utility Programs, *The Open Bioinformatics Journal,* 7, 1-8.

Austin, A. T., Yahdjian, L., Stark, J. M., Belnap, J., Porporato, A., Norton, U., Ravetta, D. A. and Schaeffer, S. M. (2004), Water pulses and biogeochemical cycles in arid and semiarid ecosystems, *Oecologia,* 141(2), 221-235.

Baldwin, D. S. and Mitchell, A. M. (2000), The effects of drying and re-flooding on the sediment and soil nutrient dynamics of lowland river-floodplain systems: A synthesis, *Regulated Rivers-Research & Management,* 16(5), 457-467.

Bandibas, J., Vermoesen, A., Degroot, C. J. and Vancleemput, O. (1994), The effect of different moisture regimes and soil characteristics on nitrous-oxide emission and consumption by different soils, *Soil Science,* 158(2), 106-114.

Banerjee, S., Helgason, B., Wang, L. F., Winsley, T., Ferrari, B. C. and Siciliano, S. D. (2016), Legacy effects of soil moisture on microbial community structure and N2O emissions, *Soil Biology & Biochemistry,* 95, 40-50.

Barnes, E. A., Power, M. E., Foufoula-Georgiou, E., Hondzo, M. and Dietrich, W. E. (2007), Upscaling river biomass using dimensional analysis and hydrogeomorphic scaling, *Geophysical Research Letters,* 34(24).

Beaulieu, J. J., Arango, C. P. and Tank, J. L. (2009), The Effects of Season and Agriculture on Nitrous Oxide Production in Headwater Streams, *Journal of Environmental Quality,* 38(2), 637-646.

Beaulieu, J. J., Tank, J. L., Hamilton, S. K., Wollheim, W. M., Hall, R. O., Mulholland, P. J., Peterson, B. J., Ashkenas, L. R., Cooper, L. W., Dahm, C. N., Dodds, W. K.,

Grimm, N. B., Johnson, S. L., McDowell, W. H., Poole, G. C., Valett, H. M., Arango, C. P., Bernot, M. J., Burgin, A. J., Crenshaw, C. L., Helton, A. M., Johnson, L. T., O'Brien, J. M., Potter, J. D., Sheibley, R. W., Sobota, D. J. and Thomas, S. M. (2011), Nitrous oxide emission from denitrification in stream and river networks, *Proceedings of the National Academy of Sciences of the United States of America,* 108(1), 214-219.

Bernot, M. J., Dodds, W. K., Gardner, W. S., McCarthy, M. J., Sobolev, D. and Tank, J. L. (2003), Comparing denitrification estimates for a texas estuary by using acetylene inhibition and membrane inlet mass spectrometry, *Applied and Environmental Microbiology,* 69(10), 5950-5956.

Bettez, N. D. and Groffman, P. M. (2012), Denitrification Potential in Stormwater Control Structures and Natural Riparian Zones in an Urban Landscape, *Environmental Science & Technology,* 46(20), 10909-10917.

Billings, S. A., Schaeffer, S. M. and Evans, R. D. (2003), Nitrogen fixation by biological soil crusts and heterotrophic bacteria in an intact Mojave Desert ecosystem with elevated CO2 and added soil carbon, *Soil Biology & Biochemistry,* 35(5), 643-649.

Biron, P. M., Robson, C., Lapointe, M. F. and Gaskin, S. J. (2004), Comparing different methods of bed shear stress estimates in simple and complex flow fields, *Earth Surface Processes and Landforms,* 29(11), 1403-1415.

Blackwood, C. B., Dell, C. J., Smucker, A. J. M. and Paul, E. A. (2006), Eubacterial communities in different soil macroaggregate environments and cropping systems, *Soil Biology & Biochemistry,* 38(4), 720-728.

Bogaard, A., Fraser, R., Heaton, T. H. E., Wallace, M., Vaiglova, P., Charles, M., Jones, G., Evershed, R. P., Styring, A. K., Andersen, N. H., Arbogast, R. M., Bartosiewic, L., Gardeisen, A., Kanstrup, M., Maier, U., Marinova, E., Ninov, L., Schafer, M. and Stephan, E. (2013), Crop manuring and intensive land management by Europe's first farmers, *Proceedings of the National Academy of Sciences of the United States of America,* 110(31), 12589-12594.

Borcard, D., Legendre, P. and Drapeau, P. (1992), Partialling out the spatial component of ecological variation, *Ecology,* 73(3), 1045-1055.

Borchard, N., Spokas, K., Prost, K. and Siemens, J. (2014), Greenhouse Gas Production in Mixtures of Soil with Composted and Noncomposted Biochars Is Governed by Char-Associated Organic Compounds, *Journal of Environmental Quality,* 43(3), 971-979.

Bormann, B. T. and Gordon, J. C. (1984), Stand density effects in young red alder plantations- productivity, photosynthate partitioning, and nitrogen-fixation, *Ecology,* 65(2), 394-402.

Bray, R. J. and Curtis, J. T. (1957), An ordination of the upland forest communities of Southern Wisconsin, *Ecological Monographs,* 27(4), 325-349.

Bru, D., Ramette, A., Saby, N. P. A., Dequiedt, S., Ranjard, L., Jolivet, C., Arrouays, D. and Philippot, L. (2011), Determinants of the distribution of nitrogen-cycling microbial communities at the landscape scale, *Isme Journal,* 5(3), 532-542.

Bruesewitz, D. A., Tank, J. L. and Hamilton, S. K. (2012), Incorporating spatial variation of nitrification and denitrification rates into whole-lake nitrogen dynamics, *Journal of Geophysical Research-Biogeosciences,* 117, 12.

Buckingham, E. (1914), On physically similar systems: illustrations of the use of dimensional equations, Physical Review.

Bukaveckas, P. A. (2007), Effects of channel restoration on water velocity, transient storage, and nutrient uptake in a channelized stream, *Environmental Science & Technology,* 41(5), 1570-1576.

Burgin, A. J. and Hamilton, S. K. (2007), Have we overemphasized the role of denitrification in aquatic ecosystems? A review of nitrate removal pathways, *Frontiers in Ecology and the Environment,* 5(2), 89-96.

Burt, T. P., Pinay, G., Matheson, F. E., Haycock, N. E., Butturini, A., Clement, J. C., Danielescu, S., Dowrick, D. J., Hefting, M. M., Hillbricht-Ilkowska, A. and Maitre, V. (2002), Water table fluctuations in the riparian zone: comparative results from a pan-European experiment, *Journal of Hydrology,* 265(1-4), 129-148.

Camargo, J. A. and Alonso, A. (2006), Ecological and toxicological effects of inorganic nitrogen pollution in aquatic ecosystems: A global assessment, *Environment International,* 32(6), 831-849.

Cameron, K. C., Di, H. J. and Moir, J. L. (2013), Nitrogen losses from the soil/plant system: a review, *Annals of Applied Biology,* 162(2), 145-173.

Canfield, D. E., Glazer, A. N. and Falkowski, P. G. (2010), The Evolution and Future of Earth's Nitrogen Cycle, *Science,* 330(6001), 192-196.

Cao, Y. P., Green, P. G. and Holden, P. A. (2008), Microbial Community Composition and Denitrifying Enzyme Activities in Salt Marsh Sediments, *Applied and Environmental Microbiology,* 74(24), 7585-7595.

Caporaso, J. G., Lauber, C. L., Walters, W. A., Berg-Lyons, D., Huntley, J., Fierer, N., Owens, S. M., Betley, J., Fraser, L., Bauer, M., Gormley, N., Gilbert, J. A., Smith, G. and Knight, R. (2012), Ultra-high-throughput microbial community analysis on the Illumina HiSeq and MiSeq platforms, *Isme Journal,* 6(8), 1621-1624.

Capps, K. A., Rancatti, R., Tomczyk, N., Parr, T. B., Calhoun, A. J. K. and Hunter, M. J. (2014), Biogeochemical Hotspots in Forested Landscapes: The Role of Vernal Pools in Denitrification and Organic Matter Processing, *Ecosystems,* 17(8), 1455-1468.

Cavigelli, M. A. and Robertson, G. P. (2000), The functional significance of denitrifier community composition in a terrestrial ecosystem, *Ecology,* 81(5), 1402-1414.

Canadian Council of Minisiters of the Environment (2012), Canadian water quality guidelines for the protection of aquatic life: Nitrate. In: Canadian environmental quality guidelines, Canadian Council of Ministers of the Environment, Winnipeg.

Chapman, J. A., Blickenderfer, M. M., Wilson, B. N., Gulliver, J. S. and Missaghi, S. (2013), Competition and growth of eight shoreline restoration species in changing water level environments, *Ecological Restoration,* 31(4), 359-367.

Chen, J. W. and Strous, M. (2013), Denitrification and aerobic respiration, hybrid electron transport chains and co-evolution, *Biochimica Et Biophysica Acta-Bioenergetics,* 1827(2), 136-144.

Chen, Z., Wang, C. H., Gschwendtner, S., Willibald, G., Unteregelsbacher, S., Lu, H. Y., Kolar, A., Schloter, M., Butterbach-Bahl, K. and Dannenmann, M. (2015), Relationships between denitrification gene expression, dissimilatory nitrate

reduction to ammonium and nitrous oxide and dinitrogen production in montane grassland soils, *Soil Biology & Biochemistry,* 87, 67-77.

Cheneby, D., Philippot, L., Hartmann, A., Henault, C. and Germon, J. C. (2000), 16S rDNA analysis for characterization of denitrifying bacteria isolated from three agricultural soils, *Fems Microbiology Ecology,* 34(2), 121-128.

Clarke, K. R. (1993), Nonparametric multivariate analysis of changes in community structure, *Australian Journal of Ecology,* 18(1), 117-143.

Cole, J. R., Wang, Q., Cardenas, E., Fish, J., Chai, B., Farris, R. J., Kulam-Syed-Mohideen, A. S., McGarrell, D. M., Marsh, T., Garrity, G. M. and Tiedje, J. M. (2009), The Ribosomal Database Project: improved alignments and new tools for rRNA analysis, *Nucleic Acids Research,* 37, D141-D145.

Compton, J. E., Harrison, J. A., Dennis, R. L., Greaver, T. L., Hill, B. H., Jordan, S. J., Walker, H. and Campbell, H. V. (2011), Ecosystem services altered by human changes in the nitrogen cycle: a new perspective for US decision making, *Ecology Letters,* 14(8), 804-815.

Corstanje, R. and Reddy, K. R. (2004), Response of biogeochemical indicators to a drawdown and subsequent reflood, *Journal of Environmental Quality,* 33(6), 2357-2366.

Crutzen, P. J., Mosier, A. R., Smith, K. A. and Winiwarter, W. (2008), N2O release from agro-biofuel production negates global warming reduction by replacing fossil fuels, *Atmospheric Chemistry and Physics,* 8(2), 389-395.

Daims, H., Lebedeva, E. V., Pjevac, P., Han, P., Herbold, C., Albertsen, M., Jehmlich, N., Palatinszky, M., Vierheilig, J., Bulaev, A., Kirkegaard, R. H., von Bergen, M., Rattei, T., Bendinger, B., Nielsen, P. H. and Wagner, M. (2015), Complete nitrification by Nitrospira bacteria, *Nature,* 528(7583), 504-509.

Daims, H., Lucker, S. and Wagner, M. (2016), A New Perspective on Microbes Formerly Known as Nitrite-Oxidizing Bacteria, *Trends in Microbiology,* 24(9), 699-712.

Dalsgaard, T., Stewart, F. J., Thamdrup, B., De Brabandere, L., Revsbech, N. P., Ulloa, O., Canfield, D. E. and DeLong, E. F. (2014), Oxygen at Nanomolar Levels Reversibly Suppresses Process Rates and Gene Expression in Anammox and Denitrification in the Oxygen Minimum Zone off Northern Chile, *Mbio,* 5(6), 14.

Dandie, C. E., Burton, D. L., Zebarth, B. J., Trevors, J. T. and Goyer, C. (2007), Analysis of denitrification genes and comparison of nosZ, cnorB and 16S rDNA from culturable denitrifying bacteria in potato cropping systems, *Systematic and Applied Microbiology,* 30(2), 128-138.

Davidson, E. A. (2009), The contribution of manure and fertilizer nitrogen to atmospheric nitrous oxide since 1860, *Nature Geoscience,* 2(9), 659-662.

Decleyre, H., Heylen, K., Tytgat, B. and Willems, A. (2016), Highly diverse nirK genes comprise two major clades that harbour ammonium-producing denitrifiers, *Bmc Genomics,* 17, 13.

Deslippe, J. R., Jamali, H., Jha, N. and Saggar, S. (2014), Denitrifier community size, structure and activity along a gradient of pasture to riparian soils, *Soil Biology & Biochemistry,* 71, 48-60.

Deutsch, B., Forster, S., Wilhelm, M., Dippner, J. W. and Voss, M. (2010), Denitrification in sediments as a major nitrogen sink in the Baltic Sea: an extrapolation using sediment characteristics, *Biogeosciences,* 7(10), 3259-3271.

Di, H. J. and Cameron, K. C. (2002), Nitrate leaching in temperate agroecosystems: sources, factors and mitigating strategies, *Nutrient Cycling in Agroecosystems,* 64(3), 237-256.

Dingman, S. L. (2008), Physical Hydrology. Second ed. Long Grove, IL: Waveland Press, Inc.

Dodla, S. K., Wang, J. J., DeLaune, R. D. and Cook, R. L. (2008), Denitrification potential and its relation to organic carbon quality in three coastal wetland soils, *Science of the Total Environment,* 407(1), 471-480.

Domeignoz-Horta, L. A., Putz, M., Spor, A., Bru, D., Breuil, M. C., Hallin, S. and Philippot, L. (2016), Non-denitrifying nitrous oxide-reducing bacteria - An effective N2O sink in soil, *Soil Biology & Biochemistry,* 103, 376-379.

Doney, S. C. (2010), The Growing Human Footprint on Coastal and Open-Ocean Biogeochemistry, *Science,* 328(5985), 1512-1516.

Dong, N. M., Brandt, K. K., Sorensen, J., Hung, N. N., Hach, C. V., Tan, P. S. and Dalsgaard, T. (2012), Effects of alternating wetting and drying versus continuous flooding on fertilizer nitrogen fate in rice fields in the Mekong Delta, Vietnam, *Soil Biology & Biochemistry,* 47, 166-174.

Du Laing, G., Rinklebe, J., Vandecasteele, B., Meers, E. and Tack, F. M. G. (2009), Trace metal behaviour in estuarine and riverine floodplain soils and sediments: A review, *Science of the Total Environment,* 407(13), 3972-3985.

Duncan, J. M., Groffman, P. M. and Band, L. E. (2013), Towards closing the watershed nitrogen budget: Spatial and temporal scaling of denitrification, *Journal of Geophysical Research-Biogeosciences,* 118(3), 1105-1119.

Ecke, R. (2005), The turbulence problem: an experimentalist's perspective, 29, Available: Los Alamos Science, Los Alamos National Laboratory.

Edgar, R. C., Haas, B. J., Clemente, J. C., Quince, C. and Knight, R. (2011), UCHIME improves sensitivity and speed of chimera detection, *Bioinformatics,* 27(16), 2194-2200.

Ellis, G., Adatia, I., Yazdanpanah, M. and Makela, S. K. (1998), Nitrite and nitrate analyses: A clinical biochemistry perspective, *Clinical Biochemistry,* 31(4), 195-220.

Elser, J. J., Fagan, W. F., Denno, R. F., Dobberfuhl, D. R., Folarin, A., Huberty, A., Interlandi, S., Kilham, S. S., McCauley, E., Schulz, K. L., Siemann, E. H. and Sterner, R. W. (2000), Nutritional constraints in terrestrial and freshwater food webs, *Nature,* 408(6812), 578-580.

Environmental Protection Agency (2015), Mississippi River/Gulf of Mexico Watershed Nutrient Task Force 2015 Report to Congress. United States Environmental Protection Agency.

Erisman, J. W., Sutton, M. A., Galloway, J., Klimont, Z. and Winiwarter, W. (2008), How a century of ammonia synthesis changed the world, *Nature Geoscience,* 1(10), 636-639.

Evans, J. R. (1989), Photosynthesis and nitrogen relationships in leaves of C3 plants, *Oecologia,* 78(1), 9-19.

Excoffier, L., Smouse, P. E. and Quattro, J. M. (1992), Analysis of molecular variance inferred from metric distances among DNA haplotypes - application to human mitochondrial-DNA restriction data, *Genetics,* 131(2), 479-491.

Fageria, N. K. and Baligar, V. C. (2005), Enhancing nitrogen use efficiency in crop plants, in Sparks, D.L. (ed.) *Advances in Agronomy, Vol 88 Advances in Agronomy*. San Diego: Elsevier Academic Press Inc, 97-185.

Fan, A. M. and Steinberg, V. E. (1996), Health implications of nitrate and nitrite in drinking water: An update on methemoglobinemia occurrence and reproductive and developmental toxicity, *Regulatory Toxicology and Pharmacology,* 23(1), 35-43.

Felber, R., Conen, F., Flechard, C. R. and Neftel, A. (2012), Theoretical and practical limitations of the acetylene inhibition technique to determine total denitrification losses, *Biogeosciences,* 9(10), 4125-4138.

Fellows, C. S., Hunter, H. M., Eccleston, C. E. A., De Hayr, R. W., Rassam, D. W., Beard, N. J. and Bloesch, P. M. (2011), Denitrification potential of intermittently saturated floodplain soils from a subtropical perennial stream and an ephemeral tributary, *Soil Biology & Biochemistry,* 43(2), 324-332.

Fernandez, A. L., Sheaffer, C. C., Wyse, D. L., Staley, C., Gould, T. J., and Sadowsky, M. J. (2016a), Associations between soil bacterial community structure and nutrient cycling functions in long-term organic farm soils following cover crop and organic fertilizer amendment, *Science of the Total Environment*, 566-567, 949-959.

Fernandez, A. L., Sheaffer, C. C., Wyse, D. L., Staley, C., Gould, T. J., and Sadowsky, M. J. (2016b), Structure of bacterial communities in soil following cover crop and organic fertilizer incorporation, *Applied Microbial Biotechnology*, 100, 9331-9341.

Fiedler, S., Vepraskas, M. J. and Richardson, J. L. (2007), Soil redox potential: Importance, field measurements, and observations, *Advances in Agronomy, Vol 94,* 94, 1-54.

Findlay, S. E. G., Mulholland, P. J., Hamilton, S. K., Tank, J. L., Bernot, M. J., Burgin, A. J., Crenshaw, C. L., Dodds, W. K., Grimm, N. B., McDowell, W. H., Potter, J. D. and Sobota, D. J. (2011), Cross-stream comparison of substrate-specific denitrification potential, *Biogeochemistry,* 104(1-3), 381-392.

Forshay, K. J. and Stanley, E. H. (2005), Rapid nitrate loss and denitrification in a temperate river floodplain, *Biogeochemistry,* 75(1), 43-64.

Fowler, D., Coyle, M., Skiba, U., Sutton, M. A., Cape, J. N., Reis, S., Sheppard, L. J., Jenkins, A., Grizzetti, B., Galloway, J. N., Vitousek, P., Leach, A., Bouwman, A. F., Butterbach-Bahl, K., Dentener, F., Stevenson, D., Amann, M. and Voss, M. (2013), The global nitrogen cycle in the twenty-first century, *Philosophical Transactions of the Royal Society B-Biological Sciences,* 368(1621), 13.

Galloway, J. N., Townsend, A. R., Erisman, J. W., Bekunda, M., Cai, Z. C., Freney, J. R., Martinelli, L. A., Seitzinger, S. P. and Sutton, M. A. (2008), Transformation of the nitrogen cycle: Recent trends, questions, and potential solutions, *Science,* 320(5878), 889-892.

Gardner, W. H. (1986), Water Content, Klute, A. (ed.), In: Methods of Soil Analysis: Part 1- Physical and Mineralogical Methods. 2nd Edition Madison, WI: Soil Science of America, 493-544.

Gohl, D. M., Vangay, P., Garbe, J., MacLean, A., Hauge, A., Becker, A., Gould, T. J., Clayton, J. B., Johnson, T. J., Hunter, R., Knights, D. and Beckman, K. B. (2016),

Systematic improvement of amplicon marker gene methods for increased accuracy in microbiome studies, *Nature Biotechnology,* 34(9), 942-949.

Gomez-Velez, J. D., Harvey, J., Cardenas, M. B. and Kiel, B. (2015), Denitrification in the Mississippi River network controlled by flow through river bedforms, *Nature Geoscience,* 8(12), 941-945.

Gongol, C. and Savage, C. (2016), Spatial variation in rates of benthic denitrification and environmental controls in four New Zealand estuaries, *Marine Ecology Progress Series,* 556, 59-77.

Graf, D. R. H., Jones, C. M. and Hallin, S. (2014), Intergenomic Comparisons Highlight Modularity of the Denitrification Pathway and Underpin the Importance of Community Structure for N2O Emissions, *Plos One,* 9(12), 20.

Groffman, P. M., Altabet, M. A., Bohlke, J. K., Butterbach-Bahl, K., David, M. B., Firestone, M. K., Giblin, A. E., Kana, T. M., Nielsen, L. P. and Voytek, M. A. (2006), Methods for measuring denitrification: Diverse approaches to a difficult problem, *Ecological Applications,* 16(6), 2091-2122.

Groffman, P. M., Butterbach-Bahl, K., Fulweiler, R. W., Gold, A. J., Morse, J. L., Stander, E. K., Tague, C., Tonitto, C. and Vidon, P. (2009), Challenges to incorporating spatially and temporally explicit phenomena (hotspots and hot moments) in denitrification models, *Biogeochemistry,* 93(1-2), 49-77.

Gu, C. H., Anderson, W. and Maggi, F. (2012), Riparian biogeochemical hot moments induced by stream fluctuations, *Water Resources Research,* 48, 17.

Guentzel, K. S., Hondzo, M., Badgley, B. D., Finlay, J. C., Sadowsky, M. J. and Kozarek, J. L. (2014), Measurement and Modeling of Denitrification in Sand-Bed Streams under Various Land Uses, *Journal of Environmental Quality,* 43(3), 1013-1023.

Harter, J., El-Hadidi, M., Huson, D. H., Kappler, A. and Behrens, S. (2017), Soil biochar amendment affects the diversity of nosZ transcripts: Implications for N2O formation, *Scientific Reports,* 7, 14.

Harvey, J. W., Bohlke, J. K., Voytek, M. A., Scott, D. and Tobias, C. R. (2013), Hyporheic zone denitrification: Controls on effective reaction depth and contribution to whole-stream mass balance, *Water Resources Research,* 49(10), 6298-6316.

Hayat, R., Ali, S., Amara, U., Khalid, R. and Ahmed, I. (2010), Soil beneficial bacteria and their role in plant growth promotion: a review, *Annals of Microbiology,* 60(4), 579-598.

Hefting, M. M., Bobbink, R. and Janssens, M. P. (2006), Spatial variation in denitrification and N2O emission in relation to nitrate removal efficiency in a n-stressed riparian buffer zone, *Ecosystems,* 9(4), 550-563.

Heiri, O., Lotter, A. F. and Lemcke, G. (2001), Loss on ignition as a method for estimating organic and carbonate content in sediments: reproducibility and comparability of results, *Journal of Paleolimnology,* 25(1), 101-110.

Henderson, S. L., Dandie, C. E., Patten, C. L., Zebarth, B. J., Burton, D. L., Trevors, J. T. and Goyer, C. (2010), Changes in Denitrifier Abundance, Denitrification Gene mRNA Levels, Nitrous Oxide Emissions, and Denitrification in Anoxic Soil Microcosms Amended with Glucose and Plant Residues, *Applied and Environmental Microbiology,* 76(7), 2155-2164.

Howarth, R., Chan, F., Conley, D. J., Garnier, J., Doney, S. C., Marino, R. and Billen, G. (2011), Coupled biogeochemical cycles: eutrophication and hypoxia in temperate estuaries and coastal marine ecosystems, *Frontiers in Ecology and the Environment,* 9(1), 18-26.

Howarth, R. W. (2008), Coastal nitrogen pollution: A review of sources and trends globally and regionally, *Harmful Algae,* 8(1), 14-20.

Howarth, R. W., Boyer, E. W., Pabich, W. J. and Galloway, J. N. (2002), Nitrogen use in the United States from 1961-2000 and potential future trends, *Ambio,* 31(2), 88-96.

Huang, Y., Zou, J. W., Zheng, X. H., Wang, Y. S. and Xu, X. K. (2004), Nitrous oxide emissions as influenced by amendment of plant residues with different C:N ratios, *Soil Biology & Biochemistry,* 36(6), 973-981.

Humbert, S., Tarnawski, S., Fromin, N., Mallet, M. P., Aragno, M. and Zopfi, J. (2010), Molecular detection of anammox bacteria in terrestrial ecosystems: distribution and diversity, *Isme Journal,* 4(3), 450-454.

Hunt, P. G., Matheny, T. A. and Szogi, A. A. (2003), Denitrification in constructed wetlands used for treatment of swine wastewater, *Journal of Environmental Quality,* 32(2), 727-735.

Huse, S. M., Welch, D. M., Morrison, H. G. and Sogin, M. L. (2010), Ironing out the wrinkles in the rare biosphere through improved OTU clustering, *Environmental Microbiology,* 12(7), 1889-1898.

Inwood, S. E., Tank, J. L. and Bernot, M. J. (2007), Factors controlling sediment denitrification in midwestern streams of varying land use, *Microbial Ecology,* 53(2), 247-258.

Isobe, K. and Ohte, N. (2014), Ecological Perspectives on Microbes Involved in N-Cycling, *Microbes and Environments,* 29(1), 4-16.

Janssen, M., Frings, J. and Lennartz, B. (2013), Do vegetated buffer strips at a drained arable site influence nitrate concentrations in the groundwater? A field-scale process study in Mecklenburg-Western Pomerania, *Hydrologie Und Wasserbewirtschaftung,* 57(2), 48-59.

Jensen, E. S., Peoples, M. B., Boddey, R. M., Gresshoff, P. M., Hauggaard-Nielsen, H., Alves, B. J. R. and Morrison, M. J. (2012), Legumes for mitigation of climate change and the provision of feedstock for biofuels and biorefineries. A review, *Agronomy for Sustainable Development,* 32(2), 329-364.

Jimenez, J. (2012), Cascades in Wall-Bounded Turbulence, *Annual Review of Fluid Mechanics, Vol 44,* 44, 27-45.

Johnson, L. B., Richards, C., Host, G. E. and Arthur, J. W. (1997), Landscape influences on water chemistry in Midwestern stream ecosystems, *Freshwater Biology,* 37(1), 193-208.

Jones, C. M., Graf, D. R. H., Bru, D., Philippot, L. and Hallin, S. (2013), The unaccounted yet abundant nitrous oxide-reducing microbial community: a potential nitrous oxide sink, *Isme Journal,* 7(2), 417-426.

Jones, C. N., Scott, D. T., Edwards, B. L. and Keim, R. F. (2014), Perirheic mixing and biogeochemical processing in flow-through and backwater floodplain wetlands, *Water Resources Research,* 50(9), 7394-7405.

Jost, L. (2007), Partitioning diversity into independent alpha and beta components, *Ecology,* 88(10), 2427-2439.

Kahle, P., Schonemann, S. and Lennartz, B. (2013), Effect of vegetated buffer strips on nitrate inputs into surface waters in drained lowland catchments, *Hydrologie Und Wasserbewirtschaftung,* 57(2), 60-68.

Kandeler, E., Deiglmayr, K., Tscherko, D., Bru, D. and Philippot, L. (2006), Abundance of narG, nirS, nirK, and nosZ genes of denitrifying bacteria during primary successions of a glacier foreland, *Applied and Environmental Microbiology,* 72(9), 5957-5962.

Kaushal, S. S., Groffman, P. M., Mayer, P. M., Striz, E. and Gold, A. J. (2008), Effects of stream restoration on denitrification in an urbanizing watershed, *Ecological Applications,* 18(3), 789-804.

Kazemzadeh, A. and Ensafi, A. A. (2001), Sequential flow injection spectrophotometric determination of nitrite and nitrate in various samples, *Analytica Chimica Acta,* 442(2), 319-326.

Kemp, M. J. and Dodds, W. K. (2002), The influence of ammonium, nitrate, and dissolved oxygen concentrations on uptake, nitrification, and denitrification rates associated with prairie stream substrata, *Limnology and Oceanography,* 47(5), 1380-1393.

Kim, H., Bae, H. S., Reddy, K. R. and Ogram, A. (2016), Distributions, abundances and activities of microbes associated with the nitrogen cycle in riparian and stream sediments of a river tributary, *Water Research,* 106, 51-61.

Kogel-Knabner, I., Amelung, W., Cao, Z. H., Fiedler, S., Frenzel, P., Jahn, R., Kalbitz, K., Kolbl, A. and Schloter, M. (2010), Biogeochemistry of paddy soils, *Geoderma,* 157(1-2), 1-14.

Kuenen, J. G. (2008), Anammox bacteria: from discovery to application, *Nature Reviews Microbiology,* 6(4), 320-326.

Lansdown, K., Heppell, C. M., Trimmer, M., Binley, A., Heathwaite, A. L., Byrne, P. and Zhang, H. (2015), The interplay between transport and reaction rates as controls on nitrate attenuation in permeable, streambed sediments, *Journal of Geophysical Research-Biogeosciences,* 120(6), 1093-1109.

Lindemann, S., Zarnoch, C. B., Castignetti, D. and Hoellein, T. J. (2016), Effect of Eastern Oysters (Crassostrea virginica) and Seasonality on Nitrite Reductase Gene Abundance (nirS, nirK, nrfA) in an Urban Estuary, *Estuaries and Coasts,* 39(1), 218-232.

Liu, X. J., Zhang, Y., Han, W. X., Tang, A. H., Shen, J. L., Cui, Z. L., Vitousek, P., Erisman, J. W., Goulding, K., Christie, P., Fangmeier, A. and Zhang, F. S. (2013), Enhanced nitrogen deposition over China, *Nature,* 494(7438), 459-462.

Loken, L. C., Small, G. E., Finlay, J. C., Sterner, R. W. and Stanley, E. H. (2016), Nitrogen cycling in a freshwater estuary, *Biogeochemistry,* 127(2-3), 199-216.

Lopez-Gutierrez, J. C., Henry, S., Hallet, S., Martin-Laurent, F., Catroux, G. and Philippot, L. (2004), Quantification of a novel group of nitrate-reducing bacteria in the environment by real-time PCR, *Journal of Microbiological Methods,* 57(3), 399-407.

Lorke, A., Muller, B., Maerki, M. and Wuest, A. (2003), Breathing sediments: The control of diffusive transport across the sediment-water interface by periodic boundary-layer turbulence, *Limnology and Oceanography,* 48(6), 2077-2085.

Madigan, M. T., Bender, K. S., Buckley, D. H., Sattley, W. M. and Stahl, D. A. (2018), *Brock Biology of Microorganisms.* Fifteenth edn. New York, NY: Pearson Education, Inc.

Mahl, U. H., Tank, J. L., Roley, S. S. and Davis, R. T. (2015), Two-Stage Ditch Floodplains Enhance N-Removal Capacity and Reduce Turbidity and Dissolved P in Agricultural Streams, *Journal of the American Water Resources Association,* 51(4), 923-940.

Manassaram, D. M., Backer, L. C. and Moll, D. M. (2006), A review of nitrates in drinking water: Maternal exposure and adverse reproductive and developmental outcomes, *Environmental Health Perspectives,* 114(3), 320-327.

Manis, E., Royer, T. V., Johnson, L. T. and Leff, L. G. (2014), Denitrification in Agriculturally Impacted Streams: Seasonal Changes in Structure and Function of the Bacterial Community, *Plos One,* 9(8), 13.

Martin, L. A., Mulholland, P. J., Webster, J. R. and Valett, H. M. (2001), Denitrification potential in sediments of headwater streams in the southern Appalachian Mountains, USA, *Journal of the North American Benthological Society,* 20(4), 505-519.

Masclaux-Daubresse, C., Daniel-Vedele, F., Dechorgnat, J., Chardon, F., Gaufichon, L. and Suzuki, A. (2010), Nitrogen uptake, assimilation and remobilization in plants: challenges for sustainable and productive agriculture, *Annals of Botany,* 105(7), 1141-1157.

McClain, M. E., Boyer, E. W., Dent, C. L., Gergel, S. E., Grimm, N. B., Groffman, P. M., Hart, S. C., Harvey, J. W., Johnston, C. A., Mayorga, E., McDowell, W. H. and Pinay, G. (2003), Biogeochemical hot spots and hot moments at the interface of terrestrial and aquatic ecosystems, *Ecosystems,* 6(4), 301-312.

Minnesota Statutes (2017). Section 103E.021, Subdivision 1.

Moore, J. W., Stanitski, C. L. and Jurs, P. C. (2010), *Chemistry: The Molecular Science.* 4th edn.: Cengage Learning.

Morris, M. W. L., Hondzo, M. and Power, M. E. (2011), Scaling Glossosoma (Trichoptera) density by abiotic variables in mountain streams, *Journal of the North American Benthological Society,* 30(2), 493-506.

Morrissey, E. M., Jenkins, A. S., Brown, B. L. and Franklin, R. B. (2013), Resource Availability Effects on Nitrate-Reducing Microbial Communities in a Freshwater Wetland, *Wetlands,* 33(2), 301-310.

Minnesota Pollution Control Agency (2013), Nitrogen in Minnesota Surface Waters: Conditions, trends, sources, and reductions, *Nitrogen in Minnesota Surface Waters*.

Mulholland, P. J., Helton, A. M., Poole, G. C., Hall, R. O., Jr., Hamilton, S. K., Peterson, B. J., Tank, J. L., Ashkenas, L. R., Cooper, L. W., Dahm, C. N., Dodds, W. K., Findlay, S. E. G., Gregory, S. V., Grimm, N. B., Johnson, S. L., McDowell, W. H., Meyer, J. L., Valett, H. M., Webster, J. R., Arango, C. P., Beaulieu, J. J., Bernot, M. J., Burgin, A. J., Crenshaw, C. L., Johnson, L. T., Niederlehner, B. R., O'Brien, J. M., Potter, J. D., Sheibley, R. W., Sobota, D. J. and Thomas, S. M.

(2008), Stream denitrification across biomes and its response to anthropogenic nitrate loading, *Nature,* 452(7184), 202-205.
Niedermeier, A. and Robinson, J. S. (2007), Hydrological controls on soil redox dynamics in a peat-based, restored wetland, *Geoderma,* 137(3-4), 18-326.
NOAA (2017) Gulf of Mexico 'dead zone' is the largest ever measured. Available at: http://www.noaa.gov/media-release/.
Nogaro, G. and Burgin, A. J. (2014), Influence of bioturbation on denitrification and dissimilatory nitrate reduction to ammonium (DNRA) in freshwater sediments, *Biogeochemistry,* 120(1-3), 279-294.
NRC (1993), *Soil and water quality: an agenda for agriculture.* Washington, DC: The National Academies Press.
O'Brien, J. M., Hamilton, S. K., Podzikowski, L. and Ostrom, N. (2012), The fate of assimilated nitrogen in streams: an in situ benthic chamber study, *Freshwater Biology,* 57(6), 1113-1125.
O'Connor, B. and Hondzo, M. (2008a), Enhancement and inhibition of denitfication by fluid-flow and dissolved oxygen flux to stream sediments, *Environmental Science & Technology,* 42(1), 119-125.
O'Connor, B. L., Harvey, J. W. and McPhillips, L. E. (2012), Thresholds of flow-induced bed disturbances and their effects on stream metabolism in an agricultural river, *Water Resources Research,* 48, 18.
O'Connor, B. L. and Hondzo, M. (2008b), Dissolved oxygen transfer to sediments by sweep and eject motions in aquatic environments, *Limnology and Oceanography,* 53(2), 566-578.
O'Connor, B. L., Hondzo, M., Dobraca, D., LaPara, T. M., Finlay, J. C. and Brezonik, P. L. (2006), Quantity-activity relationship of denitrifying bacteria and environmental scaling in streams of a forested watershed, *Journal of Geophysical Research,* 111.
Osborne, L. L. and Kovacic, D. A. (1993), Riparian vegetated buffer strips in water-quality restoration and stream management, *Freshwater Biology,* 29(2), 243-258.
Perryman, S. E., Rees, G. N., Walsh, C. J. and Grace, M. R. (2011), Urban Stormwater Runoff Drives Denitrifying Community Composition Through Changes in Sediment Texture and Carbon Content, *Microbial Ecology,* 61(4), 932-940.
Petersen, D. G., Blazewicz, S. J., Firestone, M., Herman, D. J., Turetsky, M. and Waldrop, M. (2012), Abundance of microbial genes associated with nitrogen cycling as indices of biogeochemical process rates across a vegetation gradient in Alaska, *Environmental Microbiology,* 14(4), 993-1008.
Philippot, L., Andert, J., Jones, C. M., Bru, D. and Hallin, S. (2011), Importance of denitrifiers lacking the genes encoding the nitrous oxide reductase for N2O emissions from soil, *Global Change Biology,* 17(3), 1497-1504.
Pihlatie, M., Syvasalo, E., Simojoki, A., Esala, M. and Regina, K. (2004), Contribution of nitrification and denitrification to N2O production in peat, clay and loamy sand soils under different soil moisture conditions, *Nutrient Cycling in Agroecosystems,* 70(2), 135-141.
Pina-Ochoa, E. and Alvarez-Cobelas, M. (2006), Denitrification in aquatic environments: A cross-system analysis, *Biogeochemistry,* 81(1), 111-130.

Pinay, G., Black, V. J., Planty-Tabacchi, A. M., Gumiero, B. and Decamps, H. (2000), Geomorphic control of denitrification in large river floodplain soils, *Biogeochemistry,* 50(2), 163-182.

Pinay, G., Clement, J. C. and Naiman, R. J. (2002), Basic principles and ecological consequences of changing water regimes on nitrogen cycling in fluvial systems, *Environmental Management,* 30(4), 481-491.

Pinay, G., Gumiero, B., Tabacchi, E., Gimenez, O., Tabacchi-Planty, A. M., Hefting, M. M., Burt, T. P., Black, V. A., Nilsson, C., Iordache, V., Bureau, F., Vought, L., Petts, G. E. and Decamps, H. (2007), Patterns of denitrification rates in European alluvial soils under various hydrological regimes, *Freshwater Biology,* 52(2), 252-266.

Powell, G. E., Ward, A. D., Mecklenburg, D. E. and Jayakaran, A. D. (2007), Two-stage channel systems: Part 1, a practical approach for sizing agricultural ditches, *Journal of Soil and Water Conservation,* 62(4), 277-286.

Powlson, D. S., Addisott, T. M., Benjamin, N., Cassman, K. G., de Kok, T. M., van Grinsven, H., L'Hirondel, J. L., Avery, A. A. and van Kessel, C. (2008), When does nitrate become a risk for humans?, *Journal of Environmental Quality,* 37(2), 291-295.

Prieme, A., Braker, G. and Tiedje, J. M. (2002), Diversity of nitrite reductase (nirK and nirS) gene fragments in forested upland and wetland soils, *Applied and Environmental Microbiology,* 68(4), 1893-1900.

Pruesse, E., Quast, C., Knittel, K., Fuchs, B. M., Ludwig, W. G., Peplies, J. and Glockner, F. O. (2007), SILVA: a comprehensive online resource for quality checked and aligned ribosomal RNA sequence data compatible with ARB, *Nucleic Acids Research,* 35(21), 7188-7196.

Qin, S. P., Yuan, H. J., Dong, W. X., Hu, C. S., Oenema, O. and Zhang, Y. M. (2013), Relationship between soil properties and the bias of N2O reduction by acetylene inhibition technique for analyzing soil denitrification potential, *Soil Biology & Biochemistry,* 66, 182-187.

Quinn, J. M., Cooper, A. B., Davies-Colley, R. J., Rutherford, J. C. and Williamson, R. B. (1997), Land use effects on habitat, water quality, periphyton, and benthic invertebrates in Waikato, New Zealand, hill-country streams, *New Zealand Journal of Marine and Freshwater Research,* 31(5), 579-597.

Rabalais, N. N. (2002), Nitrogen in aquatic ecosystems, *Ambio,* 31(2), 102-112.

Rabalais, N. N., Turner, R. E., Sen Gupta, B. K., Boesch, D. F., Chapman, P. and Murrell, M. C. (2007), Hypoxia in the northern Gulf of Mexico: Does the science support the plan to reduce, mitigate, and control hypoxia?, *Estuaries and Coasts,* 30(5), 753-772.

Ravishankara, A. R., Daniel, J. S. and Portmann, R. W. (2009), Nitrous Oxide (N2O): The Dominant Ozone-Depleting Substance Emitted in the 21st Century, *Science,* 326(5949), 123-125.

Rich, J. J., Heichen, R. S., Bottomley, P. J., Cromack, K. and Myrold, D. D. (2003), Community composition and functioning of denitrifying bacteria from adjacent meadow and forest soils, *Applied and Environmental Microbiology,* 69(10), 5974-5982.

Robertson, G. P. and Groffman, P. M. (2015), Nitrogen transformations, Paul, E.A. (ed.) In: Soil microbiology, ecology, and biochemistry. Fourth ed. Burlington, Massachusetts, USA: Academic Press, 421-446.

Robertson, G. P., Klingensmith, K. M., Klug, M. J., Paul, E. A., Crum, J. R. and Ellis, B. G. (1997), Soil resources, microbial activity, and primary production across an agricultural ecosystem, *Ecological Applications,* 7(1), 158-170.

Robertson, G. P. and Vitousek, P. M. (2009), Nitrogen in Agriculture: Balancing the Cost of an Essential Resource, *Annual Review of Environment and Resources Annual Review of Environment and Resources*. Palo Alto: Annual Reviews, 97-125.

Rocca, J. D., Hall, E. K., Lennon, J. T., Evans, S. E., Waldrop, M. P., Cotner, J. B., Nemergut, D. R., Graham, E. B. and Wallenstein, M. D. (2015), Relationships between protein-encoding gene abundance and corresponding process are commonly assumed yet rarely observed, *Isme Journal,* 9(8), 1693-1699.

Roley, S. S., Tank, J. L., Stephen, M. L., Johnson, L. T., Beaulieu, J. J. and Witter, J. D. (2012a), Floodplain restoration enhances denitrification and reach-scale nitrogen removal in an agricultural stream, *Ecological Applications,* 22(1), 281-297.

Roley, S. S., Tank, J. L. and Williams, M. A. (2012b), Hydrologic connectivity increases denitrifcation in the hyporheic zone and restored floodplains of an agricultural stream, *Journal of Geophysical Research,* 117(G3).

Rosch, C., Mergel, A. and Bothe, H. (2002), Biodiversity of denitrifying and dinitrogen-fixing bacteria in an acid forest soil, *Applied and Environmental Microbiology,* 68(8), 3818-3829.

Royer, T. V., David, M. B. and Gentry, L. E. (2006), Timing of riverine export of nitrate and phosphorus from agricultural watersheds in Illinois: Implications for reducing nutrient loading to the Mississippi River, *Environmental Science & Technology,* 40(13), 4126-4131.

Sanchez-Andres, R., Sanchez-Carrillo, S., Ortiz-Llorente, M. J., Alvarez-Cobelas, M. and Cirujano, S. (2010), Do changes in flood pulse duration disturb soil carbon dioxide emissions in semi-arid floodplains?, *Biogeochemistry,* 101(1-3), 257-267.

Sanford, R. A., Wagner, D. D., Wu, Q. Z., Chee-Sanford, J. C., Thomas, S. H., Cruz-Garcia, C., Rodriguez, G., Massol-Deya, A., Krishnani, K. K., Ritalahti, K. M., Nissen, S., Konstantinidis, K. T. and Loffler, F. E. (2012), Unexpected nondenitrifier nitrous oxide reductase gene diversity and abundance in soils, *Proceedings of the National Academy of Sciences of the United States of America,* 109(48), 19709-19714.

Schaller, J. L., Royer, T. V., David, M. B. and Tank, J. L. (2004), Denitrification associated with plants and sediments in an agricultural stream, *Journal of the North American Benthological Society,* 23(4), 667-676.

Schlesinger, W. H. (2009), On the fate of anthropogenic nitrogen, *Proceedings of the National Academy of Sciences of the United States of America,* 106(1), 203-208.

Schlesinger, W. H. and Burnhardt, E. S. (2013), *Biogeochemistry: An Analysis of Global Change.* 3rd edn. Waltham, MA: Elsevier.

Schlicting, H. (1987) *Boundary Layer Theory.* 7th edn. New York, NY: McGraw-Hill.

Schloss, P. D., Westcott, S. L., Ryabin, T., Hall, J. R., Hartmann, M., Hollister, E. B., Lesniewski, R. A., Oakley, B. B., Parks, D. H., Robinson, C. J., Sahl, J. W., Stres, B., Thallinger, G. G., Van Horn, D. J. and Weber, C. F. (2009), Introducing

mothur: Open-Source, Platform-Independent, Community-Supported Software for Describing and Comparing Microbial Communities, *Applied and Environmental Microbiology,* 75(23), 7537-7541.

Schmidt, T. M. and Waldron, C. (2015), Microbial diversity in soils of agricultural landscapes and its relation to ecosystem function, in Hamilton, S.K., Doll, J.E. & Robertson, G.P. (eds.) *The Ecology of Agricultural Landscapes: Long-term Research on the Path to Sustainability*. New York, New York, USA: Oxford University Press, 135-157.

Scott, D. T., Keim, R. F., Edwards, B. L., Jones, C. N. and Kroes, D. E. (2014), Floodplain biogeochemical processing of floodwaters in the Atchafalaya River Basin during the Mississippi River flood of 2011, *Journal of Geophysical Research-Biogeosciences,* 119(4), 537-546.

Scott, J. T., McCarthy, M. J., Gardner, W. S. and Doyle, R. D. (2008), Denitrification, dissimilatory nitrate reduction to ammonium, and nitrogen fixation along a nitrate concentration gradient in a created freshwater wetland, *Biogeochemistry,* 87(1), 99-111.

Seitzinger, S. P., Nielsen, L. P., Caffrey, J. and Christensen, P. B. (1993), Denitrification measurements in aquatic sediments- a comparison of 3 methods, *Biogeochemistry,* 23(3), 147-167.

Shenker, M., Seitelbach, S., Brand, S., Haim, A. and Litaor, M. I. (2005), Redox reactions and phosphorus release in re-flooded soils of an altered wetland, *European Journal of Soil Science,* 56(4), 515-525.

Shrestha, J., Niklaus, P. A., Pasquale, N., Huber, B., Barnard, R. L., Frossard, E., Schleppi, P., Tockner, K. and Luster, J. (2014), Flood pulses control soil nitrogen cycling in a dynamic river floodplain, *Geoderma,* 228, 14-24.

Shrewsbury, L. H., Smith, J. L., Huggins, D. R., Carpenter-Boggs, L. and Reardon, C. L. (2016), Denitrifier abundance has a greater influence on denitrification rates at larger landscape scales but is a lesser driver than environmental variables, *Soil Biology & Biochemistry,* 103, 221-231.

Sirivedhin, T. and Gray, K. A. (2006), Factors affecting denitrification rates in experimental wetlands: Field and laboratory studies, *Ecological Engineering,* 26(2), 167-181.

Smil, V. (2002), Nitrogen and food production: Proteins for human diets, *Ambio,* 31(2), 126-131.

Smith, C. J., Dong, L. F., Wilson, J., Stott, A., Osborn, A. M. and Nedwell, D. B. (2015), Seasonal variation in denitrification and dissimilatory nitrate reduction to ammonia process rates and corresponding key functional genes along an estuarine nitrate gradient, *Frontiers in Microbiology,* 6, 11.

Smith, D. R., Livingston, S. J., Zuercher, B. W., Larose, M., Heathman, G. C. and Huang, C. (2008a), Nutrient losses from row crop agriculture in Indiana, *Journal of Soil and Water Conservation,* 63(6), 396-409.

Smith, M. S. and Tiedje, J. M. (1979), Phases of denitrification following oxygen depletion in soil, *Soil Biology & Biochemistry,* 11(3), 261-267.

Smith, P., Martino, D., Cai, Z., Gwary, D., Janzen, H., Kumar, P., McCarl, B., Ogle, S., O'Mara, F., Rice, C., Scholes, B., Sirotenko, O., Howden, M., McAllister, T., Pan, G., Romanenkov, V., Schneider, U., Towprayoon, S., Wattenbach, M. and Smith,

J. (2008b), Greenhouse gas mitigation in agriculture, *Philosophical Transactions of the Royal Society B-Biological Sciences,* 363(1492), 789-813.

Solomon, C. T., Hotchkiss, E. R., Moslemi, J. M., Ulseth, A. J., Stanley, E. H., Hall, R. O. and Flecker, A. S. (2009), Sediment size and nutrients regulate denitrification in a tropical stream, *Journal of the North American Benthological Society,* 28(2), 480-490.

Song, K., Lee, S. H., Mitsch, W. J. and Kang, H. (2010), Different responses of denitrification rates and denitrifying bacterial communities to hydrologic pulsing in created wetlands, *Soil Biology & Biochemistry,* 42(10), 1721-1727.

Staley, C. and Sadowsky, M. J. (2016), Application of metagenomics to assess microbial communities in water and other environmental matrices, *Journal of the Marine Biological Association of the United Kingdom,* 96(1), 121-129.

Stehfest, E. and Bouwman, L. (2006), N2O and NO emission from agricultural fields and soils under natural vegetation: summarizing available measurement data and modeling of global annual emissions, *Nutrient Cycling in Agroecosystems,* 74(3), 207-228.

Strock, J. S., Kleinman, P. J. A., King, K. W. and Delgado, J. A. (2010), Drainage water management for water quality protection, *Journal of Soil and Water Conservation,* 65(6), 131A-136A.

Strohm, T. O., Griffin, B., Zumft, W. G. and Schink, B. (2007), Growth yields in bacterial denitrification and nitrate ammonification, *Applied and Environmental Microbiology,* 73(5), 1420-1424.

Tatariw, C., Chapman, E. L., Sponseller, R. A., Mortazavi, B. and Edmonds, J. W. (2013), Denitrification in a large river: consideration of geomorphic controls on microbial activity and community structure, *Ecology,* 94(10), 2249-2262.

Teranes, J. L. and Bernasconi, S. M. (2000), The record of nitrate utilization and productivity limitation provided by delta N-15 values in lake organic matter - A study of sediment trap and core sediments from Baldeggersee, Switzerland, *Limnology and Oceanography,* 45(4), 801-813.

Thornthwaite, C. W. (1948), An approach toward a rational classification of climate, *Geographical Review,* 38(1), 55-94.

Tiedje, J. (1982), Denitrification, A.L. Page, R.H.M., D.R. Keeney (ed.) In: Methods of soil analysis, part 2. Agronomy Monograph no. 9. Madison, WI: American Society of Agronomy, 1011-1026.

Tiedje, J. M., Simkins, S. and Groffman, P. M. (1989), Perspectives on measurement of denitrification in the field including recommended protocols for acetylene based methods, *Plant and Soil,* 115(2), 261-284.

Tockner, K., Pennetzdorfer, D., Reiner, N., Schiemer, F. and Ward, J. V. (1999), Hydrological connectivity, and the exchange of organic matter and nutrients in a dynamic river-floodplain system (Danube, Austria), *Freshwater Biology,* 41(3), 521-535.

Tomasek, A. A., Kozarek, J. L., Hondzo, M., Lurndahl, N., Sadowsky, M. J., Wang, P. and Staley, C. (2017), Environmental drivers of denitrification rates and denitrifying gene abundances in channels and riparian areas, *Water Resources Research,* 53(8), 6523-6538.

Townsend, A. R., Howarth, R. W., Bazzaz, F. A., Booth, M. S., Cleveland, C. C., Collinge, S. K., Dobson, A. P., Epstein, P. R., Keeney, D. R., Mallin, M. A., Rogers, C. A., Wayne, P. and Wolfe, A. H. (2003), Human health effects of a changing global nitrogen cycle, *Frontiers in Ecology and the Environment,* 1(5), 240-246.

Turner, R. E. and Rabalais, N. N. (2003), Linking landscape and water quality in the Mississippi river basin for 200 years, *Bioscience,* 53(6), 563-572.

Turner, R. E., Rabalais, N. N. and Justic, D. (2006), Predicting summer hypoxia in the northern Gulf of Mexico: Riverine N, P, and Si loading, *Marine Pollution Bulletin,* 52(2), 139-148.

USDA (2011), Carbon to nitrogen ratios in cropping systems. *In:* Service, U.N.R.C. (ed.).

USEPA (2010), Methane and nitrous oxide emissions from natural sources, Washington, DCEPA 430-R-10-001).

Van Kessel, J. S., Reeves, J. B. and Meisinger, J. J. (2000), Nitrogen and carbon mineralization of potential manure components, *Journal of Environmental Quality,* 29(5), 1669-1677.

Van Rijn, J., Tal, Y. and Schreier, H. J. (2006), Denitrification in recirculating systems: Theory and applications, *Aquacultural Engineering,* 34(3), 364-376.

Vance-Harris, C. and Ingall, E. (2005), Denitrification pathways and rates in the sandy sediments of the Georgia continental shelf, USA, *Geochemical Transactions,* 6(1), 12-18.

Venterea, R. T., Halvorson, A. D., Kitchen, N., Liebig, M. A., Cavigelli, M. A., Del Grosso, S. J., Motavalli, P. P., Nelson, K. A., Spokas, K. A., Singh, B. P., Stewart, C. E., Ranaivoson, A., Strock, J. and Collins, H. (2012), Challenges and opportunities for mitigating nitrous oxide emissions from fertilized cropping systems, *Frontiers in Ecology and the Environment,* 10(10), 562-570.

Vitousek, P. M., Aber, J. D., Howarth, R. W., Likens, G. E., Matson, P. A., Schindler, D. W., Schlesinger, W. H. and Tilman, D. (1997), Human alteration of the global nitrogen cycle: Sources and consequences, *Ecological Applications,* 7(3), 737-750.

Wall, L. G., Tank, J. L., Royer, T. V. and Bernot, M. J. (2005), Spatial and temporal variability in sediment denitrification within an agriculturally influenced reservoir, *Biogeochemistry,* 76(1), 85-111.

Wang, Y. and Qian, P. Y. (2009), Conservative Fragments in Bacterial 16S rRNA Genes and Primer Design for 16S Ribosomal DNA Amplicons in Metagenomic Studies, *Plos One,* 4(10), 9.

Wang, Y., Uchida, Y., Shimomura, Y., Akiyama, H. and Hayatsu, M. (2017), Responses of denitrifying bacterial communities to short-term waterlogging of soils, *Scientific Reports,* 7.

Ward, M. H., deKok, T. M., Levallois, P., Brender, J., Gulis, G., Nolan, B. T. and VanDerslice, J. (2005), Workgroup report: Drinking-water nitrate and health-recent findings and research needs, *Environmental Health Perspectives,* 113(11), 1607-1614.

Ward, M. H., Kilfoy, B. A., Weyer, P. J., Anderson, K. E., Folsom, A. R. and Cerhan, J. R. (2010), Nitrate Intake and the Risk of Thyroid Cancer and Thyroid Disease, *Epidemiology,* 21(3), 389-395.

Warnaars, T. A., Hondzo, M. and Power, M. E. (2007), Abiotic controls on periphyton accrual and metabolism in streams: Scaling by dimensionless numbers, *Water Resources Research,* 43(8).

Washbourne, I. J., Crenshaw, C. L. and Baker, M. A. (2011), Dissimilatory nitrate reduction pathways in an oligotrophic freshwater ecosystem: spatial and temporal trends, *Aquatic Microbial Ecology,* 65(1), 55-64.

Watts, S. H. and Seitzinger, S. P. (2000), Denitrification rates in organic and mineral soils from riparian sites: a comparison of N-2 flux and acetylene inhibition methods, *Soil Biology & Biochemistry,* 32(10), 1383-1392.

Welti, N., Bondar-Kunze, E., Mair, M., Bonin, P., Wanek, W., Pinay, G. and Hein, T. (2012), Mimicking floodplain reconnection and disconnection using N-15 mesocosm incubations, *Biogeosciences,* 9(11), 4263-4278.

Westhoek, H., Lesschen, J. P., Rood, T., Wagner, S., De Marco, A., Murphy-Bokern, D., Leip, A., van Grinsven, H., Sutton, M. A. and Oenema, O. (2014), Food choices, health and environment: Effects of cutting Europe's meat and dairy intake, *Global Environmental Change-Human and Policy Dimensions,* 26, 196-205.

White, P. J. and Brown, P. H. (2010), Plant nutrition for sustainable development and global health, *Annals of Botany,* 105(7), 1073-1080.

Wolfe, A. H. and Patz, J. A. (2002), Reactive nitrogen and human health: Acute and long-term implications, *Ambio,* 31(2), 120-125.

Woodward, K. B., Fellows, C. S., Conway, C. L. and Hunter, H. M. (2009), Nitrate removal, denitrification and nitrous oxide production in the riparian zone of an ephemeral stream, *Soil Biology & Biochemistry,* 41(4), 671-680.

Woodward, K. B., Fellows, C. S., Mitrovic, S. M. and Sheldon, F. (2015), Patterns and bioavailability of soil nutrients and carbon across a gradient of inundation frequencies in a lowland river channel, Murray-Darling Basin, Australia, *Agriculture Ecosystems & Environment,* 205, 1-8.

Xiang, S. R., Doyle, A., Holden, P. A. and Schimel, J. P. (2008), Drying and rewetting effects on C and N mineralization and microbial activity in surface and subsurface California grassland soils, *Soil Biology & Biochemistry,* 40(9), 2281-2289.

Yoon, S., Nissen, S., Park, D., Sanford, R. A. and Loffler, F. E. (2016), Nitrous Oxide Reduction Kinetics Distinguish Bacteria Harboring Clade I NosZ from Those Harboring Clade II NosZ, *Applied and Environmental Microbiology,* 82(13), 3793-3800.

Yu, K. W., Seo, D. C. and DeLaune, R. D. (2010), Incomplete Acetylene Inhibition of Nitrous Oxide Reduction in Potential Denitrification Assay as Revealed by using 15N-Nitrate Tracer, *Communications in Soil Science and Plant Analysis,* 41(18), 2201-2210.

Zhu, G. B., Wang, S. Y., Wang, W. D., Wang, Y., Zhou, L. L., Jiang, B., Op den Camp, H. J. M., Risgaard-Petersen, N., Schwark, L., Peng, Y. Z., Hefting, M. M., Jetten, M. S. M. and Yin, C. Q. (2013), Hotspots of anaerobic ammonium oxidation at land-freshwater interfaces, *Nature Geoscience,* 6(2), 103-107.

Zumft, W. G. (1997), Cell biology and molecular basis of denitrification, *Microbiology and Molecular Biology Reviews,* 61, 533-616.